INCORPORATION OF BIOACTIVE COMPOUNDS IN EMULSIONS FOR APPLICATION IN COSMETIC INDUSTRY

A THESIS PRESENTED BY

K.M. GEETHI KAUSHALYA PAMUNUWA

to the Board of Study in Chemical Sciences of the

POSTGRADUATE INSTITUTE OF SCIENCE

in partial fulfillment of the requirement

for the award of the degree of

DOCTOR OF PHYLOSOPHY

of the

UNIVERSITY OF PERADENIYA

SRI LANKA

2015

This thesis is dedicated to

my parents Mr. Todd Pamunuwa and Mrs. Jayanthi Wickramasinghe,

and to my brother Mr. Isuru Pamunuwa

DECLARATION

I do hereby declare that the work reported in this thesis was exclusively carried out by me under the supervision of Prof. Veranja Karunaratne and Prof. Nedra Karunaratne, Department of Chemistry, Faculty of Science, University of Peradeniya, Sri Lanka. It describes the results of my own independent research except where due reference has been made in the text. No part of this thesis has been submitted earlier or concurrently for the same or any other degree.

Date: 2015.11.26 ..... K.M.G.K. Pamunuwa .....

Signature of the candidate

Certified by,

1. Supervisor (Name) Veranja Karunaratne Date: 27.11.2015

(Signature) .....

2. Supervisor (Name) D. Nedra Karunaratne Date: 27.11.2015

(Signature) D. N. Karunaratne

PGIS Stamp

INCORPORATION OF BIOACTIVE COMPOUNDS IN EMULSIONS FOR APPLICATION IN COSMETIC INDUSTRY

K.M.G.K. Pamunuwa

Postgraduate Institute of Science, University of Peradeniya, Peradeniya, Sri Lanka
Department of Chemistry, University of Peradeniya, Peradeniya, Sri Lanka

Liposomes and binary systems such as cocrystals, solid solutions and eutectics are formulations that have interesting applications, especially, in pharmaceutics and cosmeceutics. The aim of this thesis work is to evaluate liposomal systems encapsulating species that have potential applications in pharmaceutical or cosmeceutical industry and to form cocrystals to enhance the pharmaceutically relevant properties of curcumin.

Liposomes were prepared using reverse-phase evaporation method, thin-film hydration method and/or proliposome method. *In vitro* release studies were carried out using the dialysis bag method while *ex vivo* skin permeation experiments with pig ears were carried out using a Franz-diffusion cell. The encapsulation efficiency and loading capacity were dependent on the lipid composition. Liposomes encapsulating the highly antioxidant methanol extract of stem-bark of *Schumacheria castaneifolia*, ferulic acid and curcumin were prepared separately. Presence of cholesterol in the lipid bilayer may have affected lipid packing and encapsulation of methanol extract of stem-bark of *Schumacheria castaneifolia*. Similarly, interactions between stearylamine in the lipid bilayer and ferulic acid may be the reason for its high encapsulation efficiency. Encapsulation efficiencies of curcumin encapsulated liposomes also appeared to be dependent on the interactions of curcumin and lipids. This study revealed that the release kinetics of encapsulated species may be modulated by changing the lipid composition. Skin permeation of ferulic acid and curcumin showed dependance on lipid composition and charge of liposomes. Thus negatively charged liposomes showed higher skin permeation properties while ferulic acid and curcumin encapsulated positively charged liposomes exhibited slower release.

Cocrystal formation using curcumin and ferulic acid was attempted using solvent evaporation, liquid-assisted grinding and neat-grinding. The products were characterized using SEM, PXRD, FT-IR, TGA, and DSC. Solvent evaporation yielded either a solid solution or a eutectic while the grinding methods yielded eutectics. Dissolution studies revealed that solid solution or eutectic formation increases the dissolution rate of curcumin and that the three methods used are equally effective. Furthermore, using a mixture of curcumin and ferulic acid confers photostability to curcumin. Also, a 1:1 (mol/mol) mixture of curcumin and ferulic acid exhibits synergistic antioxidant potential even after exposure to UV radiation.

Curcumin and ferulic acid, when used as a binary system, improves significant properties such as the dissolution rate and antioxidant potential. Basically, this study portrays the ability of liposomes and binary systems such as solid solutions and/or eutectics to enhance pharmaceuticaly and cosmeceutically relevant physical properties of antioxidants.

ACKNOWLEDGEMENTS

First of all, I would like to express my heartfelt gratitude to my supervisors Prof. Veranja Karunaratne and Prof. Nedra Karunaratne of Department of Chemistry, University of Peradeniya for their guidance, encouragement, constant support, patience, kindness and love that not only made this thesis work a success but also made me who I am today.

Also, I thank the Department of Chemistry, University of Peradeniya for allowing me to carry out my study. The academic staff and non-academic staff who helped me in numerous ways of this Department are also appreciated. Prof. Anura Wickramasinghe, Prof. Chandani Perera and Dr. Champika Hettiaracchi are specially mentioned.

I express my gratitude to Sri Lanka Institute of Nanotechnology (Slintec) for allowing me to use their laboratory facilities when necessary. Also, I extend my gratitude to my collaborators and friends at Slintec for their support, co-operation and friendship. A special mention goes to Mr. Mevan Dissanayake and Ms. Nuwanthi Katuwavila.

I am grateful to the Natural products research group of the Department of Chemistry, Faculty of Science, University of Peradeniya for providing me with a plant extract that was used in my thesis work.

Also, I am thankful to my colleagues and friends in the Department of Chemistry, University of Peradeniya for their co-operation and friendship.

In addition, I would like to thank Dr. Sanka Atapattu in Canada for helping me getting articles relevant to my study.

I acknowledge the University of Peradeniya, Sri Lanka for providing me with financial assistance through Hilda Obeysekera Research Fellowship during the first 18 months of my study period.

I am grateful to the National Science Foundation, Sri Lanka for financial assistance through a Postgraduate Research Scholarship.

Finally, I thank my parents and brother for supporting me in numerous ways, especially by providing moral support, throughout my postgraduate study period. Their encouragement and love contributed a lot for the successful completion of my degree.

TABLE OF CONTENTS

LIST OF TABLES

LIST OF FIGURES

LIST OF ABBREVIATIONS

API	Active pharmaceutical ingredient
CH	Cholesterol
CL	Cardiolipin
DPPH	1,1-diphenyl-2-picrylhydrazyl
DSC	Differential scanning calorimetry
EE	Encapsulation efficiency
FDA	U.S. Food and Drug Admininstration
FT-IR	Fourier transform infrared
HPLC	High pressure liquid chromatography
IR	Infrared
LC	Loading capacity
NHL	Curcumin encapsulated negatively charged hybrid liposomes
NL	Curcumin encapsulated negatively charged liposomes
N-PRO	Ferulic acid encapsulated negatively charged liposomes prepared by proliposome method
N-REV	Ferulic acid encapsulated negatively charged liposomes prepared by reverse phase evaporation method
N-TFH	Ferulic acid encapsulated negatively charged liposomes prepared by thin film hydration method
P80	Polysorbate 80
PA	Phosphatidic acid
PBS	Phosphate buffered saline
PC	Phosphatidyl choline
PE	Phosphatidyl ethanolamine
PG	Phosphatidyl glycerol
PHL	Curcumin encapsulated positively charged hybrid liposomes
PL	Curcumin encapsulated positively charged liposomes
P-PRO	Ferulic acid encapsulated positively charged liposomes prepared by proliposome method
P-REV	Ferulic acid encapsulated positively charged liposomes prepared by reverse phase evaporation method
PS	Phosphatidyl serine
P-TFH	Ferulic acid encapsulated positively charged liposomes prepared by film hydration method
PXRD	Powder X-ray diffraction
RES	Reticuloendothelial system
SA	Stearylamine
SM	Sphingomyelin
SEM	Scanning electron microscopy
TGA	Thermogravimetric analysis
THC	Tetrahydrocurcumin
UV	Ultraviolet

CHAPTER 1

INTRODUCTION

1.1 Liposomes

Liposomes are spherical structures made up of one or more lipid bilayers with an aqueous interior. These are closed vesicles enclosing an internal aqueous space. The internal compartment is separated from the external medium by a bilayer membrane. The lipid bilayers are composed of discrete lipid molecules. The lipid component of liposomes, usually, consists of phospholipids and lipid-soluble compounds while the aqueous component consists of an aqueous solution with water-soluble compounds (Bangham and Horne, 1964; Laouini *et al.*, 2012). A typical unilamellar liposome is shown in figure 1.

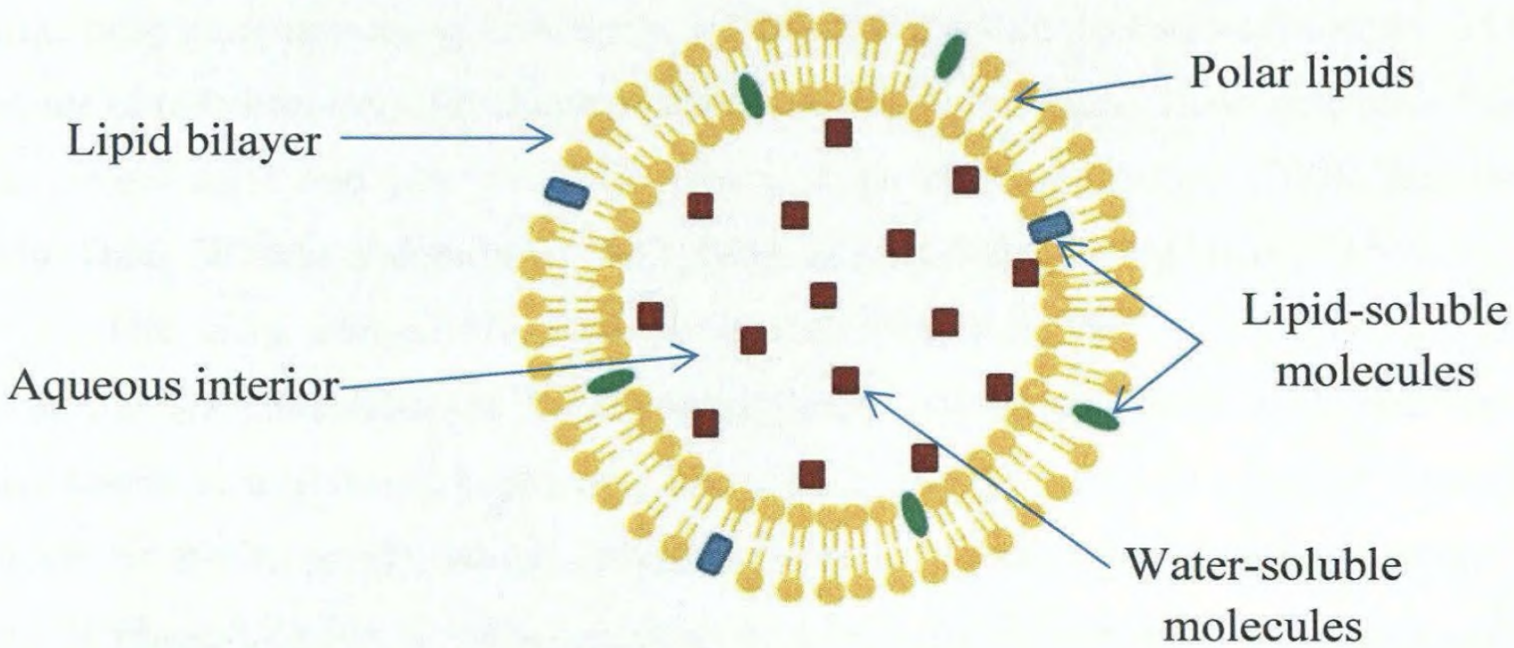

Figure 1. A typical unilamellar liposome

Numerous properties including stability, in vitro longevity, release kinetics, skin permeation and cellular uptake depend on the lipid composition of liposomes (Chen *et al.*, 2012; Fenske *et al.*, 2001; Kirby, Clarke and Gregoriadis, 1980; Maherani *et al.*, 2013). Thus, an account of the lipids used in the preparation of liposomes is given below.

1.2 Lipids

The lipidic component of liposomes consists mainly of a staple lipid that forms the structural backbone of the bilayer. In addition, numerous other minor lipid components are introduced to modulate the properties of liposomes. The types of lipids incorporated cover a wide range. In fact, the lipids incorporated can be natural or synthetic, saturated or unsaturated, ionic or non-ionic, and neutral or charged.

1.2.1 Membrane forming lipids

Lipids capable of forming lamellar structures when mixed with water include a wide variety of amphiphiles with diverse polar heads and non-polar portions. In an aqueous environment, these polar lipids form lipid bilayers so that only their hydrophilic heads are exposed to the aqueous environment while their hydrophobic tails are shielded from the aqueous solution. These lipid bilayers, then, curve to form vesicles with an aqueous interior. Vesicle forming compounds can be broadly divided into non-ionic surfactants and ionic amphiphiles. Non-ionic surfactants that form vesicles comprise sterols, and acyl or alkyl chains with single, double or triple long chains. The polar head groups of non-ionic surfactants comprise oxygen as hydroxyl or ether groups. Examples of ionic amphiphiles include cholesterol hemisuccinate, cholesterol sulfate, sodium oleate, dimethyl dioctadecyl ammonium salts and phospholipids (Berg, Tymoczko and Stryer, 2002; Brecher *et al.*, 1984; Dass, Walker and Burton, 2002; Ding, *et al.*, 2005; Watarai et.al., 1990).

The most commonly used lipids that constitute the major lipid component of liposomes are phospholipids. Glycerophospholipids have two fatty acids attached through ester bonds to a glycerol backbone. The third hydroxyl group of glycerol bears the polar portion of the molecule, which includes a moiety containing a phosphate group. Another type of phospholipids is sphingomyelin of which the backbone is sphingosine instead of glycerol (Berg *et al.*, 2002). The structures of some membrane forming lipids are depicted in figure 2.

1.2.1.1 Naturally occuring phospholipids

Phosphatidyl choline (PC)

PC, being the most readily available and the predominant lipid in natural cell membranes, usually constitutes the major component of the lipid bilayers of liposomes.

The head group of this phospholipid is phosphoryl choline. The permanent positive charge on choline and negative charge on phosphate counteracts giving a neutral yet very hydrophilic head group. Upon incorporation in a membrane, both the quarternary ammonium group of choline and phosphate group interact with adjacent molecules contributing to the tightness of packing and dispersing the local fluctuations of charge density (Berg *et al.*, 2002; Melzak *et al.*, 2012).

Phosphatidyl ethanolamine (PE)

The head group of PE is phosphoryl ethanolamine. It is neutral at neutral and low pH due to the protonation of the amine group which then counteracts the negative charge on phosphate. The hydrogen atoms attached to nitrogen interact with adjacent molecules in membranes through hydrogen bonding (Berg *et al.*, 2002; Sánchez *et al.*, 2011).

Phosphatidyl glycerol (PG)

The head group of PG consists of a glycerol moiety attached to a phosphate group via a phosphomonoester bond. In contrast to PC and PE, this molecule bears a permanent negative charge at physiological pH. The head group of PG, like those of PC and PE, forms hydrogen bonds with adjacent molecules (Berg *et al.*, 2002; Girod de Bentzmann *et al.*, 1993).

Cardiolipin (CL)

This molecule is very similar to PG, the only difference being that both ends of the head group glycerol are attached to phosphoglyceride moieties. Thus, CL comprises two negatively charged phosphates and four fatty acid chains (Berg *et al.*, 2002; Marom and Azem, 2013).

Phosphatidyl serine (PS)

A serine moiety is attached to a phosphate group which constitutes the head group of PS. Since the attachment of the serine moiety is through the hydroxyl group, the amino and carboxyl groups of serine remain free to function as zwitter ions. However, PS is negatively charged at physiological pH due to the negative charge on the phosphate group. It has been demonstrated that liposomes containing PS exhibit marked sensitivity to calcium ions in the medium and that those liposomes show stability upon freeze drying in

the presence of lyoprotectants (Berg *et al.*, 2002; Crowe, Spargo and Crowe, 1987; Martín-Molina, Rodríguez-Beas and Faraudo, 2012).

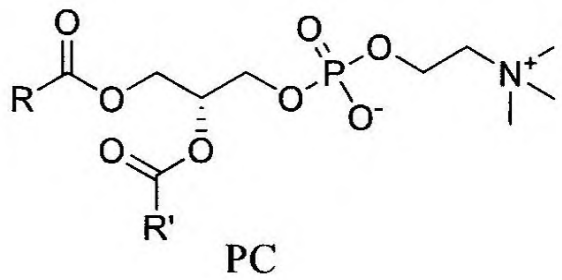

PC

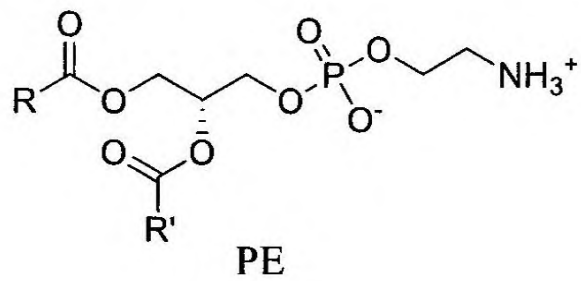

PE

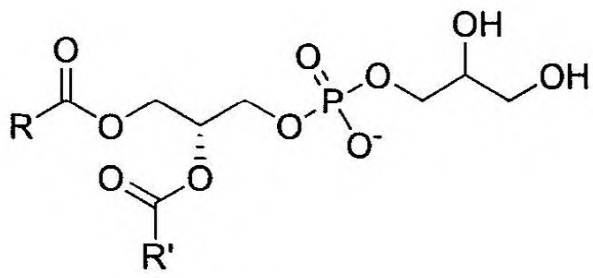

PG

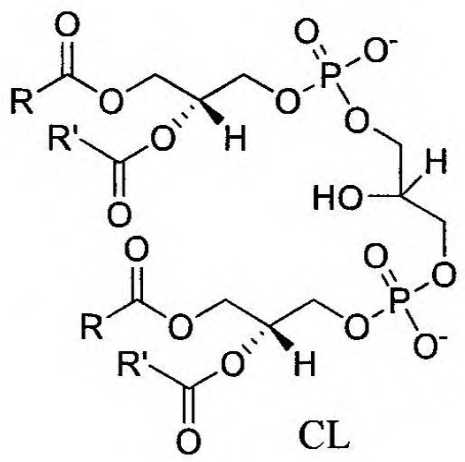

CL

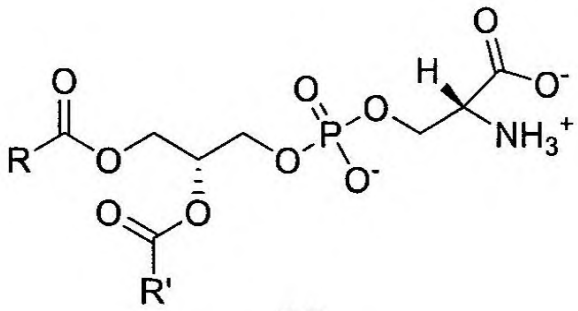

PS

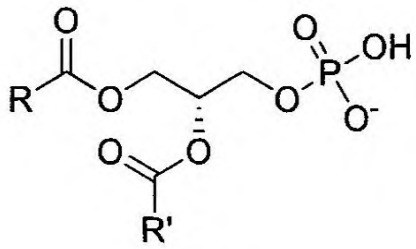

PA

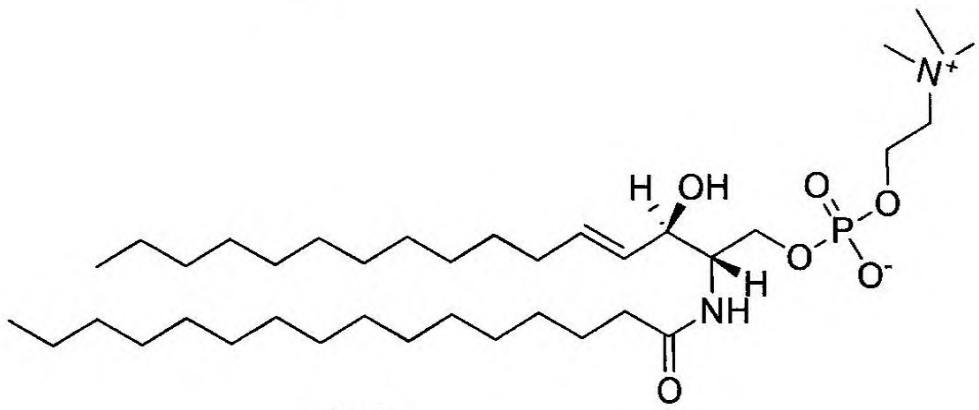

SM

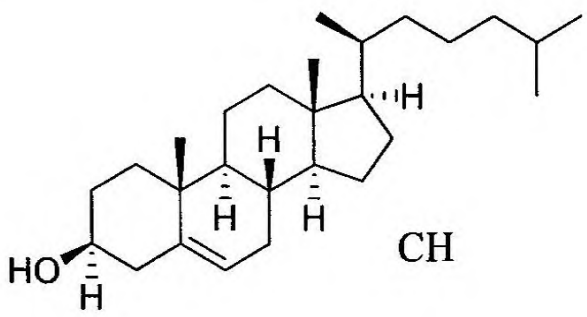

CH

Figure 2. Structures of membrane forming lipids (PC-phosphatidylcholine, PE-phosphatidylethanolamine, PG-phosphatidylglycerol, CL-cardiolipin, PS-phosphatidylserine, PA-phosphatidic acid, SM-sphingomyelin, CH-cholesterol)

Phosphatidic acid (PA)

PA is also a constituent of natural membranes. Like other phospholipids, PA contains two acyl chains attached to a glycerol backbone and the polar head is a phosphate group. Due to the negative charge on the phosphate moiety, this molecule bears a negative charge. Thus, PA is used in the preparation of negatively charged liposomes (Berg *et al.*, 2002; Kobayashi *et al.*, 2013).

Sphingomyelin (SM)

Like phosphoglycerolipids, SMs are found in the plasma membranes of animal cells. Although the percentage of SM in normal cells is low, these molecules constitute the major polar lipid in nerve tissue, specifically in myelin. The structures of SMs resemble those of phosphoglycerolipids. SM contains sphingosine and a fatty acid, collectively called a 'ceremide', as hydrophobic tails. Their polar head groups are either phosphocholine or phosphoethanolamine having no net charge. This polar lipid has been utilized to prepare liposomes in combination with other lipids, notably CH, that exhibit improved properties including pharmacokinetic and therapeutic properties (Berg *et al.*, 2002; Webb *et al.*, 1995).

Lyso-phospholipids

Lysophospholipids are derivatives of phospholipids in which either one or both fatty acids have been removed. Removal of fatty acids results through hydrolysis, and phospholipases catalyze this reaction *in vivo*. Examples of lysophospholipids include: lysophosphatidylcholine, lysophosphatidylethanolamine, lysophosphatidylinositol, lysophosphatidylserine, lysosphingomyelin and lysoglycosphingolipid. Like most lipids incorporated in liposomes, lysophospholipids alter the properties of liposomes when incorporated in the lipid bilayer of those vesicles. In fact, these derivatives of phospholipids facilitate lamellar to micellar transition, increase the phase transition temperature of the lipid bilayers, and affect release properties of liposomes (Davidsen, Mouritsen, and Jørgensen, 2002; Zuidam *et al.*, 1995).

Glycolipids

Glycolipids such as gangliosides and cerebrosides are incorporated in liposomes as minor constituents. These molecules have the same lipophilic portion as SM – ceremide – but the hydrophilic head group is a sugar moiety such as glucose, galactose or an

oligosaccharide. Incorporation of glycolipids in liposomes has shown to reduce liposomal interactions with proteins (Berg *et al.*, 2002; Ma *et al.*, 2012).

1.2.1.2 Synthetic phospholipids

In addition to natural phospholipids, synthetic phospholipids are used ubiquitously in the preparation of liposomes. In utilizing synthetic phospholipids, one can decide on the fatty acyl parts as well as the head group of the phospholipids. Also, the fatty acyl parts can be chosen to obtain optimum physical and chemical parameters such as phase transition temperature and stability, for liposomal formulations. Examples of some phospholipids frequently used in the preparation of liposomes include: dipalmitoylphosphatidylcholine (DPPC), dipalmitoylphosphatidic acid (DPPA) and dimyristoylphosphatidylcholine (DMPC) (Brecher *et al.*, 1984; Ding *et al.*, 2005; Watarai *et al.*, 1990).

1.2.1.3 Cholesterol (CH)

CH is a sterol and constitutes an essential component of biological membranes. In fact, this molecule is important for maintaining the fluidity and integrity of biological membranes. Accordingly, cholesterol is usually incorporated in the lipid bilayer of liposomes. As expected, this molecule affects many properties including fluidity, ordering of lipids and permeability of liposomal membranes (Melzak *et al.*, 2012; Senior and Gregoriadis, 1982).

1.2.1.4 Cationic lipids

Almost all cationic lipids are synthetic lipids. Examples of cationic lipids include stearylamine (SA), cetyl trimethyl ammonium bromide, dioleyl oxypropyl trimethyl ammonium chloride (DOTMA) and dioleyl trimethyl ammonium propane (DOTAP) (Dasgupta, Adhya and Basu, 2002; Fan *et al.*, 2015). Incorporation of these cationic lipids in liposomes results in cationic liposomes which repel each other, thus reducing the possibility of aggregation, flocculation and fusion (Laouini *et al.*, 2012). Furthermore, cationic liposomes can interact strongly with anionic drugs and other anionic encapsulated species, thus increasing the encapsulation efficiency of those liposomes. However, cationic liposomes interact strongly with anionic macromolecules such as proteins and nucleic acids (Zuris *et al.*, 2015). The structures of some cationic lipids are shown in figure 3.

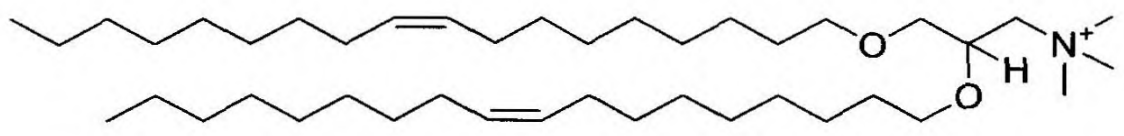

DOTMA

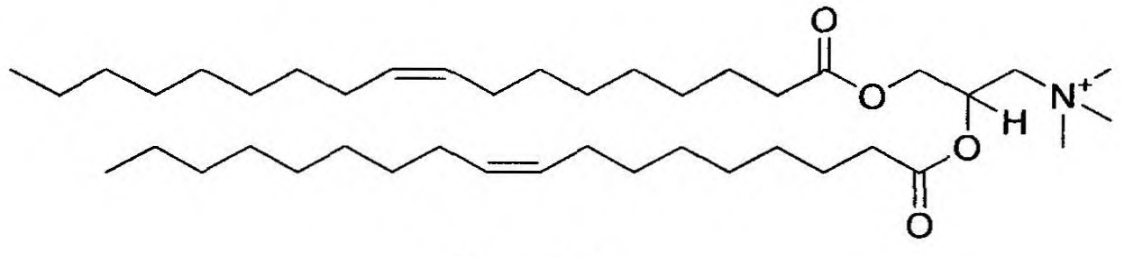

DOTAP

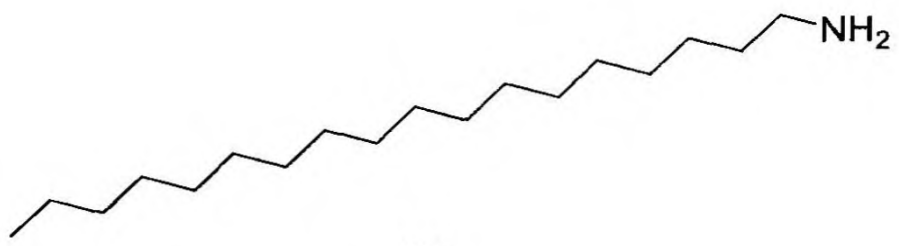

SA

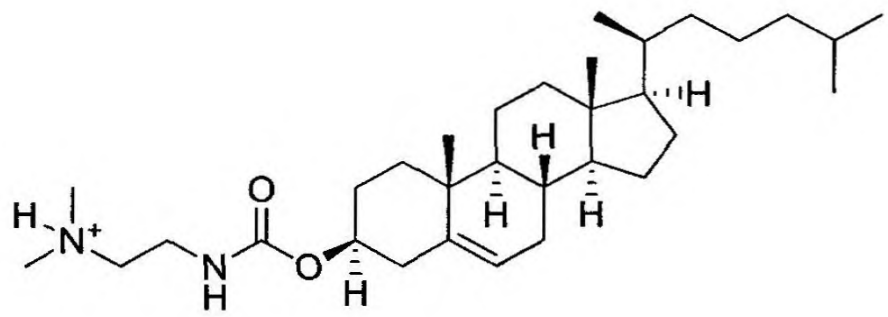

Cationic CH

Figure 3. Structures of cationic lipids (DOTMA-dioleyl oxypropyl trimethyl ammonium, DOTAP-dioleyltriethylammonium propane, SA-stearyl amine, Cationic CH – cationic cholesterol)

1.2.2 Other components incorporated in the lipid bilayers of liposomes

It is common practice to include other compounds, in addition to the main lipids used, to improve many different properties of liposomes. For instance, oleic acid and limonene are added to improve skin-penetration of bioactive agents/drugs (El Maghraby, Williams and Barry, 2004; Srisuk *et al.*, 2012). Furthermore, surfactants are incorporated in the lipid phase of liposomes to increase the flexibility of liposomes (El Maghraby, Williams, and Barry, 2000).

1.3 Aqueous component of liposomes

Liposomes are vesicles with an aqueous interior; and this aqueous interior consists of an aqueous solution with any water-soluble agent that these liposomes are designed to carry.

1.4 Categorization of liposomes

Liposomes may be categorized according to size, lamellarity, surface charge, and circulation in vivo. In addition, there are many specialized liposomes (Banerjee, 2001; Laouini *et al.*, 2012).

1.4.1 Size

According to the size (or diameter), liposomes can be categorized into: small liposomes, large liposomes, or giant liposomes. Small unilamellar vesicles have diameters in the range 20 – 100 nm. The diameters of large unilamellar vesicles are greater than 100 nm while those of giant unilamellar vesicles are greater than 1000 nm (Laouini *et al.*, 2012).

1.4.2 Lamellarity

According to the lamellarity of liposomes, these vesicles can be divided into three classes: unilamellar liposomes, multilamellar liposomes, and multivesicular liposomes. Figure 4 shows the cross sections of these different types of liposomes.

A unilamellar liposome consists of a single bilayer of polar lipids enclosing its aqueous cavity; a multilamellar liposome consists of multiple concentric bilayers of polar lipids with an aqueous interior; whereas a multivesicular liposome comprises many vesicles enclosed by a larger vesicle with a bilayer of polar lipids. As stated previously, the diameters of unilamellar liposomes are in the range 20 – 100 nm. Oligolamellar liposomes have diameters in the range 100 – 500 nm. The diameters of multilamellar liposomes are greater than 500 nm while those of multivesicular liposomes are greater than 1000 nm (Laouini *et al.*, 2012).

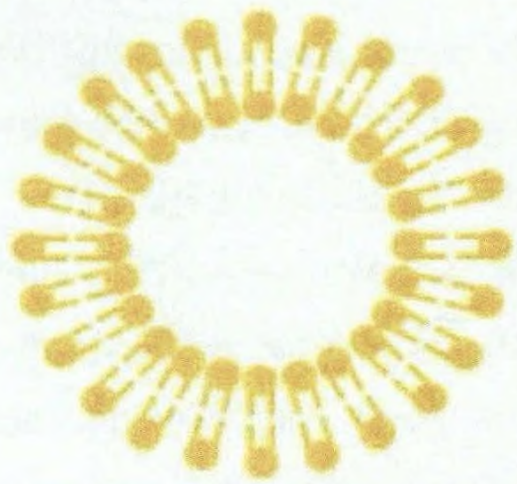

Unilamellar liposome

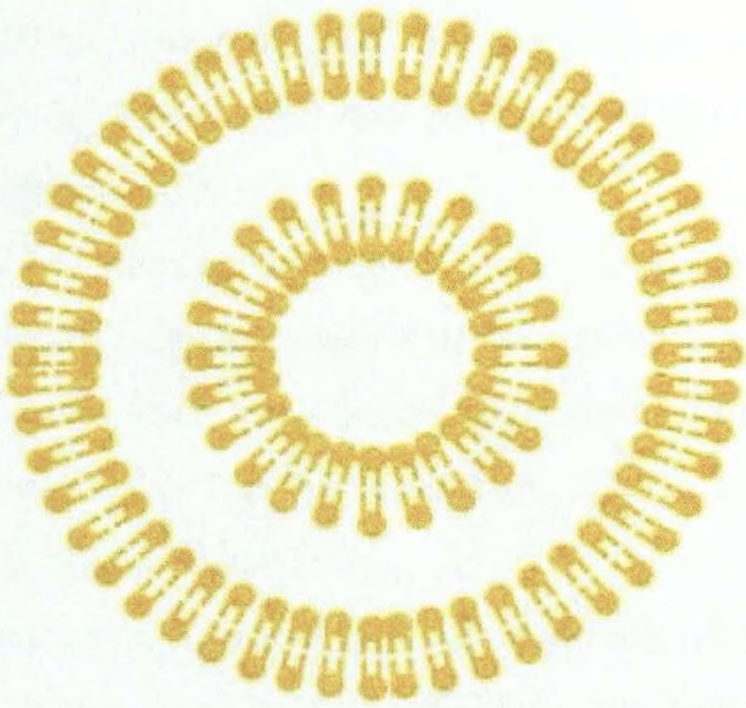

Multilamellar liposome

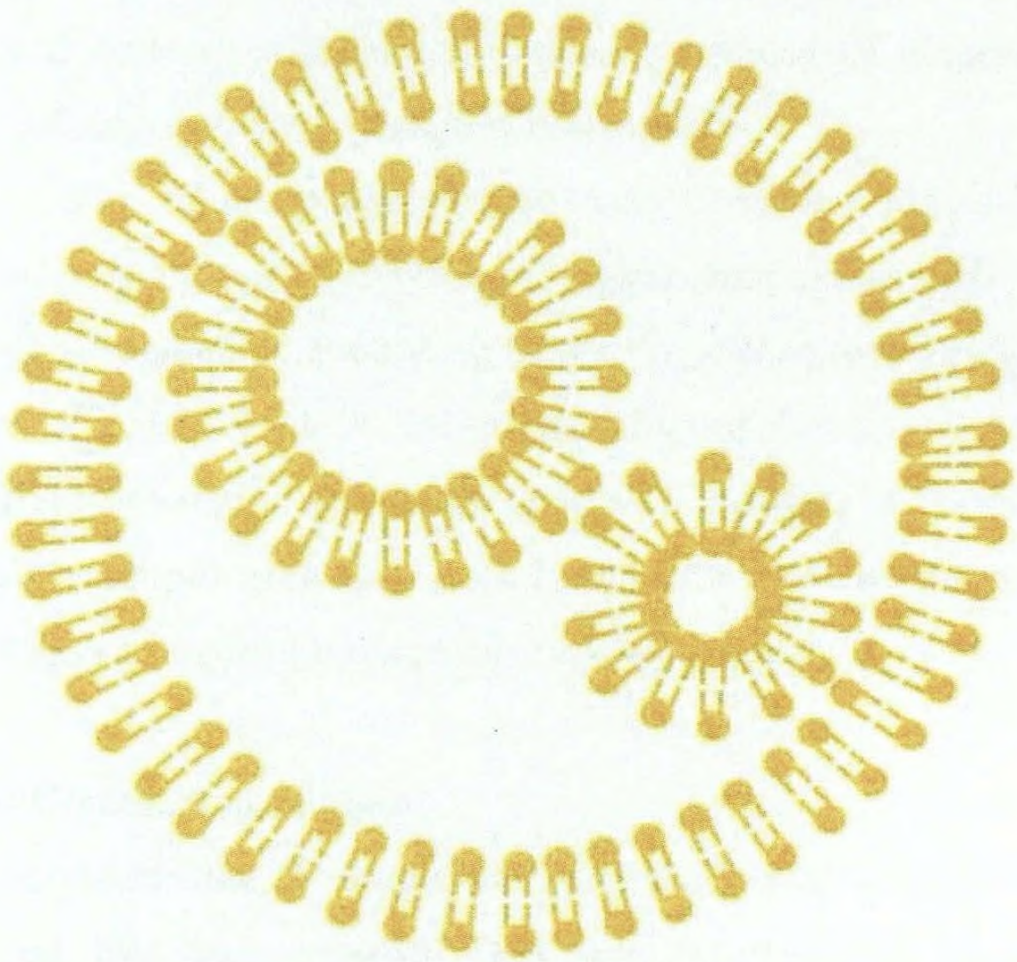

Multivesicular liposome

Figure 4. Cross sections of different types of liposomes according to the lamellar arrangement

1.4.3 Surface charge

According to the surface charge, liposomes can be divided into three main classes: neutral liposomes, negatively-charged (or anionic) liposomes, and positively-charged (or cationic) liposomes (Purohit, Sakthivel and Florence, 2001).

The lipidic phase of neutral liposomes is made up of neutral polar lipids such as PC, and/or PE. Also, other neutral lipids such as CH may be present in the lipid bilayers of liposomes. Since neutral liposomes have no surface charge, the zeta-potential of these vesicles approximate zero. Due to lack of repulsion among liposomes, these neutral liposomes tend to aggregate in solution forming bigger structures.

The lipidic phase of negatively-charged liposomes consists of negatively-charged lipids, or both negatively-charged lipids and neutral lipids. According to the degree of surface charge required, the proportion of anionic lipids used in liposome preparation is varied. Negatively-charged liposomes possess a negative zeta-potential. Since negatively-charged liposomes repel each other, a solution of negatively-charged liposomes is more stable than a solution of neutral liposomes.

The lipidic phase of positively-charged liposomes consists of positively-charged lipids, or both positively-charged lipids and neutral lipids. Like in the case of negatively-charged liposomes, according to the degree of surface charge required, the proportion of cationic lipids used in the preparation of liposomes is varied. As the name implies, positively-charged liposomes possess a positive zeta-potential. Since positively-charged liposomes repel each other, a solution of positively-charged liposomes is more stable than a solution of neutral liposomes (Laouini *et al.*, 2012).

1.4.4 Circulation *in vivo*

According to circulation properties of liposomes *in vivo*, liposomes can be broadly divided into two groups. They are conventional liposomes and sterically stabilized liposomes. The main difference between these two types of liposomes is that sterically stabilized liposomes have polymers attached to the liposomes surface whereas conventional liposomes have no such polymers attached (Immordino, Dosio and Cattel, 2006).

Sterically stabilized liposomes vs conventional liposomes

Conventional liposomes face several barriers upon intravenous administration because mechanisms to clear foreign bodies operate in the human body. When conventional liposomes are administered intravenously, certain serum proteins called 'opsonins' bind liposomes. The mononuclear phagocyte system recognizes those opsonin-bound liposomes and captures those vesicles via phagocytosis, thereby clearing the liposomes from the blood circulation (Immordino *et al.*, 2006; Patel, 1992). Furthermore, complement components initiate liposomal membrane lysis, thus releasing the encapsulants. Moreover, membrane lysis enhances the uptake of liposomes by the mononuclear phagocyte system (Devine *et al.*, 1994). In addition, liposomes interact with high density lipoproteins (HDL) and low density lipoproteins (LDL) in the blood, thus increasing the release of encapsulated drugs (Immordino *et al.*, 2006). Thus, several attempts have been made to circumvent the short comings of conventional liposomes; and sterically stabilized liposomes constitute one successful attempt.

Sterically stabilized liposomes comprise either glycolipids or hydrophilic polymers attached to the surface of liposomes, thereby forming a barrier between the liposomal surface and plasma proteins. Since opsonins are excluded from liposomal surfaces, uptake of liposomes by the mononuclear phagocyte system does not take place, thus increasing the longevity of liposomes in the blood. The most commonly used polymer in the preparation of sterically stabilized liposomes is polyethylene glycol commonly known as 'PEG'. Research on PEGylated and other types of sterically stabilized liposomes have shown promising results. In fact, several sterically stabilized liposomes are either approved or in clinical trials as drug formulations (Immordino *et al.*, 2006).

1.4.5 Specialized liposomes

In addition to the types of liposomes already described, numerous other specialized liposomes including targeted liposomes, pH-sensitive liposomes and thermo-sensitive liposomes are employed for special applications, mostly in medicine.

1.4.4.1 Targeted liposomes

Targeted liposomes are those utilized for active targeting of drugs. The surface of liposomes is modified by attaching a targeting ligand that recognizes and attaches to a receptor at the diseases site. The ligands used to modify the surface of targeted liposomes include: antibodies, peptides, aptamers or small molecules.

The type of targeted liposomes first reported was immunoliposomes in which antibodies were attached to the liposome surface (Heath, Fraley and Papahadjopoulos, 1980; Leserman *et al.*, 1980). Although other types of ligands are now preferred over antibodies due to ease of synthesis, higher purity, higher stability and nonimmunogenecity, antibodies are still commonly used in research as targeting ligands. For instance, Bhattacharyya and coworkers reported that cellular internalization of liposomes by pancreatic cells was enhanced upon presenting liposomes bearing anti-epidermal growth factor receptor antibody cetuximab (Bhattacharyya *et al.*, 2010). Moreover, the antibody derivative TfRscFv that exhibits high affinity to transferrin receptor is used as the targeting agent of immunoliposomes used in clinical trials intended to treat solid tumours (Kraft *et al.*, 2014).

1.4.5.2 pH-sensitive liposomes

Liposomes that unload their cargo upon changes in the pH of the surrounding medium are called 'pH-sensitive' liposomes. Mainly, three different strategies are utilized for making the vesicles pH-responsive. First, lipids that change their long range order upon exposure to a change in the pH may be utilized in the formation of liposomes. Second, either hydrolyzable pH-sensitive lipids or fusogenic peptides or proteins may be utilized to trigger drug release. Third, pH-sensitive polymers that destabilize the membrane or facilitate fusion with endosomes when faced with a pH change may be anchored in the lipid membrane (Felber, Hufresne, and Leroux, 2012).

pH-responsive liposomes have been evaluated for the encapsulation of numerous drugs, therapeutic agents and antigens for their delivery to many different tissues and organs. For instance, Wang and Huang demonstrated that pH-sensitive immunoliposomes may be utilized to deliver DNA (Wang and Huang, 1989). Also, it has been showed that pH-sensitive liposomes may be utilized for the intracellular delivery of the anticancer drug – doxorubicin (Obata, Tajima and Takeoka, 2010)

1.4.5.3 Thermo-sensitive liposomes

Thermo-sensitive liposomes have been developed for heat triggered drug release especially in the treatment of tumours (Weinstein *et al.*, 1979; Yatvin *et al.*, 1978). Lipids that have phase transition temperatures higher than the physiological temperature (i.e. 37 °C) are used in the development of thermosensitive liposomes. In fact, phase transition is desired in the range 39 °C – 42 °C since the tumours do not experience temperatures

higher than 42 °C during treatments (Hildebrandt *et al*, 2002; Zhang *et al*., 2011). Thermo-sensitive liposomes encapsulating numerous drugs have been investigated as antitumour therapeutic agents. Examples include vinorelbine bitartrate encapsulated thermo-sensitive liposomes that showed enhanced efficacy against lung tumour and doxorubicin encapsulated thermo-sensitive liposomes that showed enhanced efficacy against C6-glioma (Gong *et al*., 2001; Zhang *et al*., 2011).

1.5 Liposome analogues

In addition to liposomes, liposome analogues such as deformable liposomes, ethosomes and niosomes play pivotal roles in drug or bioactive agent delivery. In fact, these vesicles are investigated and utilized heavily in pharmaceutical and cosmetic industries.

1.5.1 Deformable liposomes

Deformable liposomes or transferosomes are elastic liposomes consisting of edge activators in addition to phospholipids. Edge activators destabilize the lipid bilayers, thus giving deformability to the liposome. The commonly utilized edge activators in the preparation of deformable liposomes include: Tween 20, Tween 60, Tween 80, Span 60, Span 65, Span 80, sodium cholate, sodium deoxycholate and dipotassium glycyrrhizinate (Elsayed *et al*., 2007). Actually, it has been demonstrated that the physical properties of deformable liposomes depend on the edge activator (Lee *et al*., 2005).

Although the importance of conventional liposomes in transdermal drug delivery remains controversial, deformable liposomes have shown increased skin penetration in numerous instances. For example, Liu et al. reported that the antioxidant quercetin loaded deformable liposomes showed enhanced skin penetration and conferred protection against UV B radiation (Liu *et al*., 2013). Also, deformable liposomes have shown increased skin delivery of hormones such as oestradiol and ethinylestradiol (El Maghraby, Williams and Barry, 1999; Garg *et al*., 2006). Moreover, deformable liposomes have been utilized for successful skin delivery of proteins such as insulin and human serum albumin (Guo, Ping and Zhang, 2000; Paul, Cevc and Bachhawat, 1995). Not only small molecules and proteins, but also nucleic acids may be delivered using deformable liposomes. For instance, Lee and coauthors demonstrated that sodium cholate based and sodium deoxycholate based deformable liposomes may be utilized for transdermal gene delivery (Lee *et al*, 2005).

1.5.2 Ethosomes

Ethosomes are a type of liposome analogs consisting of a high content of ethanol (20 – 45 %) in addition to phospholipids and water. Development of these vesicles was first reported by Touituo and coworkers in late 90s (Touitou *et al.*, 2000). Numerous effects of ethanol on lipid vesicles have been reported. For example, ethanol confers a negative charge to vesicles and causes the size of those vesicles to decrease. Furthermore, ethanol increases encapsulation of many drugs due to, partly, the higher solubility of those drugs in ethanol.

Ethosomes are utilized primarily for dermal and transdermal drug delivery. Touitou and coauthors suggested that ethanol – a known skin permeation enhancer – functions synergistically with vesicles and skin lipids in enhancing skin delivery of encapsulated species of ethosomes (Touitou *et al.*, 2000). Examples of ethosomal drugs that have shown enhanced skin delivery according to *in vivo* studies include hormones such as testosterone (Ainbinder and Touitou, 2005), antibiotics such as erythromycin (Godin and Touitou, 2005) and anti-inflammatory agents such as ammonium glycyrrhizinate (Paolino *et al.*, 2005).

1.5.3 Niosomes

Niosomes are liposome-like vesicles made up of mainly non-ionic surfactants instead of phospholipids (Uchegbu and Florence, 1995). Niosomes, in certain instances, preferred over conventional liposomes because the staple ingredient – non-ionic surfactants – is less costly than phospholipids and because non-ionic surfactants can be more easily derivatized than phospholipids. The areas that show interest in applications of niosomes include pharmaceutics, cosmetics and food industry (Marianecci *et al.*, 2014).

Niosomes have been evaluated for drug delivery and targeting via different routes of drug administration including: dermal and transdermal, ocular, oral, pulmonary, and parenteral (Marianecci *et al.*, 2014). In addition to drug delivery, these vesicles have been utilized for gene therapy. For instance, Zhou and coworkers utilized niosomes successfully to deliver small interfering RNA to a breast cancer cell line for gene silencing (Zhou *et al.*, 2012) Apart from the delivery of drugs or other therapeutic agents, niosomes show promise in applications in diagnostics. For example, paramagnetic agents that can be detected by nuclear magnetic resonance imaging have been delivered to tumor cells using niosomes (Luciani *et al.*, 2004).

1.6 Preparation of liposomes

The structure and physical properties of liposomes can be modulated by preparation methods. Those methods of preparation of liposomes fall under three main categories: mechanical dispersion method, solvent dispersion method, and detergent removal method. In mechanical dispersion methods, such as in sonication method and in extrusion method, lipids are dispersed mechanically in the aqueous media. In contrast, solvent dispersion methods, such as ether injection method and ethanol injection method, do not employ any mechanical means but those methods do employ organic solvents to disperse lipids in aqueous media. As the name implies, in detergent removal methods, such as dialysis and gel-permeation chromatograpy, detergents are used to introduce lipids to the aqueous media, and subsequently, detergents are removed to form liposomes in the aqueous system. Examples of different types of methods of preparation of liposomes are given below (Dua, Rana and Bhandari, 2012).

Mechanical dispersion method

- Sonication
- Extrusion through French pressure cell
- Freezing and thawing
- Thin-film hydration
- Micro-emulsification
- Membrane extrusion

Solvent dispersion method

- Ether injection
- Ethanol injection
- Reverse phase evaporation method

Detergent removal method

- Dialysis
- Detergent removal by adsorption
- Gel-permeation chromatography

1.7 Loading of drugs

Loading of substances, such as drugs, to liposomes could be conducted either passively or actively. 'Passive loading' is when drugs are encapsulated in liposomes during liposome preparation while 'active loading' is when drugs are encapsulated in liposomes after liposome preparation. Usually, hydrophobic substances are loaded passively into liposomes are encapsulation efficiencies approximating 100 % have been obtained. However, passive loading of hydrophilic substances give relatively low encapsulation efficiencies. Active loading is possible only with certain types of substances such as weak bases or weak acids. For instance, compounds with protonizable amine groups could be loaded actively by employing a pH-gradient whereas weak acids could be loaded actively by employing a calcium acetate gradient (Dua *et al.*, 2012).

1.8 Applications of liposomes

Applications of liposomes are plenteous mainly due to their colloidal size, structure, composition, various modes of action and other properties that can be tailored easily by careful utilization of suitable materials and methods. In fact, applications of liposomes include those in basic sciences, medicine, bioengineering and numerous industries such as pharmaceutical industry, cosmetic industry, agro-food industry and textile industry.

1.8.1 Basic sciences

Basic sciences to which research on liposomes has contributed a significant amount of knowledge include mathematics, physics, biophysics, physical chemistry, chemistry, biochemistry and biology. In mathematics, liposomes are used in topological studies of two-dimensional surfaces (Campelo and Hernàndez-Machado, 2006; Nomura *et al.*, 2001). In physics, liposomes are used to study aggregation behaviour and fractals (Sabín *et al.*, 2007). Also, soft and high strength materials are incorporated in liposomes in order to evaluate the role of those materials in membranes. In biophysics, liposomes are used to study the permeability of membranes and phase-transitions in two-dimensions by incorporating various lipids (Liu *et al.*, 2015). Also, liposomes are utilized in photophysics (Coelho, Rodembusch and Campo, 2014). In physical chemistry, liposomes are used to study the behaviour of colloidal particles in systems with various characteristics (Toimil *et al.*, 2012). Also, since liposomes exhibit aggregation, these vesicles are used in studies of inter- and intra- aggregate forces (Sabín *et al.*, 2007). These physico-chemical studies

increase our understanding of the evolution of life. In chemistry, liposomes are used to study photochemistry, and to conduct artificial photosynthesis in an attempt to duplicate photosynthesis (Gust, Moore and Moore, 1998). Also, liposomes are utilized for microcompartmentalization of chemical reactions, which is useful in catalysis, in investigating biomineralisation, and in synthesizing particles of colloidal dimensions (Oberholzer *et al.*, 1999). In biochemistry, liposomes are used for studies involving membrane proteins. Membrane proteins such as ion pumps and transport proteins are vital for the proper functioning of cells. Thus, knowledge of structure and function of membrane proteins provides new insight into our understanding of cellular functions. Therefore, membrane proteins are reconstituted in to the liposomal bilayer, which is a simpler artificial membrane, and studied (Tsai *et al.*, 2013). In biology, liposomes are used as model biological membranes and vesicles. Cell communication heavily depends on substances secreted in vesicles. For instance, neurotransmitters secreted in synaptic vesicles are responsible for transmitting nerve impulses. Furthermore, exo- and endo-cytosis are processes responsible for the secretion and ingestion of substances from and into cells, respectively. Moreover, Golgi apparatus secrete and ingest biomolecules via vesicles. Thus, liposomes are ideal systems to study cell function, fission and fusion (Berg *et al.*, 2002; Boucrot *et al.*, 2012).

1.8.2 Pharmaceutical industry

Pharmaceutical industry is a major industry where liposomes have a plethora of applications. Advantages of utilizing liposomes in the pharmaceutical industry, which leads to medical applications, are many fold; and include biological reasons, manufacturing reasons and physico-chemical reasons. Biological reasons are biocompatibility, biodegradability, relatively low toxicity and immunogenicity. Manufacturing reasons include ease of preparation, ease of tailoring of properties, and relatively accessible raw materials. The main physico-chemical reason is that liposomes are not in thermodynamic equilibrium but are kinetically trapped systems. Thus, unlike systems such as micelles and microemulsions, liposomes are relatively unaffected by changes in the surrounding. For instance, although micelles and microemulsions disintegrate or aggregate, liposomes conserve their structure, upon dilution. Also, the lipid bilayer presents a platform for the attachment of ligands and other molecules that affect interaction properties of liposomes.

Liposomes have been successfully used in pharmaceutical industry. Scaling up, stability and sterility issues have been solved for most cases. Large quantities of liposomes stable for relatively long periods of time can be prepared (Lasic, 1998). Sterility is achieved either by filtration through 0.2 μm filters or by using aseptic conditions (Sorgi and Huang, 1996).

Each liposome-drug system has to be carefully optimized. Further, the stability of the drug in different buffer systems and different conditions employed in formulation and storage conditions has to be evaluated. Moreover, special attention must be paid to improve the stability of liposomes when developing liposomal pharmaceutical products. In general, colloidal stability is improved by incorporating either charged lipids or lipids bearing polymers (Koutsoulas *et al.*, 2012; Quer *et al.*, 2012). Chemical stability is improved by the correct choice of lipids, addition of antioxidants or metal chelators, or optimizing the pH (Frenzel and Steffen-Heins, 2015; Peng *et al.*, 2010; See *et al.*, 2014). Biological instability can be overcome by coating the lipid membrane with polymers such as polyethylene glycol or incorporating glycolipids in the membrane (Tao, Faig and Uhrich, 2014).

Liposomes are used in the pharmaceutical industry for solubilization of poorly soluble drugs such as Amphotericin B and minoxidil that are used to treat fungal infections (Adler-moore and Proffitt, 1993; Jain *et al.*, 2010). Furthermore, liposomes are used as a means of site-avoidance of certain drugs that are toxic to certain organs. For example, liposomal Amphotericin B shows decreased nephrotoxicity while doxorubicin, which is used to treat cancer, exhibits reduced cardiotoxicity (Adler-moore and Proffitt, 1993; Scomparin *et al.*, 2015). Also, liposomes facilitate sustained or controlled release of numerous drugs. For instance, drugs used in biotherapeutics such as corticosteroids and hormones, and systemic antineoplastic drugs used to treat cancer show sustained-release and controlled-release properties, respectively, upon encapsulation in liposomes (Iwanaga *et al.*, 1997; Li *et al.*, 2013). Another purpose of using liposomes is for drug protection. Examples include insulin that is used to treat diabetes and interleukins that are used to treat cancer (Anderson *et al.*, 1994; Niu *et al.*, 2011). In addition, liposomes are utilized for RES targeting. Examples of RES targeted species via liposomes include antimalarials, vaccines, drugs used to treat macrophage located diseases and immunomodulators (Agrawal and Gupta, 2000; Ikehara *et al.*, 2008; Tsujimura *et al.*, 2009). Moreover, specific targeting is an important utility of liposomes. Specific targeting of liposomal drugs is carried out by attaching ligands, which are specific for receptors on the surface of targeted cells, on the

liposomal membrane. By this method, specific targeting of numerous therapeutic agents has been conducted (Lozano *et al.*, 2015). Another utility of liposomes is extravasation. Since tumours, inflammations and infections are associated with leaky vasculature, those diseases can be treated through extravasation of liposomal drugs (Lammers *et al.*, 2012). Accumulation of drugs in certain tissues or organs can, also, be achieved through liposomes (Al-Jamal, Al-Ahmady and Kostarelos, 2012). Further, liposomes are used for enhanced skin penetration of drugs and bioactive agents. In fact, liposomes are used as topical vehicles in dermatology (Alomrani *et al.*, 2014). Besides the utilities of liposomes stated above, those vesicles may be used as a drug depot. For instance, liposomes have exhibited promising results as drug depots in the treatment of ocular, sub-cutaneous, intra-muscular and lung diseases (Henriksen-Lacey *et al.*, 2010; Mosgoeller, Prassl and Zimmer, 2012; Yu *et al.*, 2015).

1.8.3 Medicine

Medicine is another area where liposomes play a pivotal role. In medicine, liposomes are used and have potential applications mainly in drug delivery, stimulation of immune response and vaccination, gene-therapy and medical diagnostics.

Despite the enormous number of research carried out worldwide on various aspects of the development of liposomal drug products, only about 11 liposome based drug products have been approved for human use by the US Food and Drug Administration (see Table 1). However, approximately 600 studies on liposomal drugs intended for human use are in clinical trials in US (Kraft *et al.*, 2014).

Table 1. Liposomal drugs used in medicine

Drug	Trade Name (Company)	Size (Diameter)	Disease treated
Anticancer			
Doxorubicin	Doxil / Caelyx (Janssen)	100 nm	Ovarian cancer Breast cancer Kaposi's sarcoma Multiple myeloma (in combination with bortezomib)
	Myocet (Cephalon)	80 – 90 nm	Breast cancer (in combination with cyclophosphamide)
Daunorubicin	DaunoXome (Galen)	45 – 80 nm	Kaposi's sarcoma
Cytarabine	DepoCyt (Pacira)	20 μm	Malignant Lymphomatous meningitis
Vincristine	Marqibo (Talon)	100 nm	Acute lymphoblastic leukemia
Antifungal			
Amphotericin B	AmBisome (Astellas)	< 100 nm	Antifungal Leishmaniasis
Vaccine			
Hepatitis A antigen	Epaxal (Crucell)	150 nm	Hepatitis A
Influenza antigen	Inflexal V (Crucell)	150 nm	Influenza
Analgesics			
Morphine	DepoDur (Pacira)	17 – 23 μm	Postsurgical pain
Bupivacaine	Exparel (Pacira)	24 – 31 μm	Analgesia
Other			
Verteporfin	Visudyne (QLT)	-	Age-related macular degeneration

1.8.3.1 Drug delivery

Liposomes are used mostly for drug delivery in medicine. Almost all routes of drug administration, including intravenous, intramuscular, subcutaneous, oral and topical, have been explored for liposomal drug delivery. Intravenous liposomal drug administration can be utilized to treat diseases affecting phagocytic cells. Furthermore, long-circulating liposomes have been used for intravenous drug administration. Upon intramuscular or subcutaneous liposomal drug administration, liposomes function as drug depots, in most cases. Oral route of liposomal drug delivery is advantageous due to potential higher patient compliance and ease of use. Other advantages of utilizing liposomes for oral drug delivery include increasing bioavailability of poorly water-soluble drugs, increasing intestinal membrane permeability, reducing gastrointestinal side effects and eliminating the bitter taste of oral drugs (Fricker *et al.*, 2010; Peltier *et al.*, 2006; Yang *et al.*, 2004) . Topical route of liposomal drug delivery is also very advantageous because of high patient compliance, ease of administration, etc. (Morrow *et al.*, 2007). Examples for liposomal topical drugs include corticosteroid and betamethasone dipropionate used to treat atopic eczma (Korting *et al.*, 1990; Mezei and Gulasekharam, 1980).

Liposomes, in numerous instances, have been used for passive targeting of drugs into tissues and cells. Passive targeting is essentially the utilization of the knowledge of the physiochemical properties and of the spatial and temporal distribution, including elimination, of the drug delivery vehicle to tune the pharmacokinetics of the drug in order to target the drug into a specific tissue or cell type. In some cases, the rapid intake of liposomes by phagocytic cells is exploited; while in other cases, long circulation of sterically stabilized liposomes in blood is exploited for passive targeting. Almost all FDA approved liposome based drugs are passively targeted medicines (Kraft *et al.*, 2014).

An example of a passively targeted drug is liposomal doxorubicin which is an anticancer drug. In this case, long circulation times of the delivery vehicle carrying the drug in the blood is desired to allow the liposomes to leak out of the leaky vasculature associated with tumours and to allow those vesicles to accumulate in the interstitial spaces of tumours. Thus, sterically-stabilized long circulating liposomes are used for passive targeting of doxorubicin. For instance, Doxil, which is PEGylated liposomes incorporating doxorubicin, have shown to increase the doxorubicin concentration in Kaposi's lesions of AIDS patients 10 -20 times that in normal skin (Northfelt *et al.*, 1995). DaunoXome, which is liposomal daunorubicin, also, is a long circulating liposomal medicine that is used for passive targeting. In fact, Forssen and coworkers demonstrated that tumour uptake of the

drug increased 10-fold in a murine lymphosarcoma model when liposomal daunorubicin was used as opposed to when free drug was used (Forssen, Coulter and Proffitt, 1992). Since off-target accumulation of drugs is significantly reduced upon passive targeting, the therapeutic index of those drugs may increase.

Active targeting utilizes specific receptors on the cells of target (malignant) tissues for homing of delivery vehicles loaded with drugs. Ligands that bind to those receptors are attached on the surface of liposomes. Upon administration of liposomes with targeting ligands, these delivery vehicles bind to targeted cells upon contact, thereby increasing the local drug concentration rapidly. Although active targeting should be ideal, in theory, for situations that demand rapid drug action, there are no FDA approved actively targeted liposomal drugs currently in the market (Kraft *et al.*, 2014). However, this is an area with great potential and, thus, of active research.

Numerous target receptors that can be used for active targeting have been identified through improved understanding of biology of diseases. For instance target receptors for several types of cancer, including breast cancer, ovarian cancer, lymphoma, lung cancer, murine tumor and prostate cancer, have been identified (Endsley and Ho, 2012; The Cancer Genome Atlas Network, 2012a; The Cancer Genome Atlas Network, 2012b; The Cancer Genome Atlas Research Network, 2012; The cancer Genome Atlas Research Network, 2013a; The cancer Genome Atlas Research Network, 2013b). Although there are no marketed products, there are a few ligand-conjugated liposomal drugs in clinical trials. The encapsulated species in those targeted liposomes include: oxaliplatin to treat gastroesophageal adenocarcinoma, pDNA with p53 gene to treat solid tumours, and doxorubicin to treat brain and breast cancer (Kraft *et al.*, 2014).

Multifunctional liposomes that exhibit multiple functions, also, have gained interest in liposome research, recently. For example, multivalent liposomes that recognize more than one type of receptors are in clinical trials (Kraft *et al.*, 2014). Also, multifunctional liposomes targeting cancer cells have been developed. In these liposomes, PEG coating ensures long-circulation while a hidden targeting moiety that is exposed only upon the release of PEG chains at the target site reduces off-target binding (Sawant *et al.*, 2006). Moreover, multiple drugs can be encapsulated in liposomes in treating diseases (Gomes-da-Silva *et al.*, 2012).

1.8.3.2 Stimulation of immune response and vaccination

The first step in the stimulation of an immune response is the interaction between an antigen and an antigen presenting cell (APC), that results in partial degradation of the antigen to small polypeptides. Those polypeptides then interact with either class I or class II major histocompatibility complex (MHC) molecules that bring the polypeptides to the surface of APCs. Polypeptide-MHC complex then interacts with either $CD8^+$ or $CD4^+$ T lymphocytes. Endogenous proteins of cells are presented by class I MHC molecules and thus they interact with cytotoxic or $CD8^+$ T cells; whereas exogenous proteins are presented by class II MHC molecules and thus they interact with helper or $CD4^+$ T cells. Cytotoxic T cells are the type of T cells that are directly involved in destroying tumor and virus-infected cells, and hence, priming of cytotoxic T cells has been the major challenge in stimulation of immune responses.

Intravenous injection of liposomes results in the uptake of those vesicles by splenic macrophages and liver Kupffer cells. Also, liposomal antigens have the ability to induce cytotoxic T lymphocyte responses through macrophages and dendritic cells, thereby allowing destroying of tumor and virus-infected cells (Kojima *et al.*, 2013).

1.8.3.3 Gene therapy

Cationic liposomes have been utilized to deliver pDNA that is used in gene therapeutics to the cytoplasm (Hong, 1997). However, mRNA is preferred over pDNA in gene therapy because mRNA need not enter the nucleus (Van Driessche *et al.*, 2005). In fact, liposomes have, also, been used to deliver mRNA to tumour sites (Wang *et al.*, 2013).

1.8.3.4 Medical diagnostics

In addition to the medical applications of liposomes described above, these vesicles have been utilized for medical diagnostics. Since liposomes are rapidly taken up by phagocytic cells of RES, aqueous contrast-enhancing agents encapsulated in liposomes can be targeted to the liver and spleen where liposomes accumulate. As a result, cancerous tissues can be distinguished from normal tissues using computed tomography (Selter, 1988a; Seltzer *et al.*, 1988b).

Gas filled liposomes have also been used for medical diagnostics. Since gas filled liposomes exhibit magnetic susceptibility and reflect sound well, such liposomes are utilized for magnetic resonance imaging and ultrasound imaging. For instance, Adzamli

and coworkers used gas filled liposomes for echocardiography and Simon et al used similar type of vesicles for neurosonography (Adzamli *et al.*, 1990; Simon *et al.*, 1990).

1.8.4 Bioengineering

Bioengineering is also an important field where liposomes have interesting applications. In genetic engineering and gene recombinant technology, DNA fragments containing genes of specific proteins are delivered to various cells including microorganisms. The delivered DNA fragment gets incorporated into the genetic material of that cell thereby expressing the protein or polypeptide coded by the incorporated DNA fragment (Lee *et al.*, 2014).

Transferring nucleic acids across cell membranes is challenging because of the large size, high charge and hydrophilicity of nucleic acids. However, liposomes circumvent this challenge by functioning as transfection vectors. Liposomes deliver genetic material to cells via three mechanisms. The first mechanism involves encapsulation of DNA in liposomes which act as endocytosis enhancers (Keswani, Lazebnik and Pack, 2015). The second mechanism is simulation of phosphate or diethylaminoethyl (DEAE)-dextran precipitation by liposomes (Liptay *et al.*, 1998). The third mechanism is to utilize fusogenic liposomes that cause fusion upon adsorption on the cell surface (Khatri *et al.*, 2014).

Since nucleic acids are negatively charged, positively charged liposomes are usually used in transfection to neutralize the charge. Furthermore, utilization of positively charged liposomes increases the encapsulation efficiency of nucleic acids into these vesicles. Moreover, positive charge on liposomes enables complex formation with genetic material and these complexes upon adsorption of the cell surface stimulate endocytosis or fusion. The positively-charged liposomes used in transfection are prepared by incorporating positively-charged polar lipids in the lipid bilayer (Barichello *et al.*, 2012). It has been demonstrated that positively-charged CH is superior to other types of positively-charged lipids in terms of reduced toxicity and better transfection efficiency (Gao and Huang, 1991).

1.8.5 Cosmetic industry

In addition to the already stressed properties of liposomes, these vesicles improve skin delivery of encapsulated substances (Karunaratne *et al.*, 2014). Also, liposomes contribute to hydrate the skin and to replenish lipids of the skin (Duman *et al.*, 2014; Egbaria and Weiner, 1990; Morrow *et al.*, 2007). Thus, liposomes are extensively used in the cosmetic industry. The encapsulated species of cosmetic liposomal formulations include susceptible compounds such as antioxidants, plant extracts, moisturizers, antibiotics, and recombinant proteins (Chanchal and Swarnlata, 2008; Kulkarni, Yadav, and Vaidya, 2011). Cosmetic products containing liposomes are of various types including skin creams, moisturizers, hair conditioners, sunscreens, aftershaves, lipstick, make-up and perfumes (Laouini *et al.*, 2012).

Although conventional liposomes made of natural lipids serve as excellent carriers of encapsulated substances in cosmetic industry, liposome analogues such as deformable liposomes, ethosomes and niosomes have shown better skin penetration properties. Furthermore, niosomes made of non-ionic surfactants instead of natural lipids are more stable than conventional liposomes. In addition, non-ionic surfactants used to prepare niosomes are much cheaper than natural lipids. Moreover, those vesicles can be prepared easily in large quantities. Thus, liposome analogues constitute the large portion of the cosmetic products (Morrow *et al.*, 2007; Patravale and Mandawgade, 2008).

1.8.6 Agro-food industry

Agro-food industry is an area that liposomes can be extensively used primarily because liposomes facilitate solubilization of poorly soluble substances, confer protection to susceptible compounds, and release encapsulated substances in a sustained manner.

Liposomes are made of natural lipids that are extracted from food sources. In fact, the primary sources of phospholipids of liposomes are egg yolk and soy bean. Furthermore, lipids are used in food industry to stabilize water-in-oil and oil-in-water emulsions including creams. Since liposomes are made of edible lipids, these vesicles have become attractive systems to incorporate encapsulated substances in food products.

Fermentation is a process in which liposomes are used, primarily, as sustained release systems. The encapsulated enzymes are released in a sustained manner and thus those enzymes are protected from harsh conditions of the medium in different stages of fermentation. These factors lead to shorter fermentation times and improved quality of the product. One example of utilizing liposomes in fermentation is during making cheese.

Using liposomal enzymes can reduce the cheese ripening time, providing the industry with a huge economic benefit (Fresta, Wehrli and Puglisi, 1995). Also, due to even spatial distribution of the enzymes, the cheese texture becomes better. Moreover, inconsistent flavours and bitterness, which arise due to undesirable proteolysis of enzymes at early stages of fermentation, reduces when liposomal enzymes are used (Kheadr, Vuillemard and El Deeb, 2000).

Liposomes are also used as carriers of preservatives in food industry. For instance, liposomal lysozymes are being used to destroy spoilage organisms in cheese and curd. When lysozymes are used as a preservative, these enzymes attach to casein in milk and hence get inactivated quickly. However, upon incorporation of lysozymes encapsulated in liposomes, lysozymes reside longer in the aqueous domains because liposomes localize in the aqueous spaces of those products. Thus, lysozymes remain active for a longer period of time. Also, to use natural preservatives as opposed to artificial ones is becoming popular due to health reasons. Liposomes play an important role as carriers of those natural preservatives such as vitamin C and vitamin E (Mozafari *et al.*, 2008).

Biocides such as fungicides, herbicides and pesticides have also been encapsulated in liposomes to be utilized in the agro-food industry. Liposomal biocides are less deleterious to other life forms because liposomes decrease unintended exposure of life forms to encapsulated biocides (Milne and Shelby Jr., 1999).

1.8.7 Textile industry

Applications of liposomes in the textile industry, also, are noteworthy. The characteristics of liposomes that are of immense importance for textile processing are sustained-release of encapsulates and biodegradability of liposomes. The processes of textile industry that utilize liposomes include washing and scouring, bleaching, and dyeing (Marti *et al.*, 2007).

Textile pretreatment involves washing and scouring that utilizes surfactants. The requirements an ideal surfactant used in textile industry should fulfill are biodegradability, low toxicity, use of renewable raw materials for their synthesis and multifunctionality (Clapes and Infante, 2002; Infante, Pinazo and Seguer, 1975). Phospholipids, of which liposomes are made, possess the above requirements to a very high degree. Further, the detergency power of liposomes is comparable to that of linear alkyl benzene sulphonates – a traditional surfactant used in textile industry. Moreover, liposomes do not foam, thus

distinguishing these vesicles from other surfactants used in textile industry (Sheveleva *et al.*, 2003).

Bleaching – another process of textile pretreatment – benefits from the utilization of liposomes. In fact, the advantages of employing liposomes in peroxide bleaching and chlorine bleaching have been documented (De La Maza, Parra and Bosch, 1991; Sheveleva *et al.*, 2003). For instance, using of liposomes negates the need of a wetting agent in bleaching of cotton fabrics (Alfred Kling *et al.*, 1975). Furthermore, mechanical properties and brightness of fabrics improve in the presence of liposomes in peroxide bleaching. Moreover, the rate of decomposition of peroxide decreases upon utilization of liposomes due to sustained release of peroxides or due to encapsulation of catalysts that decompose radicals (Sheveleva *et al.*, 2003). Also, excessive oxidation of wool may be prevented in bleaching of wool with chlorine (De La Maza *et al.*, 1991).

Numerous types of dyes have been encapsulated in liposomes and used in dyeing of fabrics becuase utilization of liposomes in dyeing of fabrics presents numerous advantages. For instance, liposomes improve dye exhaustion, levelness and dye-fiber bonding (Barani and Montazer, 2008).

1.9 Improving physical properties of active pharmaceutical ingredients

The majority of active pharmaceutical ingredients is solids and the main reason preventing a vast number of APIs from appearing in the market is their physical properties that are inappropriate for pharmaceutical formulations. Thus, numerous academic and industrial researchers worldwide focus on optimizing the physical properties of APIs. Examples of physical properties that need to be optimized include solubility, dissolution rate, physical and chemical stability, hygroscopicity, flowability, and compressability. Actually, various strategies are adopted to improve these properties (Qiao *et al.*, 2011). Such strategies include micronization (Cho *et al.*, 2010), salt formation (Umeda *et al.*, 2009), emulsification (Hong *et al.*, 2006), utilization of drug delivery vehicles (Morrow *et al.*, 2007), formation of eutectics (Goud *et al.*, 2012), formation of solid dispersions (Kawabata *et al.*, 2010), and more recently the formation of cocrystals (Qiao *et al.*, 2011).

1.9.1 Cocrystals

Among the numerous definitions of the term 'cocrystal', the one presented by Aakeröy and Salmon in 2005 is most widely used. According to that definition, "cocrystals are structurally homogeneous crystalline materials containing two or more components present in definite stoichiometric amounts. The cocrystal components are discrete neutral molecular reactants which are solids at ambient temperature" (Lara-Ochoa and Espinosa-Pérez, 2007; Qiao *et al.*, 2011). Pharmaceutical cocrystals are cocrystals of which at least one component is an API. The other component, which is called the 'coformer' should be a compound safe for human consumption. Usually, compounds listed as GRAS (generally recognized as safe) by FDA are used as coformers (Qiao *et al.*, 2011).

The intermolecular forces utilized in the synthesis of cocrystals include hydrogen bonding, van der Waals forces and π---π stacking interactions. Of these intermolecular forces, hydrogen bonding is the most focused (Morissette *et al.*, 2004). A few hydrogen bonding interactions utilized in cocrystal formation are shown in figure 5.

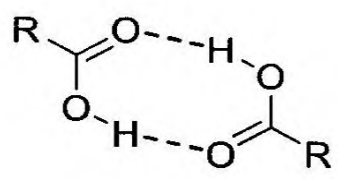

A

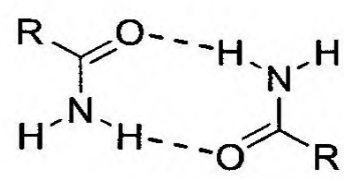

B

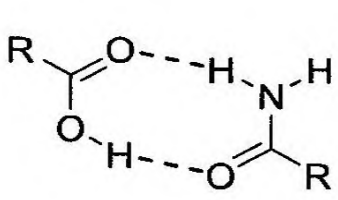

C

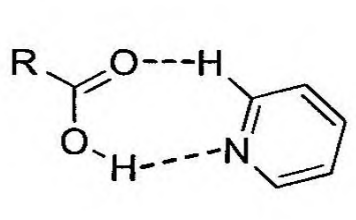

D

Figure 5. Hydrogen bonding motifs used in cocrystal formation (A - carboxylic acid-carboxylic acid, B -amine-amine, C - carboxylic acid-amine, D – carboxylic acid-pyridine)

The most commonly used methods of preparation of pharmaceutical cocrystals can be broadly divided into two groups: solution methods and grinding methods. Solution methods include evaporation cocrystallization, reaction crystallization and cooling crystallization. Grinding methods include solid-state grinding or neat-grinding and liquid-assisted grinding or solvent-drop grinding. Other seldom used methods of cocrystallization comprise application of supercritical fluid technology and application of ultrasound (Asija, Mangukia and Asija, 2013).

Evaporation cocrystallization is the evaporation of the solvent from a stoichiometric solution of the constituents of the cocrystal; and numerous pharmaceutical cocrystals have been successfully prepared using this method. For instance, Shayanfar and coworkers prepared a cocrystal of carbamazepine, which is an anticonvulsant antiepileptic drug, and nicotinamide, which is vitamin B_3, using this method (Shayanfar, Velaga and Jouyban, 2014). Furthermore, cocrystals of theophylline, which is a drug used to treat respiratory diseases, and nicotinamide has been synthesized by slow evaporation of ethanol (Lu and Rohani, 2009). Reaction crystallization is the evaporation of the solvent from a nonstoichiometric solution of the constituents of the cocrystal. This method, also, is widely used in the synthesis of cocrystals. For example, Childs and coauthors reported the formation of carbamazepine cocrystals by reaction crystallization (Childs *et al.*, 2008). Cooling crystallization involves utilization of high temperatures to solubilize the constituents of cocrystals and then changing the temperature of the system to allow cocrystallization. Examples of cocrystals formed by cooling crystallization include carbamazepine-nicotinamide cocrystal and caffeine-p-hydroxybenzoic acid cocrystal (Gagniere *et al.*, 2011; He, Chow and Tan, 2010).

Like solution methods, grinding methods have been used frequently to synthesize cocrystals. Neat grinding or solid-state grinding is a dry grinding technique where stoichiometric amounts of the constituents of cocrystals are ground either manually or mechanically. A mortar and pestle is used for manual grinding whereas a ball mill or a vibratory mill is used for mechanical grinding. Examples of cocrystals formed via neat grinding include carbamazepine-saccharin cocrystal and theophylline-nicotinamide cocrystal (Jayasankar *et al.*, 2006; Lu and Rohani, 2009). Liquid-assisted grinding or solvent drop grinding is the second type of grinding method adopted for the synthesis of cocrystals. This is a wet grinding technique where a catalytic amount of an appropriate solvent is added during grinding of the constituents of cocrystals. Numerous cocrystals have been formed using this method. For instance, Sowa and coworkers reported the

synthesis of a cocrystal of myricetin, which is an antioxidant, and piracetam, which is a nootropic drug, using liquid-assisted grinding (Sowa, Ślepokura and Matczak-Jon, 2014). Apart from the traditional solvent methods and grinding methods, a few novel methods, as stated previously, have been used for the synthesis of cocrystals. For example, Padrela and coauthors reported the formation of cocrystals of indomethacin, which is an anti-inflammatory drug, in combination with saccharin, using super critical fluid techniques (Padrela *et al.*, 2009). Moreover, Aher et al. demonstrated the application of ultrasound in the preparation of cocrystals. In fact, they reported the formation of caffeine-maleic acid cocrystals, using this technique (Aher *et al.*, 2010).

Indeed, improvements of physical properties brought about through cocrystallization of APIs should be emphasized. Solubility is an important property that has been enhanced via cocrystallization. For instance, increased solubility of ezetimibe, which is a drug prescribed to lower plasma cholesterol level, by cocrystallization in combination with methyl paraben, which is a preservative, has been demonstrated (Sugandha *et al.*, 2014). Furthermore, Bruni and coworkers showed that the solubility of loperamide hydrochloride, which is a drug used against several types of diarrhea, is increased upon cocrystallization with glutaric acid (Bruni *et al.*, 2013). In addition to increased solubility, enhanced dissolution profiles of APIs have been obtained via cocrystallization. For example, the cocrystal of itraconazole, which is an antifungal agent, and malonic acid has shown a 5-fold increase of dissolution rate compared to the free drug (Shevchenko *et al.*, 2012). Physical stability of solid forms of APIs may, also, be increased by cocrystallization. For instance, as demonstrated by Shevchenko and coauthors, itraconazole-malonic acid cocrystal does not compromise the hygroscopicity or stability of the API while two salts of itraconazole show increased hygroscopicity, although both forms increase the dissolution rate (Shevchenko *et al.*, 2012). Moreover, caffeine exhibits increased physical stability with respect to relative humidity, upon cocrystallization with oxalic acid (Trask, Samuel Motherwell and Jones, 2005). Apart from physical properties stated above, bioavailability of APIs can be increased via cocrystallization. For example, a study using mouse models demonstrated that oral bioavailability of baicalein, which shows several bioactivities including anti-inflammatory activity, can be increased by the administration of baicalein-nicotinamide cocrystals (Huang *et al.*, 2014).

Although synthesis of cocrystallization is a very attractive strategy to enhance physical properties of APIs, only a small percentage of attempts of cocrystallization have been successful. Instead of cocrystals, other forms of solids such as solid solutions or

eutectic mixtures have resulted from a number of such attempts. Interestingly, solid solutions and eutectic mixtures, also, exhibit numerous enhanced physical properties. Thus, these solid forms have become the subject of research of numerous pharmaceutical research groups worldwide.

1.9.2 Solid dispersions

Solid dispersions are solid products consisting of a crystalline or amorphous matrix and a drug dispersed in the matrix. The dispersed drug can be fully crystalline, semicrystalline or amorphous. Solid solutions are a special class of solid dispersions in which the drug is dispersed in the matrix, in the amorphous state. Solid solutions may be categorized based on many parameters. For instance, solid solutions may be divided into two groups based on the miscibility of the drug and carrier: continuous and discontinuous. In continuous solid solutions, the drug and carrier are miscible in all proportions; whereas in discontinuous solid solutions, the drug and carrier are miscible only at a definite proportion. Solid solutions may, also, be divided into three groups based on how the solute molecule is dispersed in the matrix: substitutional, interstitial and amorphous. In substitutional solid solutions, a fraction of solvent molecules of the crystal lattice are substituted by the solute molecules. In interstitial solid solutions, the solute molecules occupy interstitial spaces of solvent molecules of the crystal lattice. In amorphous solid solutions, the carrier in present in an amorphous state and the solute is dispersed at a molecular level (Chiou and Riegelman, 1971; Sinha *et al.*, 2009).

Similar to cocrystals, solid dispersions exhibit numerous attributes desirable in pharmaceutical dosage form development. First, these solid forms are utilized to increase the solubility of poorly soluble drugs. Second, solid dispersions are used to increase the dissolution rate of numerous drugs. For example, as reported by Zhang et al., the dissolution rate of finofibrate, a prodrug of fenofibric acid which lowers blood lipid levels, may be enhanced through the formation of amorphous solid dispersions (Zhang *et al.*, 2012). Third, solid dispersions may, also, increase the stability of drugs. For instance, Jang and co-researchers demonstrated that a solid dispersion of everolimus, which is a drug used in the treatment of advanced renal cell carcinoma, exhibited increased physicochemical stability compared to the drug powder (Jang and Kang, 2014). Most importantly, solid dispersions may enhance the bioavailability of drugs.

1.9.3 Eutectic mixtures

A eutectic mixture is a mixture of chemical compounds or elements, that solidifies at a temperature lower than pure compounds of elements and any other composition (Sinha *et al.*, 2009). In fact, solid eutectic mixtures consist of intimately blended fine crystals of the component species. Usually, methods of preparation of cocrystals and solid solutions may also be utilized in the preparation of eutectics. Examples of such methods include, solvent evaporation methods, grinding methods and compaction (Bi, Hwang and Morris, 2003; Cherukuvada and Nangia, 2012; Goud *et al.*, 2012). Similar to cocrystals and solid solutions, eutectic mixtures are a means of enhancing pharmaceutically important properties of APIs. For instance, Goud and coworkers formed eutectic mixtures of curcumin, that exhibited faster dissolution rates (Goud *et al.*, 2012). Also, Cherukuvada and Nangia reported the formation of a eutectic mixture of two anti-tubercular drugs, that showed fast dissolving properties (Cherukuvada and Nangia, 2012). Such increases in dissolution rates usually lead to increased bioavailability of poorly soluble drugs. Moreover, enhanced skin penetration of therapeutic agents upon eutectic formation has been reported (Fiala, Jones and Brown, 2010).

1.10 Antioxidants

Antioxidants are species that prevent the oxidation of other species. Among the many areas in which antioxidants play significant roles, pharmaceutics and medicine constitute the key areas since preventing oxidation of biological molecules is of prime importance for the proper functioning of biological systems (Sies, 1997). Following is an account of the antioxidants utilized in this thesis work.

1.10.1 Curcumin

One of the antioxidants used in this thesis work is curcumin, also called diferuloyl methane. This compound occurs naturally in the rhizome of the herb *Curcuma longa*. Curcumin has been used since ancient times in Ayurvedic medicine, in cosmetic formulations and as a spice in cooking; and recent studies have revealed a broad spectrum of biological activities of this compound (Aggarwal *et al.*, 2007; Goel, Kunnumakkara and Aggarwal, 2008). Bioactivities shown by curcumin include antioxidant, antimicrobial, anti-inflammatory and anticarcinogenic activities (Aggarwal, Kumar and Bharti, 2003; Cao *et al.*, 2015; Fu *et al.*, 2014; Govindaraj, Kandasubramanian and Kodam, 2014). Furthermore, this compound exhibits nephroprotective, hepatoprotective, antirheumatic and anti-

Alzheimer's disease properties (Chandran and Goel, 2012; Kulkarni and Chopra, 2006; Ono *et al.*, 2004; Sharma, García-Nino and Pedraza-Chaverrí, 2014). Moreover, curcumin protects against myocardial infarction and suppresses thrombosis (Jeong *et al.*, 2012; Pendurthi and Rao, 2000).

In addition to curcumin, natural analogs of curcumin from turmeric, also called 'curcuminoids' (see Figure 6) exhibit similar bioactivities to those shown by curcumin. However, the potency of these compounds differs. For instance, bisdemethoxycurcumin (BDMC) is more potent than demethoxycurcumin (DMC) or curcumin as a cytotoxic agent against ovarian cancer cells (Syu *et al.*, 1998). Furthermore, peroxynitrite scavenging activity of curcumin or DMC is higher than that of BDMC (Kim *et al.*, 2003). Moreover, BDMC is more potent than curcumin in preventing oxidative stress induced by alcohol and polyunsaturated fatty acids and in preventing hepatotoxicity induced by CCl_4 (Kamalakkannan *et al.*, 2005; Rukkumani et al., 2004) while curcumin or DMC are more potent than BDMC in protecting rats who have lead-induced neurotoxicity and in suppressing NF-κB activation (Dairam *et al.*, 2007; Sandur *et al.*, 2007).

Apart from curcuminoids, numerous metabolites of curcumin have been reported (see Figure 6). Those metabolites include dihydrocurcumin, tetrahydrocurcumin (THC), hexahydrocurcumin, hexahydrocurcuminol, curcuminglucuroide and curcumin sulphate. THC, being one of the major metabolites of curcumin, is thought to be responsible for the *in vivo* antioxidant activity of curcumin. In fact, THC is more active than curcumin as an antioxidant in numerous models. For instance, THC has been reported to be more potent than curcumin in suppressing oxidative renal damage induced by nitrilotriacetate, in preventing brain lipid peroxidation in diabetic rodents, and in conferring antioxidant effect in diabetic rats (Murugan and Pari, 2006; Okada *et al.*, 2001; Pari and Murugan, 2007). However, curcumin has been reported to be more active than THC regarding numerous bioactivities such as in modulating ABC drug transporters and in preventing skin tumor promotion in mice (Huang *et al.*, 1995; Limtrakul *et al.*, 2007).

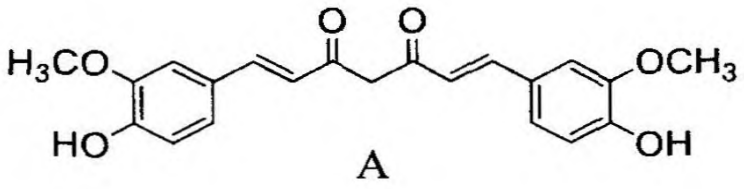

A

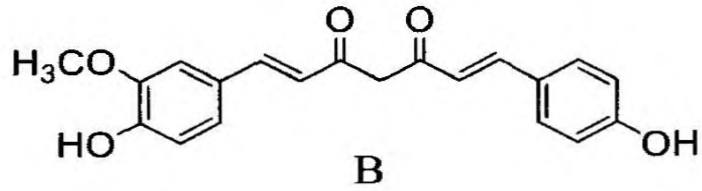

B

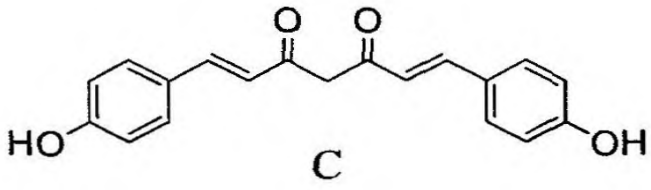

C

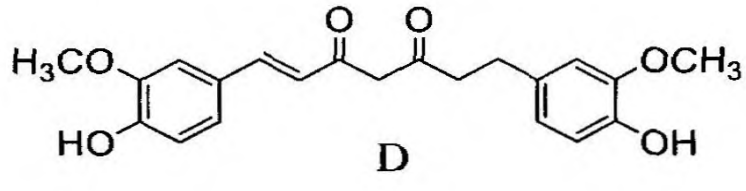

D

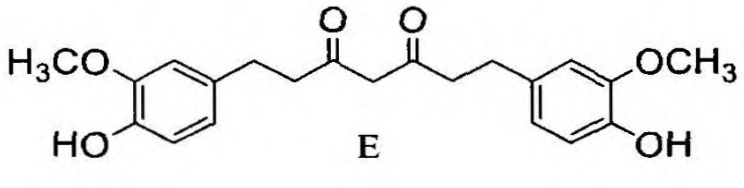

E

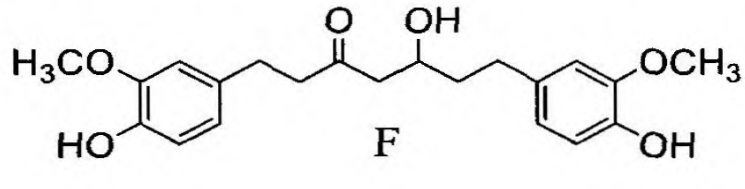

F

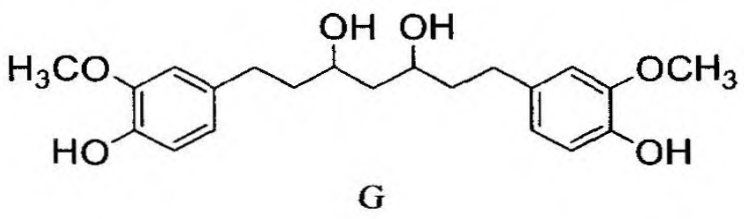

G

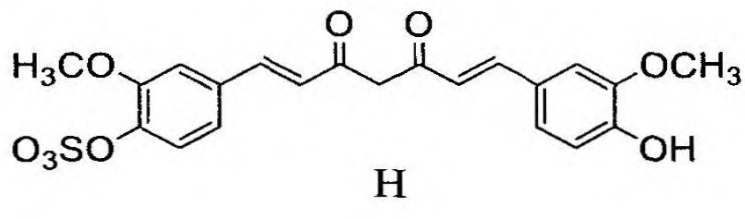

H

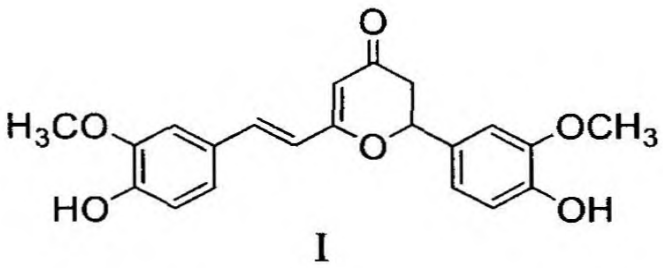

I

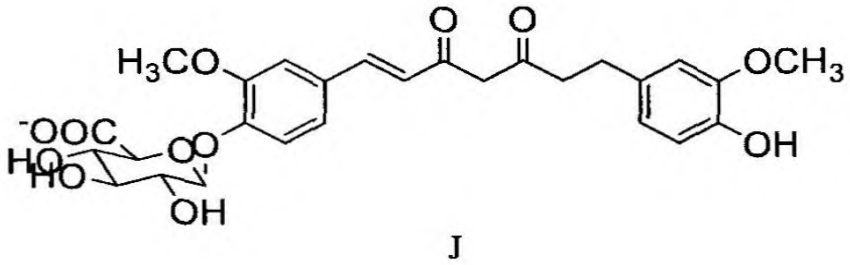

J

Figure 6. Structures of analogues of curcumin derived from turmeric and metabolites of curcumin (A-curcumin, B-demethoxycurcumin, C-bisdemethoxycurcumin, D-dihydrocurcumin, E-tetrahydrocurcumin, F-hexahydrocurcumin, G-hexahydrocurcuminol, H-curcumin sulphate, I-cyclocurcumin, J-curcuminglucuronide)

1.10.2 Ferulic acid

Ferulic acid is a phenolic compound with various attractive properties that render it a compound much desirable in cosmetic formulations and drug formulations. Numerous studies have revealed that ferulic acid is a potent antioxidant that scavenges many reactive oxygen species, thus, protecting biological systems from oxidative damage (Ogiwara *et al.*, 2002). Moreover, ferulic acid shows photoprotective properties when applied topically on the skin (Lin *et al.*, 2005). In addition, ferulic acid possesses antimutagenic and anticarcenogenic properties (Yamada and Tomita, 1996). For instance, Huang and coworkers showed that topical application of ferulic acid inhibited 12-*O*-

Tetradecanoylphorbol-13-acetate induced tumour promotion in mouse skin (Huang *et al.*, 1988). Furthermore, ferulic acid acts synergistically with other antioxidants. For example, it exhibits synergy with vitamin C and vitamin E - the major antioxidants that protect the skin (Trombino *et al.*, 2004). Ferulic acid is a natural analogue of curcumin and the structure of ferulic acid is shown in figure 7.

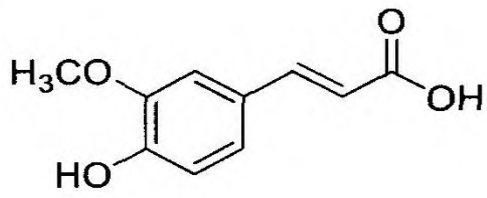

Figure 7. Structure of ferulic acid

1.11 References

Adler-moore, J.P. and Proffitt, R.T. (1993). Development, characterization, efficacy and mode of action of ambisome, a unilamellar liposomal formulation of Amphotericin B. *Journal of Liposome Research* **3(3)**, 429-450.

Aggarwal, B.B., Kumar, A. and Bharti, A.C. (2003). Anticancer potential of curcumin: preclinical and clinical studies. *Anticancer Research* **23(1)**, 363-398.

Aggarwal, B.B., Sundaram, C., Malani, N. and Ichikawa, H. (2007). Curcumin: the Indian solid gold. *Advances in Experimental Medicine and Biology* **595**, 1-75.

Agrawal, A.K. and Gupta, C.M. (2000). Tuftsin-bearing liposomes in treatment of macrophage-based infections. *Advanced Drug Delivery Reviews* **41**, 135–146.

Aher, S., Dhumal, R., Mahadik, K., Paradkar, A. and York, P. (2010). Ultrasound assisted cocrystallization from solution (USSC) containing a non-congruently soluble cocrystal component pair: caffeine/maleic acid. *European Journal of Pharmaceutical Sciences* **41**, 597-602.

Ainbinder, D. and Touitou, E. (2005). Testosterone ethosomes for enhanced transdermal delivery. *Drug Delivery* **12**, 297-303.

Alfred Kling, L., Viktor Specht, D., Carmen Hofstetter, Mannheim-Kaefertal., Gundolf Eisenberg, H. Bleaching of cellulose containing textile fiber material with a silicate-free stabilized peroxide bleaching bath, US Patent 3810391, 1975.

Al-Jamal, W.T., Al-Ahmady, Z.S. and Kostarelos, K. (2012). Pharmacokinetics & tissue distribution of temperature-sensitive liposomal doxorubicin in tumor-bearing mice triggered with mild hyperthermia. *Biomaterials* **33**, 4608-4617.

Alomrani, A.H., Shazly, G.A., Amara, A.A. and Badran, M.M. (2014). Itraconazole-hydroxypropyl-β-cyclodextrin loaded deformable liposomes: In vitro skin penetration studies and antifungal efficacy using *Candida albicans* as model. *Colloids and Surfaces B: Biointerfaces* **121**, 74–81.

Anderson, P.M., Hanson, D.C., Hasz, D.E., Halet, M.R., Blazar, B.R. and Ochoa, A.C. (1994). Cytokines in liposomes: preliminary studies with IL-1, IL-2, IL-6, GM-CSF and interferon-γ. *Cytokine* **6(1)**, 92-101.

Asija, R., Mangukia, D. and Asija, S. (2013). Pharmaceutical cocrystals: an overview. *Journal of Drug Discovery and Therapeutics* **1(3)**, 10-14.

Banerjee, R. (2001). Liposomes: Applications in medicine. *Journal of biomaterials applications* **16**, 3-21.

Bangham, A.D and Horne, R.W. (1964). Negative staining of phospholipids and their structural modification by surface-active agents as observed in the electron microscope. *Journal of Molecular Biology* **8(5)**, 660–668.

Barani, H. and Montazer, M. (2008). A review on applications of liposomes in textile processing. *Journal of Liposome Research* **18**, 249-262.

Barichello, J.M., Kizuki, S., Tagami, T., Soares, L.A.L., Ishida, T., Kikuchi, H. and Kiwada, H. (2012). Agitation during lipoplex formation harmonizes the interaction of siRNA to cationic liposomes. *International Journal of Pharmaceutics* **430**, 359– 365.

Berg, J.M., Tymoczko, J.L. and Stryer, L. (2002). *Biochemistry,* 5th edn. W.H. Freeman and Company, New York, USA.

Bhattacharyya, S., Bhattacharya, R., Curley, S. McNiven, M.A. and Mukherjee, P. (2010). Nanoconjugation modulates the trafficking and mechanism of antibody induced receptor endocytosis. *Proceedings of the National Acadamy of Sciences USA* **107(33)**, 14541-14546.

Bi, M., Hwang, S-J. and Morris, K.R. (2003). Mechanism of eutectic formation upon compaction and its effects on tablet properties. *Thermochimica Acta* **404**, 213-226.

Boucrot, E., Pick, A., Çamdere, G., Liska, N., Evergren, E., McMahon, H.T. and Kozlov, M.M. (2012). Membrane fission is promoted by insertion of amphipathic helices and is restricted by crescent BAR domains. *Cell* **149**, 124–136.

Brecher, P., Saouaf, R., Sugarman, J.M., Eisenberg, D. and LaRosa, K. (1984). Fatty acid transfer between multilamellar liposomes and fatty acid-binding proteins. *The Journal of Biological Chemistry* **259(21)**, 13395-13401

Bruni, G., Maietta, M., Maggi, L., Mustarelli, P., Ferrara, C., Berbenni, V., Freccero, M., Scotti, F., Milanese, C., Girella, A. and Marini, A. (2013). An experimental and theoretical investigation of loperamide hydrochloride-glutaric acid cocrystals. *Journal of Physical Chemistry B* **117(27)**, 8113-8121.

Campelo, F. and Hernàndez-Machado, A. (2006). Dynamic model and stationary shapes of fluid vesicles. *The European Physical Journal E* **20(1)**, 37-45.

Cao, L., Ding, W., Du, J., Jia, R., Liu, Y., Zhao, C., Shen, Y. and Yin, G. (2015). Effects of curcumin on antioxidative activities and cytokine production in Jian carp (*Cyprinus carpio var.* Jian) with CCl_4-induced liver damage. *Fish and Shellfish Immunology* **43**, 150-157.

Chanchal, D. and Swarnlata, S. (2008). Novel approaches in herbal cosmetics. *Journal of Cosmetic Dermatology* **7(2)**, 89–95.

Chandran, B. and Goel, A. (2012). A randomized, pilot study to assess the efficacy and safety of curcumin in patients with active rheumatoid arthritis. *Phytotherapy Research* **26(11)**, 1719-1725.

Chen, Y., Wu, Q., Zhang, Z., Yuan, L., Liu, X. and Zhou, L. (2012). Preparation of curcumin loaded liposomes and evaluation of their skin permeation and pharmacodynamics. *Molecules,* **17**, 5972-5987.

Cherukuvada, S. and Nangia, A. (2012). Fast dissolving eutectic compositions of two anti-tubercular drugs. *CrystEngComm, 14*, 2579-2588.

Childs, S.L., Rodríguez-Hornedo, N., Reddy, L.S., Jayasankar, A., Maheshwari, C., McCausland, L., Shipplett, R. and Stahly, B.C. (2008). Screening strategies based on solubility and solution composition generate pharmaceutically acceptable cocrystals of carbamazepine. *CrystEngComm* **10(7)**, 856-864.

Chiou, W.L. and Riegelman, S. (1971). Pharmaceutical applications of solid dispersion systems. *Journal of Pharmaceutcal Sciences* **60(9)**, 1281-1302.

Cho, E., Cho, W., Cha, K-H., Park, J., Kim, M-S., Kim, J-S., Park, H.J. and Hwang, S-J. (2010). Enhanced dissolution of megestrol acetate microcrystals prepared by antisolvent precipitation process using hydrophilic additives. *International Journal of Pharmaceutics,* **396**, 91-98.

Clapés, P. and Infante, M.R. (2002). Amino acid-based surfactants: Enzymatic synthesis, properties and potential applications. *Biocatalysis and Biotransformation* **20(4)**, 215-233.

Coelho, F.L., Rodembusch, F.S. and Campo, L.F. (2014). Synthesis, characterization and photophysics of new photoactive ESIPT lipophilic dyes. Partition experiments with different composed liposomes. *Dyes and Pigments* **110**, 134-142.

Crowe, J.H., Spargo, B.J. and Crowe, L.M. (1987). Preservation of dry liposomes does not require retention of residual water. *Proceedings of the National Academy of Sciences USA,* **84**, 1537-1540.

Dairam, A., Limson, J.L., Watkins, G.M., Antunes, E. and Daya, S. (2007). Curcuminoids, curcumin, and demethoxycurcumin reduce lead-induced memory deficits in male wistar rats. *Journal of Agricultural and Food Chemistry* **55(3)**, 1039-1044.

Dasgupta, D., Adhya, S. and Basu, M.K. (2002). The Effect of β-Tubulin-Specific Antisense Oligonucleotide Encapsulated in Different Cationic Liposomes on the Supression of Intracellular L. Donovani Parasites In Vitro. *Journal of Biochemistry* **132(1)**, 23-27.

Dass, C.R., Walker, T.L. and Burton, M.A. (2002). Liposomes containing cationic dimethyl dioctadecyl ammonium bromide: formulation, quality control, and lipofection efficiency. *Drug Delivery* **9(1)**, 11-18.

Davidsen, J., Mouritsen, O.G. and Jørgensen, K. (2002). Synergistic permeability enhancing effect of lysophospholipids and fatty acids on lipid membranes. *Biochimica et Biophysica Acta,* **1564**, 256-262.

De La Maza, A., Parra, J.L. and Bosch, P. (1991). Using liposomes in wool chlorination: Stability of chlorine liposomes and their application on wool fibres. *Textile Research Journal* **61(6)**, 357-362.

Devine, D.V., Wong, K., Serrano, K., Chonn, A. and Cullis, P.R. (1994). Liposome-complement interactions in rat serum: Implications for liposome survival studies. *Biochimica et Biophysica Acta* **1191**, 43–51.

Ding, W., Qi, X., Li, P., Maitani, Y. and Nagai, T. (2005). Cholesteryl hemisuccinate as a membrane stabilizer in dipalmitoylphosphatidylcholine liposomes containing saikosaponin-d. *International Journal of Pharmaceutics* **300**, 38–47.

Dua, J.S, Rana, A.C. and Bhandari, A.K. (2012). Liposome:Methods of preparation and applications. *International Journal of Pharmaceutical Studies and Research, 3*(2), 14-20.

Duman, G., Aslan, I., Özer, A.Y., İnanç, I, and Taralp, A. (2014). Liposome, gel and lipogelosome formulations containing sodium hyaluronate. *Journal of liposome research* **24(4)**, 259-269.

Egbaria, K. and Weiner, N. (1990). Liposomes as a topical drug delivery system. *Advanced Drug Delivery Reviews* **5**, 287-300.

El Maghraby, G.M.M., Williams, A.C. and Barry, B.W. (1999). Skin delivery of oestradiol from deformable and traditional liposomes: mechanistic studies. *Journal of Pharmacy and Pharmacology* **51**, 1123-1134.

El Maghraby, G.M.M., Williams, A.C. and Barry, B.W. (2000). Oestradiol skin delivery from ultradeformable liposomes: refinement of surfactant concentration. *International Journal of Pharmaceutics* **196(1)**, 63–74.

El Maghraby, G.M.M., Williams, A.C. and Barry, B.W. (2004). Interactions of surfactants (edge activators) and skin penetration enhancers with liposomes. *International Journal of Pharmaceutics* **276(1-2)**, 143–161.

Elsayed, M.M.A., Abdallah, O.Y., Naggar, V.F. and Khalafallah, N.M. (2007). Lipid vesicles for skin delivery of drugs: Reviewing three decades of research. *International Journal of Pharmaceutics* **332**, 1-16.

Endsley, A.N. and Ho, R.J.Y. (2012). Enhanced anti-HIV efficacy of indinavir after inclusion in CD4-targeted lipid nanoparticles. *Journal of Acquired Immune Deficiency Syndromes* **61(4)**, 417-424.

Fan, Y., Sahdev, P., Ochyl, L.J., Akerberg, J.J. and Moon, J.J. (2015). Cationic liposome–hyaluronic acid hybrid nanoparticles for intranasal vaccination with subunit antigens. *Journal of Controlled Release* **208**, 121–129.

Felber, A.E., Dufresne, M-H. and Leroux, J-C. (2012). pH-sensitive vesicles, polymeric micelles, and nanospheres prepared with polycarboxylates. *Advanced Drug Delivery Reviews* **64**, 979–992.

Fenske, D.B., Palmer, L.R., Chen, T., Wong, K.F. and Cullis, P.R. (2001). Cationic poly(ethyleneglycol) lipids incorporated into pre-formed vesicles enhance binding and uptake to BHK cells. *Biochimica et Biophysica Acta,* **1512**, 259-272.

Fiala, S., Jones, S.A. and Brown, M.B. (2010). A fundamental investigation into the effects of eutectic formation on transmembrane transport. *International journal of pharmaceutics* **393**, 68-73.

Forssen, E.A., Coulter, D.M. and Proffitt, R.T. (1992). Selective in vivo localization of daunorubicin small unilamellar vesicles in solid tumors. *Cancer Research, 52*(12), 3255-3261.

Frenzel, M. and Steffen-Heins, A. (2015). Impact of quercetin and fish oil encapsulation on bilayer membrane and oxidation stability of liposomes. *Food Chemistry* **185**, 48–57.

Fresta, M., Wehrli, E. and Puglisi, G. (1995). Neutrase entrapment in stable multilamellar and large unilamellar vesicles for the acceleration of cheese ripening. *Journal of microencapsulation* **12(3)**, 307-325.

Fricker, G., Kromp, T., Wendel, A., Blume, A., Zirkel, J., Rebmann, H., Setzer, C., Quinkert, R-O., Martin, F. and Müller-Goymann, C. (2010). Phospholipids and lipid-based formulations in oral drug delivery. *Pharmaceutical Research* **27(8)**, 1469-1486.

Fu, Y., Gao, R., Cao, Y., Guo, M., Wei, Z., Zhou, E., Li, Y., Yao, M., Yang, Z. and Zhang, N. (2014). Curcumin attenuates inflammatory responses by supressing TLR4-mediated NF-κB signaling pathway in lipopolysaccharide-induced mastitis in mice. *International Immunopharmacology* **20**, 54-58.

Gagniere, E., Mangin, D., Puel, F., Valour, J-P., Klein, J-P. and Monnier, O. (2011). Cocrystal formation in solution: Inducing phase transition by manipulating the amount of cocrystallizing agent. *Journal of Crystal Growth* **316**, 118-125.

Gao, X. and Huang, L. (1991). A novel cationic liposome reagent for efficient transfection of mammalian cells. *Biochemical and biophysical research communications* **179(1)**, 280-285.

García-Niño, W.R. and Pedraza-Chaverrí, J. (2014). Protective effect of curcumin against heavy metals-induced liver damage. *Food and chemical toxicology* **69**, 182-201.

Garg, M., Mishra, D., Agashe, H. and Jain, N.K. (2006). Ethinylestradiol-loaded ultraflexible liposomes: pharmacokinetics and pharmacodynamics. *Journal of Pharmacy and Pharmacology* **58**, 459-468.

Girod de Bentzmann, S., Pierrot, D., Fuchey, C., Zahm, J-M., Morancais, J-L. and Puchelle, E. (1993). Distearoyl phosphatidylglycerol liposomes improve surface and transport properties of CF mucus. *European Respiratory Journal* **6(8)**, 1156-1161.

Godin, B. and Touitou, E. (2005). Erythromycin ethosomal systems: physicochemical characterization and enhanced antibacterial activity. *Curr. Drug Deliv.* **2**, 269-275.

Goel, A., Kunnumakkara, A.B. and Aggarwal, B.B. (2008). Curcumin as "Curecumin": From kitchen to clinic. *Biochemical Pharmacology* **75**, 787-809.

Gomes-da-Silva, L.C., Fonseca, N.A., Moura, V., Pedroso de Lima, M.C., Simões, S. and Moreira, J.N. (2012). Lipid-based nanoparticles for siRNA delivery in cancer therapy: Paradigms and challenges. *Accounts of Chemical Research* **45(7)**, 1163-1171.

Gong, W., Wang, Z. Liu, N., Lin, W., Wang, X., Xu, D., Liu, H., Zeng, C., Xie, X., Mie, X. and Lü, W. (2001). Improving efficiency of adriamycin crossing blood brain barrier by combination of thermosensitive liposomes and hyperthermia. *Biological and Pharmaceutical Bulletin* **34**, 1058–1064.

Goud, N.R., Suresh, K., Sanphui, P. and Nangia, A. (2012). Fast dissolving eutectic compositions of curcumin. *International Journal of Pharmaceutics* **439**, 63-72.

Govindaraj, P., Kandasubramanian, B. and Kodam, K.M. (2014). Molecular interactions and antimicrobial activity of curcumin (*Curcuma longa*) loaded polyacrylonitrile films. *Materials Chemistry and Physics* **147**, 934-941.

Guo, J., Ping, Q. and Zhang, L. (2000). Transdermal delivery of insulin in mice by using lecithin vesicles as a carrier. *Drug Delivery* **7**, 113-116.

Gust, D., Moore, T.A. and Moore, A.L. (1998). Mimicking bacterial photosynthesis. *Pure and Applied Chemistry* **70(11)**, 2189-2200.

He, G., Chow, P.S. and Tan, R.B.H. (2010). Investigating the intermolecular interactions in concentration-dependent solution cocrystallization of caffein and *p*-hydroxybenzoic acid. *Crystl Growth & Design* **10(8)**, 3763-3769.

Heath, T.D., Fraley, R.T. and Papahadjopoulos, D. (1980). Antibody targeting of liposomes: Cell specificity obtained by conjugation of $F(ab')_2$ to vesicle surface. *Science,* 210, 539-541.

Henriksen-Lacey, M., Bramwell, V.W., Christensen, D., Agger, E-M., Andersen, P. and Perrie, Y. (2010). Liposomes based on dimethyldioctadecylammonium promote a depot effect and enhance immunogenicity of soluble antigen. *Journal of Controlled Release* **142**, 180-186.

Hildebrandt, B., Wust, P., Ahlers, O., Dieing, A., Sreenivasa, G., Kerner, T., Felix, R. and Riesse, H. (2002). The cellular and molecular basis of hyperthermia. *Critical Reviews in Oncology/Hematology* **43**, 33–56.

Hong, J-Y., Kim, J-K., Song, Y-K., Park, J-S. and Kim, C-K. (2006). A new self-emulsifying formulation of itraconazole with improved dissolution and oral absorption. *Journal of Controlled Release* **110**, 332-338.

Hong, K., Zheng, W., Baker, A. and Papahadjopoulos, D. (1997). Stabilization of cationic liposome-plasmid DNA complexes by polyamines and poly(ethylene glycol)-phospholipid conjugates for efficient in vivo gene delivery. *FEBS Letters, 400*, 233-237

Huang, M-T., Smart, R.C., Wong, C-Q. and Conney, A.H. (1988). Inhibitory effect of curcumin, chlorogenic acid, caffeic acid, and ferulic acid on tomor promotion in mouse skin by 12-*O*-tetradecanoylphorbol-13-acetate. *Cancer Research* **48**, 5941-5946.

Huang, Y., Zhang, B., Gao, Y., Zhang, J. and Shi, L. (2014). Baicalein-Nicotinamide cocrystal with enhanced solubility, dissolution, and oral bioavailability. *Journal of Pharmaceutical Sciences* **103(8)**, 2330-2337.

Ikehara, Y., Shiuchi, N., Kabata-Ikehara, S., Nakanishi, H., Yokoyama, N., Takagi, H., Nagata, T., Koide, Y., Kuzushima, K., Takahashi, T., Tsujimura, K. and Kojima, N. (2008). Effective induction of anti-tumor immune responses with oligomannose-coated liposome targeting to intraperitoneal phagocytic cells. *Cancer Letters* **260**, 137–145.

Immordino, M.L., Dosio, F. and Cattel, L. (2006). Stealth liposomes: review of the basic science, rationale, and clinical applications, existing and potential. *International Journal of Nanomedicine* **1(3)**, 297-315.

Infante, M.R., Pinazo, A. and Seguer, J. (1975). Non-conventional surfactants from amino acids and glycolipids: structure, preparation and properties. *Colloids and Surfaces A* **123-124**, 49-70.

Iwanaga, K., Ono, S., Narioka, K., Morimoto, K., Kakemi, M., Yamashita, S., Nango, M. and Oku, N. (1997). Oral delivery of insulin by using surface coating liposomes Improvement of stability of insulin in GI tract. *International Journal of Pharmaceutics* **157**, 73–80.

Jain, B., Singh, B., Katare, O.P. and Vyas, S.P. (2010). Development and characterization of minoxidil-loaded liposomal system for delivery to pilosebaceous units. *Journal of liposome research* **20(2)**, 105-114.

Jang, S.W. and Kang, M.J. (2014). Improved oral absorption and chemical stability of everolimus via preparation of solid dispersion using solvent wetting technique. *International Journal of Pharmaceutics* **473**, 187-193.

Jayasankar, A., Somwangthanaroj, A., Shao, Z.J. and Rodríguez-Harnedo, N. (2006). Cocrystal formation during cogrinding and storage is mediated by amorphous phase. *Pharmaceutical Research* **23(10)**, 2381-2392.

Jeong, C-W., Yoo, K.Y., Lee, S.H., Jeong, H.J., Lee, C.S. and Kim, S.J. (2012). Curcumin protects against regional myocardial ischemia/reperfusion injury through activation of RISK/GSK-3β and inhibition of p38 MAPK and JNK. *Journal of cardiovascular pharmacology and therapeutics* **17(4)**, 387-394.

Kamalakkannan, N., Rukkumani, R., Varma, P.S., Viswanathan, P., Rajasekharan, K.N. and Menon, V.P. (2005). Comparative effects of curcumin and an analogue of curcumin in carbon tetrachloride-induced hepatotoxicity in rats. *Basic & Clinical Pharmacology & Toxicology* **97**, 15-21.

Karunaratne, D.N., Dassanayake, A.C., Pamunuwa, K.M.G.K. and Karunaratne, V. (2014). Improved skin permeability of *dl*-α-tocopherol in topical macro emulsions. *International Journal of Pharmacy and Pharmaceutical Sciences* **6(6)**, 53-57.

Kawabata, Y., Yamamoto, K., Debari, K., Onoue, S. and Yamada, S. (2010). Novel crystalline solid dispersion of tranilast with high photostability and improved oral bioavailability. *European Journal of Pharmaceutical Sciences* **39**, 256-262.

Keswani, R.K., Lazebnik, M. and Pack, D.W. (2015). Intracellular trafficking of hybrid gene delivery vectors. *Journal of Controlled Release* **207**, 120–130.

Khatri, N., Baradia, D., Vhora, I., Rathi, M. and Misra, A. (2014). cRGD grafted liposomes containing inorganic nano-precipitate complexed siRNA for intracellular delivery in cancer cells. *Journal of Controlled Release* **182**, 45–57.

Kheadr, E.E., Vuillemard, J-C. and El Deeb, S.A. (2000). Accelerated Cheddar cheese ripening with encapsulated proteinases. *International Journal of Food Science & Technology* **35 (5)**, 483–495.

Kim, J.E., Kim, A.R., Chung, H.Y., Han, S.Y., Kim, B.S. and Choi, J.S. (2003). *In vitro* peroxynitrite scavenging activity of diarylheptanoids from *Curcuma longa*. *Phytotherapy Research* **17(5)**, 481-484.

Kirby, C., Clarke, J. and Gregoriadis, G. (1980). Effect of the Cholesterol Content of Small Unilamellar Liposomes on their Stability in vivo and in vitro. *Biochemistry Journal* **186**, 591-598.

Kobayashi, S., Hirakawa, K., Horiuchi, H., Fukuda, R. and Ohta, A. (2013). Phosphatidic acid and phosphoinositides facilitate liposome association of Yas3p and potentiate derepression of ARE1 (alkane-responsive element one)-mediated transcription control. *Fungal Genetics and Biology* **61**, 100-110.

Kofi Adzamli, I., Seltzer, S.E., Slifkin, M., Blau, M. and Adams, D.F. (1990). Production and characterization of Improved liposomes containing radiographic contrast media. *Investigative Radiology* 25(11), 1217-1223.

Kojima, N., Ishii, M., Kawauchi, Y. and Takagi, H. (2013). Oligomannose-Coated Liposome as a Novel Adjuvant for the Induction of Cellular Immune Responses to Control Disease Status. *BioMed Research International* **Article ID 562924**.

Korting, H.C., Zienicke, H., Schäfer-Korting, M., Braun-Falco, O. (1990). *European Journal of Clinical Pharmacology* **39(4)**, 349-351.

Koutsoulas, C., Pippa, N., Demetzos, C. and Zabka, M. (2012). The role of ζ-potential on the stability of nanocolloidal systems. *Pharmakeftiki,* **24(4)**, 106-111.

Kraft, J.C., Freeling, J.P., Wang, Z. and Ho, R.J.Y. (2014). Emerging Research and Clinical Development Trends of Liposome and Lipid Nanoparticle Drug Delivery Systems. *Journal of Pharmaceutical Sciences* **103(1)**, 29-52.

Kulkarni, P.R., Yadav, J.D. and Vaidya, K.A. (2011). Liposomes: a novel drug delivery system. *International Journal of Current Pharmaceutical Research* **3(2)**, 10-18.

Lammers, T., Kiessling, F., Hennink, W.E. and Storm, G. (2012). Drug targeting to tumors: Principles, pitfalls and (pre-) clinical progress. *Journal of Controlled Release* **161**, 175-187.

Laouini, A., Jaafar-Maalej, C., Limayem-Blouza, I., Sfar, S., Charcosset, C. and Fessi, H. (2012). Preparation, Characterization and Applications of Liposomes: State of the Art. *Journal of Colloidal Science and Biotechnology* **1**, 147-168.

Lara-Ochoa, F. and Espinosa-Pérez, G. (2007). Cocrystals Definitions. *Supramolecular Chemistry* **19(8)**, 553-557.

Lasic, D.D. (1998). Novel applications of liposomes. *Trends in Biotechnology* **16**, 307-321.

Lee, E.H., Kim, A., Oh, Y-K. and Kim, C-K. (2005). Effect of edge activators on the formation and transfection efficiency of ultradeformable liposomes. *Biomaterials* **26**, 205-210.

Lee, S., Koo, H., Na, J.H., Lee, K.E., Jeong, S.Y., Choi, K., Kim, S.H., Kwon, I.C. and Kim, K. (2014). DNA Amplification in Neutral Liposomes for Safe and Efficient Gene Delivery. *ACS Nano* **8(5)**, 4257–4267.

Leserman, L.D., Barbet, J., Kourilsky, F. and Weinstein, J.N. (1980). Targeting to cells of fluorescent liposomes covalently coupled with monoclonal antibody or protein A. *Nature* **288(5791)**, 602-604.

Li, L., ten Hagen, T.L.M., Hossann, M., Süss, R., van Rhoon, G.C., Eggermont, A.M.M., Haemmerich, D. and Koning, G.A. (2013). Mild hyperthermia triggered doxorubicin release from optimized stealth thermosensitive liposomes improves intratumoral drug delivery and efficacy. *Journal of Controlled Release* **168**, 142–150.

Limtrakul, P., Chearwae, W., Shukla, S., Phisalphong, C. and Ambudkar, S.V. (2007). Modulation of function of three ABC drug transporters, P-glycoprotein (ABCB1), mitoxantrone resistance protein (ABCG2) and multidrug resistance protein 1 (ABCC1) by tetrahydrocurcumin, a major metabolite of curcumin. *Molecular Cellular Biochemistry* **296**, 85-95.

Lin, F-H., Lin, J-Y., Gupta, R.D., Tournas, J.A., Burch, J.A., Selim, M.A., Monteiro-Riviere, N.A., Grichnik, J.M., Zielinski, J. and Pinnell, S.R. (2005). Ferulic Acid Stabilizes a Solution of Vitamins C and E and Doubles its Photoprotection of Skin. *Journal of Investigative Dermatology* **125**, 826 –832.

Liptay, S., Weidenbach, H., Adler, G. and Schmid, R.M. (1998). Colon Epithelium Can Be Transiently Transfected with Liposomes, Calcium Phosphate Precipitation and DEAE Dextran in vivo. *Digestion* **59**, 142–147.

Liu, D., Hu, H., Lin, Z., Chen, D., Zhu, Y., Hou, S. and Shi, X. (2013). Quercetin deformable liposome: Preparation and efficacy against ultraviolet B induced skin damages in vitro and in vivo. *Journal of Photochemistry and Photobiology B: Biology* **127**, 8-17.

Liu, H., Zhang, Y., Han, Y., Zhao, S., Wang, Lu, Zhang, Z., Wang, J. and Chang, J. (2015). Characterization and cytotoxicity studies of DPPC:M^{2+} novel delivery system for

cisplatin thermosensitivity liposome with improving loading efficiency. *Colloids and Surfaces B: Biointerfaces* **131**, 12–20.

Lozano, N., Al-Ahmady, Z.S., Beziere, N.S., Ntziachristos, V. and Kostarelos, K. (2015). Monoclonal antibody-targeted PEGylated liposome-ICG encapsulating doxorubicin as a potential theranostic agent. *International Journal of Pharmaceutics* **482**, 2-10.

Lu, J. and Rohani, S. (2009). Preparation and characterization of theophylline-nicotinamide cocrystal. *Organic Process Research and Development* **13(6)**, 1269-1275.

Luciani, A., Olivier, J-C., Clement, O., Siauve, N., Brillet, P-Y., Bessoud, B., Gazeau, F., Uchegbu, I.F., Kahn, E., Frija, G. and Cuenod, C.A. (2004). Glucose-receptor MR imaging of tumors: study in mice with PEGylated paramagnetic niosomes. *Radiology,* **231(1)**, 135-142.

Ma, Y., Sobkiv, I., Gruzdys, V., Zhang, H. and Sun, X-L. (2012). Liposomal glyco-microarray for studying glycolipid-protein interactions. *Analitical and Bioanalitical Chemistry* **404(1)**, 51-58.

Maherani, B., Arab-Tehrany, E., Kheirolomoom, A., Geny, D. and Linder, M. (2013). Calcein release behavior from liposomal bilayer; influence of physicochemical/mechanical/structural properties of lipids. *Biochimie,* **95**, 2018-2033.

Marianecci, C., Marzio, L.D., Rinaldi, F., Celia, C., Paolino, D., Alhaique, F., Esposito, S. and Carafa, M. (2014). Niosomes from 80s to present: The state of the art. *Advances in colloid and interface science* **205**, 187-206.

Marom, M. and Azem, A. (2013). The Use of Cardiolipin-Containing Liposomes as a Model System to Study the Interaction Between Proteins and the Inner Mitochondrial Membrane. *Methods in Molecular Biology* **1033**, 147-155.

Marti, M., Coderch, L., de la Maza, A. and Parra, J.L. (2007). Liposomes of phosphatidylcholine: A biological natural surfactant as a dispersing agent. *Coloration Technology* **123(4)**, 237-241.

Martín-Molina, A., Rodríguez-Beas, C. and Faraudo, J. (2012). Effect of Calcium and Magnesium on Phosphatidylserine Membranes:Experiments and All-Atomic Simulations. *Biophysical Journal* **102**, 2095–2103.

Melzak, K.A., Melzak, S.A., Gizeli, E. and Toca-Herrera, J.L. (2012). Cholesterol Organization in Phosphatidylcholine Liposomes: A Surface Plasmon Resonance Study. *Materials* 5, 2306-2325.

Mezei, M. and Gulasekharam, V. (1980). Liposomes - a selective drug delivery system for the topical route of administration I. Lotion dosage form. *Life Sciences* **26(18)**, 1473-1477.

Milne, C.G., Shelby Jr., P.P., Agricultural pesticide formulations, US Patent 5,958,463, 1999.

Morissette, S.L., Almarsson, Ö., Peterson, M.L., Remenar, J.F., Read, M.J., Lemmo, A.V., Ellis, S., Cima, M.J. and Gardner, C.R. (2004). High-throughput crystallization: polymorphs, satls, co-crystals and solvates of pharmaceutical solids. *Advanced drug delivery reviews* **56**, 275-300.

Morrow, D.I.J., McCarron, P.A., Woolfson, A.D. and Donnelly, R.F. (2007). Innovative Strategies for Enhancing Topical and Transdermal Drug Delivery. *The Open Drug Delivery Journal* 1, 36-59.

Mosgoeller, W., Prassl, R. and Zimmer, A. (2012). Nanoparticle-Mediated Treatment of Pulmonary Arterial Hypertension. *Methods in Enzymology* **508**, 325-354.

Mozafari, M.R., Johnson, C., Hatziantoniou, S. and Demetzos, C. (2008). Nanoliposomes and Their Applications in Food Nanotechnology. *Journal of liposome research* **18**, 309-327.

Murugan, P. and Pari, L. (2006). Antioxidant effect of tetrahydrocurcumin in streptozotocin-nicotinamide induced diabetic rats. *Life Sciences* **79**, 1720-1728.

Niu, M., Lu, Y., Hovgaard, L. and Wu, W. (2011). Liposomes containing glycocholate as potential oral insulin delivery systems: preparation, in vitro characterization, and improved protection against enzymatic degradation. *Journal of nanomedicine* **6**, 1155-1166.

Nomura, F., Nagata, M., Inaba, T., Hiramatsu, H., Hirokazu, H. and Takiguchi, K. (2001). Capabilities of liposomes for topological transformation. *Prodeeding of the National Academy of Sciences USA, **98***(5), 2340–2345.

Northfelt, D.W., Kaplan, L., Russell, J. Volberding, P.A. and Martin, F.J. (1995). Pharmacokinetics and tumor localization of DOX-SL (Stealth liposomal doxorubicin) by comparison with Adriamycin in patients with AIDS and Kaposi's sarcoma. In *Stealth Liposomes*, ed. Lasic, D. and Martin, F. CRC Press (Florida, USA), Chapter 22, 257-266.

Obata, Y., Tajima, S. and Takeoka, S. (2010). Evaluation of pH-responsive liposomes containing amino acid-based zwitterionic lipids for improving intracellular drug delivery in vitro and in vivo. *Journal of Controlled Release* **142**, 267–276.

Oberholzer, T., Meyer, E., Amato, I., Lustig, A. and Monnard, P-A. (1999). Enzymatic reactions in liposomes using the detergent-induced liposome loading method. *Biochimica et Biophysica Acta* **1416**, 57-68.

Ogiwara, T., Satoh, K., Kadoma, Y., Murakami,Y., Unten, S., Atsumi, T., Sakagami, H. and Fujisawa, S. (2002). Radical scavenging activity and cytotoxicity of ferulic acid. *Anticancer Research* **22(5)**, 2711–2717.

Okada, K., Wangpoengtrakul, C., Tanaka, T., Toyokuni, S., Uchida, K. and Osawa, T. (2001). Curcumin and especially tetrahydrocurcumin ameliorate oxidative stress-induced renal injury in mice. *The Journal of Nutrition* **131**, 2090-2095.

Ono, K., Hasegawa, K., Naiki, H. and Yamada, M. (2004). Curcumin has potent anti-amyloidogenic effects for Alzheimer's β-amyloid fibrils in vitro. *Journal of Neuroscience Research* **75(6)**, 742-750.

Padrela, L., Rodrigues, M.A., Velaga, S.P., Matos, H.A. and de Azevedo, E.G. (2009). Formation of indomethacin-saccharin cocrystals using supercritical fluid technology. *European Journal of Pharmaceutical Sciences* **38**, 9-17.

Paolino, D., Lucania, G., Mardente, D., Alhaique, F. and Fresta, M. (2005). Ethosomes for skin delivery of ammonium glycyrrhizinate: in vitro percutaneous permeation through human skin and in vivo anti-inflammatory activity on human volunteers. *Journal of Controlled Release* **106**, 99-110.

Pari, L. and Murugan, P. (2007). Antihyperlipidemic effect of curcumin and tetrahydrocurcumin in experimental type 2 diabetic rats. *Renal Failure* **29(7)**, 881-889.

Patel, H.M. (1992). Serum opsonins and liposomes: their interaction and opsonophagocytosis. *Critical Reviews in Therapeutic Drug Carrier Systems* **9(1)**, 39–90.

Patravale, V.B. and Mandawgade, S.D. (2008). Novel cosmetic delivery systems: an application update. *International Journal of Cosmetic Science* **30**, 19–33.

Paul, A., Cevc, G. and Bachhawat, B.K. (1995). Transdermal immunisation with large proteins by means of ultradeformable drug carriers. *European Journal of Immunology* **25**, 3521-3524.

Peltier, S., Oger, J-M., Lagarce, F., Couet, W. and Benoît, J-P. (2006). Enhanced oral paclitaxel bioavailability after administration of paclitaxel-loaded lipid nanocapsules. *Pharmaceutical Research* **23(6)**, 1243-1250.

Pendurthi, U.R. and Rao, L.V.M. (2000). Suppression of transcription factor Egr-1 by curcumin. *Thrombosis Research* **97**, 179-189.

Peng, X., Kong, B., Xia, X. and Liu, Q. (2010). Reducing and radical-scavenging activities of whey protein hydrolysates prepared with Alcalase. *International Dairy Journal* **20**, 360–365.

Purohit, G., Sakthivel, T. and Florence, A.T. (2001). Interaction of cationic partial dendrimers with charged and neutral liposomes. *International Journal of Pharmaceutics* **214**, 71–76.

Qiao, N., Li, M., Schlindwein, W., Malek, N., Davies, A. and Trappitt, G. (2011). Pharmaceutical cocrystals: An overview. *International Journal of Pharmaceutics* **419**, 1-11.

Quer, C.B., Elsharkawy, A., Romeijn, S., Kros, A. and Jiskoot, W (2012). Cationic liposomes as adjuvants for influenza hemagglutinin: More than charge alone. *European Journal of Pharmaceutics and Biopharmaceutics* **81**, 294–302.

Rukkumani, R., Aruna, K., Varma, P.S., Rajasekaran, K.N. and Menon, V.P. (2004). Comparative effects of curcumin and an analog of curcumin on alcohol and PUFA induced oxidative stress. *Journal of Pharmacy and Pharmaceutical Sciences* **7(2)**, 274-283.

Sabín, J., Prieto, G., Ruso, J.M. and Sarmiento, F. (2007). Fractal aggregates induced by liposome-liposome interaction in the presence of Ca 2^{+}. *The European Physical Journal E* ***24*(2)**, 201-210.

Sánchez, M., Aranda, F.J., Terual, J.A. and Ortiz, A. (2011). New pH-sensitive liposomes containing phosphatidylethanolamine and a bacterial dirhamnolipid. *Chemistry and Physics of Lipids* **164**, 16–23.

Sandur, S.K., Pandey, M.K., Sung, B., Ahn, K.S., Murakami, A., Sethi, G., Limtrakul, P., Badmaev, V. and Aggarwal, B.B. (2007). Curcumin, demethoxycurcumin, bisdemethoxycurcumin, tetrahydrocurcumin and turmerones differentially regulate anti-inflammatory and ani-proliferative responses through a ROS-independent mechanism. *Carcinogenesis* 28(8), 1765-1773.

Sawant, R.M., Hurley, J.P., Salmaso, S., Kale, A., Tolcheva, E., Levchenko, T.S. and Torchilin, V.P. (2006). "SMART" drug delivery systems: Double-targeted pH-responsive pharmaceutical nanocarriers. *Bioconjugate Chemistry,* **17(4)**, 943-949.

Scomparin, A., Salmaso, S., Eldar-Boock, A., Ben-Shushan, D., Ferber, S., Tiram, G., Shmeeda, H., Landa-Rouben, N., Leor, J., Caliceti, P., Gabizon, A. and Satchi-Fainaro, R. (2015). A comparative study of folate receptor-targeted doxorubicin delivery systems: Dosing regimens and therapeutic index. *Journal of Controlled Release* **208**, 106–120.

See, E., Zhang, W., Liu, J., Svirskis, D., Baguley, B.C., Shaw, J.P., Wang, G. and Wu, Z. (2014). Physicochemical characterization of asulacrine towards the development of an anticancer liposomal formulation via active drug loading: Stability, solubility, lipophilicity and ionization. *International Journal of Pharmaceutics* **473**, 528–535.

Selter, S. (1988a). Contrast-Carrying Liposomes: Current Status. *Investigative Radiology,* **23**, S122-S125.

Seltzer, S.E., Swensson, R.G., Rudy, P.F. and Nawfel, R.D. (1988b). Size Discrimination in Computered Tomographic Images. Effects of Feature Contrast and Display Window. *Investigative Radiology* **23(6)**, 455-462.

Senior, J. and Gregoriadis, G. (1982). Stability of small unilamellar liposomes in serum and clearance from the circulation: The effect of the phospholipid and cholesterol components. *Life Sciences,* **30(24)**, 2123-2136.

Sharma, S., Kulkarni, S.K. and Chopra, K. (2006). Curcumin, the active principle of turmeric (*Curcuma longa*), ameliorates diabetic nephropathy in rats. *Clinical and Experimental Pharmacology and Physiology* **33(10)**, 940-945.

Shayanfar, A., Velaga, S. and Jouyban, A. (2014). Solubility of carbamazepine, nicotinamide and carbamazepine-nicotinamide cocrystal in ethanol-water mixtures. *Fluid Phase Equilibria* **363**, 97-105.

Shevchenko, A., Bimbo, L.M., Miroshnyk, I., Haarala, J., Jelínková, K., Syrjänen, K., van Veen, B., Kiesvaara, J., Santos, H.A. and Yliruusi, J. (2012). A new cocrystal and salts of itraconazole: Comparison of solid-state properties, stability and dissolution behavior. *International Journal of Pharmaceutics* **436,** 403-409.

Sheveleva, I.A., Belokurova, O.A., Shcheglova, T.L. and Mel'nikov, B.N. (2003). Polyfunctional properties of liposomes in preparation of textile materials. *Fibre Chemistry* **35(1)**, 48-52.

Sies, H. (1997). Oxidative stress: oxidants and antioxidants. *Experitnental Physiology* **82,** 291-295.

Simon, R.H., Ho, S-Y., D'Arrigo, J., Wakefield, A. and Hamilton, S.G. (1990). Lipid-coated ultrastable microbubbles as a contrast agent in neurosonography. *Investigative Radiology,* 25(12), 1300-1304.

Sinha, S., Baboota, S., Ali, M., Kumar, A. and Ali, J. (2009). Solid dispersion: An alternative technique for bioavailability enhancement of poorly soluble drugs. *Journal of dispersion science and technology* **30(10)**, 1458-1473.

Sorgi, F.L. and Huang, L. (1996). Large scale production of DC-Chol cationic liposomes by microfluidization. *International Journal of Pharmaceutics* **144**, 131-139.

Sowa, M., Ślepokura, K. and Matczak-Jon, E. (2014). A 1:1 pharmaceutical cocrystal of myricetin in combination with uncommon piracetam conformer: X-ray single crystal analysis and mechanochemical synthesis. *Journal of Molecular Structure* **1058**, 114-121.

Srisuk, P., Thongnopnua, P., Raktannonchai, U. and Kanokpanont, S. (2012). Physico-chemical characteristics of methotrexate-entrapped oleic acid-containing deformable liposomes for in vitro transepidermal delivery targeting psoriasis treatment. *International Journal of Pharmaceutics* **427**, 426– 434.

Sugandha, K., Kaity, S., Mukherjee, S., Isaac, J. and Ghosh, A. (2014). Solubility enhancement of ezetimibe by a cocrystal engineering technique. *Crystal Growth & Design,* **14(9)**, 4475-4486.

Syu, W-J., Shen, C-C., Don, M-J., Ou, J-C., Lee, G-H. and Sun, C-M. (1998). Cytotoxicity of curcuminoids and some novel compounds from *Curcuma zedoaria. Journal of Natural Products* **61(12)**, 1531-1534.

Tao, L., Faig, A. and Uhrich, K.E. (2014). Liposomal stabilization using a sugar-based, PEGylated amphiphilic macromolecule. *Journal of Colloid and Interface Science* **431**, 112-116.

The Cancer Genome Atlas Network (2012a). Comprehensive molecular characterization of human colon and rectal cancer. *Nature* **487(7407)**, 330-337.

The Cancer Genome Atlas Network (2012a). Comprehensive molecular portraits of human breast tumours. *Nature* **490(7418)**, 61-70.

The Cancer Genome Atlas Research Network (2012). Comprehensive genomic characterization of squamous cell lung cancers. *Nature* **489(7417)**, 519-525.

The Cancer Genome Atlas Research Network (2013a). Genomic and epigenomic landscapes of adult de novo acute myeloid leukemia. *The New England Journal of Medicine* **368(22)**, 2059-2074.

The Cancer Genome Atlas Research Network (2013b). Integrated genomic characterization of endometrial carcinoma. *Nature* **497(7447)**, 67–73.

Toimil, P., Daviña, R., Sabín, J., Prieto, G. and Sarmiento, F. (2012). Influence of temperature on the colloidal stability of the F-DPPC and DPPC liposomes induced by lanthanum ions. *Journal of Colloid and Interface Science* **367**, 193–198.

Tønnesen, H.H., Karlsen, J. and Mostad, A. (1982). Structural Studies of Curcuminoids. I. The Crystal Structure of Curcumin. *Acta Chemica Scandinavica B* **36**, 475-479.

Touitou, E., Dayan, N., Bergelson, L., Godin, B. and Eliaz, M. (2000). Ethosomes-novel vesicular carriers for enhanced delivery: characterization and skin permeation properties. *Journal of Controlled Release,* **65**, 403-418.

Trask, A.V., Samuel Motherwell, W.D. and Jones, W. (2005). Pharmaceutical cocrystallization: Engineering a remedy for caffeine hydration. *Crystal Growth & Design* **5(3)**, 1013-1021.

Trombino, S., Serini, S., Di Nicuolo, F., Celleno, L., Ando, S., Picci, N., Calviello, G. and Palozza, P. (2004).Antioxidant effect of ferulic acid in isolated membranes and intact cells: Synergistic interactions with α-tocopherol, β-carotene, and ascorbic acid. Journal of *Agricultural and Food Chemistry* **52(8)**, 2411-2420.

Trombino, S., Serini, S., Di Nicuolo, F., Celleno, L., Andò, S., Picci, N., Calviello, G. and Palozza, P. (2004). Antioxidant effect of ferulic acid in isolated membranes and intact cells: Synergistic interactions with α-tocopherol, β-carotene, and ascorbic acid. Joutnal of *Agricultural Food Chemistry* **52(8)**, 2411-2420.

Tsai, M-F., Jiang, D., Zhao, L., Clapham, D. and Miller, C. (2013). Functional reconstitution of the mitochondrial Ca^{2+}/H^{+} antiporter Letm1. *The Journal of General Physiology* **143(1)**, 67–73.

Tsujimura, K., Ikehara, Y., Nagata, T., Koide, Y. and Kojima, N. (2009). Induction of anti-tumor immune responses with oligomannose-coated liposomes targeting to peritoneal macrophages. *Procedia in Vaccinology* **1**, 127–134.

Uchegbu, I.F. and Florence, A.T. (1995). Non-ionic surfactant vesicles (niosomes): physical and pharmaceutical chemistry. *Advances in Colloid and Interface Science* ***58***, 1-55.

Umeda, Y., Fukami, T., Furuishi, T., Suzuki, T., Tanjoh, K. and Tomono, K. (2009). Characterization of multicomponent crystal formed between indomethacin and lidocaine. *Drug Development and Industrial Pharmacy* **35(7)**, 843-851.

Van Driessche, A., Ponsaerts, P., Van Bockstaele, D.R., Van Tendeloo, V.F.I. and Berneman, Z.N. (2005). Messenger RNA electroporation: an efficient tool in immunotherapy and stem cell research. *Folia Histochemica et Cytobiologica,* **43(4)**, 213-216.

Wang, C-Y. and Huang, L. (1989). Highly efficient DNA delivery mediated by pH-sensitive immunoliposomes. *Biochemistry* **28(24)**, 9508–9514.

Wang, Y., Su, H.h., Yang, Y., Hu, Y., Zhang, L., Blancafort, P. and Huang, L. (2013). Systemic delivery of modified mRA encoding herpes simplex virus 1 thymidine kinase for targeted cancer gene therapy. *Molecular Therapy* **21(2)**, 358-367.

Watarai, S., Onuma, M., Yamamoto, S. and Yasuda, T. (1990). Inhibitory Effect of Liposomes Containing Sulfatide or Choleterol Sulfate on Syncytium Formation Induced by Bovine Immunodeficiency Virus-Infected Cells. *Journal of Biochemistry* **108(4)**, 507-509.

Webb, M., Harasym, T.O., Masin, D., Bally, M.B. and Mayer, L.D. (1995). Sphingomyelin-cholesterol liposomes significantly enhance the pharmacokinetic and therapeutic properties of vincristine in murine and human tumour models. *British Journal of Cancer* **72(4)**, 896-904.

Weinstein, J.N., Magin, R.L., Yatvin, M.B. and Zaharko, D.S. (1979). Liposomes and local hyperthermia: selective delivery of methotrexate to heated tumors. *Science* **204**, 188–191.

Yamada, J. and Tomita, Y. (1996). Antimutagenic activity of caffeic acid and related compounds. *Bioscience, Biotechnology, and Biochemistry* **60(2)**, 328-329.

Yang, S., Gursoy, R.N., Lambert, G. and Benita, S. (2004). Enhanced oral absorption of paclitaxel in a novel self-microemulsifying drug delivery system with or without concomitant use of P-glycoprotein inhibitors. *Pharmaceutical Research* **21(2)**, 261-270.

Yatvin, M.B., Weinstein, J.N., Dennis, W.H. and Blumenthal, R. (1978). Design of liposomes for enhanced local release of drugs by hyperthermia. *Science* **202**, 1290–1293.

Yu, S., Wang, Q-M., Wang, X., Liu, D., Zhang, W., Ye, T., Yang, X. and Pan, W. (2015). Liposome incorporated ion sensitive in situ gels for opthalmic delivery of timolol maleate. *International Journal of Pharmaceutics* **480**, 128-136.

Zhang, H., Wang, Z., Gong, W., Li, Z., Mei, X. and Lv, W. (2011). Development and characteristics of temperature-sensitive liposomes for vinorelbine bitartrate. *International Journal of Pharmaceutics* **414**, 56–62.

Zhang, M., Li, H., Lang, B., O'Donnell, K., Zhang, H., Wang, Z., Dong, Y., Wu, C. and Williams III, R.O. (2012). Formulation and delivery of improved amorphous fenofibrate solid dispersions prepared by thin film freezing. *European Journal of Pharmaceutics and Biopharmaceutics* **82**, 534-544.

Zhou, C., Mao, Y., Sugimoto, Y., Zhang, Y., Kanthamneni, N., Yu, B., Brueggemeier, R.W., Lee, L.J. and Lee, R.J. (2012). SPANosomes as delivery vehicles for small interfering RNA (siRNA). *Molecular Pharmaceutics* **9**, 201-210.

Zuidam, N.J., Gouw, H.K.A.E., Barenholz, Y. and Crommelin, D.J.A. (1995). Physical (in)stability of liposomes upon chemical hydrolysis: the role of lysophospholipids and fatty acids. *Biochimica et Biophysica Acta* **1240**, 101-110.

Zuris, J.A. Thompson, D.B., Shu, Y., Guilinger, J.P., Bessen, J.L., Hu, J.H., Maeder, M.L., Joung, J.K.. Chen, Z.Y. and Liu, D.R. (2015). Cationic lipid-mediated delivery of proteins enables efficient protein-based genome editing in vitro and in vivo. *Nature Biotechnology* **33**, 73–80.

CHAPTER 2

LIPOSOMES ENCAPSULATING THE HIGHLY ANTIOXIDANT METHANOL EXTRACT OF STEM-BARK OF *Schumacheria castaneifolia* VAHL: PREPARATION AND *IN VITRO* EVALUATION

2.1 Introduction

Since liposomes were first reported by Bangham and coworkers in the 1960s (Bangham, Standish and Watkins, 1965), these vesicles have been utilized for numerous purposes in various fields including pharmaceutical industry, cosmetic industry and food industry. Liposomes and liposome analogs are used mainly as drug delivery vehicles or as bioactive agent carriers (Lasic, 1998). Although numerous plant-derived pure bioactive compounds have been incorporated in liposomes, purification of these compounds involves multiple steps that are time consuming and costly. Therefore, it is desirable to encapsulate plant extracts, instead of pure compounds, in liposomes, concurrently targeting improved therapeutic efficacy and pharmacokinetics (Gortzi *et al.*, 2007; Yamamoto *et al.*, 2002).

Yamamoto and coworkers noted greater inhibitory effects on the growth of tumour cells upon encapsulation of extracts from *Ginkgo biloba* L. leaves in hybrid liposomes (Yamamoto *et al.*, 2002). Furthermore, Gortzi et. al. demonstrated that the antioxidant and antimicrobial activities of *Origanum dictamnus* extracts improved upon encapsulation in liposomes (Gortzi *et al.*, 2007). In addition, numerous plant-derived drugs, such as usnic acid, wogonin, and colchicines, have shown sustained release properties after liposomal encapsulation (Godin and Touitou, 2004; Ke *et al.*, 2007; Lira *et al.*, 2009). Liposomal encapsulation may be used as a means of enhancing skin delivery of plant-derived drugs. For example, colchicines possessing antigout properties show increased skin accumulation while catechins possessing antioxidant and anticancer properties show increased skin permeation when encapsulated in liposomes (Fang *et al.*, 2006; Godin and Touitou, 2004). In addition, numerous other benefits such as improving bioavailability, facilitating specific-targeting, reducing dose, and/or reducing dosing frequency of encapsulated material have been reported (El-Samaligy, Afifi and Mahmoud, 2006; Pripem *et al.*, 2008; Sinico *et al.*, 2005).

The cosmetic industry employs numerous plant extracts encapsulated in liposomes, notably liposomal extracts of papaya and carrot containing β-carotene (Rebmann, 2014). In this study, the methanol extract of stem bark of *Schumacheria castaneifolia* Vahl, one of the three representative species of the endemic genus Schumacheria, was encapsulated in liposomes. Sri Lankan flora consists of a high degree of endemic plants possessing potent biological activity (Bandara *et al.*, 1990). *S. castenifolia* exhibited exceptionally high antioxidant properties (Bandara *et al.*, 2011) and moderate antimicrobial properties (Bandara *et al.*, 2012) showing good potential in its use in the cosmetics/pharmaceutical applications.

Gurni and Kubitzki published, in 1981, the presence of the polyphenols: quercetin, kaempferol, quercetin 3-sulphate, kaempferol 3-sulphate, kaempferol 3,7-disulphate, prodelphinidin and procyanidin in *S. castaneifolia*, all of which may function as antioxidants (Gurni and Kubitzki, 1981). Recent studies on the methanol extract of stem bark of *S. castaneifolia* have shown the presence of polyphenolic compounds (Bandara *et al.*, 2012). In addition to its high antioxidant activity, this plant extract has moderate antimicrobial activity (Bandara *et al.*, 2012). An advantage of the extract is its insignificant cytotoxicity (Bandara *et al.*, 2011) which favours its use in pharmaceutical, cosmetic or food industries. Thus, we report herein the encapsulation of the methanol extract of stem bark of *S. castaneifolia* in liposomes with a view to studying its efficacy and release.

The properties of liposomes are dependent on the lipid composition. In fact, encapsulation efficiency and loading capacity are two important properties that usually depend on the lipid composition. It has been shown that successful encapsulation of cytochrome C required CH incorporated liposomes whereas encapsulation of vitamin E had no such constraints (Cagdas *et al.*, 2011). The effect of CH incorporation on the size of liposomes was also demonstrated by Cagdas et al. who discovered that the size of cytochrome C encapsulated and unencapsulated liposomes increased upon addition of CH, but had no effect on the size of vitamin E encapsulated liposomes (Cagdas *et al.*, 2011). Another important property- zeta potential, is dependent on the charge and nature of the lipids in the bilayer (Hurler *et al.*, 2013). The effect of the nature of lipids on stability of liposomes were demonstrated by Kokkona and coauthors who found that liposomes made of polar lipids of higher transition temperatures were more stable (Kokkona *et al.*, 2000).

Other than the properties stated above (i.e. size, zeta-potential, EE and LC), release properties of liposomes may show a pronounced variation with the lipid composition. For example, Papahadjopoulos and coworkers illustrated that incorporation of CH in

phospholipid membranes resulted in a decrease of the permeability of membranes to Na^+, K^+, Cl^- and glucose (Papahadjopoulos, Nir and Ohki, 1971).

Apart from the lipid composition, the pH and ionic strength of the release medium, also, play a critical role in determining the release properties of liposomes. For example, Baptista et al., reported that there is a significant effect of the pH of the medium on the release kinetics of dyes encapsulated in liposomes (Baptista *et al.*, 2003). Furthermore, the ionic strength of the medium may affect the release properties of the encapsulated material by compromising the stability of the liposomes (Carrión, de la Maza and Parra, 1994; Minami, Inoue and Shimozawa, 1993; Virden and Berg, 1992). Since physiologically relevant buffers differ in pH and ionic strength, release of liposomal material in those buffers may show different kinetics.

Lyoprotectants increase the stability of liposomes by preventing aggregation and fusion of liposomes. Suzuki and coauthors reported that complete prevention of aggregation and/or fusion of calcein encapsulated liposomes as well as leakage of encapsulated material is achievable by using glucose or maltose during lyophilization (Suzuki, Komatsu and Miyajima, 1996). Moreover, Harrigan and coauthors suggested that barrier properties of liposomal membranes may be enhanced by incorporation of lyoprotectants in liposomes (Harrigan, Madden and Cullis, 1990). Although lyoprotectants increase the stability and membrane barrier properties of liposomes, utilization of lyoprotectants may be undesirable if LC of liposomes is compromised.

Thus, this study was designed to evaluate the effect of lipid composition on properties such as EE, LC, size, zeta-potential, stability, and release, and to investigate the effect of release medium on the slow and sustained-release properties of liposomes encapsulating the methanol extract of stem bark of *S. castaneifolia*. The results of this study should be useful mainly in modulating properties of liposomes encapsulating plant material.

2.2 Materials and methods

2.2.1 Materials

Egg yolk PC (~ 60% TLC) and CH (assay > 98%) and DPPH were purchased from Sigma-Aldrich. Sucrose (Extra Pure) and diethyl ether were from LOBA Chemie PVT.

LTD., India. Dicloromethane, ethanol and methanol were from Sigma and other chemicals were of analytical grade. Dialysis tubing (12 400 Da MWCO) was from Sigma-Aldrich while Sephadex G50 was from GE healthcare. Deionized water filtered through a 0.2 μm filter was used for all experiments.

2.2.2 Methods

2.2.2.1 Collection and extraction of S. castaneifolia methanol extract

Plant materials of *S. castaneifolia* were collected from Thummodara region in Ratnapura, Sri Lanka. The specimen was identified by Dr. Siril Wijesundara of the Royal Botanic Gardens, Peradeniya, Sri Lanka. Stem bark was air dried and ground into particles and sequentially extracted into dichloromethane and methanol at room temperature using a bottle shaker and the extract was evaporated under reduced pressure using a rotary evaporator at room temperature.

2.2.2.2 Evaluation of antioxidant activity

The antioxidant activity of methanol extract of stem bark of *S. castaneifolia* was determined using DPPH radical scavenging assay which was expressed as IC_{50} values as described by Budzianowski and Budzianowska (Budzianowski and Budzianowska, 2006). The final concentration of DPPH in the test mixture was maintained at 1×10^{-4} mol dm^{-3} in methanol. As the positive control, α-tocopherol was used. The IC_{50} values were determined using a concentration series, ranging from 1, through 5, 10, 15, 20, 40, 60, 80 to 100 ppm of solutions. After 30 min, the absorbance at 517 nm of the test mixture was determined using a spectrophotometer (Shimadzu, UV-1800); all the tests were carried out in triplicate.

The following equation was used to calculate percent antioxidant activity:

$$Percent\ antioxidant\ activity = \frac{A_i - A_f}{A_i} \times 100$$

where, A_i is the initial absorbance of the test mixture (i.e. sum of absorbance values of DPPH solution (1×10^{-4} mol dm^{-3}) and of plant extracts at relevant concentration level) and A_f is the final absorbance of the test mixture (i.e. after 30 min).

2.2.2.3 Preparation of liposomes

Unencapsulated liposomes were prepared following the reverse phase evaporation method (Szoka Jr. and Papahadjopoulos, 1978). An emulsion was made using diethyl ether (8 ml) in which the lipids (100 mg) were dissolved to which water (2.4 ml) was added. The ratios of PC to CH used to prepare liposomes were: 10:0, 9:1, 8:2, 7:3 and 6:4.

Plant material encapsulated liposomes were prepared as described above where an emulsion was made using diethyl ether (8 ml) in which the lipids (100 mg) were dissolved to which aqueous solution (2.4 ml) of water soluble plant extract was added. Organic solvent was evaporated using a rotary evaporator to form liposomes in the aqueous phase. The total volume of each liposome solution was adjusted to 20 ml using deionized water and sonicated. Unencapsulated plant material was separated from liposomes either by centrifugation or gel filtration. Also, plant extract loaded liposomes were prepared in the presence of 2.5 % (w/v) sucrose using the same lipid ratios as above.

Preparation of each liposomal formulation was carried out in triplicate.

2.2.2.4 Determination of particle size and zeta-potential

Particle sizes of liposomes were determined using a Malvern zetasizer NanoZS (Malvern instruments, UK) fitted with a red laser of 633 nm, using dynamic light scattering technique. Liposome suspensions were diluted in deionized water, filtered with a 0.2 μm filter, and the scattering intensity was measured at an angle of 173° relative to the incident radiation after equilibrating the samples at 25 °C. The values reported are the z-average diameters of liposomes. Zeta-potentials of the same liposomal suspensions described above were measured using the Malvern zetasizer fitted with a red laser of 633 nm, using Laser Doppler Electrophoresis technique. The values reported are the z-average zeta-potentials of liposomes. In order to determine the stability variation with time, the liposomal solutions were stored at 4 °C for 2 months and the particle size and zeta-potential were measured after each month. The concentration of lipids in solution during storage was 5 mg / ml for all liposomal formulations.

2.2.2.5 Determination of loading capacity (LC)

Purified liposomes (through gel filtration) were freeze dried and 5.0 mg of dry liposomes were disrupted using a mixture of ethanol and methanol (75:25). This procedure was repeated using purified unencapsulated liposomes.

LC was determined spectrophotometrically by measuring the absorbance of disrupted plant extract encapsulated liposomes against disrupted unencapsulated liposomes at 224 nm.

The formula used to calculate the loading capacity is given below:

$$LC = \frac{Mass\ of\ encapsulated\ plant\ extract}{Mass\ of\ plant\ extract\ encapsulated\ liposomes} \times 100$$

2.2.2.6 Determination of encapsulation efficiency (EE)

EE determined spectrophotometrically was calculated using the formula given below:

$$EE = \frac{Mass\ of\ encapsulated\ plant\ extract}{Mass\ of\ plant\ extract\ initially\ introduced} \times 100$$

2.2.2.7 In vitro *release study*

Liposomes of five different lipid compositions were used for release studies conducted using the dialysis bag method in deionized water. Release from liposomes with PC : CH - 9:1 was performed in three different media: deionized water, phosphate buffered saline (pH 7.4) and artificial sweat (pH 4.7). Aliquots withdrawn from the release medium at predetermined time intervals over a period of 7 h were replenished immediately with fresh medium. The released plant extract was quantified spectrophotometrically by measuring absorbance at 210 nm - the most prominent peak of the plant extract absorbing UV radiation.

2.2.2.8 Statistical analysis

All data are presented as mean ± standard deviation (S.D.) of three parallel experiments (n = 3). Microsoft Office Excel 2007 was used for the above calculations. One way ANOVA was conducted using MINITAB 14 software to compare the results and $P < 0.05$ was considered significant.

2.3 Results and discussion

2.3.1 Antioxidant activity

Methanol extracts of plants possessing high polyphenol content usually exhibit high antioxidant activity due to their affinity for scavenging free radicals. Accordingly, the methanol extract of stem bark of *S. castaneifolia,* which has a total polyphenol content of 68.5 mg/g of gallic acid equivalents in dry plant material (Bandara *et al.*, 2012), exhibited high antioxidant activity as per DPPH radical scavenging assay. In fact, the antioxidant activity of the methanol extract of stem bark of *S. castaneifolia* (IC_{50} 9.8 ± 0.3) was comparable to that of *dl*-α-tocopherol (IC_{50} 10.9 ± 4.3) which is a highly potent antioxidant.

Synergism among multiple antioxidants is well documented. Rosmarinic acid was found to act synergistically with phenolic compounds such as quercetin or caffeic acid (Peyrat-Maillard, Cuvelier and Berset, 2003). The plant extract of *Lactuca sativa* showed synergism with quercetin indicating the synergistic activity of plant extracts (Altunkaya *et al.*, 2009). Moreover, Iacopini and co-workers studied interactions of five antioxidants in red grape and reported that quercetin, rutin and resveratrol may show synergy (Iacopini *et al.*, 2008). Indeed, the high antioxidant activity observed with the methanol extract of stembark of *S. castaneifolia* may be due to synergistic interactions among, especially, polyphenols of the extract.

2.3.2 Encapsulation efficiency and loading capacity

EE and LC were determined by using a spectrophotometric method and the values are shown in table 2. Our results indicated that EE and LC of conventional liposomes containing the methanol extract of stem bark of *S. castaneifolia* are dependent on the lipid composition. Increasing the percentage of cholesterol from 0 % to 10 %, increased the encapsulation efficiency from 66.81 % to 85.59 %. However, when the percentage of CH was increased from 10 % to 20 %, EE increased only marginally (Table 2). In fact, there was no significant difference between EEs of plant extract loaded liposomes with a CH content of 10 % and of 20 %. However, EE decreased drastically from 86.41% to 44.55% when the percentage of CH was further increased (i.e. from 20 % to 40 %). Thus, the optimum ratios of PC to CH for the encapsulation of the highly antioxidant methanol extract of stem bark of *S castaneifolia* are 9:1 and 8:2.

Table 2. Encapsulation efficiencies and loading capacities of liposomal formulations of different lipid compositions (each value is the mean of values obtained from three independent trials ± S.D.)

Liposomal formulation PC:CH	Lyoprotectant	Loading capacity (%)	Encapsulation efficiency (%)
10:0	x	6.26 ± 0.03	66.81 ± 0.38
	✓	6.73 ± 0.07	
9:1	x	7.88 ± 0.02	85.59 ± 0.26
	✓	7.99 ± 0.02	
8:2	x	7.95 ±0.02	86.41 ± 0.25
	✓	8.04 ± 0.03	
7:3	x	5.58 ± 0.03	59.05 ± 0.32
	✓	5.21 ± 0.03	
6:4	x	4.27 ± 0.03	44.55 ± 0.29
	✓	4.48 ± 0.04	

LC of liposomes prepared in the absence of the lyoprotectant, sucrose, ranged from 4.2 % to 8.0 % while that of liposomes prepared in the presence of sucrose ranged from 4.5 % to 8.0 % (Table 2). This shows that the presence of lyoprotectants has no significant effect on LCs of extract encapsulated liposomes. The variation of LC with CH content exhibited a similar pattern to that of EE. LC increased upon increasing the CH content from 0 % to 10 %. However, on further increase of CH from 10 % to 20 %, only a marginal increase of LC occurred. A drastic decrease in LC when cholesterol content exceeded 20% was observed. There was no significant difference between the loading capacity of liposomes with CH content of 10 % and of 20 %. Therefore, according to LC too, the optimum ratios of PC to CH are 9:1 and 8:2.

Basically, this study shows that EE and LC of plant material encapsulated liposomes are dependent on the lipid composition of liposomes. The increase of size of liposomes upon incorporation of CH may have contributed to the observed increase of EE and LC of liposomes. Since the methanol extract of *S. castaneifolia* is highly soluble in water, it is expected to reside mainly in the aqueous interior of liposomes. Therefore, an increase in the size of liposomes may correspond to an increase in EE and LC. Interestingly, our results are consistent with the results of Cagdas and coworkers who

demonstrated that incorporation of CH in the lipid bilayer is essential for successful encapsulation of water soluble species in liposomes (Cagdas *et al.*, 2011). In summary, the results of this study indicate that the encapsulation of water-soluble plant material may be increased by incorporating CH in the lipid bilayer of PC liposomes.

2.3.3 Particle size and zeta-potential

In this study, the effect of CH on the size and zeta-potential of unencapsulated liposomes and plant extract encapsulated liposomes was evaluated. The measurements on variation of size and zeta-potential with time of all liposomal formulations were performed immediately after preparation, after one month, and after 2 months.

2.3.3.1 Variation of particle size and zeta-potential with cholesterol content of unencapsulated liposomes

Fresh unencapsulated liposomes had hydrodynamic diameters ranging from 150 nm to 270 nm as shown in table 3.

Table 3. The variation of diameter of unloaded liposomes of different lipid compositions over a period of 2 months (Each value is the mean of three independent trials ± S.D. In each column, statistically different values are indicated by different superscripts and vice versa.)

Liposomal formulation PC:CH	**Diameter ± S.D (nm)**		
	Fresh	1 month	2 months
10:0	194.5 ± 45.0^{a}	138.1 ± 5.6^{a}	149.3 ± 7.2^{a}
9:1	264.3 ± 60.3^{a}	174.5 ± 56.5^{a}	$323.9 \pm 91.3^{a,b}$
8:2	272.7 ± 22.1^{a}	231.6 ± 47.2^{a}	434.7 ± 196.7^{b}
7:3	263.7 ± 54.6^{a}	203.5 ± 48.2^{a}	$263.5 \pm 80.5^{a,b}$
6:4	154.0 ± 18.8^{a}	196.4 ± 80.5^{a}	$198.8 \pm 45.6^{a,b}$

Incorporation of CH in the lipid bilayer brought about variation in the size of unencapsulated liposomes. Increasing the CH content resulted in a gradual increase in size to reach a maximum hydrodynamic diameter after which the size decreased. In fact, the size increased upon increasing the CH content from 0 % to 20 %. Although the size

decreased only marginally upon increasing the CH content from 20 % to 30 %, further increase in CH content to 40% decreased the size dramatically. Despite the observed variation of size with CH content, the sizes of different formulations were not significantly different. The hydrodynamic diameters measured after one month and those measured after two months exhibited a similar variation with CH content to the hydrodynamic diameters measured immediately after preparation of unloaded liposomes (Table 3). A decrease in the curvature of the bilayer due to CH incorporation may be the cause for the observed initial increase in size. The apparent decrease in the average size of liposomes, after reaching a maximum hydrodynamic diameter, can be attributed to the incompatibility of high CH content in the lipid bilayer, which may have caused CH to form other structures with smaller sizes. Actually, Finkelstein's claim for preparation of bilayers containing equal ratios of lecithin and CH (Finkelstein, 1974), was contested by Ibarguren and coworkers who illustrated that the actual amount of CH present in the lipid bilayers was much less than the expected amount (Ibarguren *et al.*, 2010). Indeed, this finding supports our claim about the formation of CH rich structures of smaller sizes. The variation of size with CH content was evident even after one month and two months of preparation.

Table 4. The variation of zeta-potential of unloaded liposomes of different lipid compositions over a period of 2 months (Each value is the mean of three independent trials ± S.D. In each column, statistically different values are indicated by different superscripts and vice versa.)

Liposomal formulation PC:CH	**Zeta-potential ± S.D (mV)**		
	Fresh	1 month	2 months
10:0	-31.6 ± 6.1^{a}	-54.2 ± 14.8^{a}	-52.9 ± 4.4^{a}
9:1	$-43.0 \pm 2.6^{a,b}$	-64.4 ± 4.1^{a}	$-58.3 \pm 1.6^{a,b}$
8:2	$-42.8 \pm 6.9^{a,b}$	-52.6 ± 0.6^{a}	-61.9 ± 3.5^{b}
7:3	-45.2 ± 3.7^{b}	-61.7 ± 3.4^{a}	-60.7 ± 2.4^{b}
6:4	$-35.2 \pm 0.4^{a,b}$	-60.9 ± 3.7^{a}	-65.0 ± 2.0^{b}

The average zeta-potentials of fresh unloaded liposomes ranged between -32.0 mV and -45.0 mV gradually becoming more negative with increasing CH content (Table 4). A significant difference between the zeta-potential of liposomal formulation containing only

PC (i.e. -31.6 ± 6.1) and that of liposomal formulation containing a CH content of 30 % (i.e. – 45.2 ± 3.7) was observed. Further increase of CH content, from 30 % to 40 %, led to an insignificant increase in the zeta-potential (-35.2 ± 0.4, Table 4). One month old liposomes did not show variation of zeta-potential with CH content. However, after two months, liposomes suspending in solution exhibited zeta-potentials which became gradually more negative with increasing CH content. The zeta-potential of liposomal formulation containing only PC was significantly different from those of liposomal formulations containing CH above 20 %.

The average zeta-potentials of fresh unloaded liposomes indicate that unloaded liposomes stable in solution can be prepared using PC and CH in the ratios given. However, based on work by Hurler et al., it was expected that liposomes with zeta-potentials close to zero would form since both PC and CH are neutral at physiological pH (Hurler *et al.*, 2013). Negative zeta-potentials observed in this study may be due to the presence of other negatively charged phospholipids such as PA, PS and PI, in addition to neutral PC, in the PC that was used for the preparation of liposomes (Kuksis, 1992). Besides, PC used in this study was only of 60 % purity. Furthermore, incorporation of CH resulted in liposomes of more negative zeta-potentials. This information suggests that interactions between PC and CH favour the phosphate group of PC to be exposed to the external environment, under the conditions used to measure the zeta-potential. Indeed, this observation is consistent with the report by Xia and Xu who suggested that the hydroxyl group of CH may interact with the choline group of PC, thereby exposing the phosphate group of PC to the external environment (Xia and Xu, 2005). Although zeta-potentials of unloaded liposomes gradually decreased to reach a minimum upon increasing the CH content, further increase of CH content resulted in a slight increase of the zeta-potential. Formation of CH-rich structures with less negative or zero zeta-potential may be the cause for the observed increase of the zeta-potential. Although one month old liposomes did not show variation of zeta-potential with time, two month old liposomes stable in solution demonstrated the ability of CH to favour orientation of the phosphate group of PC to the external environment probably via hydrogen bonding with the choline group.

2.3.3.2 Variation of particle size and zeta-potential with time of unloaded liposomes

The stability of unloaded liposomes in solution was investigated by measuring the size and zeta-potential with time for a period of two months. All liposomal formulations showed precipitation of lipidic structures with time, most probably due to fusion and / or

aggregation of those structures. Table 3 and table 4 give the sizes and zeta-potentials of liposomes remaining in the suspension, repectively.

Unloaded liposomes did not show a significant variation of size with time. However, all liposomal formulations except the liposomal formulation with a CH content of 40 % showed a decrease of size one month after preparation (Table 3). This reflects the removal of large liposomes from the suspension due to precipitation as a result of fusion or aggregation. As shown in table 3, all liposomal formulations showed an increase in size upon storage from one month to two months due to fusion and/or aggregation of liposomes. Since the variation of size with time was statistically insignificant, our results indicate that unloaded liposomes stable over a period of 2 months may be prepared using PC and CH.

As shown in table 4, the average zeta-potentials of unloaded liposomes decreased after one month of preparation. Liposomes with low charge have a lower degree of repulsion among vesicles and tend to fuse and / or aggregate and then precipitate from the solution. Although the zeta-potentials of one-month old liposomes and those of two-month old liposomes showed no significant difference, the difference between the zeta-potential of fresh liposomes and those of two-month old liposomes of each formulation was statistically significant, except of the formulation containing only PC. This result indicates that aggregation and subsequent removal of liposomes with less negative zeta-potentials from the suspension occur mainly during the first month of storage, after which the liposomes suspending in solution remain stable over a period of two months.

2.3.3.3 Variation of particle size and zeta-potential with cholesterol content of liposomes containing plant extract

Similar to unloaded liposomes, fresh liposomes containing plant extract showed variation of size with cholesterol content (Table 5). The hydrodynamic diameter increased gradually upon increasing the CH content from 0% to 30 % beyond which the size decreased dramatically. In fact, there was a statistically significant difference between the hydrodynamic diameters of liposomes with a CH content of 30 % and 40 %.

Loaded liposomes remaining in the suspension after one month of preparation exhibited a pronounced variation of the average hydrodynamic diameter with CH content (see Table 5). The size increased gradually upon increasing the CH content from 0 % to 40 %. The difference in sizes of liposomes with CH contents of 0 %, 10 % and 20 % were not significant. When the CH content exceeded 30 % (i.e. CH content of 30 % and 40 %), the

size increase was significantly greater than those of liposomes with lower CH content. Loaded liposomes remaining in the suspension after two months of preparation also exhibited a variation of the average hydrodynamic diameter with CH content (Table 5). Similar to one month old liposomes, the hydrodynamic diameters of two months old liposomes increased with increasing CH content. In fact, this variation was even more pronounced than the variation showed by the liposomes after one month of preparation. The sizes of liposomes with10 % CH or lower, did not show a significant difference. However, the sizes of the liposomes were significantly different at higher CH contents (i.e. CH contents of 20 %, 30 % and 40 %). In addition, these high CH liposomes were also significantly different from each other.

Table 5. The variation of diameter of plant extract-loaded liposomes of different lipid compositions over a period of 2 months (Each value is the mean of three independent trials ± S.D. In each column, statistically different values are indicated by different superscripts and vice versa.)

Liposomal formulation PC:CH	**Diameter ± S.D (nm)**		
	Fresh	1 month	2 months
10:0	$168.2 \pm 7.9^{a,b}$	149.2 ± 32.4^{a}	151.4 ± 16.4^{a}
9:1	$189.5 \pm 8.4^{a,b}$	179.5 ± 24.6^{a}	175.1 ± 6.8^{a}
8:2	$206.9 \pm 6.9^{a,b}$	208.5 ± 30.8^{a}	239.7 ± 20.5^{b}
7:3	228.1 ± 36.2^{a}	319.5 ± 14.4^{b}	376.5 ± 14.1^{c}
6:4	156.8 ± 37.5^{b}	364.8 ± 71.7^{b}	455.7 ± 35.7^{d}

Like in the case of unloaded liposomes, the initial increase of size may be due to the decrease in the curvature of the bilayers while the subsequent decrease of average size may be due to the formation of CH-rich structures with low hydrodynamic diameters. These results indicate that the effect of CH on the size of unloaded liposomes and plant extract loaded liposomes is similar. In fact, the effect of CH on size was more evident in loaded liposomes. Also, one month old liposomes and two month old liposomes showed a gradual increase in size with increasing CH content. Thus, the size of plant extract encapsulated liposomes may be modulated by varying the lipid composition, specifically the ratio of PC to CH. Since the size affects other properties of liposomes, including EE,

release kinetics, skin permeation and biodistribution (Hurler *et al.*, 2013), size modulation of plant material encapsulated liposomes may enable fine tuning of liposomes with respect to other properties.

As shown in table 6, fresh loaded liposomes and one month old loaded liposomes exhibited no significant variation of zeta-potential with CH content. However, zeta-potentials of loaded liposomes suspending in solution after two months of preparation decreased gradually with increasing CH content. In fact, the zeta-potential of liposomes with no CH and that of liposomes with 40 % CH were significantly different. This variation of zeta-potential may be due to the interactions of CH and choline group of PC to expose the phosphate group to the external solution, as explained under section 3.3.3.2. Basically, zeta-potentials of plant material encapsulated liposomes indicate that encapsulated liposomes stable in solution can be prepared using PC and CH.

Table 6. The variation of zeta-potential of plant extract-loaded liposomes of different lipid compositions over a period of 2 months (Each value is the mean of three independent trials ± S.D. In each column, statistically different values are indicated by different superscripts and vice versa.)

Liposomal formulation PC:CH	**Zeta-potential ± S.D (mV)**		
	Fresh	1 month	2 months
10:0	-58.2 ± 4.3^{a}	-45.0 ± 7.1^{a}	-38.7 ± 8.9^{a}
9:1	-69.0 ± 9.1^{a}	-51.7 ± 7.1^{a}	$-47.0 \pm 2.9^{a,b}$
8:2	-65.3 ± 3.8^{a}	-60.1 ± 0.1^{a}	$-49.5 \pm 6.8^{a,b}$
7:3	-65.2 ± 0.6^{a}	-58.5 ± 3.7^{a}	$-53.4 \pm 3.2^{a,b}$
6:4	-65.8 ± 4.5^{a}	-54.4 ± 5.5^{a}	-54.1 ± 5.4^{b}

2.3.3.4 Variation of particle size and zeta-potential of plant extract containing liposomes with time

All five different formulations of loaded liposomes showed aggregation and precipitation with time. The degree of precipitation increased with increasing CH content. Table 5 gives the sizes of liposomes remaining in the suspension.

Liposomes with no or low CH content (PC to CH – 10:0, 9:1 and 8:2) showed no significant variation of size with time. In contrast, liposomal formulations with higher CH

contents (PC to CH – 7:3 and 6:4) showed significant increase of size with time. This suggests that high CH contents in plant extract loaded liposomes favour aggregation and / or fusion of liposomes.

In contrast to the zeta-potentials of unloaded liposomes, those of loaded liposomes became less negative with time (Table 6). In fact, the difference between the zeta-potential of fresh liposomes and two months old liposomes was significant of liposomal formulations with a CH content of 10%, 20 % and 30 %. However, precipitation of lipidic structures, most probably with less negative zeta-potentials, with time was observed even with loaded liposomes. Thus, it was expected that the average zeta-potentials would become more negative with time. This anomaly may be due to leakage of small quantities of encapsulated material with time. Encapsulated polyphenols, upon leakage, have the potential to interact with phosphate groups of PC through hydrogen bonding, thus shielding the negative charge of PC leading to liposomes with less negative zeta-potentials which gives rise to increased aggregation.

Numerous authors have demonstrated the effectiveness of approaches to increase the stability of liposomes. For instance, Dragicevic-Curic et al. showed that the size of the liposomes could be maintained by incorporating liposomes in hydrogels made of carbomer (Dragicevic-Curic *et al.*, 2010). Thus, incorporation of plant extract encapsulated liposomes in a gel may increase the stability.

2.3.4 *In vitro* release studies

The effect of CH on sustained release properties of liposomes encapsulating the methanol extract of stem bark of *S. castaneifolia* was evaluated using deionized water as the release medium.

Our results reveal that the release of the encapsulated plant material from liposomes made of PC (assay ~ 60%, TLC) and CH is dependent on the lipid composition of liposomes (see Figure 8). In fact, the liposomes became progressively leaky as the amount of CH was increased from 0 % (w/w) to 20 % (w/w) beyond which the release profiles overlapped. This result is consistent with the literature showing the dependence of release of encapsulated species on the lipid composition of liposomes (Mourtas *et al.*, 2007).

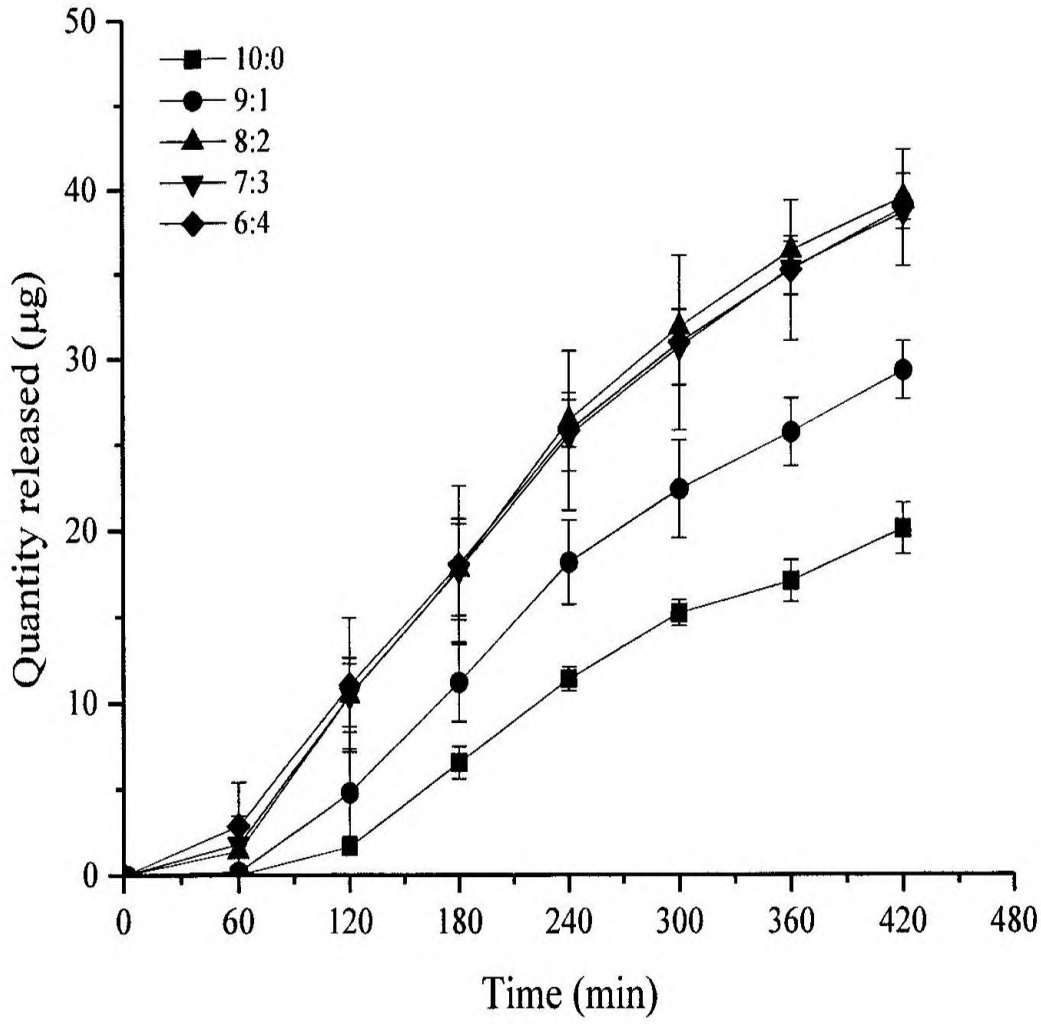

Figure 8. Release profiles of *S. castaneifolia* methanol extract from different liposomal formulations of different lipid compositions (i.e ratio of PC to CH)

Lipid packing and fluidity of membranes depend on the CH content. Therefore, incorporation of CH affects the permeability of the encapsulated material from liposomes (Nitsche and Kasting, 2013). Raffy and Teissie suggested that CH increases the ordering of lipids in the membrane, thus making the membrane less leaky (Raffy and Teissié, 1999). However, Xiang and Anderson reported that incorporation of CH in phospholipid bilayers, depending on the amount incorporated may sometimes increase the permeability of the encapsulants (Xiang and Anderson, 1997). In fact, we observed increased release of encapsulated material upon increasing CH content in the lipid bilayer. The differences among loaded liposomes in this study include differences of size and LC in addition to the difference of CH content. These factors also may affect the release kinetics of encapsulated material from liposomes.

In addition to size and LC, the amount of phospholipids was different among the five liposomal formulations. Thus, as stated previously, in addition to PC, other phospholipids present in egg yolk could interact with encapsulated polyphenols through

hydrogen bonding, thus retarding their release. As the CH content was increased up to 40 %, the PC (of 60% purity) content was decreased from 100 % to 60 %. Thus, theoretically, the content of other phospholipids also should decrease with increasing CH content. Since the degree to which encapsulated polyphenols can interact with phospholipids decreases with increasing CH content, the release of encapsulated material may increase with decreasing phospholipid content. Thus, the observed variation of release profiles of different liposomal formulations may most probably be due to a combined effect of size, encapsulated amount and lipid composition of loaded liposomes.

Release studies were conducted in deionized water and in two physiologically relevant buffer systems - PBS (pH 7.4) and artificial sweat (pH 4.7) - in order to study the effect of media on the release kinetics of loaded liposomes.Liposomes with the ratio of PC to CH - 9:1, which showed intermediate release were selected for the study.

As depicted in figure 9, slow and sustained release of encapsulated material from liposomes occurred up to 7 h in all types of media used, beyond which release was not monitored. The release profile of the plant extract from the liposomes in deionized water and in PBS which was of higher ionic strength overlapped. This suggests that the effect of salt concentration and hence that of ionic strength on the release kinetics of chemical constituents of the methanol extract of stem bark of *S. castaneifolia* from liposomes is negligible at least up to the ionic strength of PBS. However, the release profile of plant extract in artificial sweat was significantly different from those of above in that it was much slower. The lower pH of artificial sweat compared to other two media may be one reason for this difference. In a medium of pH as low as 4.7, a greater percentage of phenolic groups will remain protonated. This protonation will lead to lower solubility of polyphenols in artificial sweat than in aqueous component of liposomes. Thus, liposomal polyphenols will tend to remain in the vesicles rather than to leak out.

In addition to differences in release kinetics, we observed aggregation of liposomes during release studies in artificial sweat, which was not observed in deionized water or in PBS. The much higher ionic strength of artificial sweat than that of PBS may have contributed to the aggregation observed in artificial sweat. Indeed, higher concentrations of salts result in faster aggregation of liposomes. For instance, using NaCl, NaBr and Na_2SO_4, Carrion and coworkers demonstrated that aggregation of liposomes occurs faster in solutions of higher ionic strength (Carrión *et al.*, 1994).

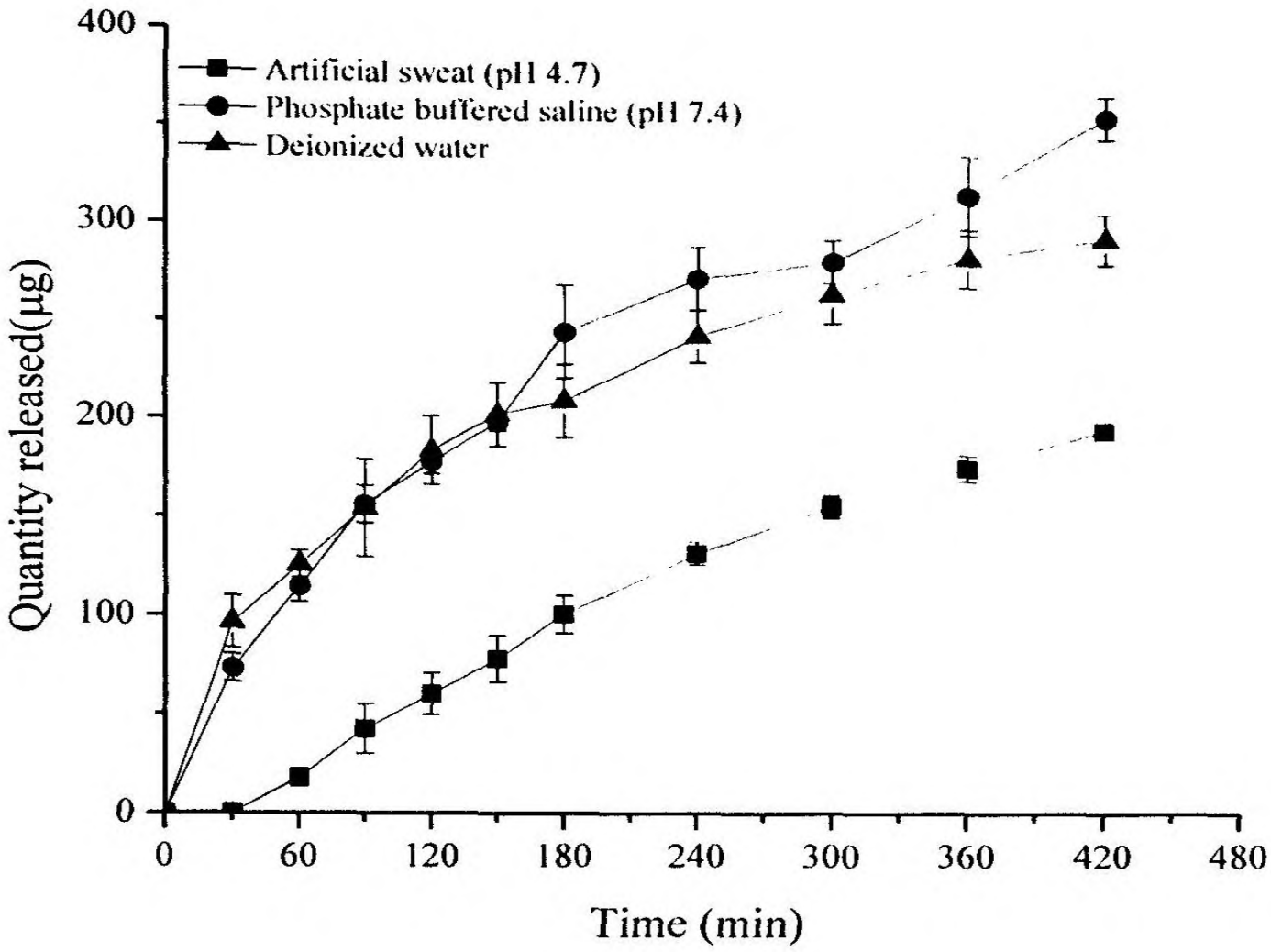

Figure 9. Release profiles of *S. castaneifolia* from liposomal formulation PC:CH - 9:1 in different media

These results indicate that this liposomal formulation may be used for slow and sustained release of the chemical constituents of the methanol extract of stem bark of *S.castaneifolia* in physiological buffers. Moreover, if loaded liposomes are incorporated in topical formulations, only a small quantity of the extract will release to sweat, as indicated by the release profile in artificial sweat. However, upon penetration of liposomes through the stratum corneum to deeper layers of the skin, the extract will release faster, as indicated by the relative position of release profile in PBS.

2.4 Conclusion

The highly antioxidant methanol extract of stem bark of *S. castaneifolia* was successfully encapsulated in conventional liposomes made of PC (assay approx. 60 %) and CH. The optimum ratios of PC to CH were 9:1 and 8:2 (w/w) in terms of EE and LC. The presence of sucrose - a lyoprotectant - does not affect LC of plant extract encapsulated liposomes.

The change in the lipid composition had mixed results on the properties of liposomes. When unencapsulated liposomes were examined, the change in lipid composition towards an increase in CH content had minimum effect on the stability and aggregation properties of the liposomes. In addition, the size of liposomes did not show significant variation. However, loading the *S. castaneifolia* extract indicated pronounced changes to the size, charge and stability with time as well as the release profile of the encapsulated liposomes. Thus, loaded liposomes should be either lyophilized or incorporated in a viscous medium such as a gel as means of storage in order to increase the stability of the liposomes.

Conventional liposomes encapsulating the methanol extract of stembark of *S. castaneifolia* can be used as a slow and sustained release system of the plant extract. The sustained release properties can be modulated by changing the lipid composition. Furthermore, release of encapsulated plant material depends of the medium to which the encapsulated material is released. In fact, release of encapsulated plant material in artificial sweat is much slower than in PBS or in deionized water. Thus, conventional liposomes may be suitable for topical formulations where sustained release of plant material is desired.

2.5 References

Altunkaya, A., Becker, E.M., Gökmen, V. and Skibsted, L.H. (2009). Antioxidant activity of lettuce extract (*Lactuca sativa*) and synergism with added phenolic antioxidants. *Food Chemistry* **115**, 163-168.

Bandara, B.M.R., Hewage, C.M., Jayamanne, L., Karunaratne, V., Bandara, K.A.N.P., Adikaram, N.K.B., Pinto, M.R.M. and Wijesundara, D.S.A. (1990). Biologocal activity of some steam distillates from leaves of ten species from Rutaceous plants. *Journal of National Science Council Sri Lanka* **18**, 71.

Bandara, R.M.C.J., Abeykoon, D.M.B., Bandara, B.M.R., Wickramasinghe, A., Wijesundara, D.S.A., Karunaratne, D.N. and Karunaratne, V. (2011). Antioxidant, cytotoxic and phytotoxic activities of *Schumacheria castaneifolia*, a plant endemic to Sri Lanka. *Proceedings of Peradeniya University Research Sessions (PURSE)* **16**,156.

Bandara, R.M.C.J., Alahakoon, A.M.C.S.B., Bandara, B.M.R., Wickramasinghe, A., Karunaratne, D.N., Karunaratne, V., Rajapakse, R.G.S.C. and Wijesundara, D.S.A. (2012). Total polyphenol content and antimicrobial activity of *Schumacheria castaneifolia* and *Schumacheria alnifolia*. *Proceedings of Peradeniya University Research Sessions (PURSE)* **17**, 177.

Bangham, A.D., Standish, M.M. and Watkins, J. C. (1965). Diffusion of univalent ions across the lamellae of swollen phospholipids. *Journal of Molecular Biology* **13**, 238-252.

Baptista, A.L.F., Coutinho, P.J.G., Real Oliveira, M.E.C.D. and Rocha Gomes, J.I.N. (2003). Effect of pH on the control release of microencapsulated dye in lecithin liposomes. II. *Journal of Liposome Research* **13(2)**, 123-130.

Budzianowski, J. and Budzianowska, A. (2006). Chromatographic and spectrophotometric analyses of the DPPH free radical scavenging activity of the fractionated extracts from *Lamium album* L., *Lamium purpureum* L. and *Viscum album* L. *Herba Polonica* **52(1/2)**, 51-57.

Cagdas, F.M., Ertugral, N., Bucak, S. and Atay, N.Z. (2011). Effect of preparation method and cholesterol on drug encapsulation studies by phospholipid liposomes. *Pharmaceutical Development and Technology* **16(4)**, 408-414.

Carrión, F.J., de la Maza, A. and Parra, J.L. (1994). The influence of ionic strength and lipid bilayer charge on the stability of liposomes. *Journal of Colloid and Interface Science* **164**, 78-87.

Dassanayake, M.D. (1996). *A revised handbook to the flora of Ceylon,* Vol. X, Oxford and IBH Publishing Co. Pvt. Ltd., New Delhi, India.

Dragicevic-Curic, N., Winter, S., Krajisnik, D., Stupar, M., Milik, J., Graefe, S. and Fahr, A. (2010). Stability evaluation of temoporfin-loaded liposomal gels for topical application. *Journal of Liposome Research* **20(1)**, 38-48.

El-Samaligy, M.S., Afifi, N.N. and Mahmoud, E.A. (2006). Evaluation of hybrid liposomes-encapsulated silymarin regarding physical stability and in vivo performance. *International Journal of Pharmaceutics* **319(1-2)**, 121-129.

Fang, J-Y., Hwang, T-L., Huang, Y-L. and Fang, C-L. (2006). Enhancement of the transdermal delivery of catechins by liposomes incorporating anionic surfactants and ethanol. *International Journal of Pharmaceutics* **310(1-2)**, 131-138.

Finkelstein, A. (1974). Bilayers: formation, measurements, and incorporation of components. *Methods in Enzymology* **32(C)**, 489-501.

Godin, B. and Touitou, E. (2004). Mechanism of bacitracin permeation enhancement through the skin and cellular membranes from an ethosomal carrier. *Journal of Controlled Release* **94(2-3)**, 365-379.

Gortzi, O., Lalas, S., Chinou, I. and Tsaknis, J. (2007). Evaluation of the antimicrobial and antioxidant activities of *Origanum dictamnus* extracts before and after encapsulation in liposomes. *Molecules* **12(5)**, 932-945.

Gurni, A.A. and Kubitzki, K. (1981). Flavonoid chemistry and systematics of the Dilleniaceae. *Biochemical Systematics and Ecology* **9(2/3)**, 109-114.

Harrigan, P.R., Madden, T.D. and Cullis, P.R. (1990). Protection of liposomes during dehydration or freezing. *Chemistry and Physics of Lipids* **52**, 139-149.

Hurler, J., Žakelj, S., Mravljak, J., Pajk, S., Kristl, A., Schubert, R. and Škalko-Basnet, N. (2013). The effect of lipid composition and liposome size on the release properties of liposomes-in-hydrogel. *International Journal of Pharmaceutics* **456**, 49-57.

Iacopini, P., Baldi, M., Storchi, P. and Sebastiani, L. (2008). Catechin, epicatechin, quercetin, rutin and resveratrol in red grape: content, *in vitro* antioxidant activity and interactions. *Journal of Food Composition and Analysis* **21**, 589-598.

Ibarguren, M., Alonso, A., Tenchov, B.G. and Goñi, F.M. (2010). Quantitation of cholesterol incorporation into extruded lipid bilayers. *Biochimica et. Biophysica Acta* **1798**, 1735-1738.

Ke, X., Xu, Y., Yan, F. and Ping, Q-N. (2007). Preparation of wogonin liposomes and its pharmacokinetics in rats. *Journal of China Pharmaceutical University* **38(6)**, 502-506.

Kokkona, M., Kallinteri, P., Fatouros, D. and Antimisiaris, S.G. (2000). Stability of SUV liposomes in the presence of cholate salts and pancreatic lipases: efffect of lipid composition. *European Journal of Pharmaceutical Sciences* **9**, 245-252.

Kuksis, A. (1992). Yolk lipids. *Biochimica et Biophysica Acta* **1124**, 205-222.

Lasic, D.D. (1998). Novel applications of liposomes. *Trends in Biotechnology* **16**, 307-321.

Lira, M.C.B., Ferraz, M.S., da Silva, D.G.V.C., Cortes, M.E., Teixeira, K.I., Caetano, N.P., Sinisterra, R.D., Ponchel, G. and Santos-Magalhães, N.S. (2009). Inclusion complex of usnic acid with β-cyclodextrin: characterization and nanoencapsulation into liposomes. *Journal of Inclusion Phenomena and Macrocyclic Chemistry* **64(3-4)**, 215-224.

Minami, H., Inoue, T. and Shimozawa, R. (1993). Aggregation kinetics of dimyristoylphosphatidylglycerol vesicles induced by divalent cations. *Journal of Colloid and Interface Science* **158**, 460-465.

Mourtas, S., Fotopoulou, S., Duraj, S., Sfika, V., Tsakiroglou, C. and Antimisiaris, S.G. (2007). Liposomal drugs dispersed in hrdrogels: effect of liposome, drug and gel properties on drug release kinetics. *Colloids Surfaces B: Biointerfaces* **55**, 212-227.

Nitsche, J.M. and Kasting, G.B. (2013). Permeability of fluid-phase phospholipid bilayers: assessment and useful correlations for permeability screening and other applications. *Journal of Pharmaceutical Sciences* **102(6)**, 2005-2032.

Papahadjopoulos, D., Nir, S. and Ohki, S. (1971). Permeability properties of phospholipid membranes: effect of cholesterol and temperature. *Biochimica et Biophysica Acta* **266**, 561-583.

Peyrat-Maillard, M.N., Cuvelier, M.E. and Berset, C. (2003). Antioxidant activity of phenolic compounds in 2,2'-azobis (2-amidinopropane) dihydrochloride (AAPH)-induced oxidation: synergistic and antagonistic effects. *Journal of American Oil Chemists' Society* **80(10)**, 1007-1012.

Priprem, A., Watanatorn, J., Sutthiparinyanont, S., Phachonpai, W. and Muchimapura, S. (2008). Anxiety and cognitive effects of quercetin liposomes in rats. *Nanomedicine: Nanotechnology, Biology and Medicine* **4**, 70-78.

Raffy, S. and Teissié, J. (1999). Control of lipid membrane stability by cholesterol content. *Biophysical Journal* **76**, 2072-2080.

Rebmann, H., Composition for cosmetic, pharmaceutical or dietary applications, U.S. Patent 8,652,494 B2, 2014.

Sinico, C., Logu, A.D., Lai, F., Valenti, D., Manconi, M., Loy, G., Bonsignore, L. and Fadda, A.M. (2005). Liposomal incorporation of *Artemisia arborescens* L. essential oil and in vitro antiviral activity. *European Journal of Pharmaceutics and Biopharmaceutics* **59(1)**, 161-168.

Suzuki, T., Komatsu, H. and Miyajima, K. (1996). Effects of glucose and and its oligomers on the stability of freeze-dried liposomes. *Biochimica et Biophysica Acta* **1278**, 176-182.

Szoka Jr., F. and Papahadjopoulos, D. (1978). Procedure for preparation of liposomes with large internal aqueous space and high capture by reverse-phase evaporation. *Proceedings of the National Academy of Sciences USA* **75(9)**, 4194-4198.

Virden, J.W. and Berg, J.C. (1992). NaCl-induced aggregation of dipalmitoylphosphatidylglycerol small unilamellar vesicles with varying amounts of incorporated cholesterol. *Langmuir* **8(6)**, 1532-1537.

Xia, S. and Xu, S. (2005). Ferrous sulfate liposomes: preparation, stability and application in fluid milk. *Food Research International* **38**, 289-296.

Xiang, T-X. and Anderson, B.D. (1997). Permeability of acetic acid across gel and liquid-cyrstalline lipid bilayers conforms to free-surface-area theory. *Biophysical Journal* **72**, 223-237.

Yamamoto, S., Nakano, K., Ishikawa, C., Yamamoto, M., Matsumoto, Y., Iwahara, M., Furusaki, S. and Ueoka, R. (2002). Enhanced inhibitory effects of extracts from *Ginkgo*

biloba L. leaves encapsulated in hybrid liposomes on the growth of tumor cells in vitro. *Biochemical Engineering Journal* **12**, 125-130.

CHAPTER 3

EFFECT OF LIPID COMPOSITION AND PREPARATION METHOD ON PROPERTIES OF FERULIC ACID ENCAPSULATED LIPOSOMES

3.1 Introduction

Liposomes, vesicular structures with lipid bilayers and an aqueous interior, play a pivotal role as drug delivery vehicles, in pharmaceutical industry and in cosmetic industry. Therefore, numerous strategies are adopted to prepare liposomes with varying properties, thus enabling those liposomes to function even more effectively (Laouini *et al.*, 2012).

The model bioactive agent used in this study is ferulic acid which is a potent antioxidant having numerous other important bioactivities (Lin *et al.*, 2005; Ogiwara *et al.*, 2002). It is an amphiphilic molecule which shows intermediate solubility in water, and thus this drug is expected to behave differently than both hydrophilic and hydrophobic encapsulants.

Liposomal ferulic acid has been the subject of investigations of numerous research groups. For instance, Chen and coworkers studied the skin penetration and deposition of ferulic acid from vesicular delivery systems such as conventional liposomes, deformable liposomes, invasomes and ethosomes. They demonstrated that vesicular systems enhanced skin permeation of ferulic acid (Chen, Liu and Fahr, 2010). Another study conducted by Zhang et al. revealed that liposome-in-chitosan microspheres showed better slow release properties of ferulic acid than free ferulic acid or chitosan microspheres (Zhang *et al.*, 2011). In addition, Qin and coauthors reported successful encapsulation of ferulic acid in liposomes using calcium acetate gradient method (Qin *et al.*, 2008). However, the effect of method of preparation and charge on properties of ferulic acid encapsulated liposomes has remained unexplored.

Changing the method of preparation of liposomes usually alters properties such as size, lamellarity, and encapsulation efficiency; and hence, may affect release kinetics and skin permeation properties (Akbarzadeh *et al.*, 2013). Thus, ferulic acid encapsulated liposomes were prepared using three methods – reverse phase evaporation method, thin

film hydration method and proliposome method – and the properties of those liposomes were evaluated and compared.

Changing the lipid composition, also, alters the properties of liposomes. In fact numerous authors have reported the effect of charge, which is brought about by changing the lipid composition of liposomes, on the properties of liposomes (Gillet *et al.*, 2011; Park *et al.* 2011). Thus, both negatively charged liposomes and positively charged liposomes, encapsulating ferulic acid were prepared, and the properties of those liposomes were evaluated and compared.

The aim of this research project was to investigate the effect of method of preparation and lipid composition on the properties of ferulic acid encapsulated liposomes. Furthermore, the effect of liposomal encapsulation of ferulic acid on release properties and skin permeation properties of ferulic acid was evaluated. In addition to providing insight into the optimum method/s and lipid compositions for the preparation of ferulic acid encapsulated liposomes, this study will provide knowledge that will be very useful for future engineering of liposomal formulations encapsulating amphiphilic drugs and bioactive agents.

3.2 Materials and methods

3.2.1 Materials

Egg yolk PC (~ 60% TLC), CH (assay > 98%) and ferulic acid (≥ 99.0 %, HPLC) were purchased from Sigma-Aldrich. Dichloromethane, ethanol and methanol were from Sigma. Other chemicals were of analytical grade. Dialysis tubing (12 000 MWCO) was from Sigma-Aldrich. Fresh pig ears were obtained from a local slaughter house. Deionized water filtered through a 0.2 μm filter was used for all experiments.

3.2.2 Methods

3.2.2.1 Preparation of negatively charged liposomes

Reverse phase evaporation method

PC (100 mg), CH (40 mg) and ferulic acid (1 mg) were dissolved in a mixture of chloroform and ethanol, and a thin film of lipids was made in a round bottom flask. These compounds were, then, redissolved in ether (10 ml), and PBS (pH 7.4) was added to the round bottom flask. Then, the mixture was sonicated to form an emulsion. Next, the organic solvent was evaporated to form a suspension of liposomes and the final volume was made to 10 ml using PBS. Finally, the liposome suspension was sonicated in a bath sonicator for 5 min, thus forming 'ferulic acid encapsulated negatively charged liposomes prepared by reverse phase evaporation method' (N-REV).

Thin film hydration method

PC (100 mg), CH (40 mg) and ferulic acid (1 mg) were dissolved in a mixture of chloroform and ethanol, and a thin film of lipids was made in a round bottom flask. Next, PBS (10 ml) was added to the round bottom flask, and the thin film was hydrated by stirring. The liposome suspension was kept at 4 °C in a refrigerator overnight to complete hydration. Finally, the liposome suspension was sonicated at 4 °C in a bath sonicator for 5 min, thus forming 'ferulic acid encapsulated negatively charged liposomes prepared by thin film hydration method' (N-TFH).

Proliposome method

PC (100 mg), CH (40 mg) and ferulic acid (1 mg) were dissolved in 250 µl of ethanol by heating the mixture at 60 °C for 5 min. Next, PBS (1 ml) was added to the solution, and it was stirred to form a proliposome mixture to which 9 ml of PBS was added drop-wise over a period of 15 min while stirring. Finally, the liposome suspension was sonicated in a bath sonicator at 4 °C for 5 min, thus forming 'ferulic acid encapsulated negatively charged liposomes prepared by proliposome method' (N-PRO).

3.2.2.2 Preparation of positively-charged liposomes

Reverse phase evaporation method

PC (100 mg), CH (40 mg), SA (20 mg) and ferulic acid (1 mg) were dissolved in a mixture of chloroform and ethanol, and a thin film of lipids was made in a round bottom flask. These compounds were, then, redissolved in ether (10 ml), and PBS (pH 7.4) was added to the round bottom flask. Then, the mixture was sonicated to form an emulsion. Next, the organic solvent was evaporated to form a suspension of liposomes and the final volume was made to 10 ml using PBS. Finally, the liposome suspension was sonicated in a bath sonicator for 5 min, thus forming 'ferulic acid encapsulated positively charged liposomes prepared by reverse phase evaporation method' (P-REV).

Thin film hydration method

PC (100 mg), CH (40 mg), SA (20 mg) and ferulic acid (1 mg) were dissolved in a mixture of chloroform and ethanol, and a thin film of lipids was made in a round bottom flask. Next, PBS (10 ml) was added to the round bottom flask, and the thin film was hydrated by stirring. The liposome suspension was kept at 4 °C in a refrigerator overnight to complete hydration. Finally, the liposome suspension was sonicated at 4 °C in a bath sonicator for 5 min, thus forming 'ferulic acid encapsulated positively charged liposomes prepared by thin film hydration method' (P-TFH).

Proliposome method

PC (100 mg), CH (40 mg), SA (20 mg) and ferulic acid (1 mg) were dissolved in 250 µl of ethanol by heating the mixture at 60 °C for 5 min. Next, PBS (1 ml) was added to the solution, and it was stirred to form a proliposome mixture to which 9 ml of PBS was added drop-wise over a period of 15 min while stirring. Finally, the liposome suspension was sonicated in a bath sonicator at 4 °C for 5 min, thus forming 'ferulic acid encapsulated positively charged liposomes prepared by proliposome method' (P-PRO).

3.2.2.3 Determination of encapsulation efficiency

The EE of ferulic acid encapsulated charged liposomes was determined using a spectrophotometric method. Briefly, the liposome suspension was centrifuged at 20,700 rpm at 4 °C for 20 min. twice, and then, the supernatant was withdrawn. Supernatant was

diluted with methanol, and then ferulic acid determination was carried out by measuring absorbance at 321 nm.

The standard curve of ferulic acid for the determination of ferulic acid was constructed by using a series of standard solutions of ferulic acid of concentrations 2 mg/L, 4 mg/L, 6 mg/L, 8 mg/L, and 10 mg/L.

The formula used for the calculation of EE is given below.

$$EE = \frac{Total\ amount\ of\ feruic\ acid - Amount\ of\ ferulic\ acid\ in\ supernatant}{Total\ amount\ of\ ferulic\ acid\ initially\ introduced} \times 100$$

3.2.2.4 Determination of loading capacity

The LC of ferulic acid encapsulated charged liposomes was determined using a spectrophotometric method.

The formula used for the calculation of LC is given below.

$$LC = \frac{Mass\ of\ encapsulated\ ferulic\ acid}{Mass\ of\ ferulic\ acid\ encapsulated\ liposomes} \times 100$$

3.2.2.5 Determination of particle size

Particle sizes of liposomes were determined using a Malvern zetasizer NanoZS (Malvern instruments, UK) fitted with a red laser of 633 nm, using dynamic light scattering technique. Liposome suspensions were diluted in deionized water, filtered with a 0.45 μm filter, and the scattering intensity was measured at an angle of 173° relative to the incident radiation after equilibrating the samples at 25 °C. The values reported are the z-average diameters of liposomes.

3.2.2.6 Determination of zeta-potential

Zeta-potentials of the same liposomal suspensions described above were measured using the Malvern zetasizer fitted with a red laser of 633 nm, using Laser Doppler Electrophoresis technique. Samples were equilibrated at 25 °C before taking measurements. The values reported are the z-average zeta-potentials of liposomes.

3.2.2.7 *In vitro* release studies

In vitro release studies were conducted using ferulic acid encapsulated liposomes following the dialysis bag method. Briefly, 5 ml of liposomal suspension was put in a dialysis bag; which was then immersed in 20 ml of PBS in a beaker. The release medium was stirred constantly using a magnetic stirrer thoughout the experiment. Aliquots of 1.5 mL were withdrawn from the release medium at predetermined time intervals and the release medium was replenished immediately with fresh buffer. The withdrawn aliquots were used for the determination of released ferulic acid. This experiment was conducted in triplicate.

In vitro release studies were carried out using both negatively charged liposomes and positively charged liposomes prepared using the reverse phase evaporation method, thin-film hydration method and proliposome method.

Release profiles of free ferulic acid and different liposomal formulations were fitted to seven different models: Zero order, First order, Higushi, Hixon-Crowell, Korsemeyer-Peppas, Baker-Lonsdale, and Gompertz. The model that exhibited the adjusted R-square closest to unity was selected as the best fit.

The functions of the models considered are given below (Lokhandwala, Deshpande and Deshpande, 2013):

Zero order model

$$Q_t = Q_o + K_o\, t$$

where;

Q_t – amount of drug dissolved in time t

Q_o – initial amount of drug in solution

K_o – zero order release constant

First order model

$$\log C_t = \log C_o - Kt/2.303$$

where;

C_o – initial concentration of drug

C_t – concentration of drug at time t

K – first order rate constant

Higuchi model

$$Q = K_H \times t^{1/2}$$

where;

Q – amount of drug released in time t per unit area

K_H – Higushi dissolution constant

t – time

Hixson-Crowell model

$$W_0^{1/3} - W_t^{1/3} = \kappa t$$

where;

W_o – initial amount of drug in the pharmaceutical dosage form

W_t – remaining amount of drug at time t

κ – constant incorporating surface-volume relation

Korsmeyer-Peppas model

$$M_t/M_\infty = K t^n$$

where;

M_t/M_∞ - fraction of drug released at time t

K – release rate constant

n – release exponent

Baker-Lonsdale model

$$\frac{3}{2}\left[1 - \left(1 - \frac{M_t}{M_\infty}\right)^{2/3}\right] \frac{M_t}{M_\infty} = Kt$$

where;

M_t/M_∞ - fraction of drug released at time t

K – release rate constant

Gompertz model

$$X(t) = X_{max}\, e^{[-\alpha e^{\beta \log t}]}$$

where;

$X(t)$ – percent dissolved at time t

X_{max} – maximum dissolution

α – undissolved proportion at time t

β – dissolution rate

3.2.2.8 *Ex vivo* skin permeation studies

Preparation of pig ear skin

First, pig ear was washed thoroughly with deionized water and the skin was removed from the cartilage using a scalpel. After that, the fat layer was removed from the skin to obtain full thickness pig ear skin. A circular portion of full thickness pig ear skin was used for each skin permeation experiment. Sectioned pig ear skin was equilibrated in PBS (pH 7.4) for 1 h before using for the experiment.

Ex vivo skin permeation experiments

Skin permeation experiments were carried out using a Franz-diffusion cell. Briefly, after filling the receiver compartment completely with fresh PBS (pH 7.4) solution, the water jacket was connected to a water supply at 25 °C. Next, sectioned pig ear skin was placed between donor and receiver compartments of the Franz diffusion cell such that the epidermal side was on the donor side, and the two compartments were clamped together tightly. Then, the liposomal suspension (5 mL) was applied on the skin through the donor compartment. The receiver solution was stirred continuously using a magnetic stirrer throughout the experiment at a constant rate. An aliquot of 1 ml was withdrawn from the receiver compartment at predetermined time intervals and the receiver solution was replenished with fresh buffer immediately. Each withdrawn aliquot was diluted with 3 ml of methanol and this solution was analyzed for ferulic acid after filtering it using a 0.45 µm filter. Sampling was continued for 24 h. After that, the pig ear skin was removed from the Franz-diffusion cell and was immersed in 10 ml of methanol. After 12 h, this methanol

solution was filtered through a 0.45 µm filter and was analyzed for ferulic acid using a spectrophotometer. This experiment was carried out in triplicate.

Ex vivo skin permeation experiments were carried out using free ferulic acid and all types of liposomal fomulations except P-REV.

Calculation of percentage drug permeation, cumulative drug permeation, flux(J) and permeability (Kp)

The percentage drug permeation after each time interval was calculated using the following equation.

$$Percentage\ drug\ permeation\ = \frac{Cumulative\ mass\ of\ drug\ permeated}{Total\ mass\ of\ drug\ initially\ introduced} \times 100$$

The cumulative mass of drug permeated (Q) after each time interval was calculated using the following equation.

$$Q = \{\, C_n V + \sum_{i=1}^{n-1} C_i\, S \,\}$$

where,

Q – Cumulative mass of drug permeated (µg)

C_n – Concentration of drug in receiver compartment at n^{th} sampling interval (µg/mL)

V – Volume of Franz-diffusion cell (mL)

C_i – Concentration of drug in i^{th} sample (µg/mL)

S – Volume of sampling aliquot (mL)

The average steady state flux (J) was calculated using the following equation.

$$J = \frac{dQ}{dt} \cdot \frac{1}{A}$$

where,

A – Surface area of the skin

dQ/dt – Slope of the plot Q vs. t

The skin permeability (K_p) is given by the following equation.

$$K_p = \frac{J}{\Delta C}$$

where,

ΔC – Difference in drug concentration of donor and receiver compartments at a given time

The average permeability (K_p(ave)) was calculated using the following equation.

$$K_p(ave) = \frac{\Sigma(J/\Delta C)}{N}$$

where,

N – Number of intervals

3.2.2.9 Statistical analysis

All data are presented as mean ± standard deviation (S.D.) of three parallel experiments (n = 3). Microsoft Office Excel 2007 was used for the above calculations. One way ANOVA was conducted using MINITAB 14 software to compare the results and $P < 0.05$ was considered significant. Curve fitting for drug release models was carried out using OriginPro 9 software.

3.3 Results and discussion

In this study, the effect of charge on the properties of ferulic acid encapsulated liposomes was evaluated. Actually, incorporation of charged lipids in the lipid bilayers of liposomes has become commonplace due to various reasons. Firstly, charged lipids are incorporated to increase the surface charge density of liposomes in order to prevent liposomes from aggregation, flocculation and fusion. Also, charged lipids are incorporated to increase the distance between adjacent lipid bilayers of multilamellar liposomes, which in turn increases the internal aqueous volume of liposomes (Banerjee, 2001). Secondly, incorporation of charged lipids in liposomes allows one to introduce controlled instability into liposomes. For instance, although PE forms bilayers at neutral pH, it forms non-bilayer aggregates at lower pHs (Adlakha-Hutcheon *et al.*, 1999; Lasic, 1998). Thirdly, charged liposomes are incorporated for their functional groups which may be utilized for surface modification of liposomes. For example, proteins and other molecules may be conjugated with charged lipids which also function as anchors of those conjugated structures to the liposome. Finally, imparting a charge to liposomes has, in numerous cases, shown to give desirable attributes such as improved encapsulation efficiency, sustained release properties and skin-penetration properties to liposomes (Oh *et al.*, 2011; Park *et al.*, 2011) .

The effect of method of preparation on the properties of ferulic acid encapsulated liposomes was evaluated in this study, in addition to the effect of charge. The methods used for preparing liposomes were reverse-phase evaporation method, thin-film hydration method and proliposome method. Each of these methods is associated with different advantages and disadvantages, thus making the determination of the optimum method an important step in the development of liposomal pharmaceutical formulations. The reverse phase evaporation method exhibits high encapsulation efficiencies for hydrophilic drugs and produces large unilamellar vesicles (Laouini *et al.*, 2012; Szoka Jr. and Papahadjopoulos, 1978). On the other hand, thin film hydration method exhibits high encapsulation efficiencies for hydrophobic drugs and produces multilamellar vesicles (Chen *et al.*, 2012; Laouini *et al.*, 2012). A disadvantage of both of these techniques is the exposure of the drug to organic solvents. Furthermore, minute quantities of organic solvents used in the preparation may remain in the final liposomal formulation. An advantage of proliposome method is the possibility of utilizing this method for large-scale preparing of liposomes. This method is particularly suitable for the encapsulation of lipophilic drugs in liposomes (Dua, Rana and Bhandari, 2012). Unlike the other two

methods used in this study, the proliposome method does not require the utilization of harmful organic solvents. In fact, the proliposome method uses only ethanol which is much tolerated by the human body. In this work, the effect of method of preparation was evaluated not only on EE but also on other properties including in vitro release and skin permeation properties.

3.3.1 Encapsulation efficiency and loading capacity

The effect of method of preparation and charge of liposomes on EE and LC was evaluated in this study and the values obtained for different liposomal formulations are shown in table 7.

Table 7. Encapsulation efficiency and loading capacity of different liposomal formulations. Each value represents mean ± S.D. (n = 3). Significantly different values are followed by different superscripts on each column and vice versa ($p < 0.05$).

Liposomal formulation	EE (%)	LC (%)
N-REV	69.93 ± 2.47^{a}	0.50 ± 0.02^{a}
N-TFH	71.64 ± 0.23^{a}	$0.51 \pm 0.00^{a,b}$
N-PRO	72.98 ± 0.39^{a}	0.52 ± 0.00^{b}
P-REV	Not determined	Not determined
P-TFH	81.34 ± 1.05^{b}	$0.51 \pm 0.01^{a,b}$
P-PRO	80.66 ± 0.44^{b}	$0.50 + 0.00^{a,b}$

As indicated in table 7, the charge of liposomes has a significant effect on EE of ferulic acid encapsulated liposomes. In fact, the EEs of the two types of positively charged liposomes were significantly higher than those of the three types of negatively charged liposomes. SA, which is the chemical compound incorporated in the lipid bilayer to impart a positive charge to liposomes, remains protonated at neutral pH, and thus, may interact strongly with deprotonated negatively charged ferulic acid molecules via mainly electrostatic interactions. These interactions may be the cause of the higher EEs exhibited by positively charged liposomes. Thus, positively charged liposomes, especially those vesicles containing SA, may be more appropriate for the encapsulation of ferulic acid with high encapsulation efficiencies.

Although EE was dependent on charge and thus lipid composition of liposomes, this parameter was independent of the method of preparation of liposomes used in this study. Thus, either reverse phase evaporation method, thin film hydration method or proliposome method can be used to prepare negatively charged ferulic acid encapsulated liposomes with similar EEs; while either thin film hydration method or proliposome method can be used to prepare positively charged ferulic acid encapsulated liposomes with similar EEs. Under the experimental conditions of this study, P-REVs were unable to be separated from the aqueous phase by centrifugation; and thus, were not analyzed.

The LCs of ferulic acid encapsulated liposomes approximated 0.5 %. This relatively low value may be a result of the low drug/lipid ratio used in the preparation of liposomes. Also, the high EEs observed may be due to the relatively low drug/lipid ratio used in this study. Indeed, the possibility of increasing EE by lowering the drug/lipid ratio in the preparation of liposomes has been demonstrated by numerous authors (Tardi *et al.*, 2007). Although EE was dependent on the charge of liposomes, the effect of charge and method of preparation was negligible on LC. Thus, the lipid compositions and methods utilized in this study are equally appropriate to obtain ferulic acid encapsulated liposomes with a LC of 0.5 %.

3.3.2 Particle size and zeta-potential

The properties of liposomes usually depend heavily on their physical characteristics such as particle size and zeta-potential. Thus, those characteristics of ferulic acid encapsulated liposomes were analyzed and the values are given in table 8.

Table 8. Diameter, polydispersity index and zeta-potential of different liposomal formulations. Each value represents mean ± S.D. (n = 3). Significantly different values are followed by different superscripts and vice versa ($p < 0.05$).

Liposomal formulation	Diameter (nm)	Polydispersity index	Zeta-potential (mV)
N-REV	289.5 ± 9.7^{a}	0.242 ± 0.014^{a}	-63.6 ± 3.4^{a}
N-TFH	329.8 ± 7.0^{b}	0.206 ± 0.002^{a}	-61.6 ± 4.5^{a}
N-PRO	253.5 ± 1.8^{a}	0.254 ± 0.011^{a}	-61.3 ± 3.4^{a}
P-REV	Not determined	Not determined	Not determined
P-TFH	420.3 ± 27.0^{c}	0.263 ± 0.023^{a}	$+20.1 \pm 5.9^{b}$
P-PRO	624.4 ± 17.2^{d}	0.389 ± 0.053^{b}	$+6.3 \pm 2.1^{c}$

According to table 8, the incorporation of SA in the lipid bilayer/s of ferulic acid encapsulated liposomes increases the size of those vesicles. In fact, the diameters of positively charged liposomes were significantly greater than those of negatively charged liposomes. Moreover, the method of preparation has a significant effect on the size of ferulic acid encapsulated liposomes. In fact, the sizes of N-REV and N-PRO were similar; whereas that of N-TFH was much larger. Thus, either reverse phase evaporation method or proliposome method may be utilized to prepare smaller (i.e. 200 nm – 300 nm) ferulic acid encapsulated liposomes. The two types of positively charged liposomes were also different in size, such that the size of P-PRO was much larger than that of P-TFH. Therefore, unlike in the case of negatively charged liposomes, thin film hydration method may be utilized to prepare smaller (i.e. approximately 400 nm) positively charged ferulic acid encapsulated liposomes.

Polydispersity index is indicative of the homogeneity of the liposomes in size, which is of utmost importance in most instances for improved therapeutic efficacy of liposomal drugs. As indicated in table 8, negatively charged ferulic acid encapsulated liposomes exhibited lower polydispersity indices than positively charged liposomes. This difference in polydispersity index indicates that the incorporation of SA in liposomes may result in liposomes less homogenous in size. However, the polydispersity indices of positively charged liposomes were dependent on the method of preparation. In fact, the polydispersity index of P-TFH was significantly smaller than that of P-PRO, and was similar to those of negatively charged liposomes. Thus, thin film hydration method may be used to yield positively charged liposomes with high homogeneity.

The zeta-potential which is indicative of the charge is a significant parameter of liposomes. In fact, dependence of important properties such as release of encapsulants, skin permeation and cellular uptake of liposomes on the zeta-potential have been reported (Gillet *et al.*, 2011; Kim *et al.*, 1994; Stefanutti *et al.*, 2014). According to table 8, the zeta-potentials of ferulic acid encapsulated liposomes depend heavily on the lipid composition. Specifically, the incorporation of SA in the lipid bilayers of liposomes results in positively charged liposomes. The zeta-potentials of negatively charged liposomes were independent of the method of preparation, and thus, either reverse phase evaporation method, thin film hydration method or proliposome method may be utilized in the preparation of stable negatively charged ferulic acid encapsulated liposomes. Although the zeta-potentials of negatively charged liposomes were similar, those of positively charged liposomes were dependent on the method of preparation. In fact, the zeta-potential of P-TFH was more

positive than that of P-PRO, and thus thin film hydration method is more appropriate to prepare positively charged ferulic acid encapsulated liposomes under the experimental conditions of this study.

3.3.3 *In vitro* release

Liposomal encapsulation is commonly used as a means of improving slow-release properties of encapsulated species. There are numerous instances where release properties have been modulated by changing the lipid composition and charge of liposomes (Chen *et al*., 2012; Kim *et al*., 1994). Also, the type (i.e. lamellarity, size) of liposomes utilized may have a significant effect on release properties (Maherani *et al*., 2013). Thus, the release properties of free ferulic acid and ferulic acid encapsulated liposomes that differ in lipid composition, charge and type are evaluated and the release profiles are depicted in figure 10.

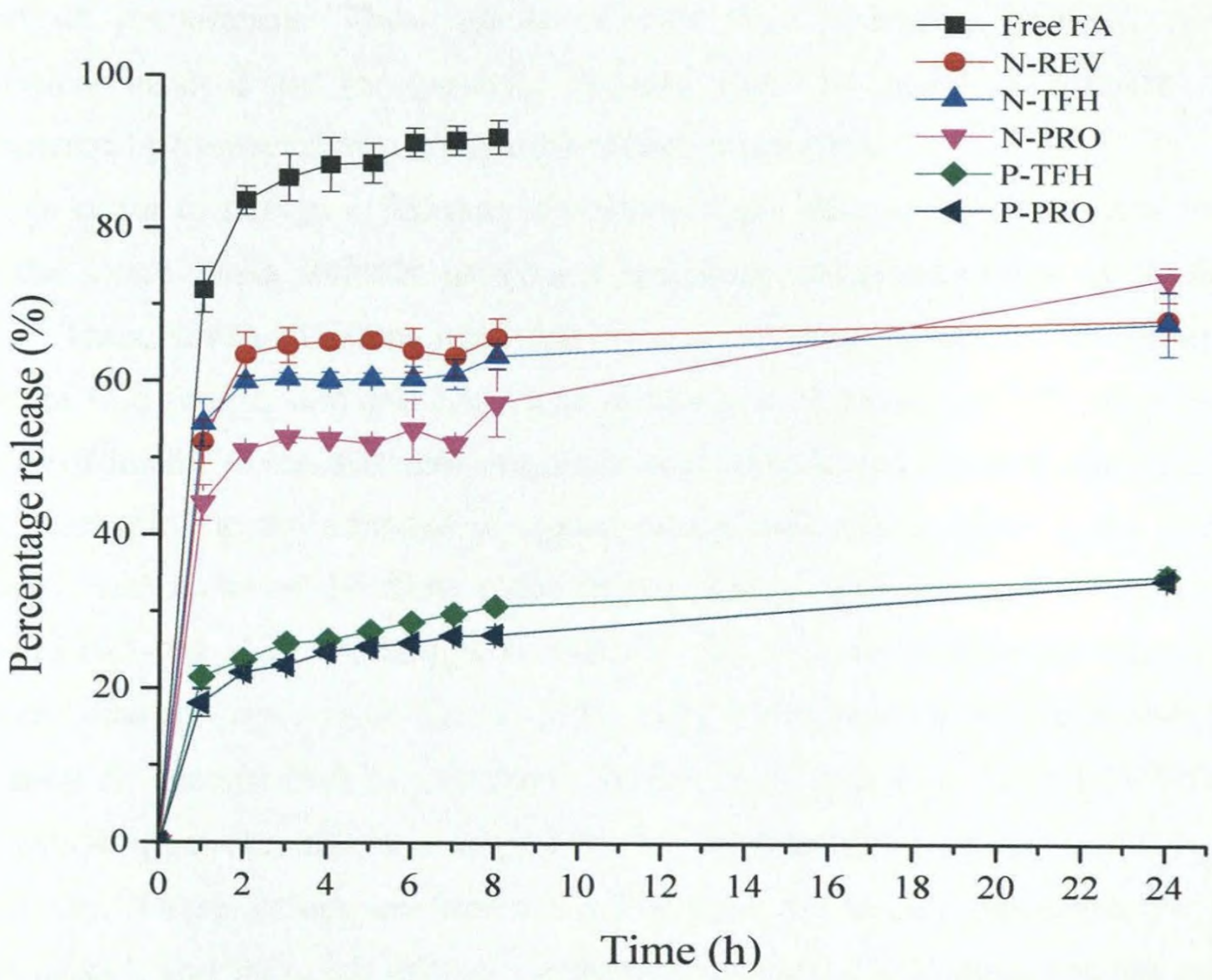

Figure 10. The release profiles of free ferulic acid (FA) and different types of ferulic acid encapsulated liposomal formulations (n = 3)

As shown in figure 10, the five types of ferulic acid encapsulated liposomes exhibited much slower release of ferulic acid than free ferulic acid. Thus, liposomal encapsulation is an effective means of improving slow release of ferulic acid irrespective of the charge or type of liposomes. Moreover, the two types of positively charged liposomes exhibited much slower release of ferulic acid than negatively charged liposomes. In fact, the percentage release of ferulic acid from negatively charged liposomes ranged from 68 % to 73 % while that from positively charged liposomes approximated 34 % - 35 %, at 24 h. Thus, these results show that the release properties may be improved further by utilizing positively charged ferulic acid encapsulated liposomes. Specifically, incorporating SA in the lipid bilayers of ferulic acid encapsulated liposomes is an effective strategy that enhances slow release of ferulic acid. One major reason for the slower release properties exhibited by SA-containing liposomes may the strong electrostatic interactions of SA and ferulic acid, that hinder the escape of ferulic acid from liposomes. Although the release behaviour of liposomal ferulic acid was dependent on the charge or lipid composition of liposomes, it was independent of the method of preparation. Thus, either of thin film hydration method, reverse phase evaporation method or proliposome method may be used to prepare ferulic acid encapsulated liposomes that exhibit slow release properties.

In order to design efficacious liposomal drug delivery systems, it is imperative to know the exact mass transfer processes and drug release kinetics of those liposomal systems. Thus, seven different drug release models were tested for the observed release profiles of free ferulic acid and liposomal ferulic acid. The adjusted R-square values of the release profiles for seven different drug release models tested are given in table 9.

According to the adjusted R-square values indicated in table 9, the release profiles of free FA and those of the three types of negatively charged liposomes (i.e. N-REV, N-TFH, N-PRO) fit best to Gompertz model. The release profiles of the two types of positively charged liposomes (i.e. P-TFH, P-PRO) fit best to Korsmeyer-Peppas model while they fit second best to Gompertz model. Although P-TFH and P-PRO fit best to Korsmeyer-Peppas model, the exponent 'n' of the two curves are 0.16 and 0.17, respectively. These values are much smaller than the values described by Korsmeyer-Peppas model, and thus, the release mechanism of ferulic acid does not fall under Fickian diffusion, anamolous transport or case-II transport (Siepmann and Peppas, 2001). Therefore, it is more appropriate to describe the drug release mechanisms of all liposomal formlations using Gompertz model. The initial brust release of ferulic acid shown by the

liposomal formulations may be due to the rapid release of ferulic acid attached to the external surface of lipid membranes of liposomes and due to the concentration gradient between the dialysis bag and the surrounding release medium. The slow release phase that follows may be due to partitioning of ferulic acid between the liposomes and release medium, before ultimately reaching a maximum.

Table 9. Adjusted R-square values of free ferulic acid and different liposomal formulations of curve fitting for seven different drug release models

Formula -tion	Adjusted R-square						
	Zero order	First order	Higuchi	Hixson-Crowell	Korsmeyer -Peppas	Baker - Lonsdale	Gompertz
Free FA	0.3940	0.6529	0.7113	0.5848	0.8887	0.7920	0.9910
N-REV	0.0632	0.1644	0.3885	0.0991	0.5423	0.7132	0.9948
N-TFH	0.0960	0.6999	0.4170	0.1559	0.8518	0.6287	0.9814
N-PRO	0.3511	0.8760	0.6707	0.5280	0.8022	0.6364	0.8423
P-TFH	0.2990	0.6755	0.6672	0.3433	0.9850	0.6560	0.8799
P-PRO	0.3926	0.7222	0.7468	0.4449	0.9830	0.7287	0.8486

3.3.4 *Ex vivo* skin permeation

As stated previously, ferulic acid possesses antioxidant and anticancer activities. Thus, skin permeation of this bioactive compound is desired for pharmaceutical and cosmetic applications. In this work, *ex vivo* skin permeation experiments were carried out using a Franz-diffusion cell using excised full thickness pig ear skin as a substitute to the human skin. The skin permeation profiles are depicted in figure 11 and values pertaining to skin permeation experiments are shown in table 10.

As depicted in figure 11, the three types of negatively charged liposomes exhibited much greater skin permeation of ferulic acid than both the two types of positively charged liposomes and free ferulic acid in PBS. Free ferulic acid in PBS and P-PRO showed the lowest degree of skin penetration (Table 10). The cumulative percent permeation at 24 h of P-TFH was higher than those of free ferulic acid and P-PRO; but was much lower than those of negatively charged liposomes. In fact, the cumulative percent permeation of ferulic acid at 24 h of negatively charged liposomes was greater than two-fold those of free ferulic acid and P-PRO, and approximately 1.7 or 1.8 fold that of P-TFH. Thus, the skin

permeation of liposomal ferulic acid depends clearly on the charge of liposomes. Also, our results reveal that negatively charged liposomes may be utilized to facilitate skin penetration of ferulic acid.

Apart from charge, the types of liposomes used in this study differ in a few other parameters including size and release properties. Thus, the observed variation of skin permeation of liposomes may be a function of at least some if not all of those parameters. Furthermore, incorporation of SA has shown to increase the gel-to-liquid crystalline phase transition temperature (see Chapter 4). The decrease in the liquidity of the lipid membranes of the positively charged liposomes may also be a reason for the lower skin permeability of ferulic acid from those vesicles. Actually, Chen and coworkers forwarded a similar argument to explain the skin penetration behavior of curcumin from liposomes made of phospholipids with different phase-transition temperatures (Chen *et al*., 2012).

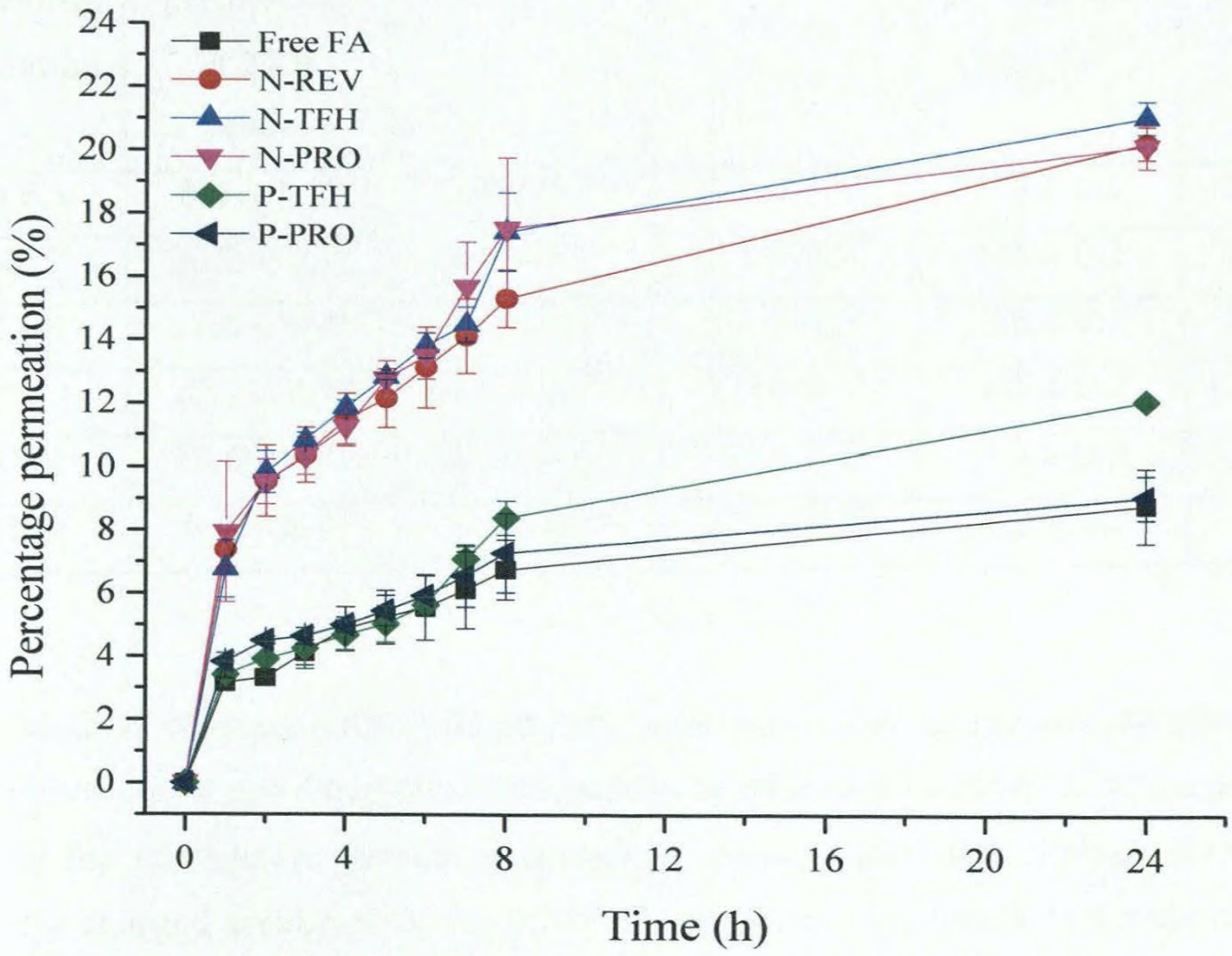

Figure 11. *Ex vivo* skin permeation profiles of free ferulic acid (FA) and different ferulic acid-loaded formulations (n = 3)

According to table 10, free ferulic acid and P-PRO showed the lowest cumulative percent permeation, average flux and average permeability; P-TFH showed slightly higher values than free ferulic acid and P-PRO; whereas, the three types of negatively charged liposomes showed the highest values. The average flux values of negatively charged liposomes were approximately 2 fold that of free ferulic acid while the average permeability values of negatively charged liposomes were approximately 2.5 fold that of free ferulic acid. These results indicate that negatively charged ferulic acid encapsulated liposomes are superior to positively charged liposomes in skin penetration of ferulic acid, under the experimental conditions of this study.

Table 10. Cumulative percent permeation at 24 h, average flux (J(ave)), average permeability (Kp(ave)), skin deposition per unit area and cumulative percent skin deposition at 24 h from different ferulic acid-containing formulations. Each value represents mean ± S.D. (n=3).

Ferulic acid-containing formulation	Cumulative percent permeation at 24 h (%)	J(ave) /10^{-1} (μg / h . cm^2)	K_p(ave) /10^{-3} (cm / h)	Skin deposition per unit area (μg / cm^{-2})	Cumulative percent skin deposition at 24 h (%)
Free FA	8.8 ± 1.2^{a}	2.0 ± 0.3^{a}	3.2 ± 0.5^{a}	1.3 ± 0.1	$2.3 \pm 0.1^{a,b}$
N-REV	20.2 ± 0.5^{b}	4.1 ± 0.1^{b}	8.1 ± 0.2^{b}	1.5 ± 0.2	3.1 ± 0.5^{a}
N-TFH	21.0 ± 0.5^{b}	4.4 ± 0.1^{b}	8.4 ± 0.3^{b}	1.5 ± 0.1	$2.9 \pm 0.2^{a,b}$
N-PRO	20.1 ± 0.7^{b}	4.3 ± 0.2^{b}	8.0 ± 0.3^{b}	1.5 ± 0.2	$2.9 \pm 0.3^{a,b}$
P-TFH	12.0 ± 0.2^{c}	2.8 ± 0.0^{c}	4.5 ± 0.1^{c}	1.3 ± 0.3	$2.3 \pm 0.4^{a,b}$
P-PRO	9.0 ± 0.7^{a}	2.1 ± 0.2^{a}	3.3 ± 0.3^{a}	1.2 ± 0.2	2.2 ± 0.3^{b}

Method of preparation affected the performance of negatively charged liposomes and positively charged liposomes differently. In fact, the method of preparation had no effect on the cumulative percent permeation, average flux and average permeability of negatively charged ferulic acid encapsulated liposomes, whereas it had a significant effect on those parameters of positively charged liposomes. As indicated in table 10, P-TFH is superior to P-PRO. These results show that reverse phase evaporation method, thin film hydration method or proliposome methods are equally effective in the preparation of negatively charged ferulic acid encapsulated liposomes while thin film hydration method is

more effective than proliposome method in preparing positively charged liposomes for skin permeation of ferulic acid.

Although cumulative skin permeation, average flux and average permeability were highly dependent on the charge of liposome, percentage skin deposition and skin deposition per unit area appear to be independent of the charge or method of preparation of ferulic acid encapsulated liposomes. The only significant difference in percentage skin deposition was between N-REV and P-PRO, which may be attributed to the large difference in size and charge of the two types of vesicles. Basically, these results indicate that either negatively charged or positively charged liposomes may be utilized for the skin deposition of ferulic acid.

3.4 Conclusion

Charge and/or method of preparation impart significant effects on properties such as EE, LC, size, polydispersity index, zeta-potential, release properties and skin permeation properties of ferulic acid encapsulated liposomes.

Positively charged liposomes prepared by incorporating SA in the lipid bilayers of liposomes may be utilized to obtain liposomes with higher EEs (i.e. approx. 80 %) than negatively charged liposomes. Since EE was independent of the method of preparation under the experimental conditions, either reverse phase evaporation method, thin film hydration method or proliposome method may be used in the preparation of liposomes. In general, LC was independent of both charge and method of preparation.

The charge and method of preparation have a profound effect on size of ferulic acid encapsulated liposomes. The polydispersity index also depends on charge, and this parameter indicates that negatively charged liposomes more homogenous than positively charged liposomes may be prepared under the experimental conditions of this study. The zeta-potential depends on the lipid composition and indicates that egg yolk PC and CH may be utilized to form stable negatively charged ferulic acid encapsulated liposomes while egg yolk PC, CH and SA may be utilized to form positively charged liposomes.
This study reveals that liposomal encapsulation of ferulic acid irrespective of the method of preparation may be utilized for slow release of ferulic acid. As expected, the release of ferulic acid depends on the charge of liposomes. In fact, positively charged liposomes may be employed for much slower release of ferulic acid than negatively charged liposomes.

Also, this work shows that negatively charged liposomes are superior to positively charged liposomes for skin penetration of ferulic acid. However, both negatively charged

liposomes and positively charged liposomes are equally effective in skin deposition of ferulic acid. The method of preparation has only negligible effect on skin permeation and skin deposition of ferulic acid.

3.5 References

Adlakha-Hutcheon, G., Bally, M.B., Shew, C.R. and Madden, T.D. (1999). Controlled destabilization of a liposomal drug delivery system enhances mitoxantrone antitumor activity. *Nature biotechnology* **17(8)**, 775-779.

Akbarzadeh, A., Rezaei-Sadabady, R., Davaran, S., Joo, S.W., Zarghami, N., Hanifehpour, Y., Samiei, M., Kouhi, M. and Nejati-Koshki, K. (2013). Liposome: classification, preparation, and applications. *Nanoscale Research Letters* **8**, 102-110.

Banerjee, R. (2001). Liposomes: Applications in Medicine. *Journal of biomaterials applications* **16**, 3-21.

Chen, M., Liu, X. and Fahr, A. (2010). Skin Delivery of Ferulic Acid from Different Vesicular Systems. *Journal of Biomedical Nanotechnology* **6(5)**, 577-585.

Chen, Y., Wu, Q., Zhang, Z., Yuan, L., Liu, X. and Zhou, L. (2012). Preparation of curcumin loaded liposomes and evaluation of their skin permeation and pharmacodynamics. *Molecules,* **17**, 5972-5987.

Dua, J.S, Rana, A.C. and Bhandari, A.K. (2012). Liposome:Methods of preparation and applications. *International Journal of Pharmaceutical Studies and Research, 3*(2), 14-20.

Gillet, A., Compère, P., Lecomte, F., Hubert, P., Ducat, E., Evrard, B. and Piel, G. (2011). Liposome surface charge influence on skin penetration behaviour. *International Journal of Pharmaceutics* **411**, 223-231.

Kim, C-K., Lee, M-K., Han, J-H. and Lee, B-J. (1994). Pharmacokinetics and tissue distribution of methotrexate after intravenous injection of differently charged liposome-entrapped methotrexate to rats. *International Journal of Pharmaceutics* **108**, 21-29.

Lokhandwala, H., Deshpande, A. and Deshpande, S. (2013). Kinetic modeling and dissolution profiles comparison: An overview. *International Journal of Pharma and Bio Sciences* **4(1)**, 728-737.

Laouini, A., Jaafar-Maalej, C., Limayem-Blouza, I., Sfar, S., Charcosset, C. and Fessi, H. (2012). Preparation, Characterization and Applications of Liposomes: State of the Art. *Journal of Colloidal Science and Biotechnology* **1**, 147-168.

Lasic, D.D. (1998). Novel applications of liposomes. *Trends in Biotechnology* **16**, 307-321.

Lin, F-H., Lin, J-Y., Gupta, R.D., Tournas, J.A., Burch, J.A., Selim, M.A., Monteiro-Riviere, N.A., Grichnik, J.M., Zielinski, J. and Pinnell, S.R. (2005). Ferulic Acid Stabilizes a Solution of Vitamins C and E and Doubles its Photoprotection of Skin. *Journal of Investigative Dermatology* **125**, 826 –832.

Maherani, B., Arab-Tehrany, E., Kheirolomoom, A., Geny, D. and Linder, M. (2013). Calcein release behavior from liposomal bilayer; influence of physicochemical/mechanical/structural properties of lipids. *Biochimie,* **95**, 2018-2033.

Ogiwara, T., Satoh, K., Kadoma, Y., Murakami,Y., Unten, S., Atsumi, T., Sakagami, H. and Fujisawa, S. (2002). Radical scavenging activity and cytotoxicity of ferulic acid. *Anticancer Research* **22(5)**, 2711–2717.

Oh, E.K., Jin, S-E., Kim, J-K., Park, J-S., Park, Y. and Kim, C-K. (2011). Retained topical delivery of 5-aminolevulinic acid using cationic ultradeformable liposomes for photodynamic therapy. *European Journal of Pharmaceutical Sciences* **44(1-2)**, 149-157.

Park, S-J., Choi, S.G., Davaa, E. and Park, J-S. (2011). Encapsulation enhancement and stabilization of insulin in cationic liposomes. *International Journal of Pharmaceutics* **415**, 267-272.

Park, S-J., Choi, S.G., Davaa, E. and Park, J-S. (2011). Encapsulation enhancement and stabilization of insulin in cationic liposomes. *International Journal of Pharmaceutics* **415**, 267-272.

Qin, J., Chen, D.W., Lu, W.G., Xu, H., Yan, C.Y., Hu, H.Y., Chen, B.Y., Qiao, M.X. and Zhao, X.L. (2008). Preparation, Characterization, and Evaluation of Liposomal Ferulic Acid In Vitro and In Vivo. *Drug development and industrial pharmacy* **34(6)**, 602-608.

Siepmann, J. and Peppas, N.A. (2001). Modeling of drug release from delivery systems based on hydroxypropyl methylcellulose (HPMC). *Advanced drug delivery reviews* **48**, 139-157.

Stefanutti, E., Papacci, F., Sennato, S., Bombelli, C., Viola, I., Bonincontro, A., Bordi, F., Mancini, G., Gigli, G. and Risuleo, G. (2014). Cationic liposomes formulated with DMPC and a gemini surfactant traverse the cell membrane without causing a significant bio-damage. *Biochimica et Biophysica Acta,* **1838**, 2646–2655.

Szoka Jr., F. and Papahadjopoulos, D. (1978). Procedure for preparation of liposomes with large internal aqueous space and high capture by reverse-phase evaporation. *Proc Natl Acad Sci USA* **75(9)**, 4194-4198.

Tardi, P.G., Gallagher, R.C., Johnstone, S., Harasym, N., Webb, M., Bally, M.B. and Mayer, L.D. (2007). Coencapsulation of irinotecan and floxuridine into low cholesterol-containing liposomes that coordinate drug release in vivo. *Biochimica et Biophysica Acta* **1768**, 678–687.

Zhang, J., Yuan, H., Lin, D., Tnag, Q. and Xu, X. (2011). Study on pharmacokinetics of ferulic acid loaded liposome-in-chitosan microspheres in rats. *Zhongguo Zhongyao Zazhi* **36(13)**, 1751-1754.

CHAPTER 4

EFFECT OF LIPID COMPOSITION ON PROPERTIES OF CURCUMIN ENCAPSULATED LIPOSOMES

4.1 Introduction

Curcumin is a natural compound that exhibits numerous important bioactivities. However, the poor bioavailability and low stability of this bioactive compound hinder its use as a pharmaceutical ingredient. Among the numerous strategies adopted to overcome these limitations, liposomal encapsulation has been studied extensively (Lu *et al.*, 2012; Takahashi *et al.*, 2009). Interestingly, liposomal systems can be used to enhance important properties such as sustained release and skin delivery of bioactive agents in addition to improving bioavailability and stability.

Liposomal encapsulation of curcumin has improved numerous important properties of this bioactive agent with potential applications in many different fields. Curcumin encapsulated liposomes have been utilized in developing antimicrobial surfaces for the food industry (Dogra *et al.*, 2015). Furthermore, Shin and coauthors suggested that curcumin nanoliposomes coated with chitosan may be suitable for applications in the food industry due to the increased bioavailability, mucoadhesive properties and storage stability exhibited by those nanoparticles (Shin *et al.*, 2013). Another field that conducts research to enhance numerous aspects of liposomal curcumin is pharmaceutics. Research in pharmaceutics has revealed that liposomal curcumin exhibits higher therapeutic efficacy against several malignancies than free curcumin. For instance, increased anticancer, antitumor, and anti-inflammatory properties of liposomal curcumin have been reported (Basnet *et al.*, 2012; Narayanan et al., 2009; Ranjan *et al.*, 2013). Also, it has been demonstrated that the lipid composition of liposomes affects the bioactivity of curcumin encapsulated liposomes. For instance, Dhule and coworkers showed that the antitumor activity of curcumin against osteosarcoma cell lines enhanced upon incorporation of C6 ceramide in the lipid bilayer of liposomes (Dhule *et al.*, 2014). This work focused on investigating the effect of lipid composition of liposomes on properties of curcumin encapsulated liposomes.

The lipid composition of liposomes constitutes a main factor that determines the properties of liposomes and the effect of lipid composition on the properties of liposomes is well documented. Examples of properties of liposomes affected by the lipid composition include size, zeta-potential, stability, encapsulation efficiency, release properties, and skin permeation properties (Bouarab *et al.*, 2014; Chen *et al.*, 2012; Hurler *et al.*, 2013;). Thus, the lipid composition can be varied to modulate such properties of liposomes to make those liposomes well suited for their intended application.

The aim of this research was to evaluate the effect of charge and surfactants, individually and in combination, on the properties of curcumin encapsulated liposomes. In this work, egg yolk phosphatidylcholine was used as the staple polar lipid in the preparation of liposomes while cholesterol was used as a minor component. The surfactant – polysorbate 80 – was incorporated in the preparation of deformable liposomes while stearylamine was utilized in the preparation of positively charged liposomes. The properties of liposomes considered were size, zeta-potential, encapsulation efficiency, loading capacity, in vitro release and skin delivery of curcumin. Also, thermal analysis was carried out to investigate the degradation behavior and phase transition temperatures of curcumin encapsulated liposomes. The expected outcomes of this study were to develop liposomal formulations that facilitate slow-release and improved skin delivery of curcumin and to acquire knowledge of the behavior of charged lipids and surfactants in liposomal formulations, that will be useful in the future engineering of liposomal systems.

4.2 Materials and methods

4.2.1 Materials

Egg yolk PC (~ 60% TLC), CH (purity ≥ 99 %), P80, SA (assay 90 %), curcumin (assay ≥ 65 % (HPLC), ethanol (HPLC grade), methanol (HPLC grade), phosphoric acid (85 % wt. % in water), and dialysis membrane (MWCO 12 000) were purchased from Sigma-Aldrich. Chloroform (reagent grade) was obtained from Fisher Scientific. Deionized water filtered through a 0.2 μm filter was used throughout the study. Fresh pig ears were obtained from a local slaughter house.

4.2.2 Methods

4.2.2.1 Preparation of liposomes

Preparation of curcumin encapsulated negatively charged liposomes (NL)

Thin-film hydration method was used to prepare NL. Briefly, PC (200 mg) and CH (50 mg) were dissolved in chloroform (50 ml) in a round bottom flask to which an ethanol solution of 10 mg of curcumin was added. Then, a thin film of lipid soluble components was prepared by evaporating the organic solvent under reduced pressure using a rotary evaporator (Heidolph - Laborota 4000). Any residual solvent was removed by keeping the round bottom flask with the thin film of lipids in a vacuum oven over night. Next, the thin film of lipids was hydrated using deionized water. The resultant liposomal solution was allowed to stand at 4 °C overnight to complete hydration. After that, the liposomal solution was sonicated for 10 min at 4 °C using a bath sonicator (Branson 2510).

Preparation of curcumin encapsulated negatively charged hybrid liposomes (NHL)

Thin-film hydration method was used to prepare NHL. The same procedure as above was followed after dissolving PC (200 mg), CH (25 mg) and P80 (25 mg) in chloroform (50 ml) in a round bottom flask to which an ethanol solution of 10 mg of curcumin was added.

Preparation of curcumin encapsulated positively charged liposomes (PL)

Thin-film hydration method was used to prepare PL. The same procedure as above was followed after dissolving PC (200 mg), CH (25 mg) and SA (25 mg) in chloroform (50 ml) in a round bottom flask to which an ethanol solution of 10 mg of curcumin was added.

Preparation of curcumin encapsulated positively charged hybrid liposomes (PHL)

Thin-film hydration method was used to prepare PHL. The same procedure as above was followed after dissolving PC (200 mg), CH (25 mg), SA (25 mg) and P80 (25 mg) in chloroform (50 ml) in a round bottom flask to which an ethanol solution of 10 mg of curcumin was added.

4.2.2.2 Determination of encapsulation efficiency and loading capacity

The EE and LC of curcumin encapsulated liposomes were determined using a HPLC method. First, unencapsulated curcumin was removed from liposomes by dialyzing the liposomal solutions against deionized water at 4 °C for 3 days. Next, the amount of encapsulated curcumin was determined by HPLC analysis after disrupting the liposomes in ethanol.

The above procedure was repeated for the determination of EE and LC of all four types of liposomes.

The formula used to calculate the EE is given below.

$$Encapsulation\ efficiency = \frac{Amount\ of\ curcumin\ encapsulated\ in\ liposomes}{Amount\ of\ curcumin\ initially\ introduced} \times 100$$

The formula used to calculate the LC is given below.

$$Loading\ capacity = \frac{Mass\ of\ curcumin\ encapsulated\ in\ liposomes}{Total\ mass\ of\ curcumin\ encapsulated\ liposomes} \times 100$$

4.2.2.3 Determination of particle size and zeta-potential

Particle sizes of liposomes were determined using a Malvern zetasizer NanoZS (Malvern instruments, UK) fitted with a red laser of 633 nm, using dynamic light scattering technique. Liposome suspensions were diluted in deionized water, filtered with a 0.2 μm filter, and the scattering intensity was measured at an angle of 173° relative to the incident radiation after equilibrating the samples at 25 °C. The values reported are the z-average diameters of liposomes. Zeta-potentials of the same liposomal suspensions described above were measured using the Malvern zetasizer fitted with a red laser of 633 nm, using Laser Doppler Electrophoresis technique. The values reported are the z-average zeta-potentials of liposomes.

4.2.2.4 Thermal analysis

Thermogravimetric analysis

TGA was carried out using a thermogravimetric analyzer (TA Instruments SDT Q600). An alumina crucible was used to hold approximately 5 mg of sample in the crucible. The sample was heated from room temperature to 800 °C at a heating rate of 20 °C/min under a high purity nitrogen flow of 100 mL/min.

TGA was carried out following the procedure described above using PC, CH, P80, SA, curcumin, NL, NHL, PL and PHL.

Differential scanning calorimetry

DSC was performed on a DSC Q200 DSC. A 4-6 mg portion of the sample was placed in crimped but vented aluminum pans and heated at a rate of of 10 °C/min in the temperature range of -40 °C - +80 °C. The sample was purged by a stream of dry nitrogen flowing at 50 mL/min.

DSC was carried out following the procedure described above using NL, NHL, PL and PHL. Four cycles of heating and cooling were conducted for each sample.

4.2.2.5 *In vitro* release studies

5 mL of liposomal solution was put in dialysis tubing (12 000 MWCO) and then both ends were sealed. The dialysis tubing with liposomal solution was immersed in PBS of pH 6.8 containing 20 % (v/v) ethanol and 0.5 % (v/v) P80. The release medium was stirred at a constant rate using a magnetic stirrer. 1 mL aliquots were removed at predetermined time intervals and the release medium was replenished immediately with fresh medium. Withdrawn aliquots were analyzed by HPLC. This experiment was conducted in triplicate.

In vitro release studies were carried out following the procedure described above using NL, NHL, PL and PHL.

Release profiles of curcumin encapsulated different liposomal formulations were fitted to six different drug release models: Zero order, First order, Higushi, Hixon-Crowell, Korsemeyer-Peppas, and Gompertz. The model that exhibited the adjusted R-square closest to unity was selected as the best fit.

The functions of the models considered are given under section 3.2.2.7.

4.2.2.6 *Ex vivo* skin permeation and skin deposition of curcumin

Excised pig ear skin was used for *ex vivo* skin permeation studies. The receiver compartment of a Franz cell was filled with buffer (PBS, pH 6.8) containing ethanol - 20 % (v/v) and P80 - 0.5 % (v/v). The excised epidermis was placed between the donor and receiver compartments and 5 mL of liposomal solution was introduced through the donor compartment. 1 mL aliquots were withdrawn from the receiver compartment at predetermined time intervals for 8 h and the receiver solution was replenished immediately with fresh buffer. Withdrawn aliquots were analyzed by HPLC.

After 8 h, pig ear skin used for permeation study was removed from the Franz cell, and liposomes on the skin were removed using tissue and absorbent cotton wool. Next, the skin was immersed in 25 mL of ethanol and was stirred for 12 h. The ethanol solution was then analyzed for curcumin using HPLC. This experiment was conducted in triplicate.

Ex vivo skin permeation and skin deposition studies were carried out following the procedure described above using NL, NHL, PL and PHL.

4.2.2.7 HPLC determination of curcumin

HPLC determination of curcumin was carried out using an Agilent HPLC. Each sample was filtered through a 0.2 μm PTFE filter and was injected using an autosampler. A phosphate buffer of pH 2.2 and acetonitrile were used for gradient elution and the retention time was 11.5 min. Detection was carried out using a dioade array detector at 425 nm.

4.2.2.8 Statistical analysis

All data are presented as mean ± standard deviation (S.D.) of three parallel experiments (n = 3). Microsoft Office Excel 2007 was used for the above calculations. One way ANOVA was conducted using MINITAB 14 software to compare the results and $P < 0.05$ was considered significant. Curve fitting for different drug release models was carried out using OriginPro 9 software.

4.3 Results and discussion

4.3.1 Encapsulation efficiency and loading capacity

The EE and LC values obtained for each type of liposomes are shown in table 11.

Table 11. Encapsulation efficiencies and loading capacities of different liposomal formulations. Values are reported as mean ± S.D. (n = 3).

Liposomal formulation	EE (%)	LC (%)
NL	87.8 ± 4.3	3.4 ± 0.2
NHL	77.8 ± 5.7	3.0 ± 0.2
PL	57.5 ± 1.3	2.2 ± 0.1
PHL	54.5 ± 2.2	1.9 ± 0.1

The EEs of curcumin encapsulated liposomes spanned from 55 % to 88 %. These high EEs may be due to the utilization of the thin film hydration method, which usually gives high EEs for the encapsulation of hydrophobic species, for the preparation of liposomes in this study. The EEs of NL and NHL are actually comparable with the values reported by Chen and coworkers who used soy bean PC or egg yolk PC with CH and Tween 80 for the preparation of curcumin encapsulated liposomes (Chen *et al.*, 2012).

Although the liposomes exhibited relatively high EEs, those values depended on the lipid composition of curcumin encapsulated liposomes. Liposomes consisting of only PC and CH in the lipid component showed the highest EE which is 87.8 ± 4.3 %. When P80 was incorporated in the lipid bilayer, the EE decreased by 11 % to reach 77.8 ± 5.7 %. The EE of SA incorporated PL was 57.5 ± 1.3 %; a pronounced decrease. Consistent with the negatively charged liposomes, incorporation of P80 along with SA, further decreased the EE to 54.5 ± 2.2 %. However, this decrease was negligible, indicating that the effect of P80 on the EE diminishes in the presence of SA. The decrease of EE upon the incorporation of P80 and SA may be because these compounds decrease the space available for curcumin in the lipid bilayers of liposomes.

The LCs ranged from 1.9 ± 0.1 % to 3.4 ± 0.2 % and depended on the lipid composition. Like EEs, LCs decreased upon incorporation of P80 or SA. Also, the effect of SA superseded that of P80 when both species were present together.

Although P80 and SA decrease the encapsulation of curcumin, it is unreasonable to generalize this effect over all surfactants and positively charged species incorporated in the lipid component. Surfactants and such positively charged species incorporated in the lipid bilayers show great diversity in their structures so that their effects on the arrangement of lipids in the lipid bilayers also vary widely. Thus, it can be concluded that P80 and SA have a detrimental effect on the EE of curcumin in liposomes made of egg yolk PC and CH, most probably due to competition among P80, SA and curcumin for space in the lipid bilayers of liposomes, and thus, that conventional liposomes (NL) are superior in terms of EE and LC in this context.

4.3.2 Particle size and zeta-potential

The particle size and zeta-potential of each type of liposomes were analyzed using a Malvern zetasizer. The values obtained are shown in table 12.

Table 12. Diameter, polydispersity index and zeta-potential of different types of curcumin encapsulated liposomes. Each value represents mean ± S.D. (n = 3). Statistically different values are followed by different superscripts and vice versa, in each column.

Liposomal formulation	Diameter (nm)	Polydispersity index	Zeta-potential (mV)
NL	284.2 ± 6.3^{a}	0.296 ± 0.046^{a}	-57.4 ± 3.5^{a}
NHL	225.7 ± 5.0^{b}	0.293 ± 0.020^{a}	-48.7 ± 1.7^{b}
PL	226.8 ± 10.9^{b}	0.399 ± 0.038^{b}	$+42.0 \pm 0.3^{c}$
PHL	265.3 ± 3.3^{c}	$0.363 \pm 0.059^{a,b}$	$+48.2 \pm 0.8^{d}$

The mean diameters ranged from 225 nm to 285 nm, exhibiting their suitability for pharmaceutical applications. The statistically different values indicate that the size of curcumin encapsulated liposomes depends on the lipid composition. NLs were the largest vesicles. Upon incorporation of P80 in the lipid bilayer, the size decreased significantly, most probably because of the large head group of this surfactant that may increase the curvature of the vesicles (cf. NL and NHL). Similar to the incorporation of P80, the incorporation of SA in the lipid bilayer to form positively charged liposomes resulted in smaller vesicles (cf. NL and PL). However, unlike P80, SA consists of only a small polar head group. Thus, increase of the curvature of the lipid bilayer by SA only is highly

unlikely. However, interactions of SA with curcumin and / or CH may lead to the formation of smaller vesicles. Since both P80 and SA contributed to the formation of smaller vesicles, it was expected that the size would further decrease upon their incorporation together to form PHL. In contrast, PHLs were larger than both NHLs and PLs. These size differences reveal that SA and P80 have an antagonistic effect with respect to size of liposomes made of egg yolk PC and CH. Basically, our results indicate that P80 and SA can be used to modulate the size of curcumin encapsulated liposomes, especially intended for pharmaceutical applications.

Although the incorporation of P80 had a significant effect on the size, it had no effect on the polydispersity index of liposomes. Thus, this surfactant can be used to prepare homogeneous populations of curcumin encapsulated liposomes. According to the polydispersity indeces of the four types of liposomes, NLs and NHLs are more homogenous than PLs and PHLs. These results indicate that the incorporation of SA contributes to the formation of more dispersed populations of liposomes. Thus, if the application demands a narrow size distribution of liposomes, other positively charged lipids should be utilized instead of SA.

The zeta-potentials reveal that curcumin encapsulated liposomes stable in solution can be prepared incorporating P80 and/or SA in liposomes made of egg yolk PC and CH. Although the lipids, PC and CH, and the surfactant P80 bear no net charge, liposomes made using those species were negatively charged. In fact, the zeta-potential of NL was - 57.4 ± 3.5 mV while that of NHL was - 48.7 ± 1.7 mV. This negative charge may have resulted due to the orientation of the phosphate group of PC towards the external aqueous component of the lipid bilayer, facilitated by CH. In fact, this phenomenon was observed with free liposomes and plant extract encapsulated liposomes as mentioned in Chapter 2. These results indicate that the effect of CH on the orientation of the head group of PC is either unaffected or augmented by the presence of curcumin in the bilayer. Upon incorporation of P80 in curcumin encapsulated liposomes, the liposomes remained negatively charged; however, the zeta-potential increased (i.e. became less neagative) significantly. This increase may be due to the shielding of the phosphate groups of PC by the ethoxy moieties of the head groups of P80. Thus, P80 may be utilized to increase the zeta-potential of negatively charged liposomes made of PC and CH. Positively charged liposomes resulted when SA was incorporated in the lipid bilayer of curcumin encapsulated liposomes. Thus, SA can be utilized to prepare cationic curcumin liposomes successfully. As in the case of anionic liposomes, the incorporation of P80 had a

significant effect on the zeta-potential of cationic liposomes. Again, upon incorporation of P80, the zeta-potential increased probably due to the shielding of phosphate groups of PC in the bilayer by P80. Thus, P80 increases the zeta-potential of both negatively charged and positively charged curcumin encapsulated liposomes.

4.3.3 Thermal analysis

4.3.3.1 Thermogravimetric analysis

The four types of curcumin encapsulated liposomes and their constituents were subject to TGA and their main degradation temperatures and the corresponding weight losses are given in table 13.

Table 13. The main degradation temperatures and corresponding weight losses of curcumin encapsulated liposomes and their constituents

Compound / formulation	Degradation temperature (°C)	Corresponding weight loss (%)
Phosphatidylcholine	344.63 378.84	52.05 29.18
Cholesterol	352.03 439.90	69.95 19.36
Polysorbate 80	413.54	96.92
Stearylamine	262.57	95.88
Curcumin	380.45	58.92
NL	368.29	77.09
NHL	368.06	85.18
PL	353.64	75.59
PHL	359.22	85.76

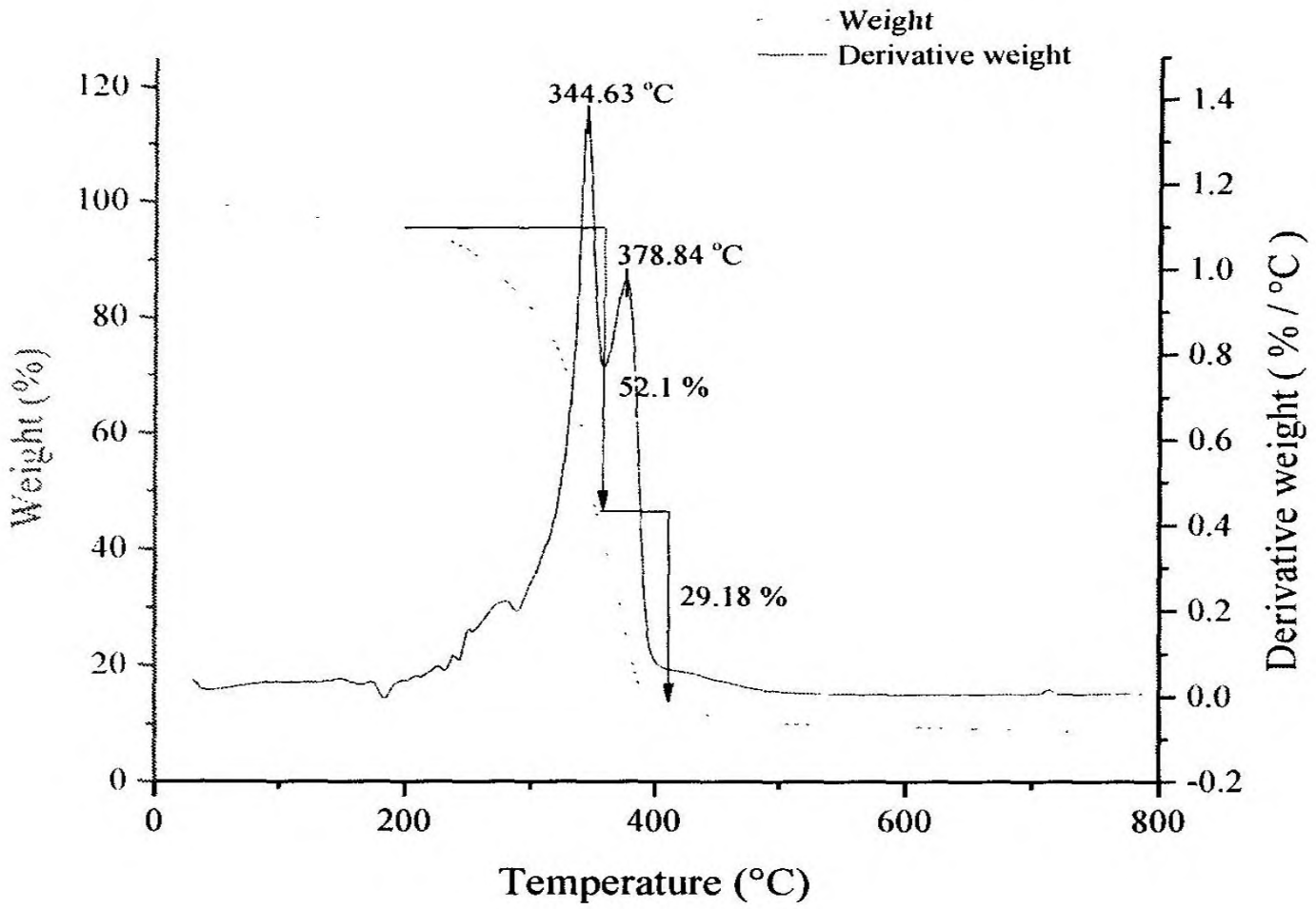

Figure 12. Weight and derivative weight versus temperature of TGA of phosphatidylcholine

The TGA profile of phosphatidylcholine is shown in figure 12. PC exhibited two main degradation temperatures; one at 344.6 °C which corresponded to a weight loss of 52.1 % and the other at 378.8 °C which corresponded to a weight loss of 29.2 %. The residual weight at 800 °C was only 8.4 %.

The TGA profile of cholesterol is shown in figure 13. CH, also, exhibited two main degradation temperatures. The major one was at 352.0 °C corresponding to a weight loss of 70.0 % while the other was at 439.9 °C corresponding to a weight loss of 19.4 %. The residual weight at 800 °C was only 3.9 %.

The TGA profile of polysorbate 80 is shown in figure 14. P80 showed one degradation temperature at which almost all P80 was degraded. In fact, a weight loss of 96.9 % occurred at 413.5 °C. The residual weight at 800 °C was negligible.

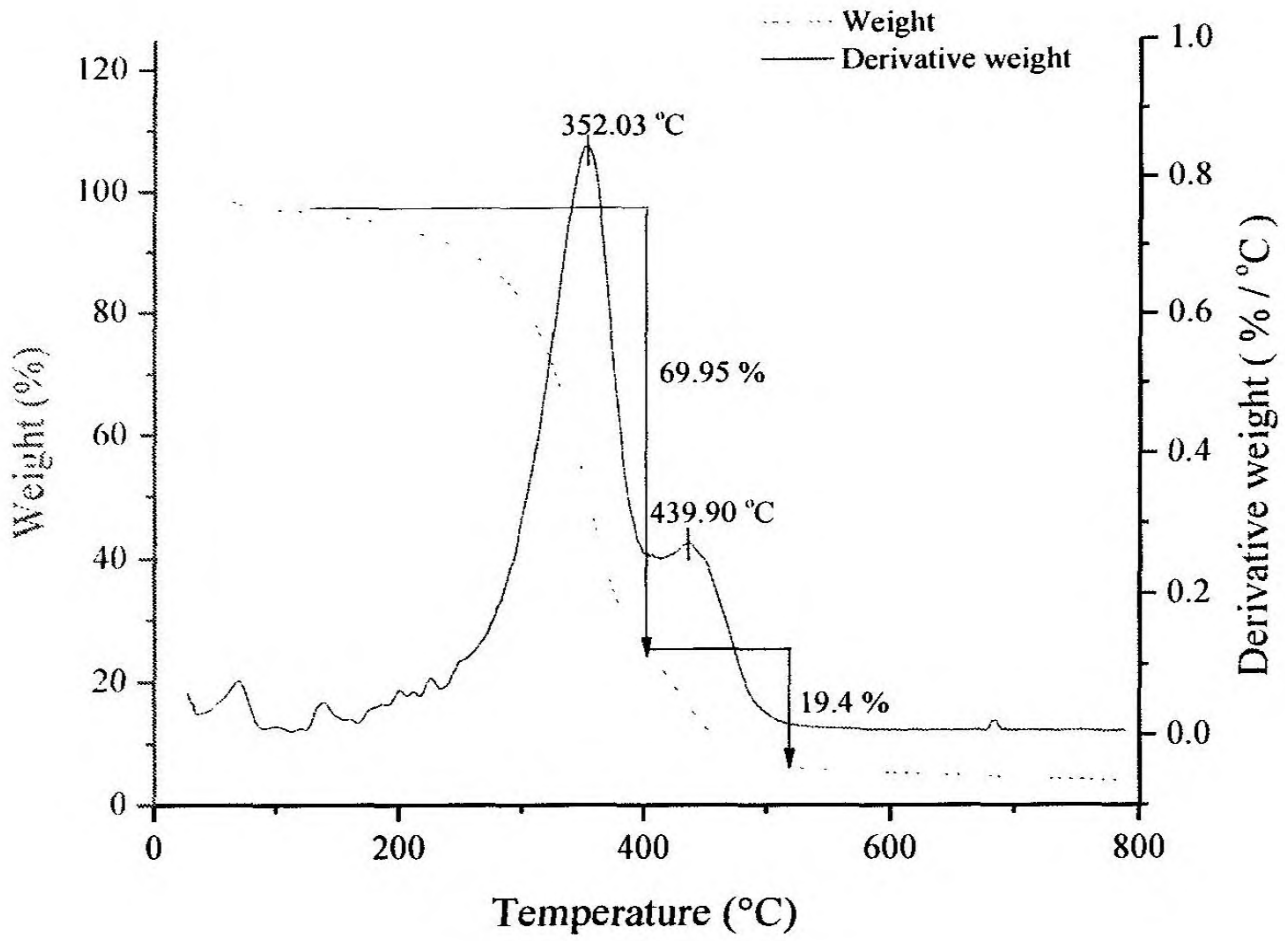

Figure 13. Weight and derivative weight versus temperature of TGA of cholesterol

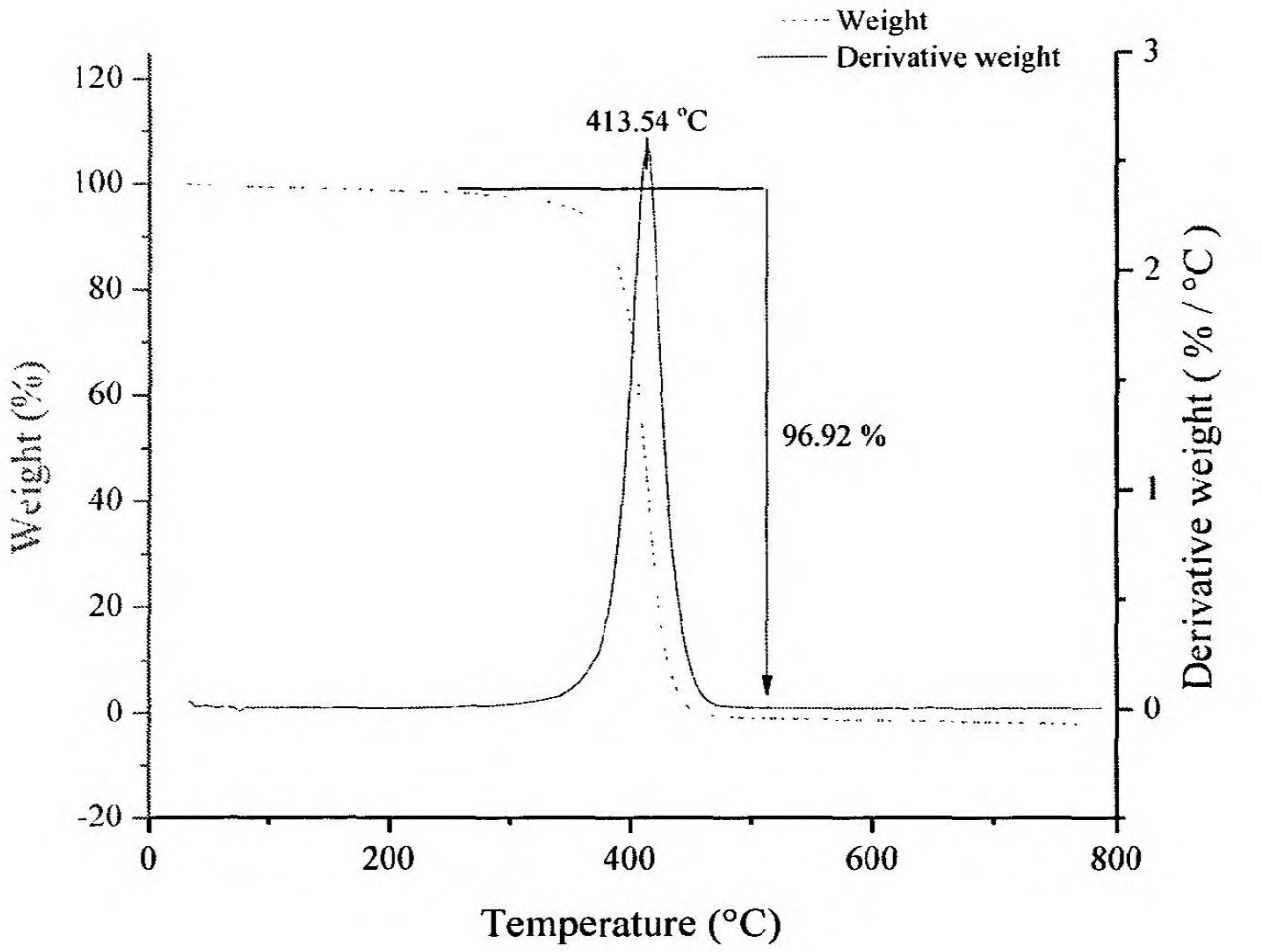

Figure 14. Weight and derivative weight versus temperature of TGA of polysorbate 80

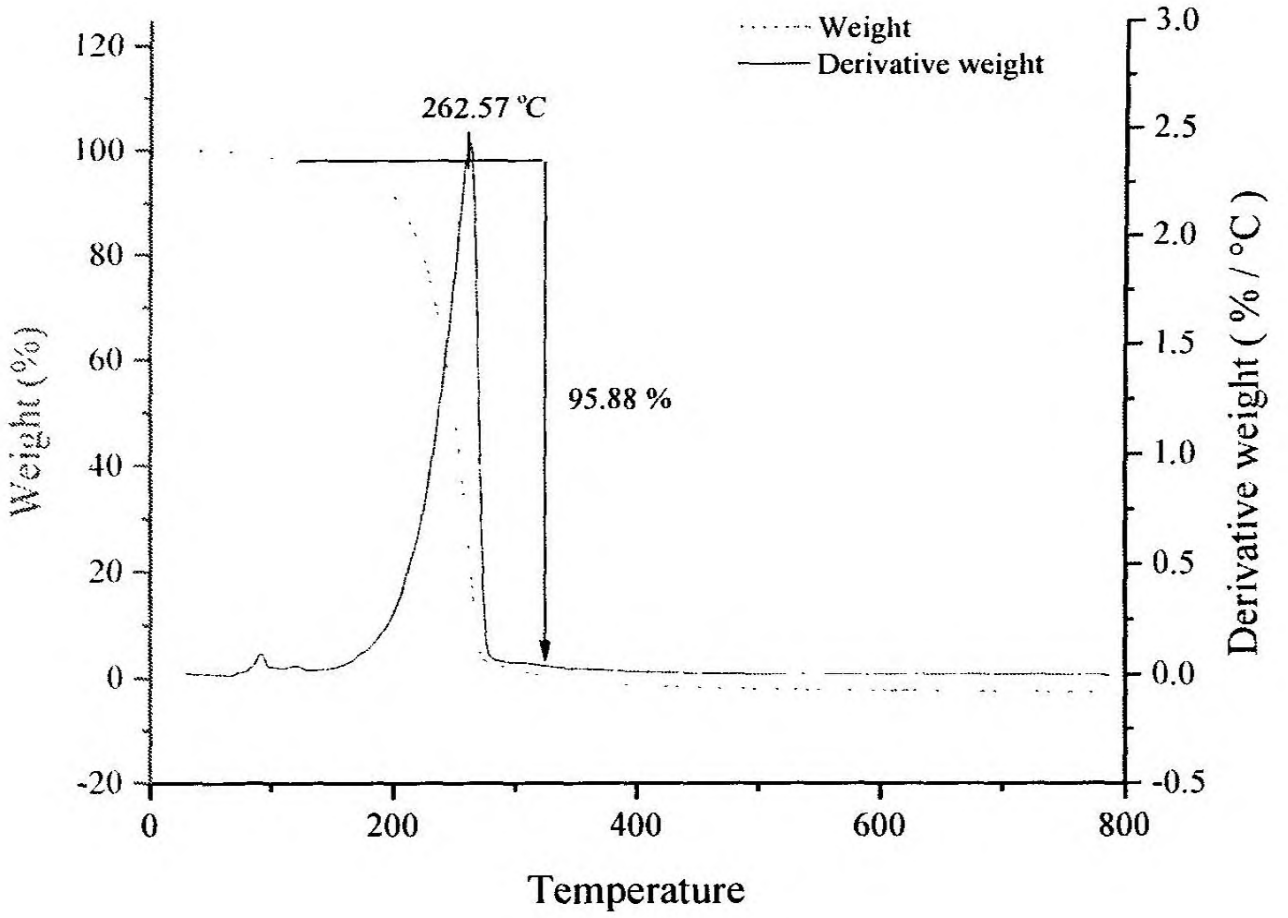

Figure 15. Weight and derivative weight versus temperature of TGA of stearylamine

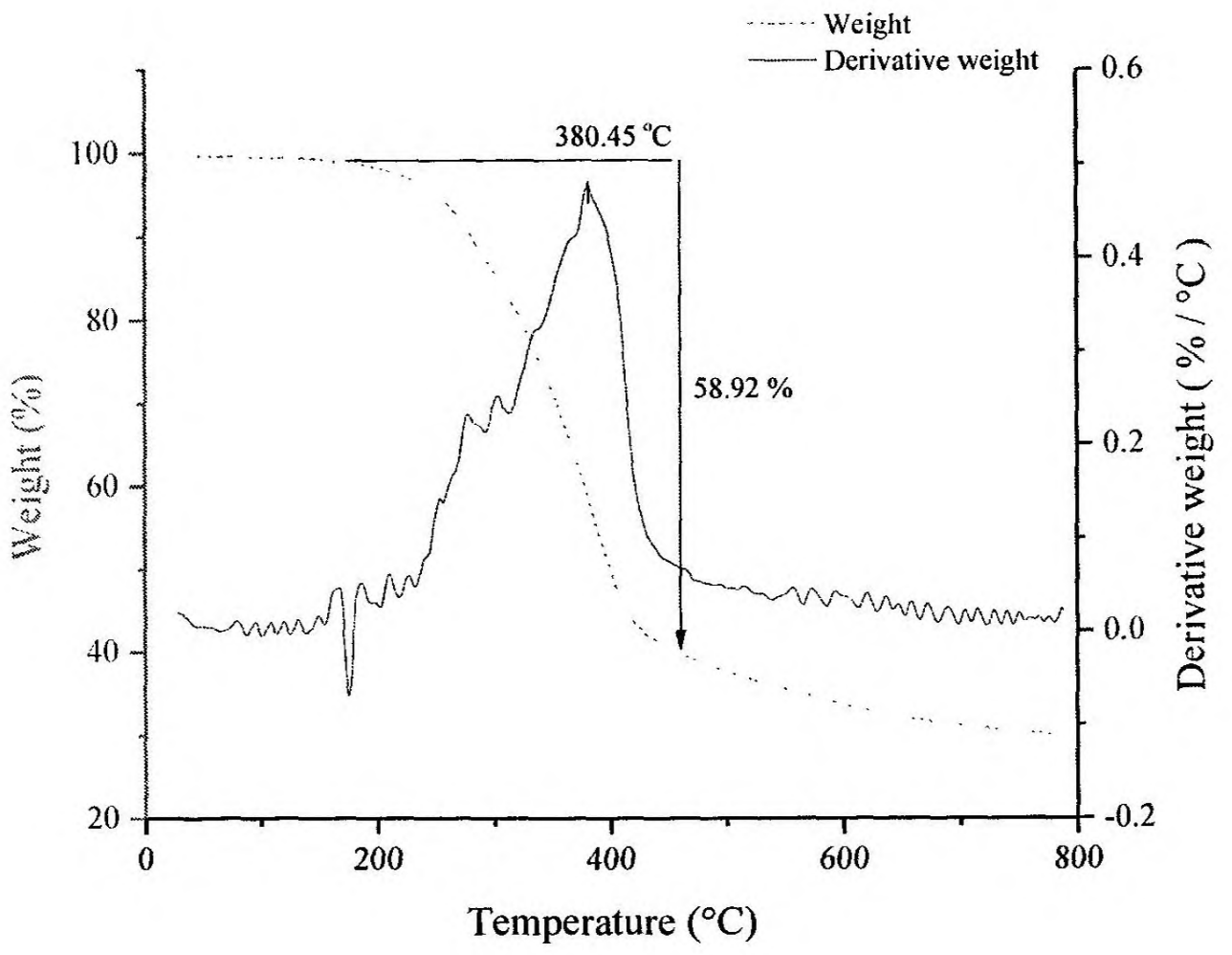

Figure 16. Weight and derivative weight versus temperature of TGA of curcumin

The TGA profile of stearylamine is shown in figure 15. Similar to the degradation profile of P80, the degradation profile of SA consisted of only one degradation temperature. This degradation temperature was at 262.6 °C and the corresponding weight loss was 95.9 %. The residual weight was negligible.

The TGA profile of curcumin is shown in figure 16. Curcumin showed degradation at 380.4 °C and the corresponding weight loss was 58.9 %. The residual weight at 800 °C was 30.1 %.

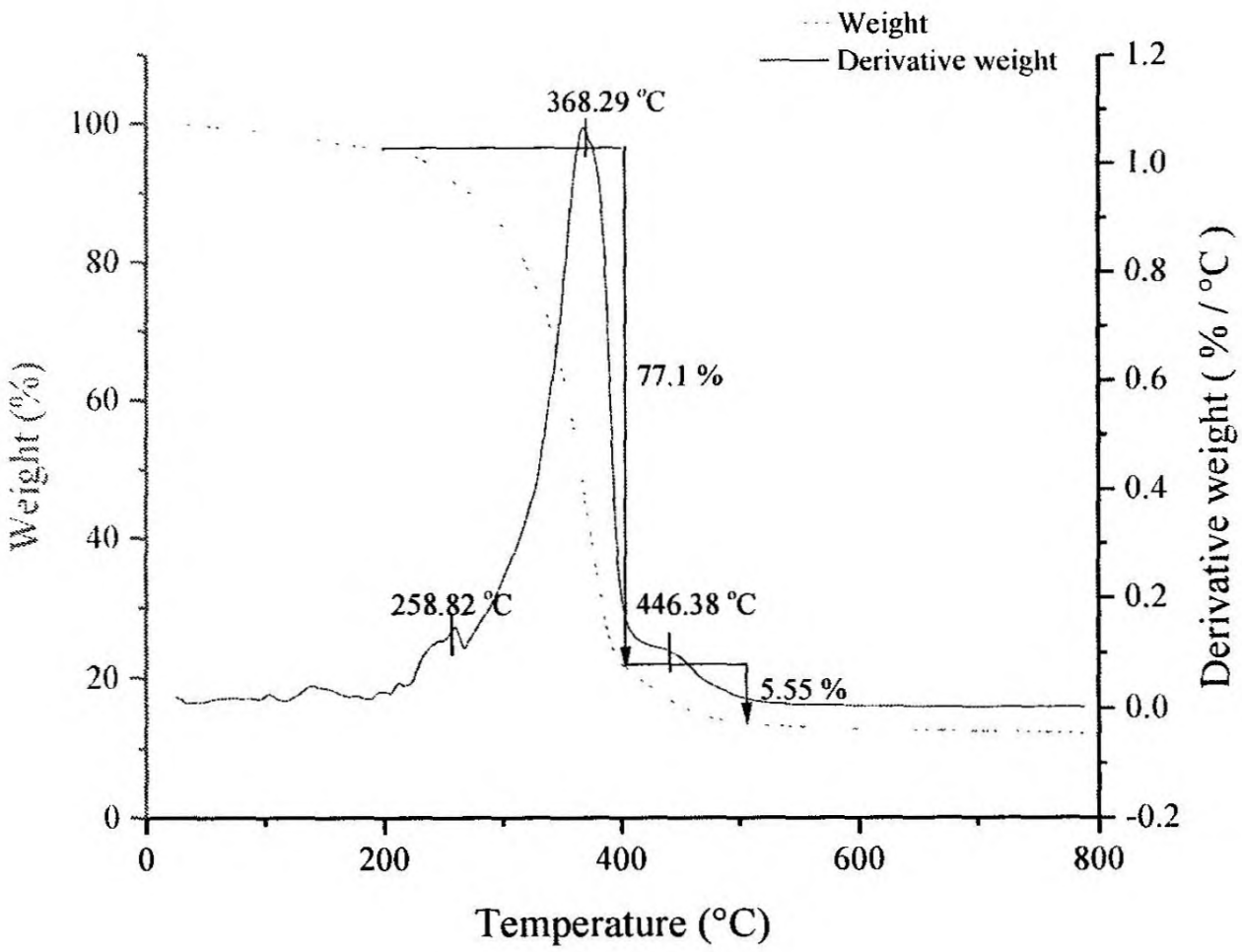

Figure 17. Weight and derivative weight versus temperature of TGA of curcumin encapsulated negatively charged liposomes

The TGA profile of NL is shown in figure 17. NL exhibited the main degradation peak at 368.3 °C that corresponded to a weight loss of 77.1 %. Minor degradation peaks were at 258.8 °C and 446.4 °C. The residual weight at 800 °C was 12.2 %.

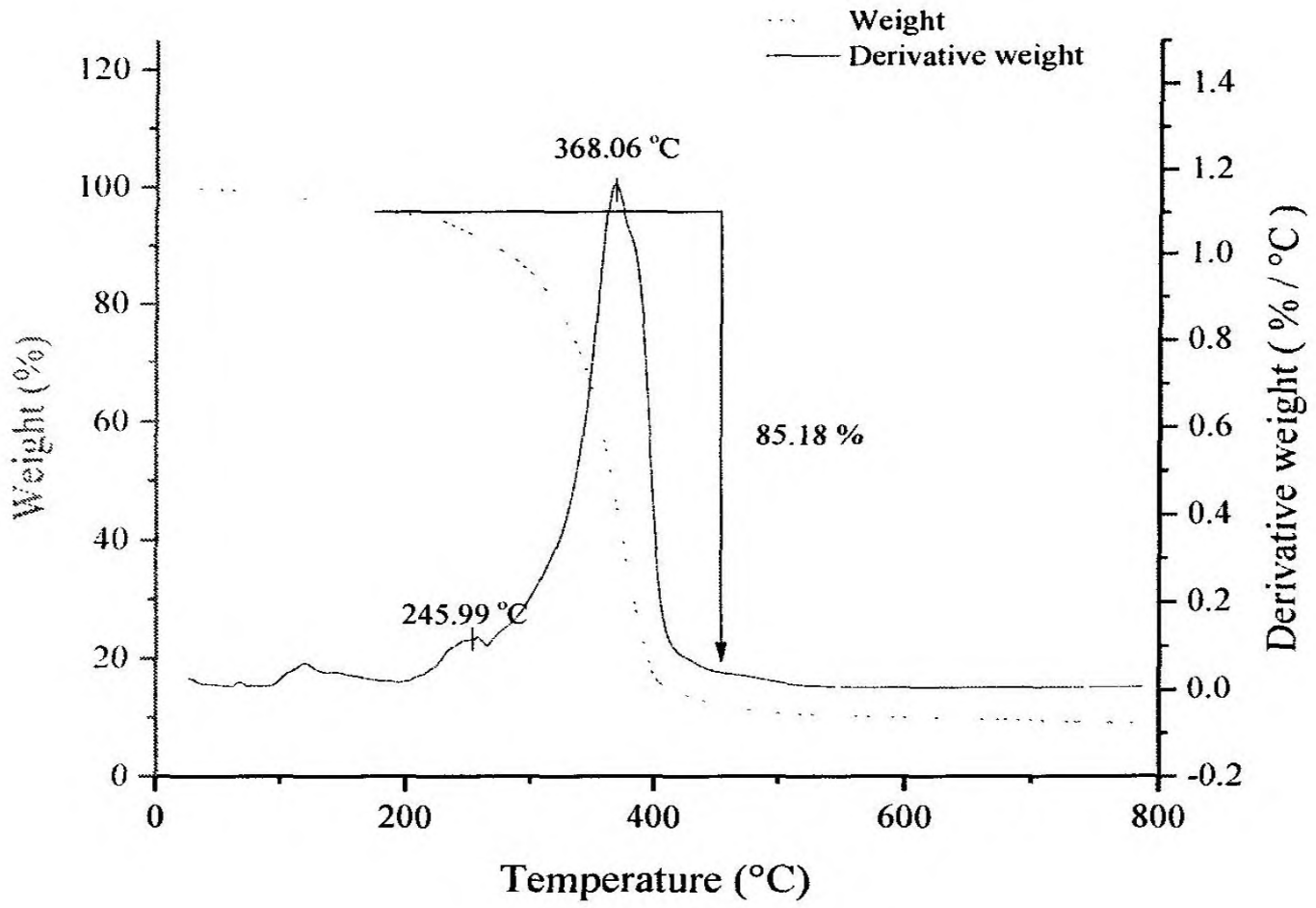

Figure 18. Weight and derivative weight versus temperature of TGA of curcumin encapsulated negatively charged hybrid liposomes

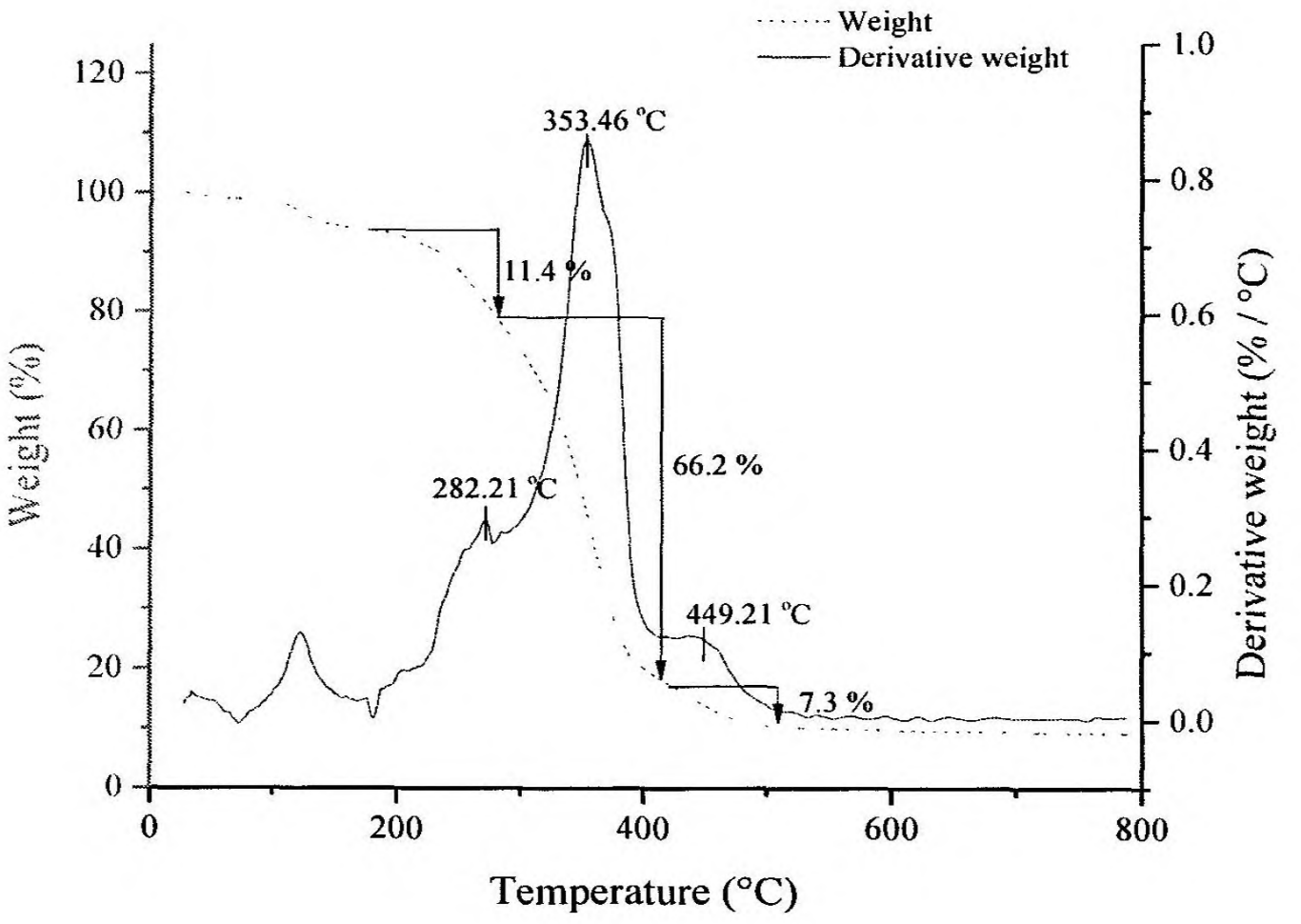

Figure 19. Weight and derivative weight versus temperature of TGA of curcumin encapsulated positively charged liposomes

The TGA profile of NHL is shown in figure 18. NHL showed a main degradation temperature at 368.1 °C that corresponded to a weight loss of 85.2 %. In addition, it showed a minor degradation temperature at 246.0 °C. The residual weight at 800 °C was 9.0 %.

Compared to both types of liposomes bearing a negative charge, the two types of liposomes bearing a positive charge - PL and PHL - exhibited main degradation peaks at lower temperatures.

The TGA profile of PL is shown in figure 19. PL exhibited main degradation at 353.6 °C where a weight loss of 66.2 % occurred. This temperature is approximately 15 °C lower than the main degradation temperatures of the two types of negatively charged liposomes. In addition to the main degradation temperature, this type of liposomes exhibited two minor degradation temperatures: one at 282.2 °C corresponding to a weight loss of 11.4 % and the other at 449.2 °C corresponding to a weight loss of 7.3 %. The residual weight at 800 °C was 9.2 %.

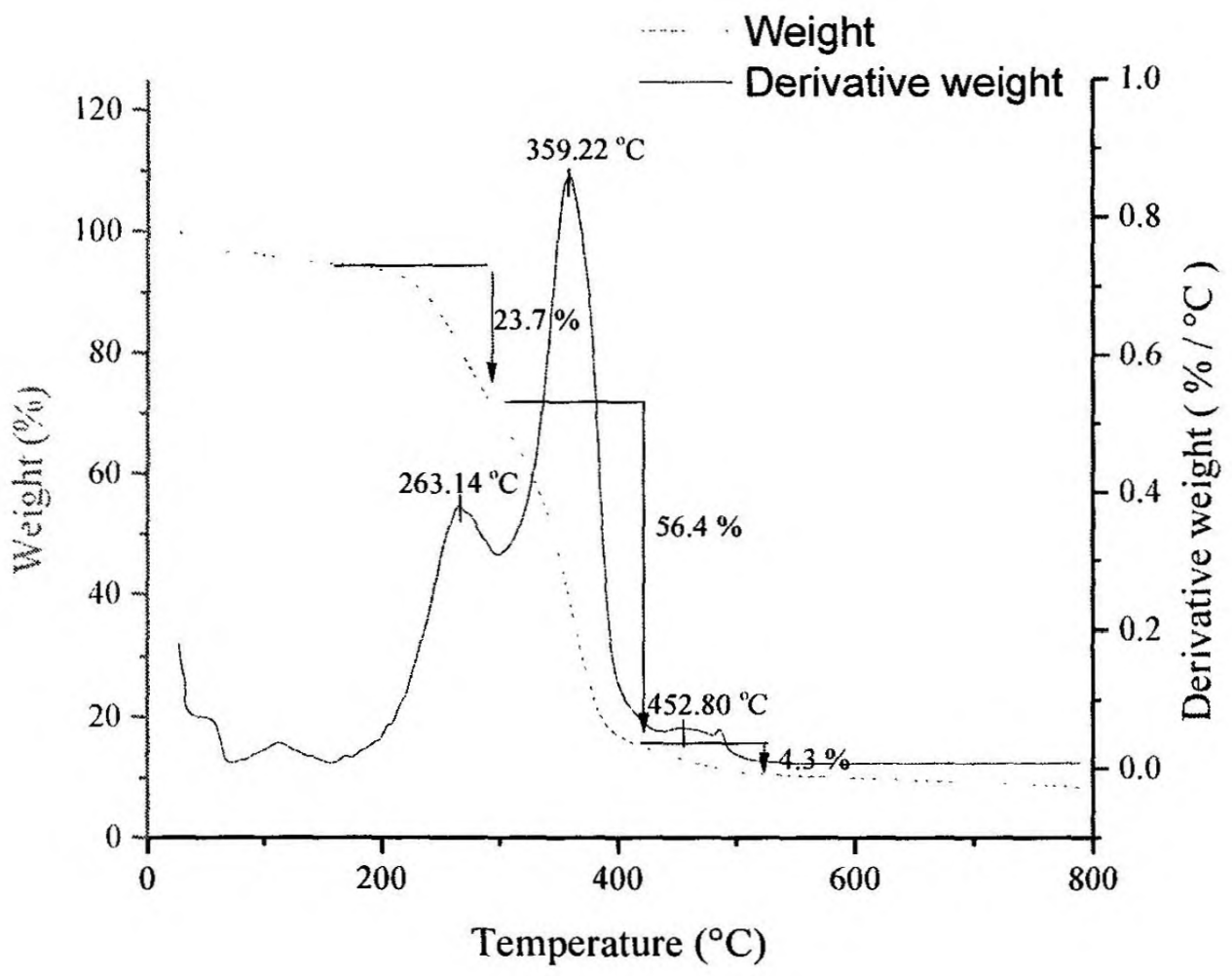

Figure 20. Weight and derivative weight versus temperature of TGA of curcumin encapsulated positively charged hybrid liposomes

The TGA profile of PHL is shown in figure 20. PHL exhibited degradation at 359.2 °C where a weight loss of 56.4 % occurred. This degradation temperature is approximately 10 °C lower than those of NL and NHL while this temperature is approximately 5 °C higher than that of PL. In addition to the main degradation temperature, PHL showed two minor degradation temperatures: one at 263.1 °C corresponding to a weight loss of 23.7 % and another at 452.8 °C corresponding to a weight loss of 4.3 %. The residual weight at 800 °C was 8.4 %.

In general, TGA profiles indicate the two types of negatively charged liposomes exhibit negligible degradation around 250 °C whereas the two types of positively charged liposomes exhibit more pronounced degradation at 282 °C and 263 °C. This higher percentage of weight loss shown by positively charged liposomes is due to the presence of SA which undergoes degradation at 262.57 °C in those liposomes.

Furthermore, these results clearly indicate that incorporation of SA in the lipid bilayer of curcumin encapsulated liposomes results in a depression of the main degradation temperature by 10 – 15 °C making those vesicles more susceptible to thermal degradation. In addition, these results indicate that although the main degradation temperature is unaffected by incorporation of P80 in negatively charged liposomes, the main degradation temperature may be increased by approximately 5 °C by incorporating P80 in positively charged liposomes. Thus, thermal stability of curcumin encapsulated positively charged liposomes may be increased by incorporating P80.

Despite this subtle variation of the main degradation temperatures, both negatively and positively charged liposomes are unlikely to undergo thermal degradation during manufacturing or storing because manufacturing and storing temperatures are much lower than the degradation temperatures exhibited by those liposomal formulations.

4.3.3.2 Differential scanning calorimetry

The heating curves of DSC of the four types of liposomes are shown in figure 21. According to the heating curves, PL and PHL exhibited higher melting temperatures than NL and NHL. In fact, the melting temperatures of NL and NHL were 14.8 °C and 14.2 °C, respectively; while those of PL and PHL were 40.6 °C and 50.8 °C, respectively.

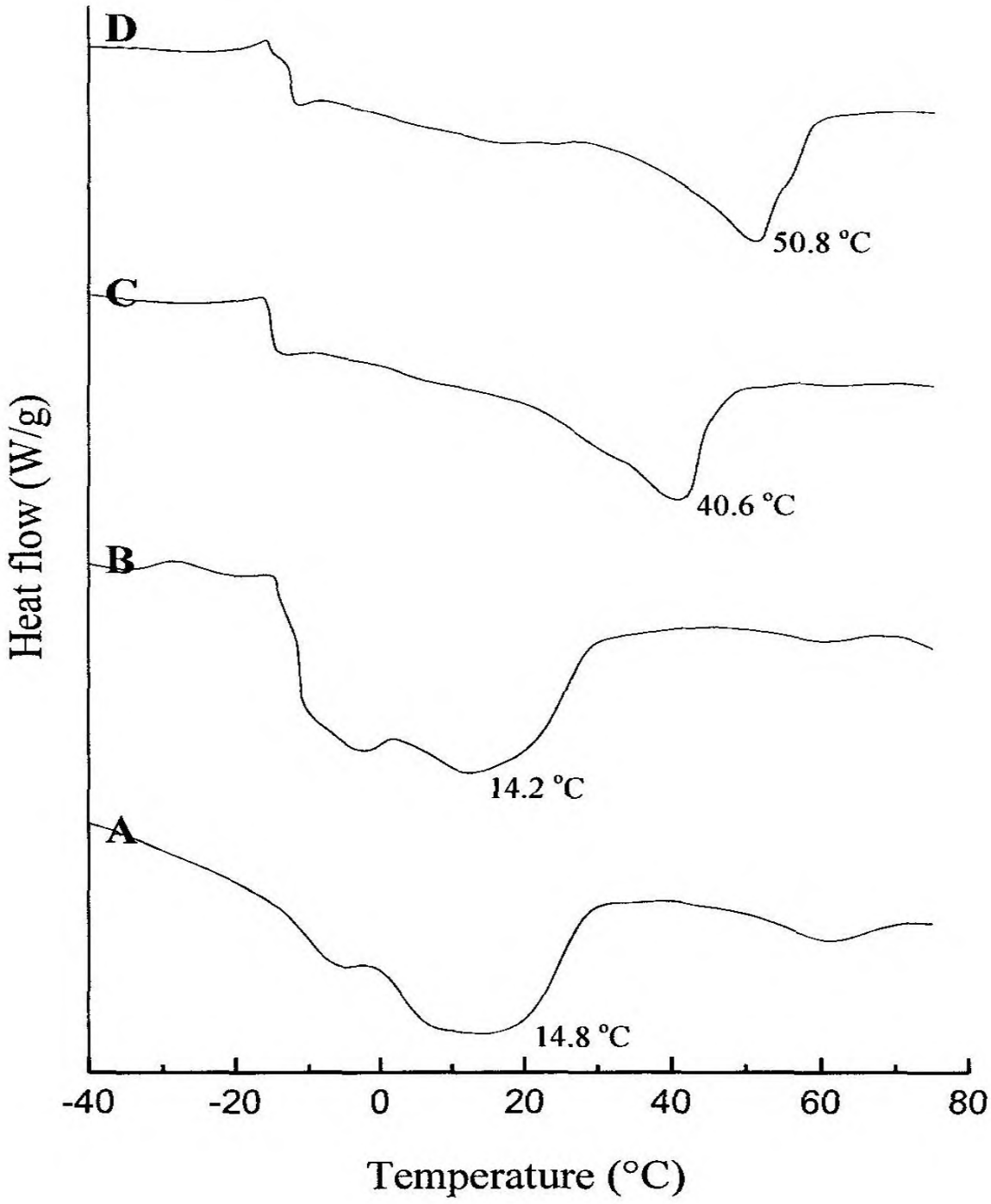

Figure 21. DSC heating curves of four types of curcumin encapsulated liposomes; A - negatively charged liposomes, B - negatively charged hybrid liposomes, C - positively charged liposomes, D - positively charged hybrid liposomes

The cooling curves of DSC of the four types of liposomes are shown in figure 22.

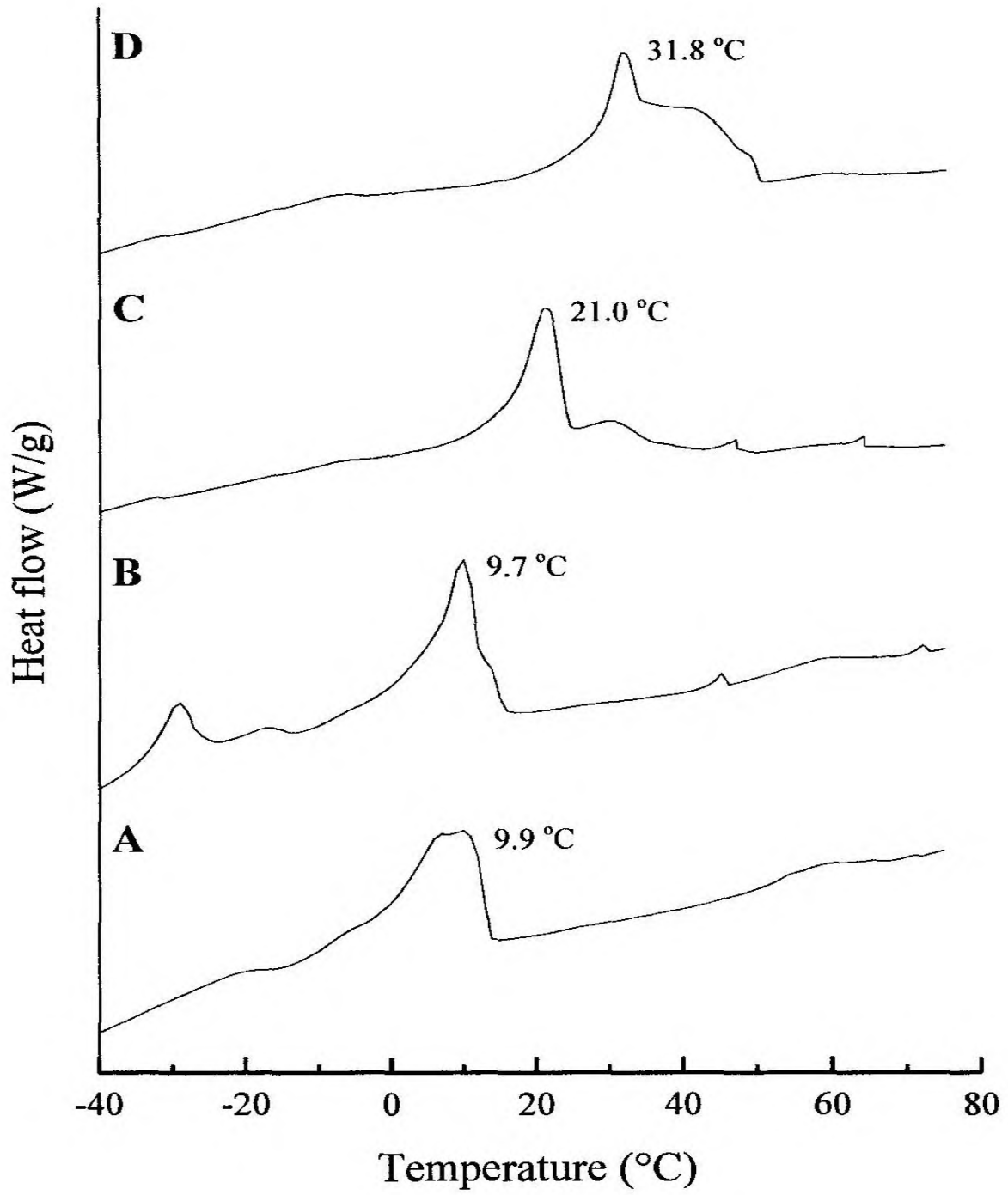

Figure 22. DSC cooling curves of four types of curcumin encapsulated liposomes; A - negatively charged liposomes, B - negatively charged hybrid liposomes, C - positively charged liposomes, D - positively charged hybrid liposomes

The cooling curves revealed that the crystallization temperatures of the two types of positively charged liposomes were higher than those of the two types of negatively charged liposomes. In fact, the crystallization temperatures of NL and NHL were 9.9 °C and 9.7 °C, respectively; while those of PL and PHL were 21.0 °C and 31.8 °C, respectively.

Melting and crystallization temperatures depend heavily on the lipid composition. The difference between the melting temperature of NL and that of NHL was negligible.

Accordingly, the difference between the crystallization temperatures of those types of liposomes, also, was negligible. Furthermore, these results indicate that the lipid bilayer of negatively charged liposomes exists mainly in the liquid crystalline state at room temperature. The melting and crystallization temperatures of the two types of curcumin encapsulated positively charged liposomes are much higher than those of the two types of negatively charged liposomes. Moreover, these results indicate that positively charged liposomes exist mainly in the gel state at room temperature. Unlike the melting temperatures of negatively charged liposomes, those of positively charged liposomes were significantly different. In fact, the melting temperature of PHL is 10 °C higher than that of PL. Accordingly, the crystallization temperature of PHL is, also, approximately 10 °C higher than that of PL. These results indicate that incorporation of SA in the lipid bilayer results in ordering of lipids in the bilayer, thus favouring the gel state. These features may affect release properties and skin permeation properties of curcumin encapsulated liposomes.

4.3.4 *In vitro* release properties

One important feature of liposomes is their ability to act as sustained release systems. This desirable property of liposomes can be enhanced by incorporating charged lipids in the lipid composition during liposome preparation. Insulin encapsulated in cationic liposomes has shown better sustained-release properties (Park *et al.*, 2011). However, dibucaine encapsulated anionic liposomes with better sustained-release properties than positively charged liposomes have been reported (Nounou *et al.*, 2006). Thus, the effect of charge of liposomes on the release properties of curcumin encapsulated liposomes was evaluated in this study.

The effect of surfactants is evaluated to a smaller extent than the effect of charge, on the release properties of liposomes. However, surfactants usually play significant roles in enhancing skin delivery of encapsulated species of liposomes (Elsayed *et al.*, 2007). Thus, P80 was incorporated in liposomes and its effect on the release properties of curcumin encapsulated liposomes was evaluated.

The *in vitro* release profiles of the four types of curcumin encapsulated liposomes are shown in figure 23.

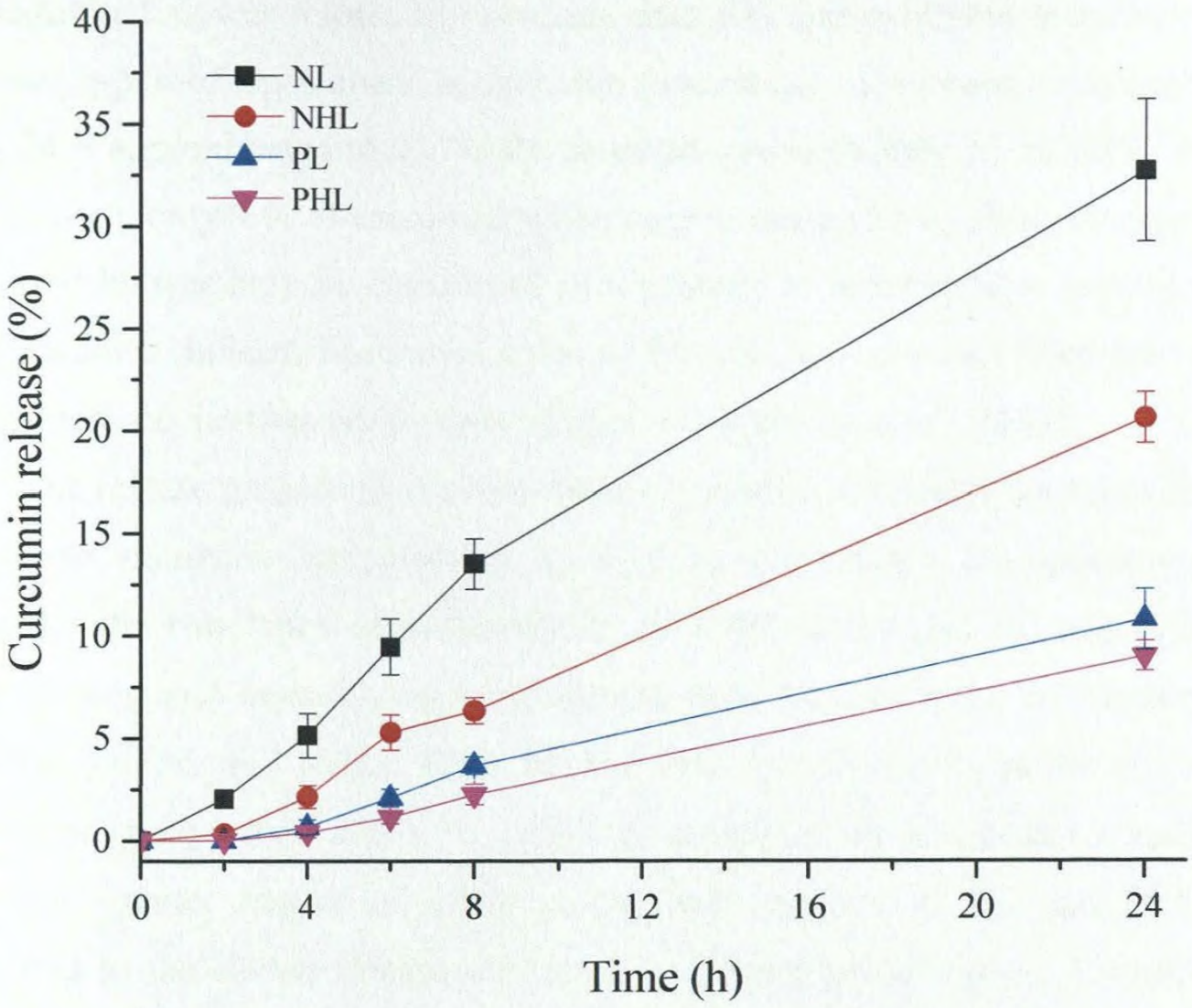

Figure 23. *In vitro* release profiles of the four types of curcumin encapsulated liposomes in PBS of pH 6.8; NL - negatively charged liposomes, NHL - negatively charged hybrid liposomes, PL - positively charged liposomes, PHL - positively charged hybrid liposomes

The release profiles of curcumin encapsulated liposomes are consistent with the literature. Specifically, Chen and coworkers showed that the release percentage of curcumin at 24 h from liposomes made of egg yolk PC and CH was 45 – 50 % (Chen *et al.*, 2012). We obtained a comparable value – 32 % - for liposomes with a similar lipid composition (see NL of figure 23). The observed decrease in the release of our study may be due to the lower temperature at which the experiments were carried out. In fact, Chen et al. conducted release studies at 37 °C whereas we carried out the studies at 25 °C. Furthermore, Chen and coauthors reported that around 65 % of curcumin was released from the liposomes at 48 h (Chen *et al.*, 2012). Thus, we can expect our experiments to exhibit a lower degree of release, probably of approximately 50 %, at 48 h.

According to the *in vitro* release profiles of different types of liposomes encapsulating curcumin, NL and NHL showed faster release of curcumin compared to PL and PHL, exhibiting a pronounced effect of charge on the release properties of curcumin

encapsulated liposomes. NL released the highest amount of curcumin (32 %), during 24 h. NHL exhibited slower release of curcumin than NL, but exhibited faster release than the other two types of liposomes. In fact, the percentage of curcumin released from NHL during 24 h approximated to 21 %. PL released approximately 11 % while PHL released approximately only 9 % of encapsulated curcumin, during 24 h. Thus, incorporation of SA in the lipid bilayer may be considered as a strategy to achieve slow release of curcumin from liposomes. Indeed, liposomes made of PC and SA have exhibited slower release of encapsulated species than other types of liposomes (Hurler *et al.*, 2013).

The release properties of curcumin encapsulated liposomes appear to correlate with their phase transition temperatures as well as the charge of liposomes. As stated previously, the two types of positively charged liposomes (i.e. PL and PHL) exhibited higher melting and crystallizing temperatures than the two types of negatively charged liposomes (i.e. NL and NHL). Thus, PL and PHL remain mainly in the more ordered gel state at room temperature while NL and NHL remain in the less ordered liquid crystalline state. This greater degree of order in the lipid bilayers of PL and PHL may have contributed to the slower release exhibited by these types of lipids. A similar reasoning was put forward by Chen and coworkers who argued that the higher melting temperature of hydrogenated soybean phospholipids (HSPC) was indicative of lower membrane liquidity, while liposomes made from natural unsaturated counterparts possess higher membrane liquidity, resulting in slower release of curcumin by the HSPC liposomes (Chen *et al.*, 2012).

As depicted by figure 23, slower release of curcumin may be achieved by incorporating P80 in negatively charged liposomes. In fact, the release of curcumin was decreased by 34 % upon the incorporation of P80 in negatively charged liposomes. However, the effect of P80 on the release of curcumin from positively charged liposomes was less pronounced. In fact, the decrease was only 18 %. Thus, it can be concluded that P80 may be utilized to achieve slow release of curcumin, especially from negatively charged liposomes.

All liposomal formulations may function as drug depots since all formulations exhibited relatively slow release properties. However, since the two types of positively charged liposomes exhibited much slower release than the two negatively charged liposomes, positively charged liposomes may be suitable for prolonged release of curcumin. Basically, one can choose a certain type of liposomal formulation depending on the pharmacokinetics desired for the intended application.

Drug release kinetic studies were carried out to select a model that best describes the release behaviour of the four different curcumin encapsulated liposomal formulations. According to table 14 that indicates the adjusted R-square values for the six different models tested, either Gompertz model, zero order model or Hixson-Crowell model can be used to describe the release kinetics of the curcumin encapsulated liposomal formulations used in this study. However, the release profiles fit best to Gompertz model. In general, the two types of negatively charged liposomes (i.e. NL and NHL) exhibit gradual release of curcumin with time while the two types of positively charged liposomes (i.e. PL and PHL) show a lag time followed by gradual release of curcumin with time.

Table 14. Adjusted R-square values of different liposomal formulations of curve fitting for six different drug release models

Formulation	Adjusted R-square					
	Zero order	First order	Higuchi	Hixson - Crowell	Korsmeyer - Peppas	Gompertz
NL	0.9830	0.6830	0.8817	0.9917	0.9672	0.9987
NHL	0.9917	0.5406	0.8218	0.9919	0.8961	0.9908
PL	0.9832	0.6703	0.7937	0.9837	0.8796	0.9992
PHL	0.9777	0.7740	0.7372	0.9766	0.9425	0.9998

4.3.5 *Ex vivo* skin permeation and skin deposition

According to *ex vivo* skin permeation studies, none of the liposomal formulations used in this study facilitated skin penetration of curcumin during a period of 8 h. However, all types of liposomal formulations facilitated skin deposition of curcumin (see Table 15).

Table 15. Percentage skin deposition and amount of deposition of curcumin from different types of liposomes. Values are indicated as mean ± S.D. (n = 3).

Liposomal formulation	Percentage of skin deposition (%)	Amount deposited (μg / cm^2)
NL	7.3 ± 0.6	25.7 ± 2.2
NHL	2.9 ± 0.5	8.6 ± 1.4
PL	1.9 ± 0.3	4.4 ± 0.6
PHL	1.1 ± 0.2	2.5 ± 0.5

Although no skin penetration occurred under the experimental conditions of this study, Chen and coworkers reported skin penetration of curcumin from liposomes made from either egg yolk phospholipids, soybean phospholipids or hydrogenated phospholipids. In fact, they reported a percentage permeation of approximately 5 % at 8 h. The difference in permeation results of our study and the study conducted by Chen et al. may be due to the smaller size of liposomes used by them. In fact, the particle sizes of their liposomes were less than 100 nm whereas those of our liposomes ranged from 200 nm – 300 nm. Furthermore, Chen and coauthors used rat abdominal skin whereas we used full thickness pig ear skin. This difference in the type of skin used also may have contributed to the discrepancies of the two studies (Chen *et al.*, 2012).

In general, the two types of negatively charged liposomes exhibited a higher percentage of skin deposition of encapsulated curcumin than the two types of positively charged liposomes. Thus, skin delivery of liposomal curcumin is dependent on the charge of liposomes. Actually, numerous authors have illustrated the effect of charge of liposomes on their skin-penetration properties. For example, Gillet and coworkers illustrated that negatively-charged liposomes prepared by the addition of 1,2-dimyristoyl-sn-glycero-3-phosphate (DMPA) or dicetylphosphate (DCP) to the lipid composition showed better skin-penetration properties compared to neutral liposomes or posively-charged liposomes (Gillet *et al.*, 2011). In contrast, Oh et. al. reported that cationic ultradeformable liposomes are suitable for topical delivery of 5-aminolevunic acid (Oh *et al.*, 2011). These different effects of charge on skin-penetration ability of liposomes necessitate the optimization of charge of liposomes for each individual bioactive agent. According to the amount of skin deposition, negatively charged liposomes are the most suitable type of liposomes for skin delivery of curcumin.

Edge activators and skin-penetration enhancers are substances that improve the skin permeability of liposomal bioactive agents, especially when incorporated in liposomes. P80 which is also called tween 80 has shown to increase skin delivery of many subtances. For instance, Maghraby and coworkers demonstrated that ultradeformable liposomes preparared by incorporating surfactants, such as tween 80, span 80 or sodium cholate, in liposomes show better skin delivery of oestradiol than traditional liposomes or a saturated solution of oestradiol (El Maghraby, Williams and Barry, 1999; El Maghraby, Williams and Barry, 2000). According to the skin deposition results of this study, P80 has an effect on the skin delivery of curcumin. However, it imparts a negative effect. In fact, it decreased skin deposition of curcumin by 60 % upon incorporation in negatively charged

liposomes and by 42 % upon incorporation in positively charged liposomes. Thus, under the experimental conditions of this study, ionic lipids are better than their P80-containing counterparts with respect to skin delivery of curcumin.

4.4 Conclusion

This study reveals that the charge of liposomes and the presence of surfactants impart a pronounced effect on the properties of curcumin encapsulated liposomes and that those factors may be exploited to modulate the properties of those vesicles.

Egg yolk PC and CH with or without P80 may be utilized to form negatively charged liposomes. Positively charged liposomes can be formed by incorporating SA in liposomes made of egg yolk PC and CH with or without P80.

The encapsulation efficiency depends heavily on the lipid composition of curcumin encapsulated liposomes. All formulations exhibited relatively high EEs. The two types of negatively charged liposomes were superior in terms of EE and LC to the two types of positively charged liposomes. Moreover, incorporation of P80 resulted in a decrease of those parameters.

P80 and SA if incorporated separately result in curcumin encapsulated liposomes of smaller size. Since, numerous important properties such as biodistribution depend on the particle size, different ratios of these substances may be utilized to alter the size of liposomes. Incorporation of P80 results in an increase in the zeta-potential and thus it may be utilized for tuning of zeta-potential of curcumin encapsulated liposomes.

Incorporation of SA influences the liquidity of lipid bilayers of curcumin encapsulated liposomes. This decreased liquidity may affect numerous other properties such as release properties and skin delivery of liposomal curcumin.

The charge of liposomes has a significant effect on the release properties of liposomal curcumin. In fact, the two types of positively charged liposomes show better slow release properties of curcumin. Incorporation of P80 further decreases the rate of release.

Negatively charged liposomes show better skin deposition of liposomal curcumin than positively charged liposomes. Under the experimental conditions of this study, incorporation of P80 has a detrimental effect on skin delivery of liposomal curcumin.

In summary, egg yolk PC, CH, P80 and SA may be used to form stable curcumin encapsulated liposomes and to modulate properties of those vesicular drug delivery vehicles. Negatively charged liposomes facilitate better encapsulation and skin delivery while positively charged liposomes show better slow release properties.

4.5 References

Basnet, P., Hussain, H., Tho, I. and Skalko-Basnet, N. (2012). Liposomal delivery system enhances anti-inflammatory properties of curcumin. *Journal of Pharmaceutical Sciences* **101(2)**, 598–609.

Bouarab, L., Maherani, B., Kheirolomoom, A., Hasan, M., Aliakbarian, B., Linder, M. and Arab-Tehrany, E. (2014). Influence of lecithin–lipid composition on physico-chemical properties of nanoliposomes loaded with a hydrophobic molecule. *Colloids and Surfaces B: Biointerfaces* **115**, 197–204.

Chen, Y., Wu, Q., Zhang, Z., Yuan, L., Liu, X. and Zhou, L. (2012). Preparation of curcumin loaded liposomes and evaluation of their skin permeation and pharmacodynamics. *Molecules,* **17**, 5972-5987.

Dhule, S.S., Penfornis, P., He, J., Harris, M.R., Terry, T., John, V. and Pochampally, R. (2014). The combined effect of encapsulating curcumin and C6 ceramide in liposomal nanoparticles against osteosarcoma. *Molecular Pharmaceutics* **11(2)**, 417–427.

Dogra, N., Choudhary, R., Kohli, P., Haddock, J.D., Makwana, S., Horev, B., Vinokur, Y., Droby, S. and Rodov, V. (2015). Polydiacetylene Nanovesicles as Carriers of Natural Phenylpropanoids for Creating Antimicrobial Food-Contact Surfaces. *Journal of Agricultural Food Chemistry* **63(9)**, 2557-2565.

El Maghraby, G.M.M., Williams, A.C. and Barry, B.W. (1999). Skin delivery of oestradiol from deformable and traditional liposomes: mechanistic studies. *Journal of Pharmacy and Pharmacology* **51**, 1123-1134.

El Maghraby, G.M.M., Williams, A.C. and Barry, B.W. (2000). Oestradiol skin delivery from ultradeformable liposomes: refinement of surfactant concentration. *International Journal of Pharmaceutics* **196(1)**, 63–74.

Elsayed, M.M.A., Abdallah, O.Y., Naggar, V.F. and Khalafallah, N.M. (2007). Lipid vesicles for skin delivery of drugs: Reviewing three decades of research. *International Journal of Pharmaceutics* **332**, 1-16.

Gillet, A., Compère, P., Lecomte, F., Hubert, P., Ducat, E., Evrard, B. and Piel, G. (2011). Liposome surface charge influence on skin penetration behaviour. *International Journal of Pharmaceutics* **411**, 223-231.

Hurler, J., Žakelj, S., Mravljak, J., Pajk, S., Kristl, A., Schubert, R. and Škalko-Basnet, N. (2013). The effect of lipid composition and liposome size on the release properties of liposomes-in-hydrogel. *International Journal of Pharmaceutics* **456**, 49– 57.

Lu, Y., Ding, N., Yang, C., Huang, L., Liu, J. and Xiang, G. (2012). Preparation and in vitro evaluation of a folate-linked liposomal curcumin formulation. *Journal of liposome research* **22(2)**, 110-119.

Narayanan, N.K., Nargi, D., Randolph, C. and Narayanan, B.A. (2009). Liposome encapsulation of curcumin and resveratrol in combination reduces prostate cancer incidence in PTEN knockout mice. *International Journal of Cancer* **125(1)**, 1-8.

Nounou, M.M., El-Khordagui, L.K., Khalafallah, N.A. and Khalil, S.A. (2006). *In vitro* release of hydrophilic and hydrophobic drugs from liposomal dispersions and gels. *Acta Pharmaceutica* **56** , 311–324.

Oh, E.K., Jin, S-E., Kim, J-K., Park, J-S., Park, Y. and Kim, C-K. (2011). Retained topical delivery of 5-aminolevulinic acid using cationic ultradeformable liposomes for photodynamic therapy. *European Journal of Pharmaceutical Sciences* **44(1-2)**, 149-157.

Park, S-J., Choi, S.G., Davaa, E. and Park, J-S. (2011). Encapsulation enhancement and stabilization of insulin in cationic liposomes. *International Journal of Pharmaceutics* **415**, 267-272.

Ranjan, A.P., Mukerjee, A., Helson, L., Gupta, R. and Vishwanatha, J.K. (2013). Efficacy of liposomal curcumin in a human pancreatic tumor xenograft model: Inhibition of tumor growth and angiogenesis. *Anticancer Research* **33(9)**, 3603-3610.

Shin, G.H., Chung, S.K., Kim, J.T., Joung, H.J. and Park, H.J. (2013). Preparation of chitosan-coated nanoliposomes for improving the mucoadhesive property of curcumin using the ethanol injection method. *Journal of Agricultural Food Chemistry* **61(46)**, 11119–11126.

Takahashi, M., Uechi, S., Takara, K., Asikin, Y. and Wada, K. (2009). Evaluation of an oral carrier system in rats: Bioavailability and antioxidant properties of liposome-encapsulated curcumin. *Journal of Agricultural and Food Chemistry* **57(19)**, 9141–9146.

CHAPTER 5

SYNTHESIS OF CURCUMIN - FERULIC ACID COCRYSTALS AND APPLICATIONS OF EUTECTIC COMPOSITION

5.1 *Introduction*

A cocrystal is a crystalline, multicomponent molecular complex composed of solids in a definite stoichiometric ratio in the crystal lattice. The components of cocrystals interact via noncovalent interactions. In fact, the traditional OH….O strong hydrogen bonds, other types of hydrogen bonds, van der Waals forces, halogen bonding and π-π interactions are utilized in the synthesis of cocrystals (Lara-Ochoa and Espinosa-Pérez, 2007). Pharmaceutical cocrystals are composed of an Active Pharmaceutical Ingredient (API) and a coformer, another ingredient safe for human consumption. Examples of such pharmaceutical cocrystals include carbamazepine-saccharin, indomethacin-saccharin, itraconazole-L-malic acid and adefovir dipivoxil-suberic acid or succinic acid (Jung, Lee and Kim, 2013; Kudo and Takiyama, 2014; Ober, Montgomery and Gupta, 2013; Padrela *et al.*, 2009). Cocrystallization usually alters physico-chemical properties such as solubility, dissolution rate, stability, and bioavailability of its constituents. For instance, cocrystallization of carbamazepine with numerous coformers including nicotonamide and saccharin significantly enhanced the solubility of this API while cocrystallization of thyeophilline resulted in increased dissolution rates (Good and Rodríguez-Hornedo, 2009; Padrela *et al.*, 2014). Furthermore, theophilline cocrystals exhibited increased physical stability (Trask, Sam Motherwell and Jones, 2006). Also, carbamazepine showed enhanced oral absorption profiles when cocrystallized with saccharin in addition to exhibiting improved solubility, dissolution and stability (Hickey *et al.*, 2007). While most pharmaceutical cocrystals are composed of an API and an inert coformer, in this research, deviating from the norm, we attempted to produce a cocrystal composed of two bioactive ingredients – curcumin and ferulic acid - that exhibit closely related bioactivities.

Curcumin is derived from the rhizome of the herb *Curcuma longa.* Curcumin is pharmacologically active in a number of aspects such as antimicrobial, antioxidant and anti-cancer (Ahmad *et al.*, 2008). However, curcumin exhibits very poor bioavailability partly due to its low solubility in aqueous media. In fact, only

low levels of curcumin were detected in plasma and tissues when this bioactive compound was administered at a high dose (Anand *et al.*, 2007). Photostablity of curcumin is also a question. It has been demonstrated that curcumin undergoes rapid degradation especially upon UV irradiation (Tønnesen, Másson and Loftsson, 2002). Thus, to assure that the targeted dose and the effective dose administered are the same, means of increasing stability of curcumin should be investigated. Moreover, the stability of curcumin is dependent on the media in which it is dissolved. In fact, curcumin is unstable in alkaline and neutral media; over 90% decomposition occurs within 30 minutes at pH 7.4 buffer medium. However, the degradation is much slower in acidic media (Wang *et al.*, 1997). The cocrystals create a platform to improve physicochemical properties such as solubility and stability of curcumin, thereby enhancing its bioavailability.

Curcumin undergoes keto- enol tautomerism and the curcumin molecule in the crystal structure exists in enol form. The enol form is stabilized by intra molecular hydrogen bonding and this cis-enol ring has a planar configuration. In the crystal structure of curcumin, one phenol ring and the cis-enol ring are coplanar while the other phenol ring is rotated by an angle of approximately 45°. The two enol "carbonyl" oxygens present strong H bond acceptors. The presence of intramolecular hydrogen bonds between neighboring OH and OCH_3 groups of this two aromatic rings has important implications regarding preferred molecular structures. Thus, intermolecular interactions of crystals of curcumin consist of H-bonds as well as π-stacking (Tønneson, Karlsen and Mostad, 1982). Ferulic acid, being a structural analogue of curcumin, may participate in similar interactions as curcumin in crystal structures.

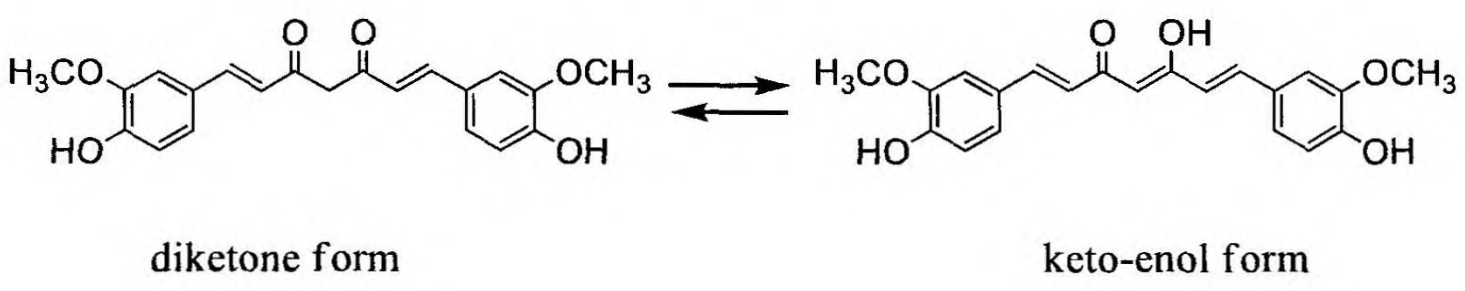

Figure 24. Keto-enol tautomerism of curcumin

In this study, the co-former utilized in cocrystal formation was ferulic acid which is a structural analogue of curcumin and a potent antioxidant (Trombino *et al.*, 2004). Ferulic

acid is biosynthesized from phenylalanine and tyrosine in plants and can be readily extracted via conventional solvent extraction or microwave-assisted extraction (Setyaningsih *et al.*, 2015). Ferulic acid, being a phenolic compound, has the ability to form a phenoxy radical which is resonance stabilized. The presence of a methoxy group at the *ortho* position and the presence of a conjugated group at the *para* position further stabilize the phenoxy radical. This resonance stabilization accounts for the antioxidant potential of ferulic acid. In fact, the ability of ferulic acid to scavenge both reactive oxygen species (ROS) and reactive nitrogen species (RNS) has been reported (Ogiwara *et al.*, 2002). Due to, mainly, the antioxidant properties of ferulic acid, this molecule exhibits numerous other significant bioactivities such as anticancer, antimutagenic and antimicrobial (Srinivasan, Sudheer and Menon, 2007), that make this compound an ideal conformer for cocrystallization of curcumin.

Curcumin and ferulic acid – APIs used in this research – have been used as components of cocrystals. For instance, Samphui and coworkers reported the formation of cocrystals of curcumin in combination with resorcinol and with pyrogallol (Sanphui *et al.*, 2011), and Chow et al. reported the formation of cucrcumin cocrystals in combination with phloroglucinol (Chow *et al.*, 2014). The ability of ferulic acid to form cocrystals has also been demonstrated. For example, Swapna and coauthors reported the formation of cocrystals of isoniazid with ferulic acid (Swapna, Maddileti and Nangia, 2014). Although cocrystallization of both curcumin and ferulic acid with other substances has been reported, cocrystallization of the above two APIs together has not been reported. In fact, recently Goud et al. demonstrated the formation of a simple eutectic mixture instead of a cocrystal when cocrystallisation of curcumin and ferulic acid was attempted (Goud *et al.*, 2012). Likewise, not only cocrystals, but also other products such as solid dispersions, solid solutions and simple eutectic mixtures may result when cocrystallization of APIs is attempted through numerous methods including rational design of cocrystals. Nevertheless, those products also, like cocrystals, possess several attributes desirable for pharmaceutical formulations. For instance both solid solutions and eutectic mixtures have shown to increase equilibrium solubility, dissolution rate and physical stability of APIs. Thus, as illustrated by Goud and coauthors, products of cocrystallization, although unsuccessful, may be useful (Goud *et al.*, 2012).

Solid solutions and eutectic mixtures are ubiquitously utilized in pharmaceutical formulations. A solid solution is a type of solid dispersions in which the drug in amorphous state is dispersed in a carrier matrix. A eutectic system is a mixture of chemical

compounds or elements that has a single chemical composition that solidifies at a lower temperature than any other composition. This composition is known as the *eutectic composition* (Sinha *et al.*, 2009). Eutectic compositions of numerous APIs with ingredients safe for human consumption have been reported. Curcumin – the primary bioactive agent utilized in this study – also forms eutectic mixtures with numerous compounds. For example, Goud and coauthors illustrated that curcumin formed eutectic mixtures with nicotinamide, ferulic acid, hydroquinone, p-hydroxybenzioc acid and L-tartaric acid upon mechano-chemical grinding and that those eutectic mixtures showed increased intrinsic and powder dissolution rates (Goud *et al.*, 2012).

Formation of cocrystals can be carried out employing a number of methods, the most commonly used ones being solvent methods and grinding methods (Qiao *et al.*, 2011). In this research, synthesis of curcumin-ferulic acid cocrystals was attempted via three methods: cocrystallization from solvent evaporation, neat grinding, and liquid assisted grinding.

This thesis explains our attempt to synthesize curcumin cocrystals with ferulic acid in the stoichiometric ratio of 1:1 (mol/mol) which has previously been reported to result in a eutectic mixture. Also, characterization of products of cocrystallization via microscopic methods, FT-IR and Raman spectroscopy, powder X-ray diffraction, thermogravimetric analysis and differential scanning calorimetry is discussed. Furthermore, powder dissolution rates of the products of cocrystallization and that of curcumin alone are compared. Moreover, photostability, thermal stability and antioxidant activity of curcumin, of ferulic acid and of eutectic composition of curcumin and ferulic acid are compared and discussed since it is imperative to enhance these properties both during dosage form development and storage and even after administration.

5.2 Materials and methods

5.2.1 Materials

Curcumin (purity 99%) was purchased from Lobal Chemie. *trans*-Ferulic acid (purity 99%), KBr (FT-IR grade), DPPH, ethanol (HPLC grade), methanol (HPLC grade), acetonitrile (HPLC grade) and phosphoric acid (85 % wt. % in water), were purchased from Sigma-Aldrich. Deionized water filtered through a 0.2 μm filter was used throughout the study.

5.2.2 Methods

5.2.2.1 Synthesis of ferulic acid – curcumin cocrystals

Synthesis of ferulic acid-curcumin cocrystals was attempted via three methods: cocrystallization through solvent evaporation, liquid-assisted grinding, and neat grinding.

Neat grinding (C)

A 1:1 mixture of *trans*-ferulic acid (52 mg; 0.00027 mol) and curcumin (100 mg; 0.00027 mol) was ground for 30 min.

Liquid- assisted grinding (D)

A 1:1 mixture of *trans*-ferulic acid (52 mg; 0.00027 mol) and curcumin (100 mg; 0.00027 mol) was ground for 30 min with a catalytic amount of ethanol.

Cocrystallization through solvent evaporation (E)

A 1:1 mixture of *trans*-ferulic acid (52 mg; 0.00027 mol) and curcumin (100 mg; 0.00027 mol) was dissolved in ethanol at 30 °C for 30 min and the resultant solution was left for cooling at room temperature. After 2 days, the crystals were filtered, washed with the mother liqueur, and dried in a vacuum oven at 30 °C for 24 hr.

5.2.2.2 HPLC analysis

The composition of the crystals was determined through HPLC analysis using a C_{18} column. A phosphoric acid buffer of pH 2.2 and acetonitrile were used for gradient elution. The percentage of acetonitrile was increased from 23 % to 75 % gradually over a period of 13 min. Next, 100 % acetonitrile was eluted for 5 min. A constant flow rate of 1 mL/min was used throughout the analysis. The wavelengths used for the detection of eluents were 321 nm, 279 nm, 267 nm, 254 nm and 231 nm.

5.2.2.3 Characterization of crystals by optical microscopy

The images of crystals resulted from cocrystallization by solvent evaporation (E) were obtained from an Olympus DP72 optical microscope.

5.2.2.4 Characterization of crystals by SEM

Microstructural analysis was carried out using a Hitachi Tabletop Microscope - Hitachi SU6600 (Hitachi High-Technologies Europe GmbH, Germany) - with an electron beam voltage of 5 kV. The samples were placed on a piece of carbon sticky tabs and stored in a desiccator for 1 h in order to remove residual moisture. Afterwards, they were sputter coated with a thin layer of gold (E-1010 Ion sputter, Hitachi) for 15 s in order to reduce charging and improve image quality.

5.2.2.5 Characterization of crystals by FT-IR and Raman spectroscopy

Bruker Vertex 80 FT-IR spectrometer with Ram-FT module (RAM II) was used to record IR and Raman spectra. IR spectra were recorded in diffuse reflectance mode on samples dispersed in KBr. Raman spectra were recorded on compressed samples contained on the sample holder.

5.2.2.6 Characterization of crystals by PXRD

PXRD was recorded on Bruker D8 FOCUS diffractometer (Bruker AXS, New Delhi) using Cu-Kα X-radiation (λ = 1.5418 °A) at 40 kV and 40 mA power. The diffraction patterns were collected over the 2θ range 5° - 50° at a scan rate of 0.02 °/sec.

5.2.2.7 Thermal analysis

The thermal stability of ferulic acid, curcumin and the products of cocrystallization was examined by DSC (Figure 8) and TGA (Figure 9).

Thermogravimetric analysis

TGA was carried out in TA Instrument - SDT Q600 thermogravimetric analyzer. An alumina crucible was used to hold 10 mg of sample uniformly at the bottom of the crucible. The sample was heated from room temperature to 800 °C at a heating rate 10 °C/min under a high purity nitrogen flow of 100 mL/min.

Differential Scanning Calorimetry

DSC was performed on Q200 DSC. A 4-6 mg portion of the sample was placed in crimped but vented aluminum pans and the temperature range was 30 - 250 °C at a heating rate of 5 °C/min. The sample was purged by a stream of dry nitrogen flowing at 100 mL/min.

5.2.2.8 Determination of solubility

The solubility of curcumin, C, D and E in a 50% (v/v) ethanol solution was determined. Briefly, a 45 mg of the solid was sieved through a 250 μm mesh and the powder was directly poured into 400 mL of dissolution medium (50% ethanol). The rotation was fixed at 50 rpm and the absorbance of curcumin in solution was determined colourimetrically at 425 nm at varying intervals using a Schimadzu UV 3600 UV-Vis spectrophotometer. The experiment was continued upto 5 h at 25 °C.

5.2.2.9 Assessment of thermal stability

Thermal stability of ferulic acid, of curcumin and of eutectic mixture of ferulic acid and curcumin was carried out at three different temperatures. The samples were prepared of concentration 0.1 mM in ethanol. Next, the solutions were incubated at 25 °C and the solutions were analyzed through HPLC at every 1 h interval. Similar procedures were carried out for stability assessment at 37 °C and at 70 °C. Each experiment was carried out in triplicate.

5.2.2.10 Assessment of photostability

Solutions of curcumin, ferulic acid and E of concentration 10 ppm were prepared in ethanol. Those solutions were exposed to both UV A and B radiation concurrently. Spectra of solutions of curcumin, ferulic acid and E were monitored at 30 min intervals for 180 min.

Also, assessment of photostability was carried out by exposing samples to diffuse light and to UV radiation. In brief, solutions of curcumin, ferulic acid and eutectic mixtures were prepared of concentration 0.1 mM in ethanol. The solutions were exposed either to diffuse light or to UV radiation. The degradation of curcumin and ferulic acid was monitored through HPLC analysis. The intensity of curcumin was determined at 425 nm and ferulic acid at 321 nm. Each experiment was carried out in triplicate.

5.2.2.11 Assessment of antioxidant properties

Solutions of ferulic acid, of curcumin, and of eutectic mixture of ferulic acid and curcumin were prepared for a concentration of 0.050 mM. The compounds to be tested were added into a 1 mM methanol solution of DPPH. The final concentration of DPPH was maintained at 100 μM. After mixing the solutions, those mixtures were kept protected

from UV radiation. The absorbance of remaining DPPH was determined colourimetrically at 514 nm after 30 minutes using a Schimadzu UV 3600 UV-Vis spectrophotometer. The concentrations of the compounds tested were 5.0, 10.0, 15.0, 20.0, 25.0, 30.0, 35.0, 40.0 and 45.0 μM. DPPH assay for each concentration of each compound or compound mixture was carried out in triplicate.

5.2.2.12 Statistical analysis

Results indicated are the means of results of three independent experiments. Values are indicated as mean ± S.D (standard deviation). Microsoft excel 10 software was used for the calculations. ANOVA was used to determine statistical significance and $p < 0.05$ was considered significant. Curve fitting for the determination of IC_{50} values was carried out using ZigmaPlot 10.0 software.

5.3. Results and discussion

In this work, cocrystallization of curcumin was attempted with ferulic acid as the coformer. Although there are numerous methods of cocrystallization, each method presents advantages and disadvantages unique to that particular method. Thus, three commonly employed methods of cocrystallization: Evaporation cocrystallization, liquid-assisted grinding and neat grinding, were utilized in this study.

The main advantage of evaporation cocrystallization is the production of cocrystals suitable for analyzing using single crystal X-ray diffraction (Qiao *et al.*, 2011). However, the solution crystallization process suffers from several drawbacks. The solvent employed can interfere with the intermolecular interactions of the cocrystal, resulting in the incorporation of the solvent into crystal lattice. Also, this method requires a large volume of solvents.

Grinding provides an easier way to synthesize cocrystals while avoiding the drawbacks of solution crystallization. The act of solid state grinding and liquid-assisted grinding induces chemical change, which is known as mechanochemistry. Liquid-assisted grinding method confers several advantages over solution crystallization. For instance, the relative solubility of the API and coformer is not a concern. Moreover, neat grinding which is a solvent-free solid-state cocrystallisation method eliminates the possibility of forming undesired solvates. However, the inability to obtain single crystals is a disadvantage of liquid-assisted grinding and neat grinding. The other disadvantages include the less degree of purity in comparison to liquid

crystallization and the increase in crystalline disorder which accompanies some materials upon energetic grinding.

The following sections of this chapter describe characterization and discuss properties of the products of cocrystallization of curcumin and ferulic acid.

5.3.1 Composition of products of cocrystallization

The products of cocrystallization (i.e. C, D and E) were analyzed by HPLC. According to the analysis, the stoichiometric molar ratio of curcumin to ferulic acid of the products of cocrystallization was 1:1.

5.3.2 Characterization of products of cocrystallization by optical microscopy

5.3.2.1 Optical micrographs of product of solvent evaporation

Optical micrographs of E are shown in figure 25. These images demonstrate the crystalline nature of the product. In fact, these crystals assume a long tubular morphology with blunt ends.

Figure 25. Optical micrographs of the product of solvent evaporation

5.3.2.2 Optical micrographs of the product of liquid-assisted grinding

Optical micrographs of the product of liquid-assisted grinding are shown in figure 26. These images reveal that the product of liquid-assisted grinding is less crystalline than the product of solvent evaporation.

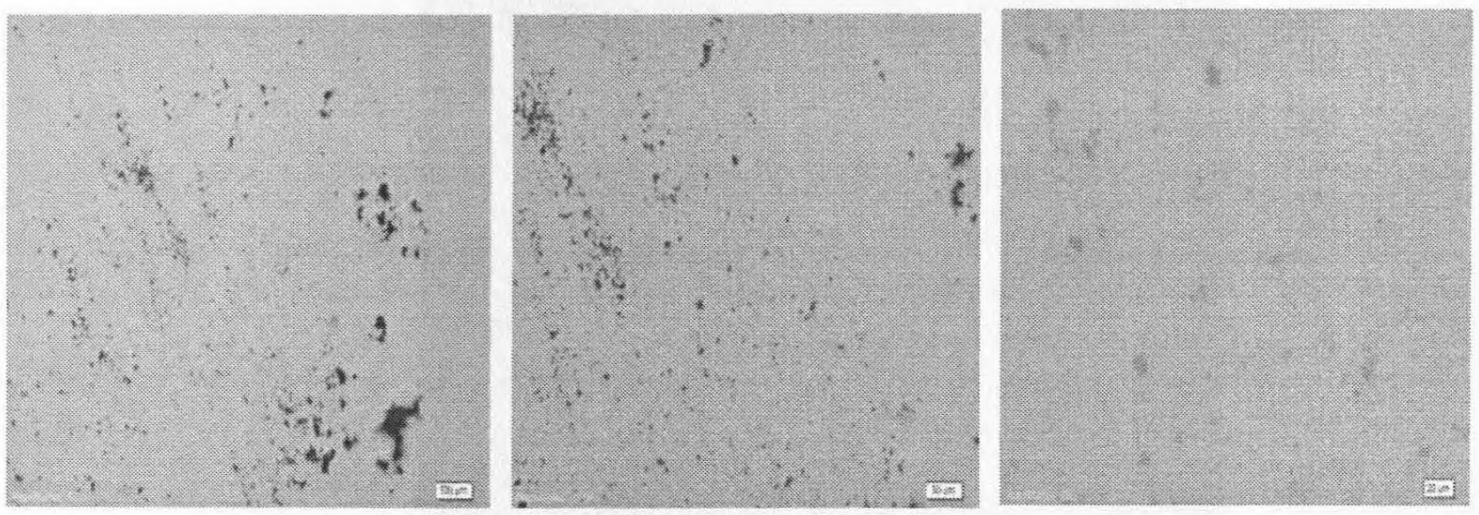

Figure 26. Optical micrographs of the product of liquid-assisted grinding

5.3.3 Characterization of products of cocrystallization by SEM

Only E was characterized by SEM because of its crystallinity. SEM images of E are shown in figure 27.

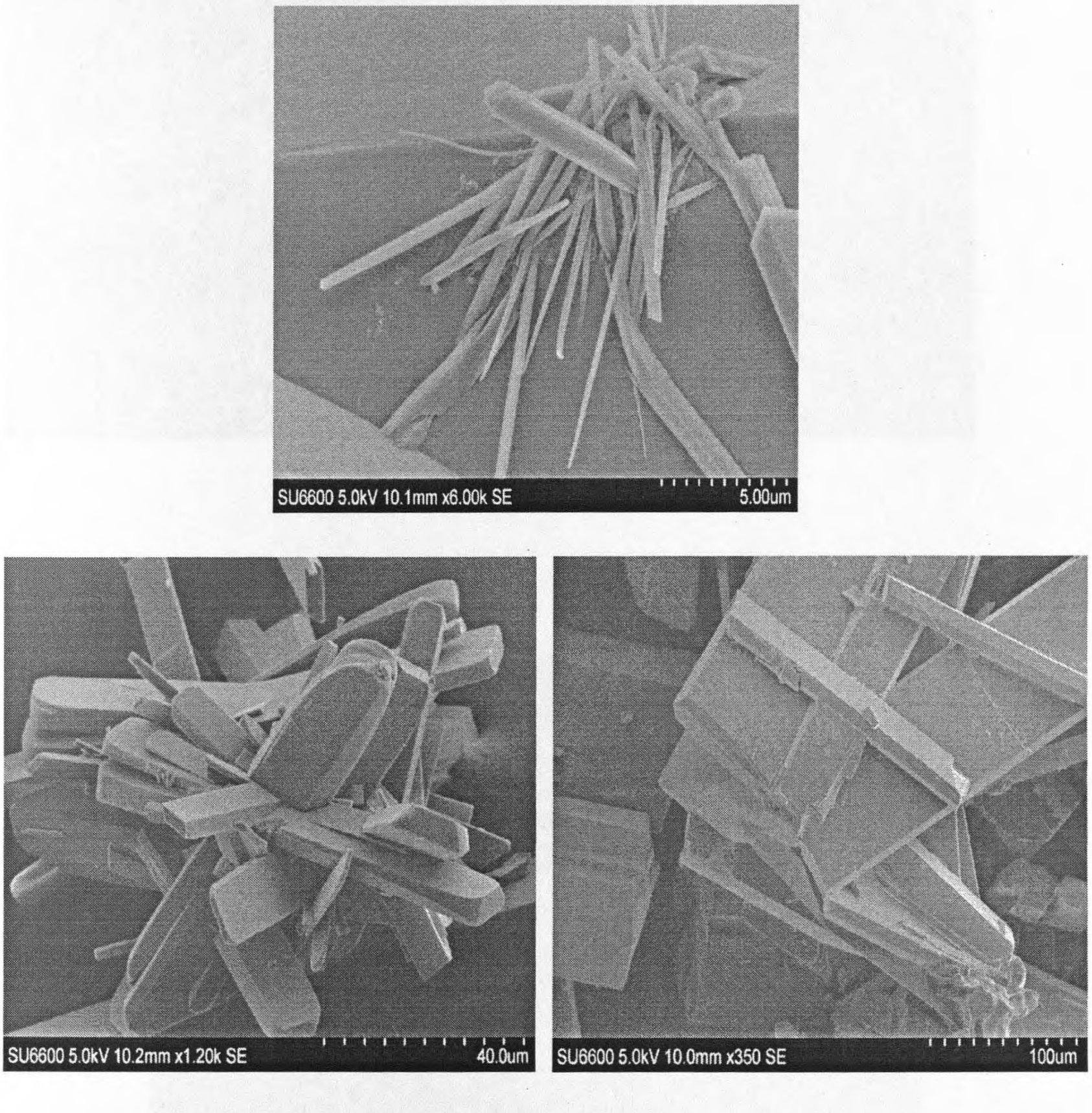

Figure 27. SEM images of the product of cocrystallization by solvent evaporation (E)

The SEM images of ferulic acid (A) and curcumin (B) are shown in figure 28 and figure 29, respectively.

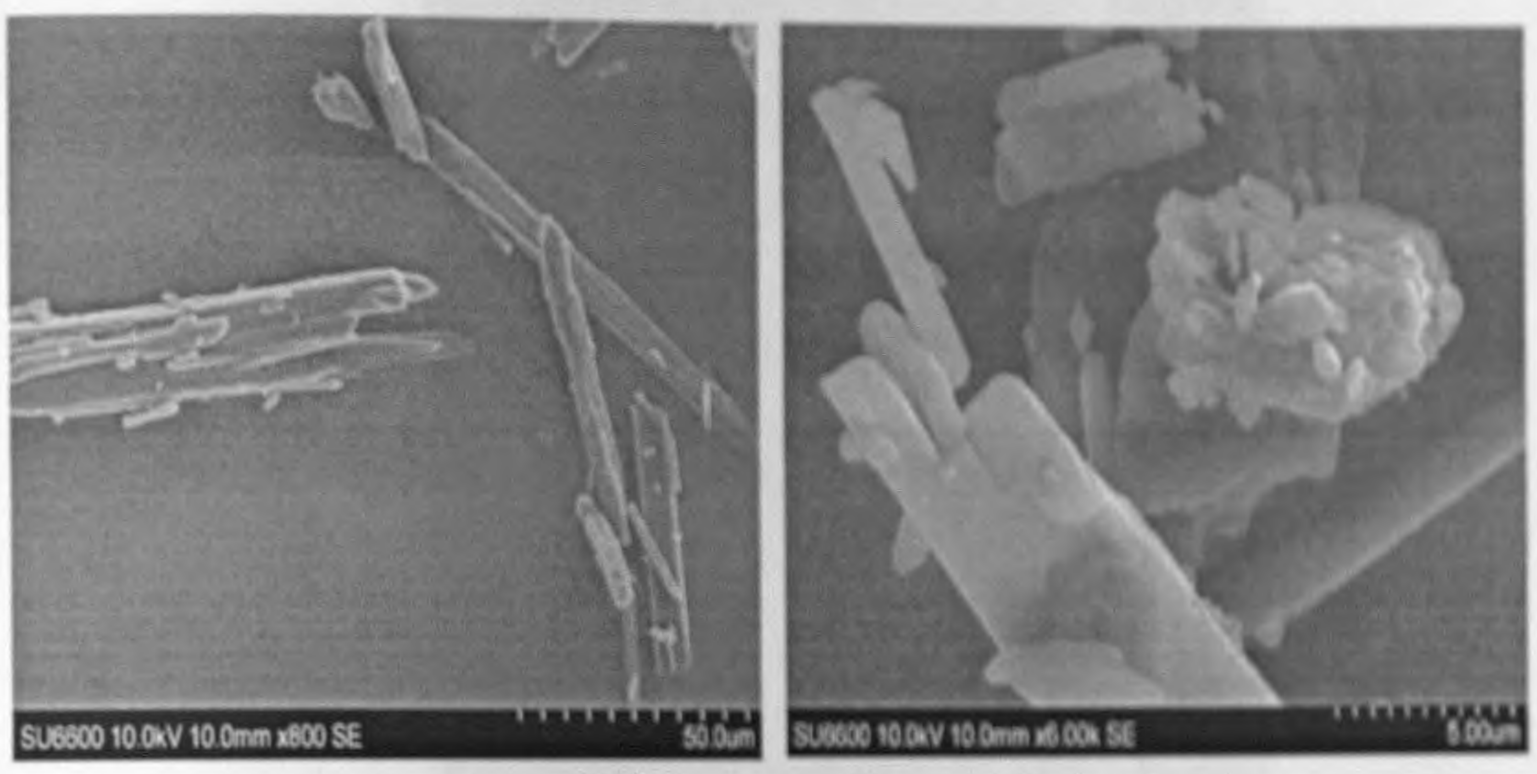

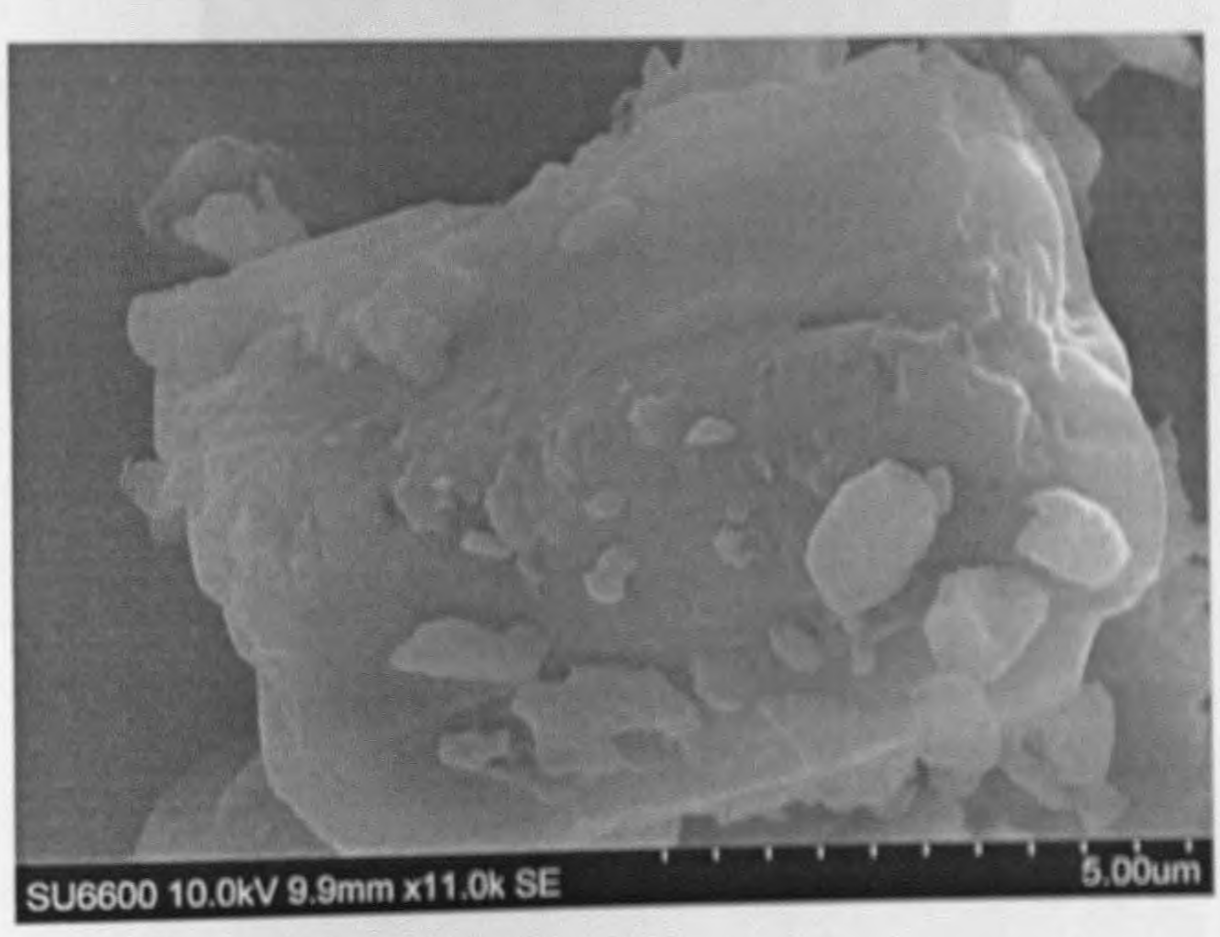

Figure 28. SEM images of ferulic acid

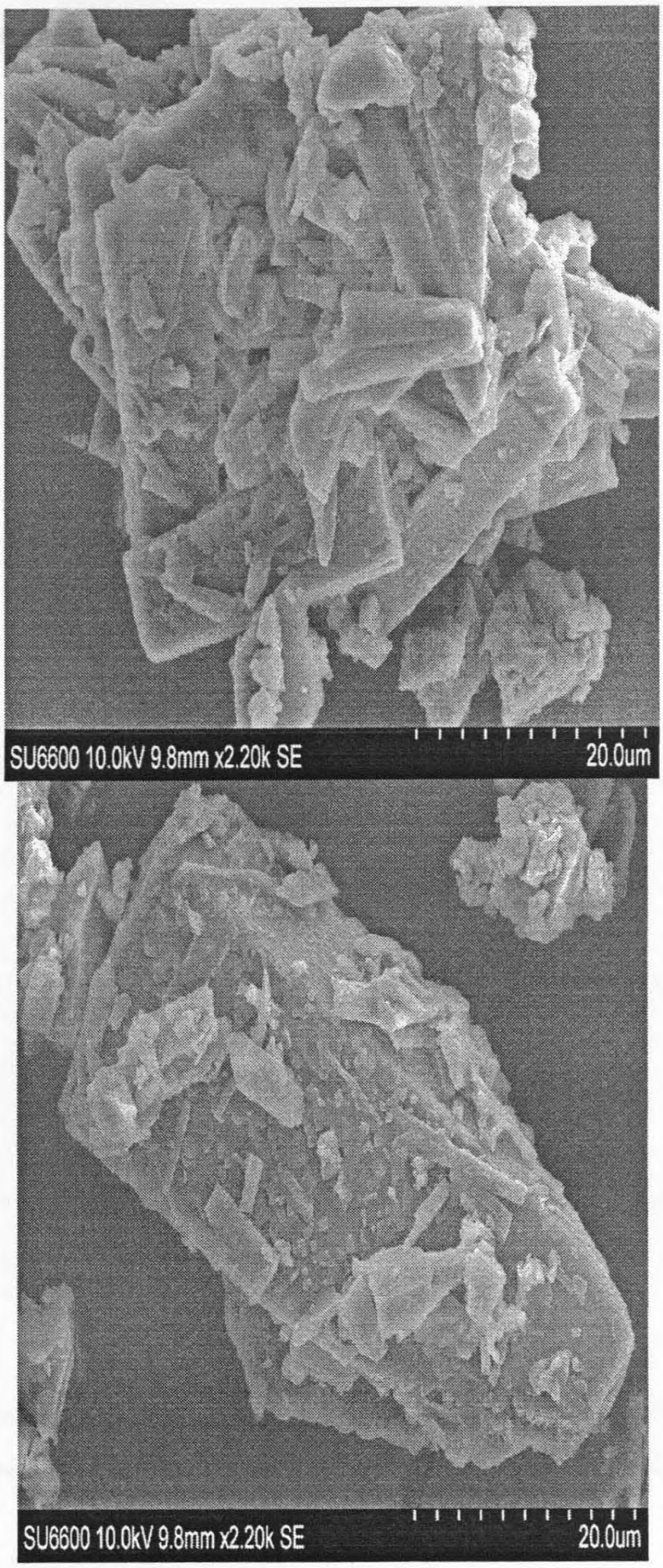

Figure 29. SEM images of curcumin

The SEM examination of E showed crystals of long prisms with various trapezoidal and pentagonal cross-sections. The crystals are distinctly different in morphology from their API and co-former.

5.3.4 Characterization of products of cocrystallization by PXRD

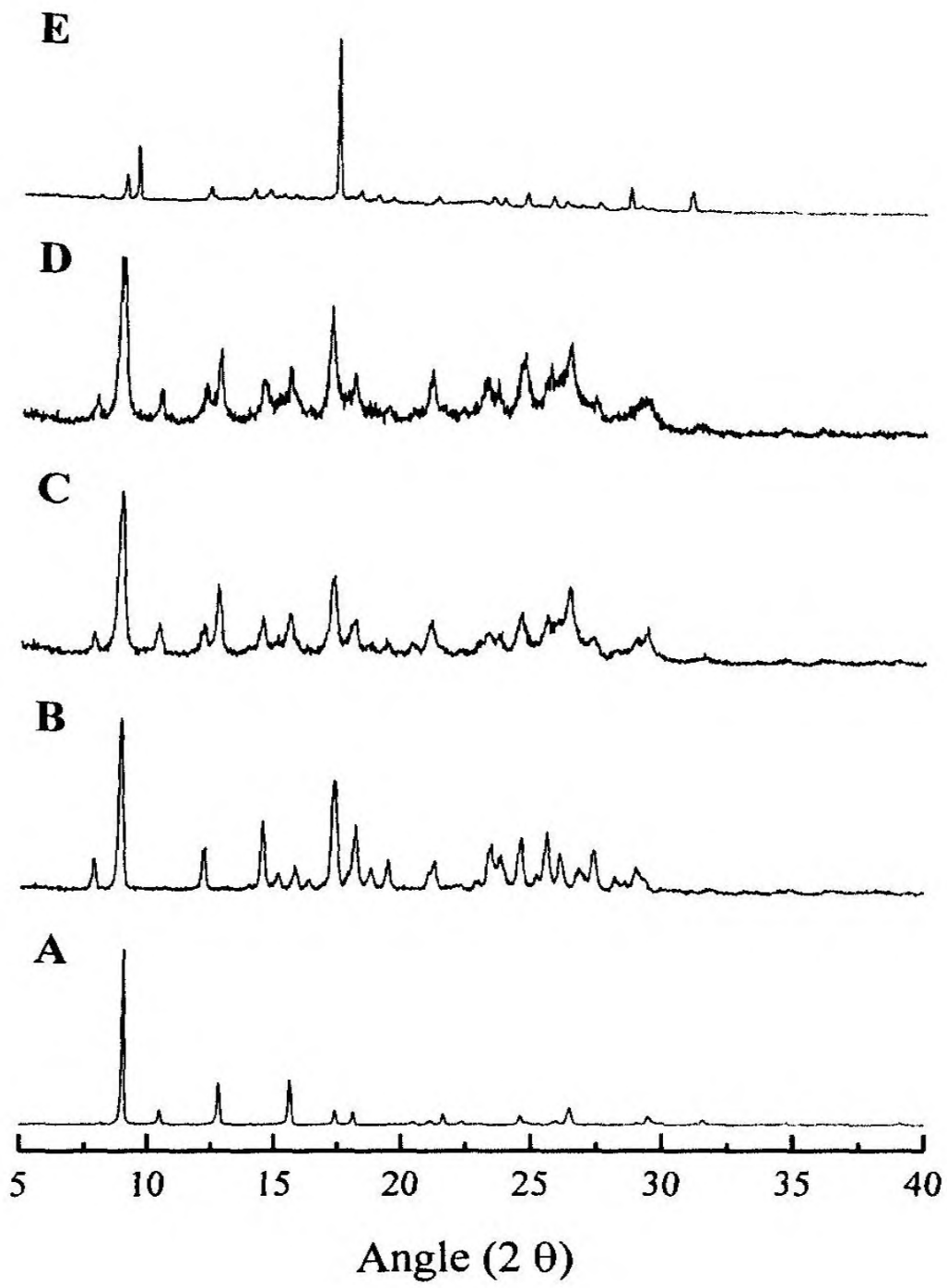

Figure 30. PXRD pattern of ferulic acid (A), curcumin (B), product of neat grinding (C), product of liquid-assisted grinding (D) and product of solvent evaporation (E)

PXRD patterns of curcumin (B), ferulic acid (A), and the products of cocrystallization by neat grinding (C), liquid-assisted grinding (D) and solvent evaporation (E) are shown in figure 30. Diffraction peaks of pure ferulic acid have almost disappeared in the diffraction pattern of E. For instance, peaks at 10.462°, 12.795°, 20.448° and 29.477° of the diffraction pattern of ferulic acid are absent in the diffraction pattern of E. However, a few diffraction peaks of pure ferulic acid are present

in low intensity in the diffraction pattern of the new product. The diffraction patterns of pure curcumin and E are somewhat similar, although numerous diffraction peaks of pure cucrcumin have shifted in the diffraction pattern of the new product. In addition, a number of new diffraction peaks of the product of solvent evaporation became visible: most notably those at 9.447°, 14.051°, 19.013°, and 31.031°. It suggests that the product of cocrystallization by solvent evaporation may be a new cocrystal. At least, this product may be close to a solid solution of ferulic acid in curcumin. Powder X-ray diffraction patterns of the product of neat grinding (C) and that of liquid-assisted grinding (D) are very similar. Those diffraction patterns consist of peaks of the diffraction patterns of both curcumin and ferulic acid. Diffraction peaks of C and D are of much lower intensity than those of pure components and the product of cocrystallization by solvent evaporation. Also, the diffraction patterns of C and D lack sharp diffraction peaks. These features indicate the lower degree of crystallinity of the products of grinding (i.e. C and D).

5.3.5 Characterization of products of cocrystallization by FT-IR and Raman spectroscopy

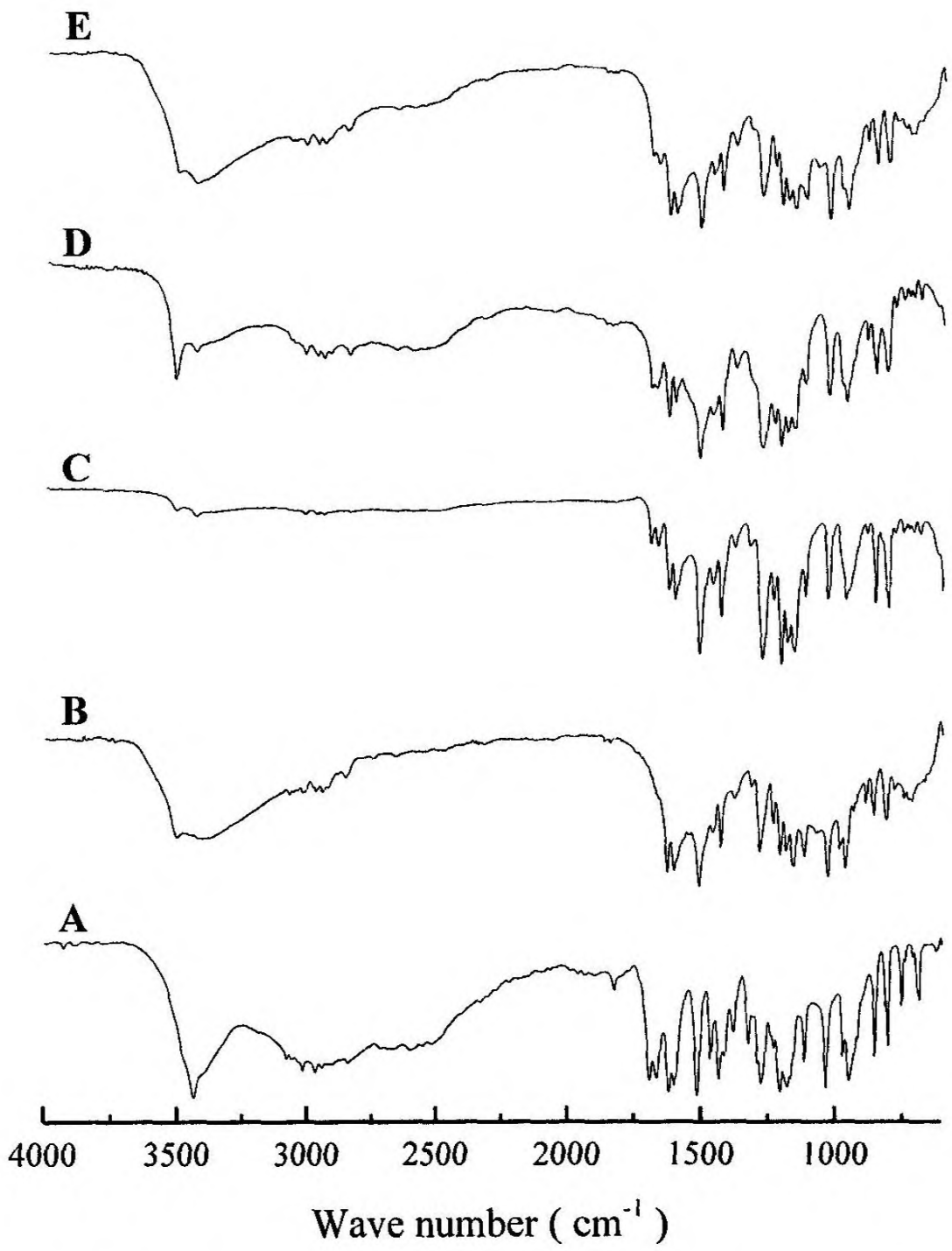

Figure 31. IR spectra of ferulic acid, curcumin and products of cocrystallization; ferulic acid (A), curcumin (B), product of neat grinding (C), product of liquid-assisted grinding (D), product of crystallization by solvent evaporation (E)

Table 16. Wave numbers of IR active stretching vibrations of functional groups of APIs and products of cocrystallization; Ferulic acid (A), Curcumin (B), product of neat grinding (C), product of liquid-assisted grinding (D), product of cocrystallization by solvent evaporation (E)

Formulation / Compound	IR active stretching vibrations; Wave number (cm^{-1})			
	O - H	C = O	Aryl alkyl ether C - O - C	Phenyl C - O
A	3438.34 (sh)	1691.37 (s)	1276.57	1232.44
B	3407.17 (br) 3510.24	1627.94 (s)	1283.83	1233.14
C	3435.09 3510.28	1624.23 1691.37 (w)	1275.90	1232.65
D	3440.81 3514.18	1627.64 1691.47 (w)	1277.84	1234.37
E	3436.36 (br)	1626.97 1691.47 (w)	1280.67	1234.37

Hydroxyl groups are present in both ferulic acid and curcumin, and accordingly, bands corresponding to O – H stretching vibrations were clearly visible in the spectra of the two APIs as well as the three types of products obtained from the different methods of cocrystallization. Ferulic acid showed a sharp strong absorption band at 3438 cm-1 due to the presence of the phenolic O-H. In addition, a broad band that centered around 3000 cm^{-1} appeared as a result of dimer formation through the carboxylic acid group. Hydrogen bonding of the ferulic acid dimer is shown in figure 32. The O-H absorption band of curcumin was markedly different from those of ferulic acid. In fact, the phenolic O-H absorption occurred at 3407 cm^{-1} as a strong and broad band. This indicates the high degree of hydrogen bonding that occurs in curcumin. Also, a small peak at 3510 cm^{-1} superimposed on the broad phenolic O-H band was present. This peak may be due to the small number of free O-H groups present in curcumin. The product of neat grinding (C) exhibited absorption at 3435 cm^{-1} as a result of O-H stretching. The position of this band is significantly different from that of curcumin. Also, a band of less intensity was present at 3510 cm^{-1} representing free O-H groups. Similar to C, the product of liquid assisted grinding (D) showed two bands as a result of O-H groups; one at 3440 cm^{-1} and another at

3514 cm^{-1}, corresponding to hydrogen bonded and free O-H groups, respectively. The product from crystallization by solvent evaporation (E) showed an O-H absorption band similar to that of curcumin, although the peak shifted to a higher wave number. In fact, the band appeared at 3407 cm^{-1} in curcumin whereas it appeared at 3436 cm^{-1} in E. Also, the broad band around 3000 cm^{-1} that appeared in the spectrum of ferulic acid is absent in the spectrum of E. These results indicate that ferulic acid dimers present in pure ferulic acid are absent in the products of cocrystallization, especially in E. Also, these results show that the hydrogen bonding pattern of curcumin changes upon combination with ferulic acid via methods of cocrystallization.

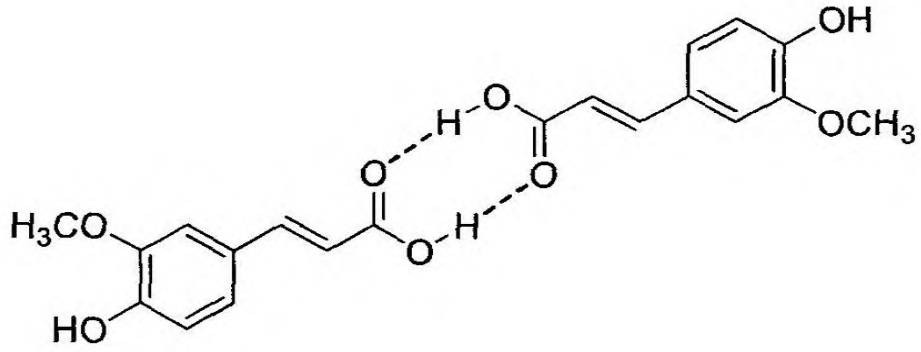

Figure 32. Hydrogen bonding of the ferulic acid dimer

Carbonyl groups, common to both curcumin and ferulic acid, are also involved in hydrogen bonding in these APIs. The carbonyl group of the carboxylic acid group of ferulic acid is involved in hydrogen bonding resulting in dimer formation in pure ferulic acid. Hence, it showed a strong absorption band at 1620 cm^{-1}. Also, the carbonyl groups of free carboxylic acid groups exhibited a strong absorption band at 1691 cm^{-1}. The absorption of carbonyl groups of curcumin occurred at 1628 cm^{-1}. In all three products of cocrystallization (i.e. C, D and E), the predominant absorption band corresponding to carbonyl groups appeared at 1624 cm^{-1} – 1628 cm^{-1}. The intensity of bands at 1691 cm^{-1} was much low. These results indicate that a significantly larger proportion of carboxylic acid groups of ferulic acid are involved in hydrogen bonding in the products of cocrystallization than in free ferulic acid.

In contrast to the vibrations of hydroxyl groups and to those of carbonyl groups, vibrations of aryl alkyl ether C-O-C bonds occurred within a very narrow range of wave lengths, in all five systems investigated (i.e. A-E). In fact, this range of wave lengths was from 1275 cm^{-1} to 1284 cm^{-1}. Similarly, the vibrations of phenyl C-O bond occurred within

a very narrow range of wavelengths. In fact, this range of wave lengths was from 1232 cm-1 to 1235 cm^{-1}. Thus, IR spectra do not reveal information on the involvement of either aryl alkyl ether C-O-C bonds or phenyl C-O bonds in intermolecular bond formation of the products of cocrystallization.

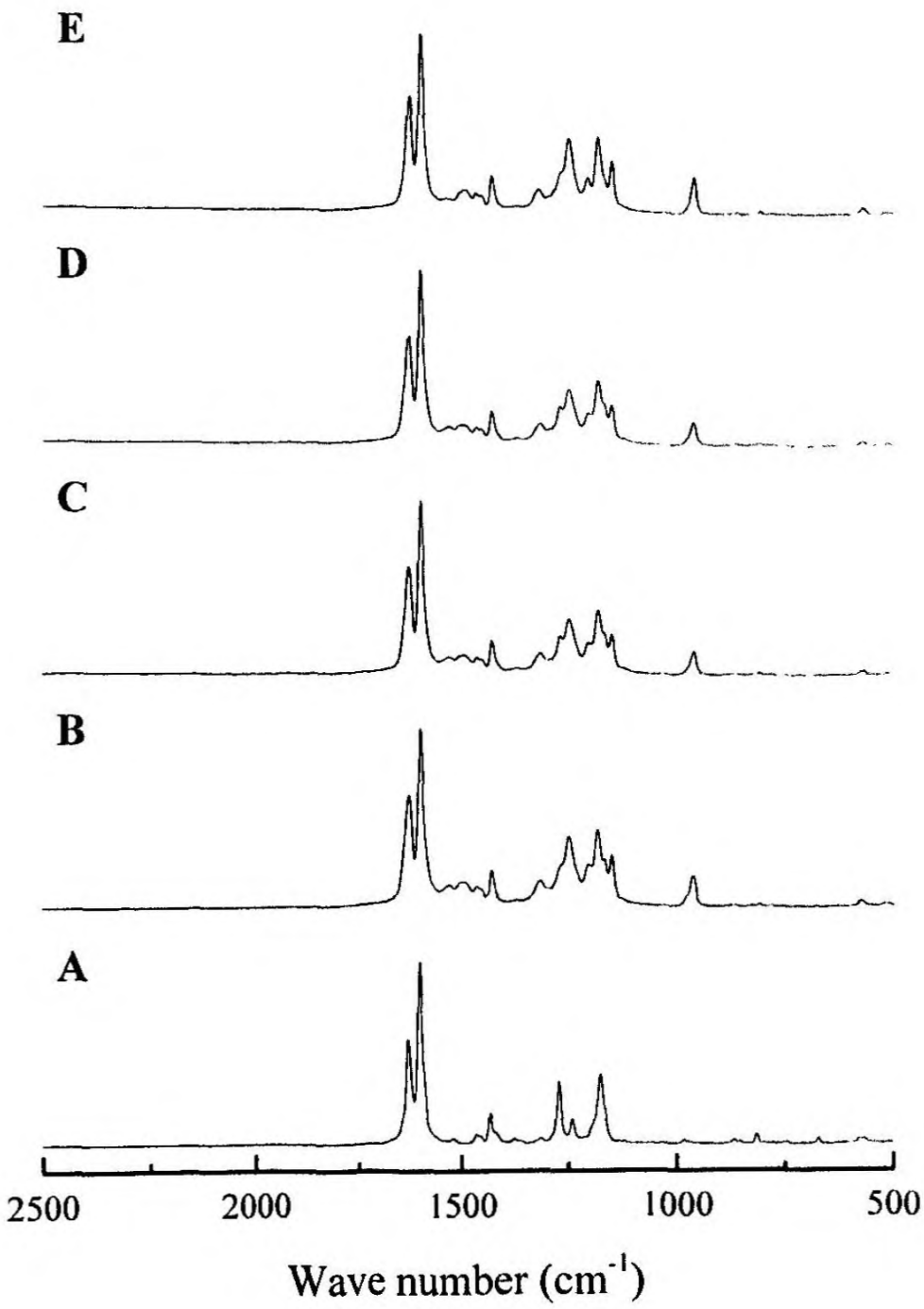

Figure 33. Raman spectra of ferulc acid, curcumin, and products of cocrystallization; ferulic acid (A), curcumin (B), product of neat grinding (C), product of liquid-assisted grinding (D), product of cocrystallization by solvent evaporation (E)

Table 17. Wave numbers of Raman active vibrations of APIs and products of cocrystallization; ferulic acid (A), curcumin (B), product of neat grinding (C), product of liquid-assisted grinding (D), product of cocrystallization by solvent evaporation (E)

Formulation/ compound	Raman active vibrations; wave number (cm^{-1})				
	C=O	C=C	Aromatic C=C	Aryl alkyl ether C-O-C	Phenol C-O
A	1629.60	1602.09	1432.98	1272.87	1241.41
B	1627.38	1600.99	1430.42		1250.39
C	1627.96	1601.10	1430.61	1271.07	1250.20
D	1628.06	1601.16	1430.66	1271.20	1250.20
E	1627.12	1600.78	1430.19	1207.93	1250.54

Raman spectra of the bioactive agents and the products of cocrystallization are depicted in figure 33 and the wave numbers of Raman active vibrations of functional groups are indicated in table 17. Raman spectra of ferulic acid, curcumin and the products of cocrystallization exhibited peaks corresponding to the vibrations of carbonyl groups in the range 1627 cm^{-1} – 1630 cm^{-1}. Thus, there are only negligible changes in Raman active C=O vibrations upon combination of the APIs through methods of cocrystallization. Also, according to Raman spectra, variation of vibrations of double bonds and aromatic double bonds is very subtle.

Ferulic acid exhibited a peak corresponding to the vibrations of C-O-C bonds of aryl alkyl ether group at 1273 cm^{-1}. However, vibrations of this moiety of curcumin appeared to be Raman inactive. The product of neat grinding (C) and that of liquid-assisted grinding (D) showed peaks very close to that of ferulic acid, indicating the presence of ferulic acid in those formulations. Interestingly, the product of cocrystallization by solvent evaporation (E) exhibited a peak markedly different from all other species. In fact, the peak corresponding to C-O-C vibrations appeared at 1208 cm^{-1} in E. This is approximately 65 cm^{-1} lower than the peaks of other species. This change in the wave number indicates an involvement of the aryl alkyl ether C-O-C bonds in intermolecular bond formation in E. In fact, the oxygen atom of the ether group can function as a hydrogen bond donor.

Phenyl C-O is another group that can participate in hydrogen bond formation. Ferulic acid and curcumin showed peaks that were apart from about 9 cm^{-1}, corresponding to the vibrations of this bond. In fact, the peak of A appeared at 1241 cm^{-1} whereas that of

B appeared at 1250 cm^{-1}. Interestingly, the peak at 1241 cm^{-1} of ferulic acid was absent in the spectra of all three products of cocrystallization (i.e. C, D and E). The peak at 1250 cm^{-1} that appeared in the spectrum of curcumin was present in the spectra of C, D and E. This result indicates that the phenyl C-O bond of ferulic acid undergoes some change, most probably participates in intermolecular hydrogen bonding with curcumin, in the products of cocrystallization.

In sum, the IR and Raman spectroscopic analysis of the products of cocrystallization shows that the vibrational frequencies match those of the components (i.e. APIs). However, hydrogen bonding alters the force constants of both the donor and acceptor groups. Specifically, the O-H group of curcumin, and the C=O, aryl alkyl ether C-O-C and phenol C-O groups of ferulic acid appear to participate in new or altered hydrogen bond formation in the products of cocrystallization. It can therefore be concluded that hydrogen bonding of the components has been altered during cocrystallization.

5.3.6 Thermal analysis

5.3.6.1 Thermogravimetric analysis

Ferulic acid (A), curcumin (B) and E were selected for TGA.

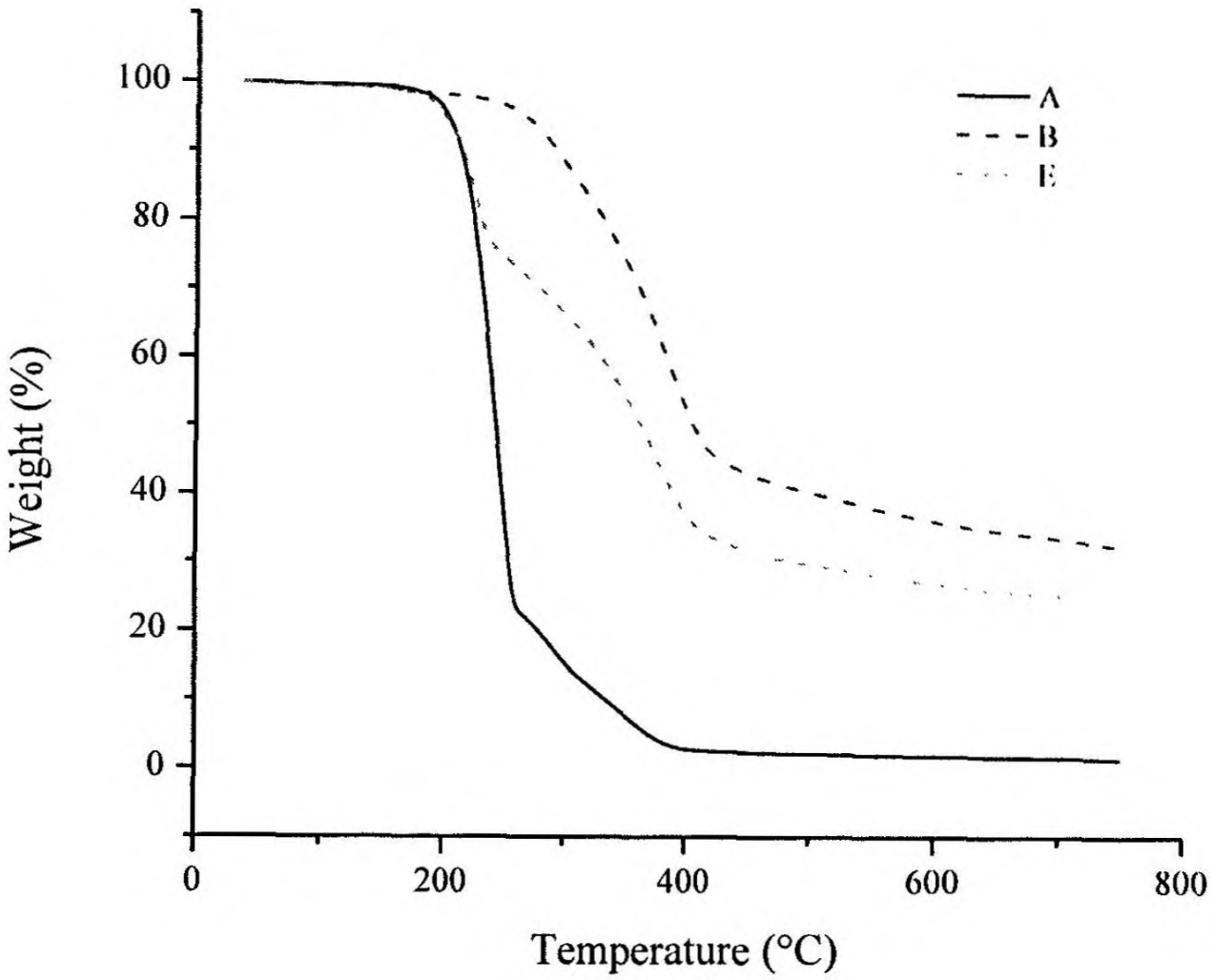

Figure 34. Thermograms of ferulic acid (A), curcumin (B) and the product of cocrystallization by solvent evaporation (E)

The thermograms of A, B and E are shown in figure 34. The thermograms reveal that the thermal stability of curcumin is higher than that of ferulic acid. As expected, E, which contains both ferulic acid and curcumin, shows an intermediate stability.

The TGA profile of ferulic acid is shown in figure 35 which shows the main degradation temperature of ferulic acid is at 243.9 °C corresponding to a weight loss of 77.4 %. The residual weight was negligible and was only 1.6 % at 750 °C.

The TGA profile of curcumin is shown in figure 36. According to this TGA profile, the main degradation temperature of curcumin is at 391.2 °C which corresponds to a weight loss of 55.8 %. The residual weight was 30.1 % at 750 °C.

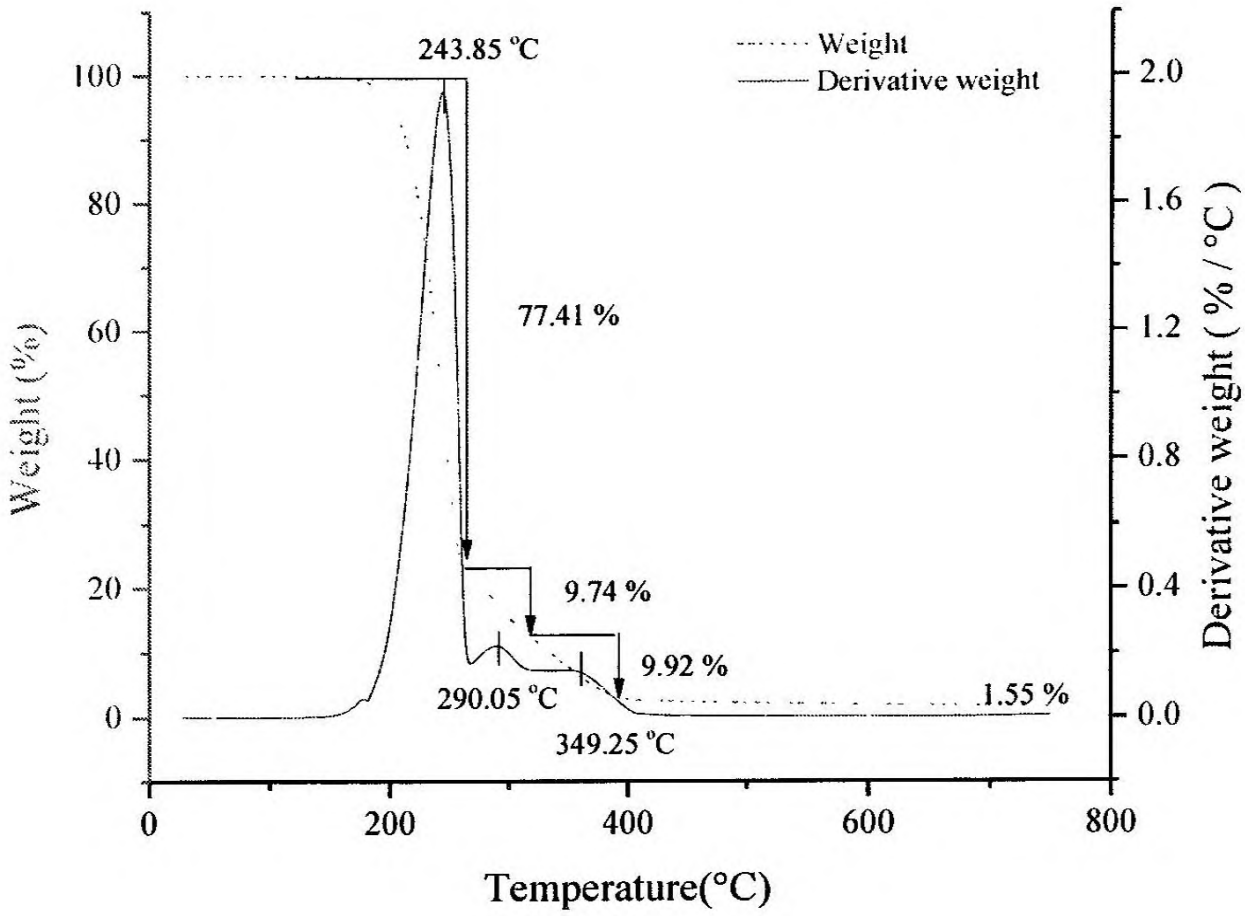

Figure 35. Weight and derivative weight versus temperature of ferulic acid

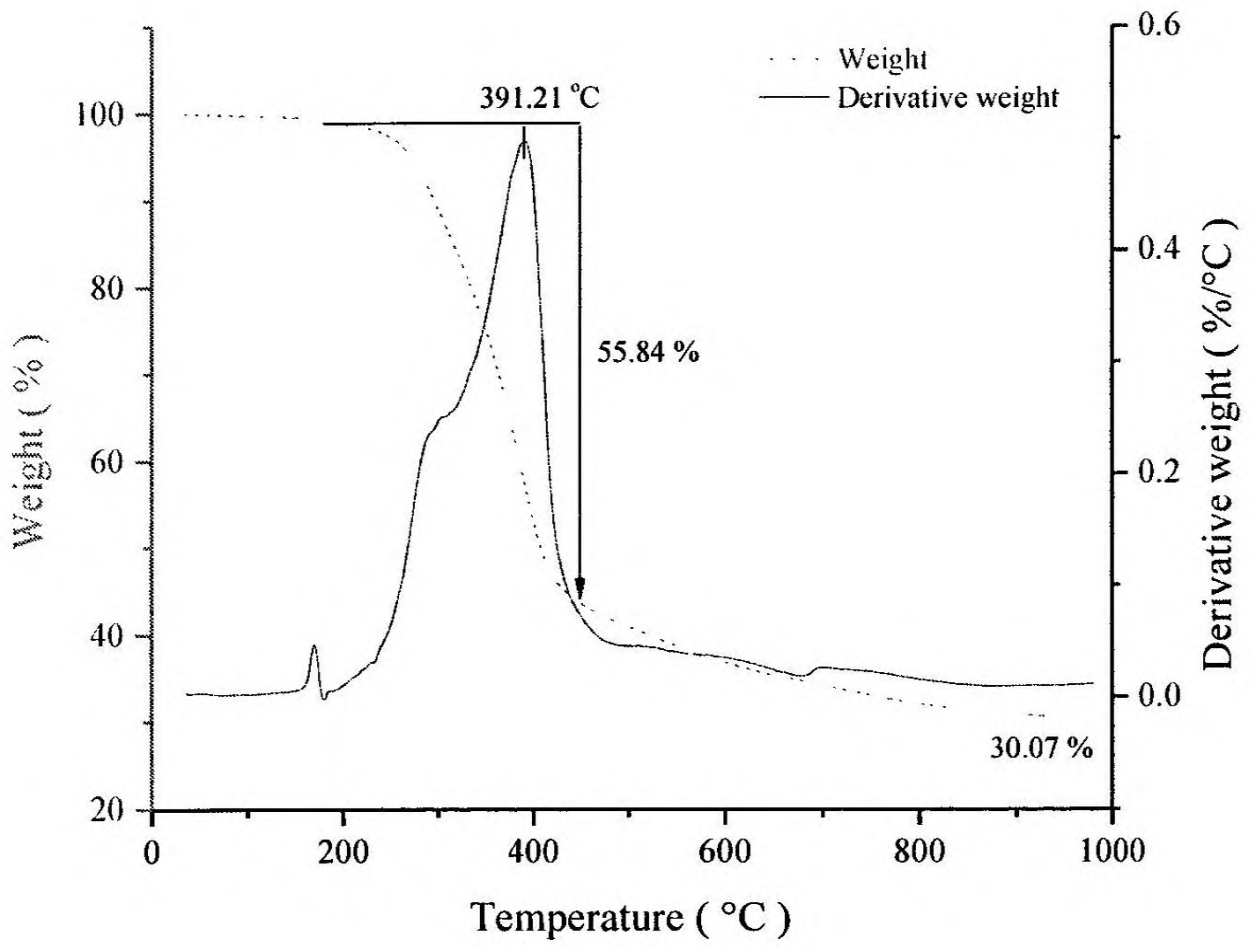

Figure 36. Weight and derivative weight versus temperature of curcumin

The TGA profile of the product of cocrystallization by solvent evaporation (E) is shown in figure 37. As expected, this TGA profile exhibits two main degradation temperatures; one at 223.9 °C which corresponds to a weight loss of 24.9 % and the other at 377.1 °C which corresponds to a weight loss of 43.70 %. Considering the degradation temperatures and percentage weight losses it can be concluded that degradation of ferulic acid in E occurs at 223.9 °C. This temperature is approximately 20 °C lower than the main degradation temperature of pure ferulic acid (cf. 243.9 °C). Likewise, it can be concluded that degradation of curcumin in E occurs at 377.1 °C. This temperature is approximately 14 °C lower than the main degradation temperature of pure curcumin (cf. 391.2 °C). These results indicate that both ferulic acid and curcumin become more susceptible to thermal degradation upon crystal formation by solvent evaporation. The possible increase in the internal energy of the lattice, that is caused by the insertion of ferulic acid molecules in the curcumin crystal structure, may be the cause for this increased susceptibility to temperature, of both ferulic acid and curcumin in E.

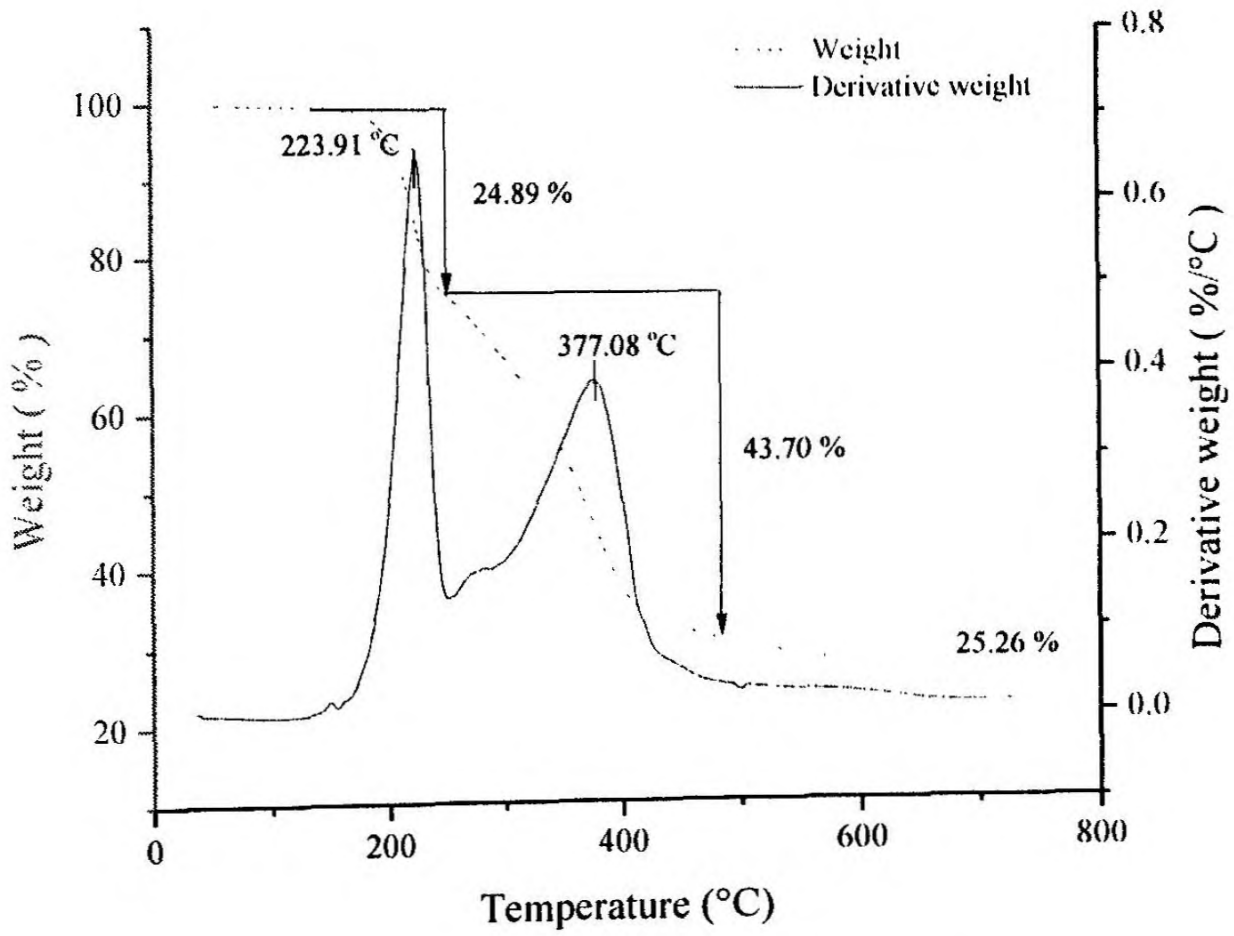

Figure 37. Weight and derivative weight versus temperature of the product of cocrystallization by solvent evaporation

5.3.6.2 Differential scanning calorimetry

The melting temperatures of ferulic acid, curcumin and all three products of cocrystallization were analyzed by DSC. The DSC thermograms of those species are depicted in figure 38.

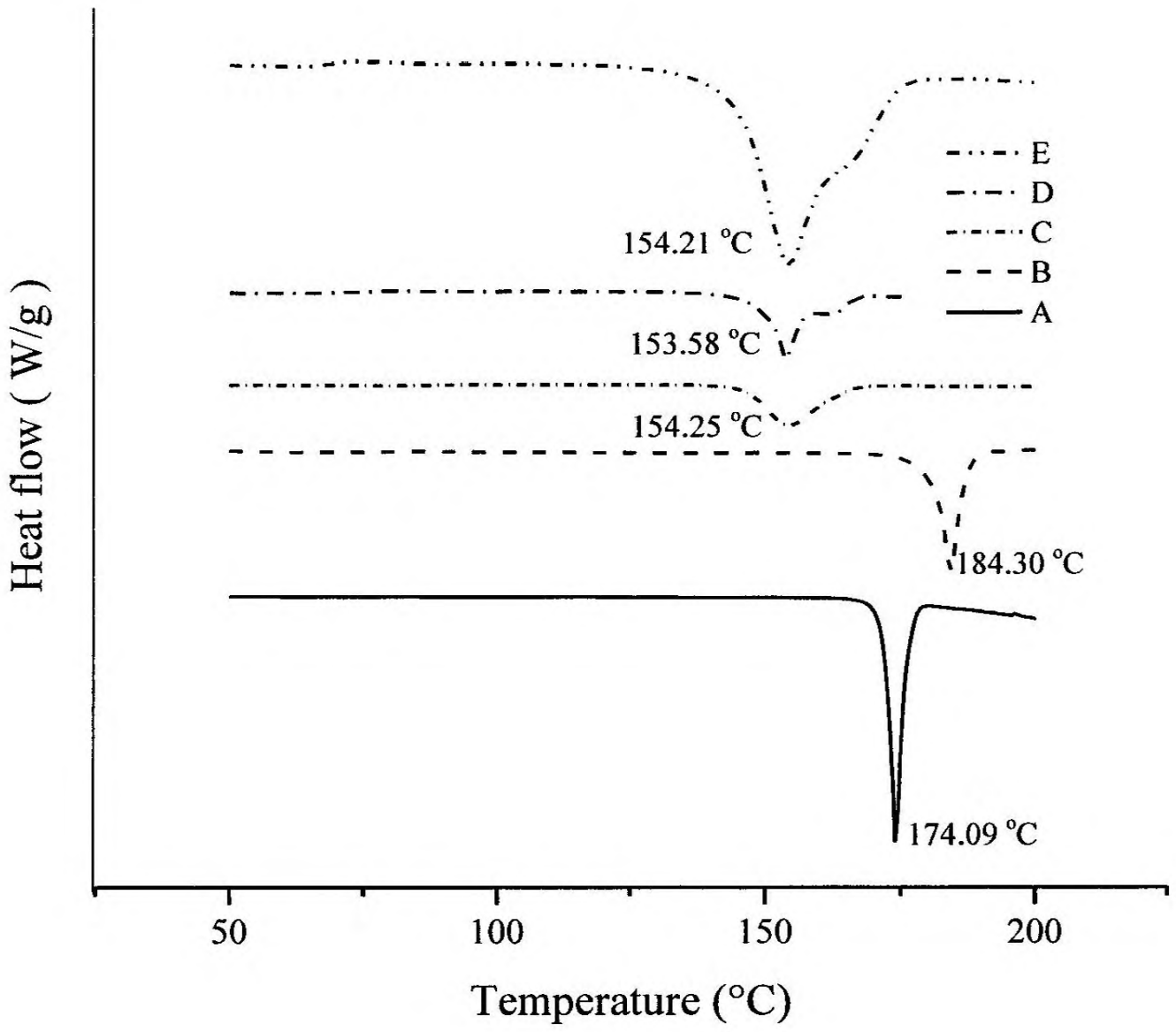

Figure 38. DSC thermograms of ferulic acid, curcumin, and the products of cocrystallization; Ferulic acid (A), curcumin (B), product of neat grinding (C), product of liquid-assisted grinding (D), and product of cocrystallization by solvent evaporation (E)

The APIs - ferulic acid and curcumin – showed relatively sharp endothermic peaks in DSC profiles. The melting temperatures of these compounds, ferulic acid and curcumin, were 174.1 °C and 184.3 °C, respectively. All three products of cocrystallization exhibited lower melting temperatures than starting materials; and those temperatures were very similar. In fact, the melting temperatures of the product of neat grinding (C), product of

liquid-assisted grinding (D) and product of cocrystallization by solvent evaporation (E) were 154.2 °C, 153.6 °C and 154.2 °C, respectively.

DSC profiles suggest that C and D are eutectic phases. Solid eutectic mixtures are a result of the minor component being supersaturated in the lattice of the major component (Gorniak *et al.*, 2011). However, as stated by Goud and coauthors, in the present scenario, the two components are mixed in stoichiometric ratios; and thus, one can make a distinction between major and minor components only superficially (Goud *et al.*, 2012). The supersaturation of one component in the lattice of the other component results in multiple solid solution phases that allow each component to retain its lattice structure. However, the interfaces between those phases consist of much weaker intermolecular interactions, unfulfilled bonds and imperfect atomic arrangements. Actually, eutectic mixtures comprise multiple solid solution phases with such incoherent boundaries. Due to their microstructures, eutectic mixtures possess higher internal energy than their starting materials, leading to lower melting points (Das *et al.*, 2009). The lower melting temperatures of the products of cocrystallization are indicative of the higher free energy of those solid forms. Since C and D exhibited lower melting endotherms while showing no characteristic peaks in the PXRD pattern, and IR and Raman spectra, it can be concluded that neat grinding and liquid-assisted grinding had resulted in binary eutectic compositions of curcumin and ferulic acid. The product of cocrystallization by solvent evaporation (E) also exhibited a melting temperature lower than those of the starting material. Thus, it is highly unlikely that E be a cocrystal. However, since the PXRD pattern of E approximates that of curcumin, E is most probably a solid solution of curcumin wherein ferulic acid constitutes the dispersed phase.

The solubilization mechanisms of crystalline phases are related to the increase of the solvent affinity and/or decrease of the lattice energy. In fact, the decrease in lattice energy is indicated by the decrease of the melting point. Due to the lowering of the melting point of the products of cocrystallization, these solid forms are expected to show higher dissolution rates and solubilities than curcumin which is the relatively insoluble species. Also, since the melting points of C, D and E approximate to the same temperature (i.e. 154 °C), these solid forms are expected to show similar dissolution properties.

5.3.7 Determination of dissolution

Solubility is of paramount importance as a physiochemical property of pharmaceutical compounds. Solubility is important in the bioavailability of

pharmaceutical compounds. The concentration of the substance in equilibrium with an excess of the undissolved substance is defined as the solubility. The dissolution rate is the rate at which the equilibrium is reached.

According to reported data, the solubility of curcumin – the API of this study - is very low (8.7 mg/L). It has a lower solubility below pH 7, and thus, it shows very low oral bioavailability. Utilizing higher pHs in pharmaceutical formulations is also problematic because investigations have revealed that its stability is less in neutral and in basic media (Wang *et al.*, 1997). However, curcumin is highly soluble in EtOH and acetone. Thus, the solvent system used for dissolution studies was 50% EtOH in water.

Although, curcumin shows low solublity in water, the coformer - ferulic acid - is relatively more soluble in water. Thus, pharmaceutical solid forms such as eutectics, solid solutions and cocrystals that curcumin forms in combination with ferulic acid are expected to exhibit higher solubilities and dissolution rates.

The direct exposure of cocrystal/eutectic composition to the solvent necessitates uniform distribution of particle size. Smaller particles with larger surface area have higher solubility. Particles of near uniform distribution were obtained by sieving through 250 μm mesh.

Powder dissolution rates of pharmaceutical formulations are measured routinely since increased dissolution rates usually accompany increased bioavailability of drugs/bioactive agents. Accordingly, powder dissolution rates of curcumin and the products of different methods of cocrystallization were measured after sieving the bioactive agents and formulations through a 250 μm mesh so that the effect of particle size on the dissolution of different formulations was removed. As predicted, the powder dissolution rates of the products of different methods of cocrystallization were higher than that of curcumin (see Figure 39). In fact the dissolution rates of the products of cocrystallization exhibited a two-fold increase than that of curcumin (see Table 18). The average dissolution rate of curcumin, which exhibited the lowest dissolution rate, over the period of 4 h is $(85.2 \pm 3.5) \times 10^{-3}$ mg/min. Interestingly, as expected by the similar melting temperatures, the powder dissolution profiles of the products of different methods of cocrystallization were very simiar that they almost overlapped. However, the dissolution rate of the product of solution crystallization was slightly higher than those of the products of neat grinding and liquid assisted grinding. In fact, the powder dissolution rates of the product of neat grinding, of the product of liquid-assisted grinding and of the

product of solution crystallization are 174.0 ± 3.5 × 10^{-3} mg/min, 174.3 ± 8.1 × 10^{-3} mg/min, and 187.1 ± 2.7 × 10^{-3} mg/min, respectively.

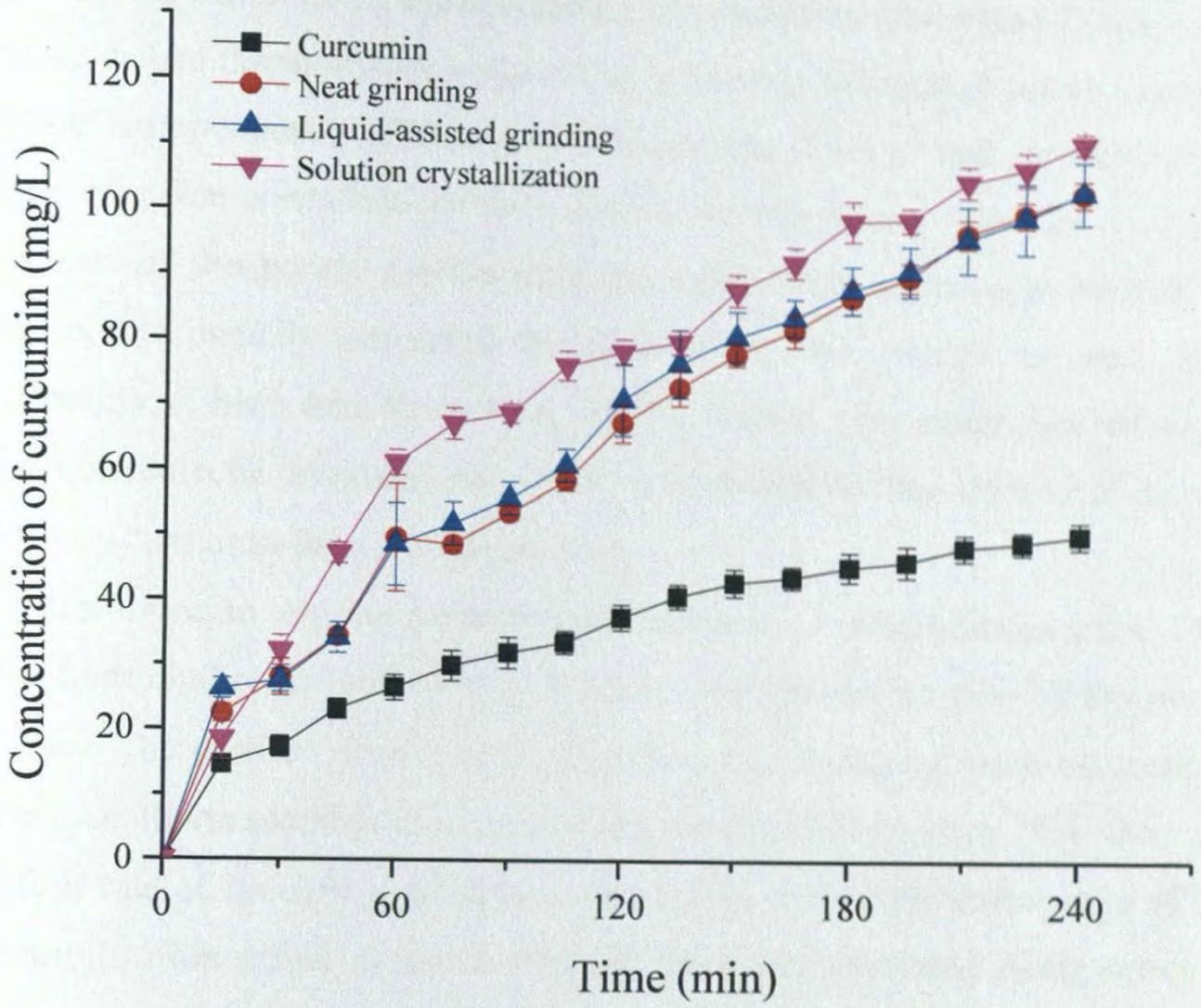

Figure 39. Powder dissolution profiles of curcumin and products of cocrystallization in 50 % ethanol-water

Table 18. Concentration of curcumin at 240 min and average dissolution rates of curcumin and products of cocrystallization

Formulation	Concentration of curcumin at 240 min (mg/L)	Average dissolution rate × 10^3 (mg/min)
Curcumin	.51.1 ± 2.1	.85.2 ± 3.5
Neat grinding (C)	104.4 ± 2.1	174.0 ± 3.5 (× 2.0)
Liquid-assisted grinding (D)	104.6 ± 4.9	174.3 ± 8.1 (× 2.0)
Solution crystallization (E)	112.3 ± 1.6	187.1 ± 2.7 (× 2.2)

As shown in figure 39, the dissolution profiles of C and D, which are eutectic mixtures of curcumin and ferulic acid, overlap and exhibit a two fold increase in the

dissolution rate at 240 min. Numerous factors contribute to this increase in dissolution rates showed by those eutectic mixtures, and following is a description of those factors.

The small size of solid crystallites of eutectic mixtures contributes to the increased dissolution rate exhibited by those eutectics. As stated by Chiou and Riegelman, eutectics may be described thermodynamically as "an intimately blended physical mixture of its two crystalline components" (Chiou and Riegelman, 1971), and accordingly, eutectics comprise very fine crystalline particles. Due to the reduction of the size of crystallites, the surface area of the poorly soluble drug increases. This increase in surface area of the poorly soluble usually increases its dissolution rate, which in turn increases its bioavailability (Chiou and Riegelman, 1971). Indeed, the small size of crystallites of curcumin in eutectic mixtures may have contributed to the enhanced dissolution rate exhibited by curcumin-ferulic acid eutectics.

In addition to the fine particle size in eutectics, a solubilization effect of the carrier or more hydrophilic component may increase the dissolution rate of the poorly soluble component. The carrier - ferulic acid - dissolves fast, bringing more curcumin in contact with the dissolution medium due to the microstructure of eutectics. This may increase the dissolution rate of the API – curcumin – especially during the early stage of dissolution. This solubilization effect of the carrier has been demonstrated using many APIs. For instance, Goldberg and coworkers demonstrated this phenomenon by showing that a physical mixture of acetaminophen and urea dissolves much faster than pure acetaminophen of similar particle sizes (Goldberg *et al.*, 1966). Moreover, Bates rationalized the increased dissolution of reserpine in a physical mixture of reserpine and polyvinylpyrrolidone using a similar phenomenon (Bates, 1969).

Prevention of aggregation and agglomeration of the fine crystallites of the poorly soluble APIs, also, is a major contributor to enhanced dissolution rates exhibited by eutectics. An aggregate may be defined as "a particle or an assembly of particles held together by strong inter- or intra-molecular or atomic cohesive forces" while an agglomerate may be defined as "a gathering of two or more particles and/or aggregates held together by relatively weak cohesive forces". In both of these cases, a dramatic reduction of surface area occurs, which is detrimental to dissolution rates. Although fine particles usually increase the dissolution rate of poorly soluble drugs, stronger van der Waal attractions present due to increased surface energy of those particles lead to aggregations or agglomerations. Thus, the dissolution rate may not exhibit the expected degree of increase. However, since the formation of aggregates and agglomerations of the

poorly soluble drug do not usually occur, the dissolution rate markedly increases in the case of eutectics (Chiou and Riegelman, 1971). Of course, the absence of aggregations and agglomerations may have contributed significantly to the enhanced dissolution rate exhibited by curcumin in C and D.

Wettability and dispersibility are, also, factors that influence the dissolution rate. In eutectics and in other solid dispersion systems, including solid solutions, the poorly soluble species is dispersed in a water-soluble matrix. Since the fine crystallites of the API are intimately surrounded by the water-soluble carrier, the API is brought into contact with the dissolution medium upon dissolution of the carrier, that result in wetting of the drug particles. Increased wetting, then, leads to increased dissolution rates (Chiou and Riegelman, 1971). Indeed, wettability and dispersibility may have significantly affected the dissolution rate of all products of cocrystallization.

Metastable crystalline materials constitute solid forms that exhibit increased solubility and faster dissolution (Chiou and Riegelman, 1971). According to the PXRD pattern, IR and Raman spectra, and thermograms, it may be inferred that E is a solid solution in which curcumin exists in a metastable form. Thus, the higher internal energy of this crystalline form may have contributed to the increased dissolution rate shown by E.

5.3.8 Thermal stability

Thermal stability of the antioxidants – ferulic acid and curcumin – were evaluated via HPLC analysis at three different temperatures: 25 °C at which the formulations are stored, 37 °C which represents physiological temperature, and 70 °C which represents the manufacturing temperature of topical formulations such as emulsions. Our results indicate that ferulic acid and curcumin are stable, whether used individually or as a mixture, at the selected temperatures over a period of 8 h (see Figures 40, 41 and 42). However, these antioxidants exhibited this apparent stability only when these compounds were protected from light.

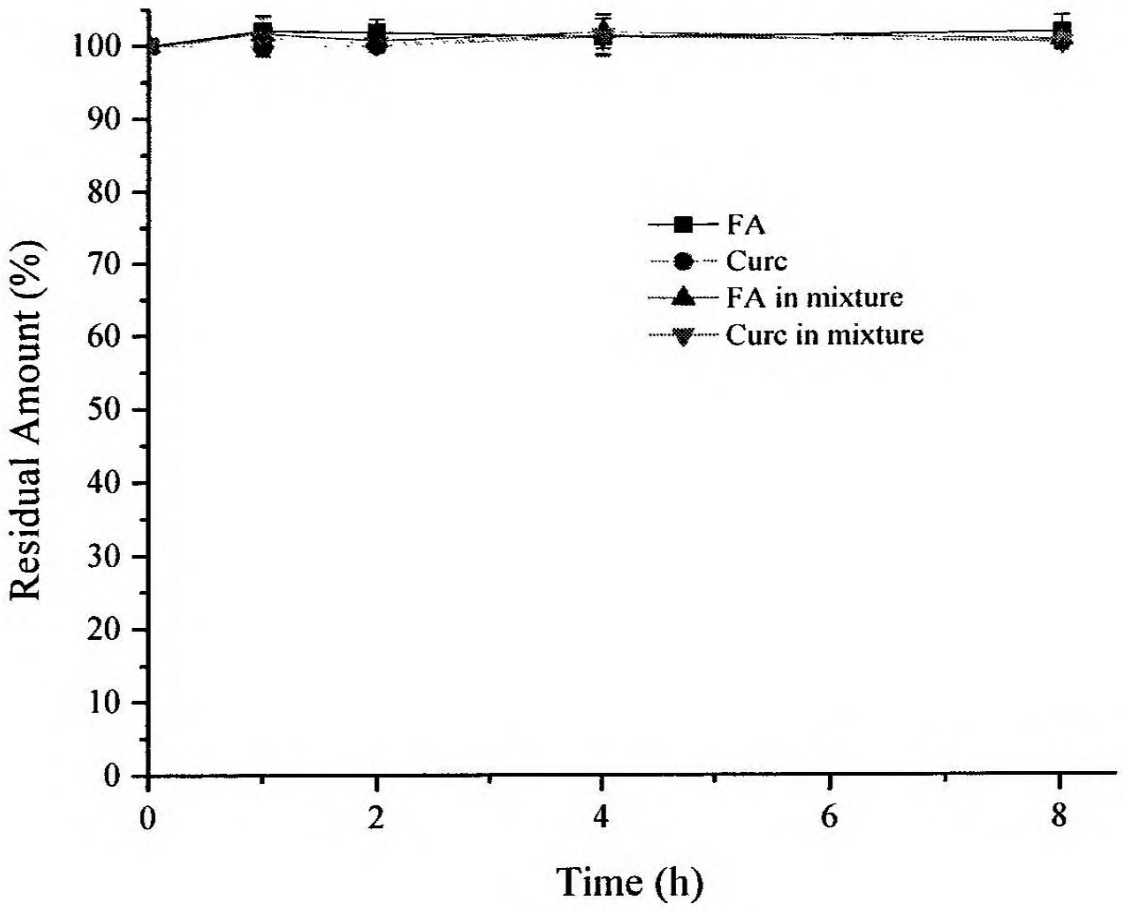

Figure 40. Residual amounts of ferulic acid (FA) and curcumin (Curc) at 25 °C separately and in combination over a period of 8 h

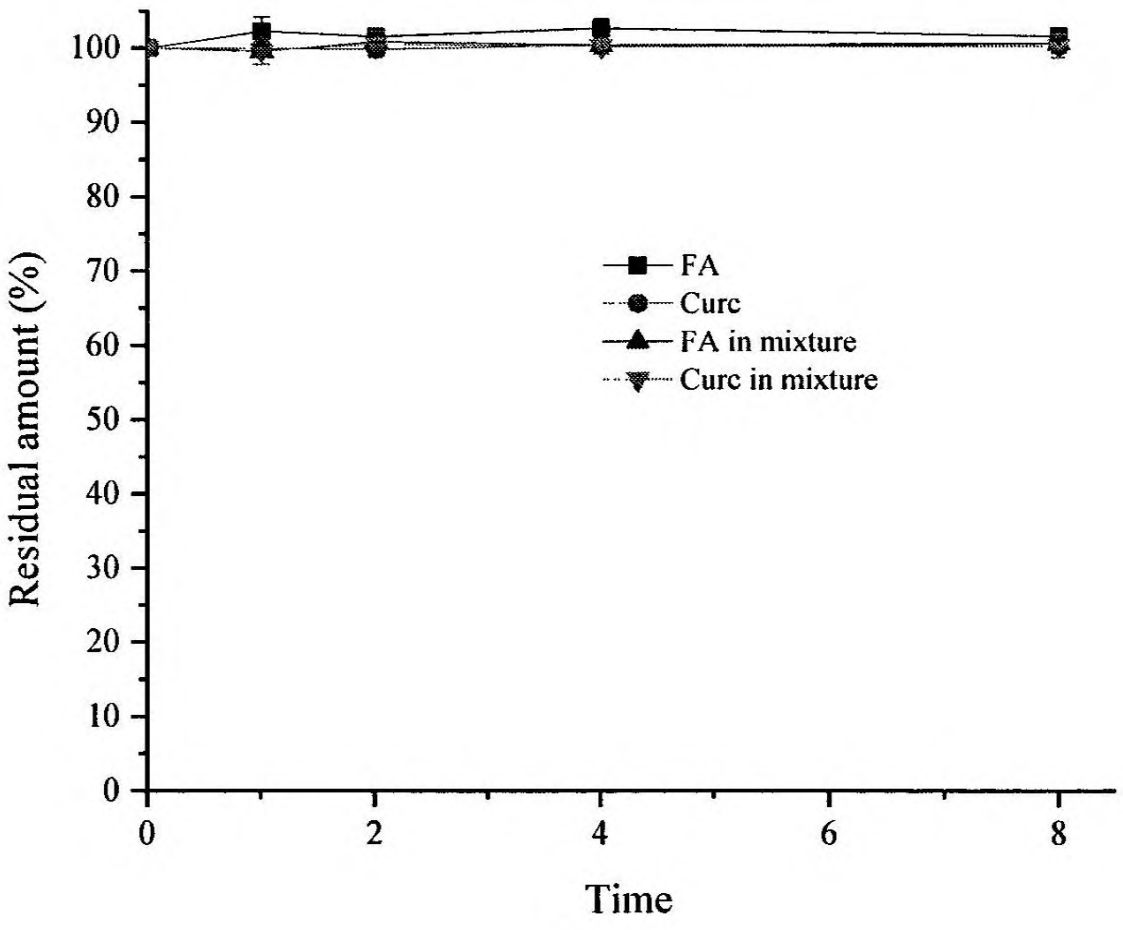

Figure 41. Residual amounts of ferulic acid (FA) and curcumin (Curc) at 37 °C separately and in combination over a period of 8 h

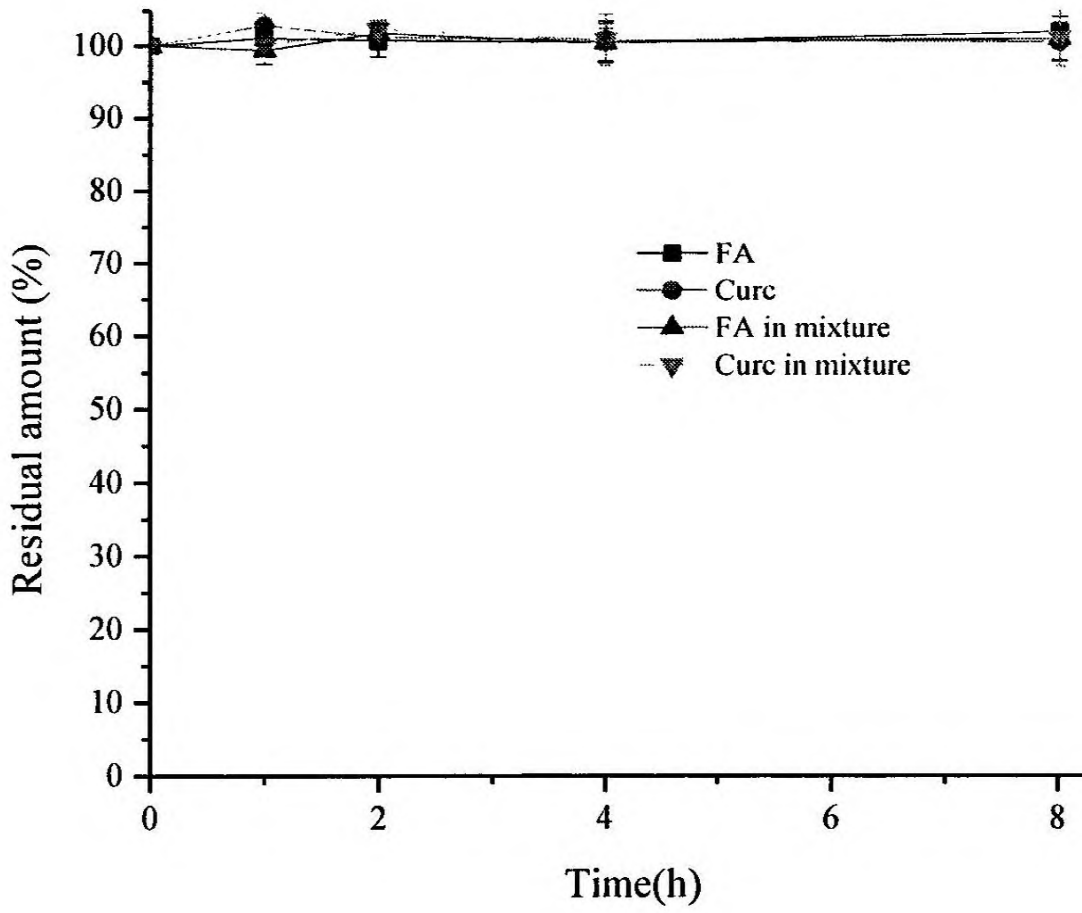

Figure 42. Residual amounts of ferulic acid (FA) and curcumin (Curc) at 70 °C separately and in combination over a period of 8 h

5.3.9 Photostability

In order to evaluate the stability of ferulic acid, curcumin and E, ethanol solutions of them were exposed to both UV A and UV B radiation simultaneously and the spectra were recorded. Figure 43 depicts the spectra of ferulic acid upon irradiation of UV light. Absorbance at 321 nm decreased upto 60 min beyond which absorbance remained the same. Thus, according to these spectra, degradation of ferulic acid occurs mainly in the first hour of UV exposure, after which the ferulic acid solution becomes stable.

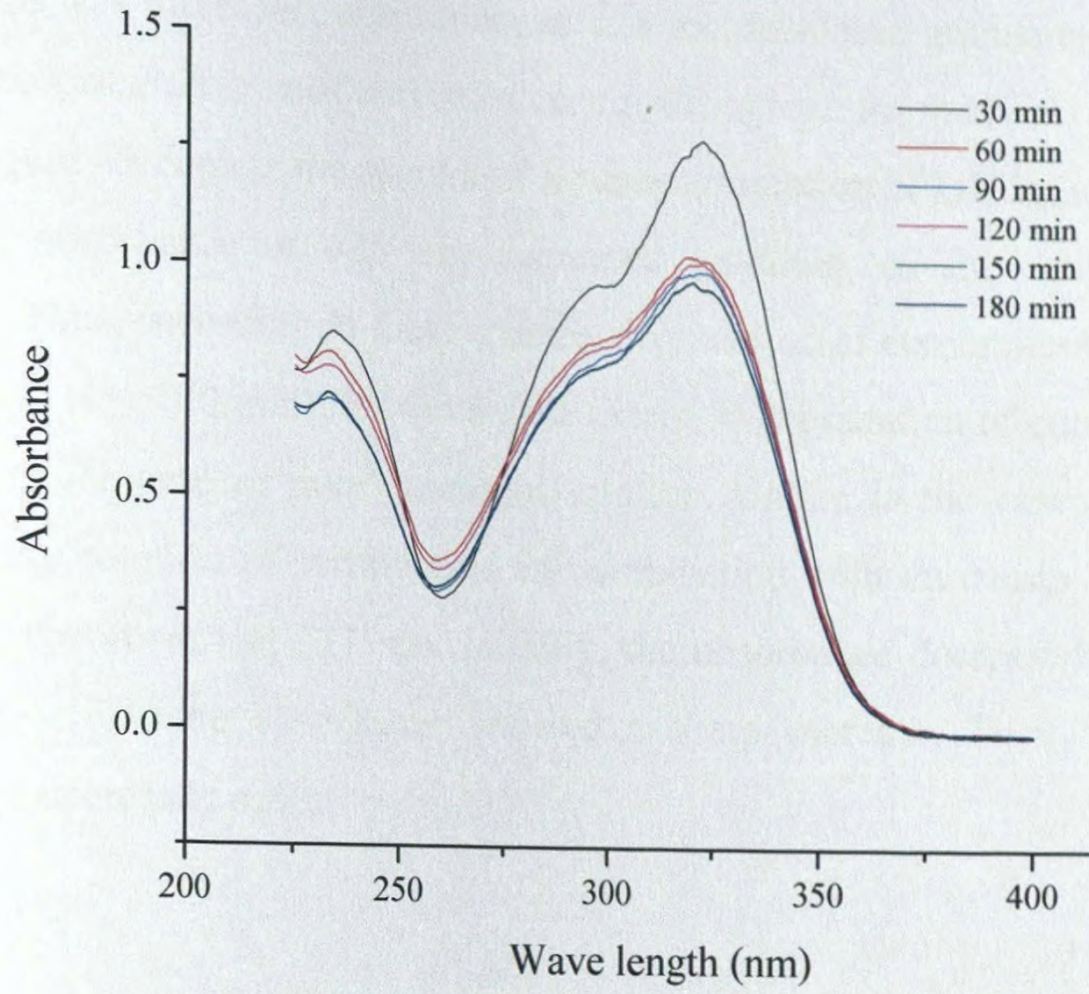

Figure 43. The profiles of absorbance vs wavelength for a solution of ferulic acid, upon UV irradiation

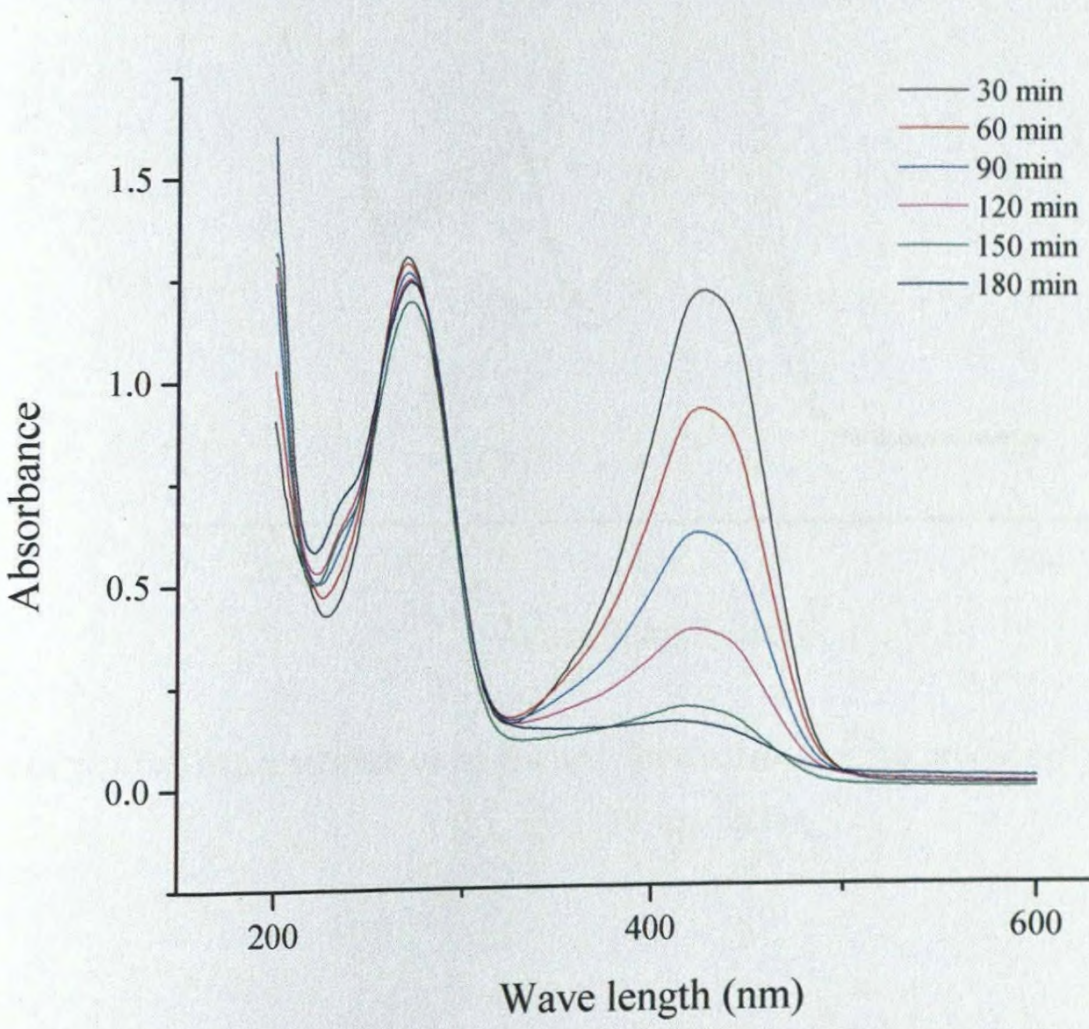

Figure 44. The profiles of absorbance vs wavelength for a solution of curcumin, upon UV irradiation

Figure 44 depicts the spectra of curcumin upon irradiation of UV light. As the time of exposure was increased, absorbance at 425 nm decreased gradually. Thus, according to these spectra, degradation of curcumin occurs throughout the study period (i.e. 180 min).

Figure 45 depicts the spectra of E, upon irradiation of UV light. Like in the case of curcumin, absorbance at 425 nm decreased gradually as the time of exposure was increased. Thus, according to these spectra, degradation of curcumin occurs throughout the study period (i.e. 180 min). However, the extent of degradation of curcumin appears to be less than in the case of pure curcumin solution. Unlike in the case of pure ferulic acid solution, the solution of ferulic acid in combination with curcumin exhibited an erratic pattern of absorbance at 321 nm. Initially, the absorbance decreased gradually up to 90 min. after which the absorbance showed a sharp increase. Then, after 120 min, the absorbance decreased again.

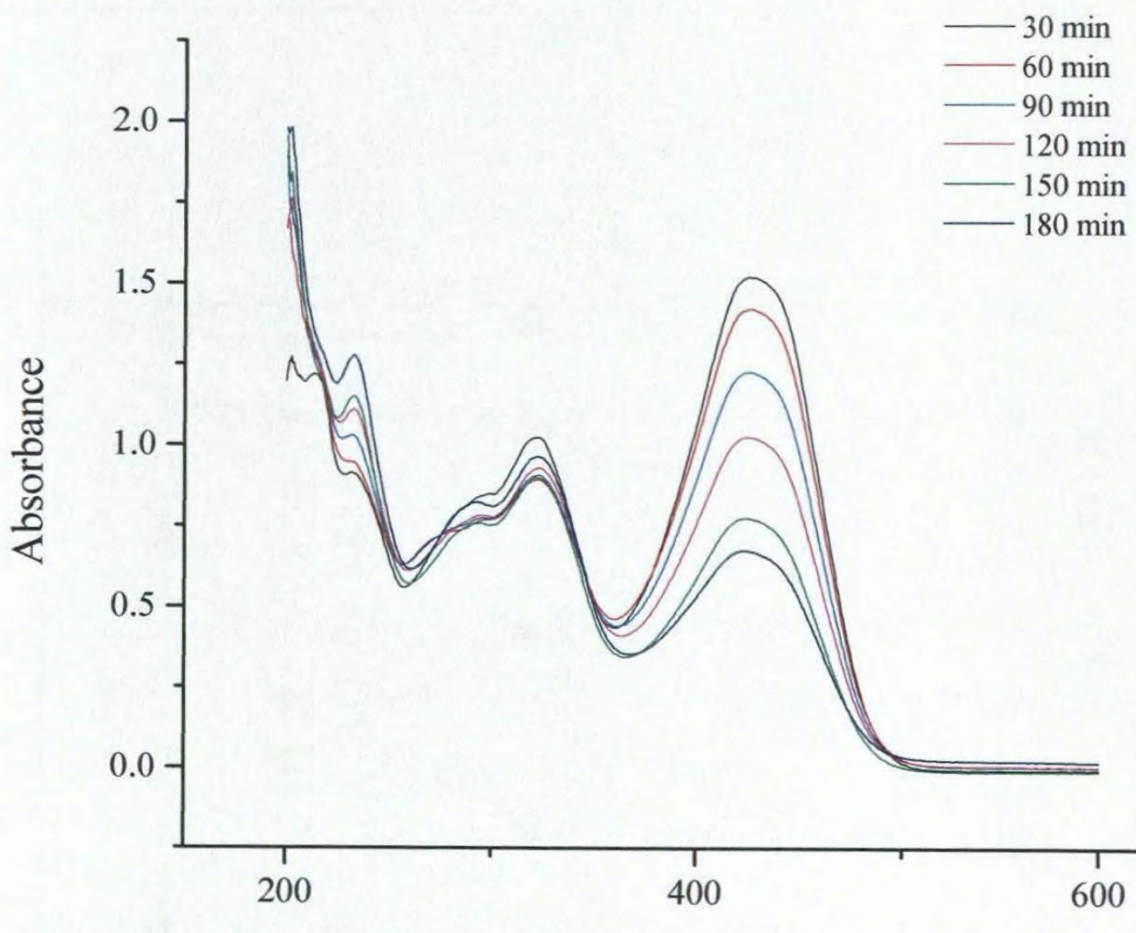

Figure 45. The profiles of absorbance vs wavelength for a solution of the product of solution crystallization (E), upon UV irradiation

In order to determine the stability of ferulic acid and curcumin in diffuse light and upon irradiation of UV light quantitatively and to investigate the degradation products of

those species, ethanol solutions of ferulic acid, of curcumin and of a mixture of those two bioactive compounds were exposed to diffuse light, and to both UV A and UV B radiation simultaneously. The resultant solutions were then analyzed by HPLC. HPLC peaks of the degradation products were identified by comparing the relative polarities of those species. The degradation products and their retention times are given in table 19.

Table 19. Retention times of ferulic acid, curcumin and their main degradation products

Compound	Retention time (min)	Detection wave length (nm)
Ferulic acid	4.2	321
Curcumin	11.5	425
Vanillin	4.4	321
Hexenal	8.1	321

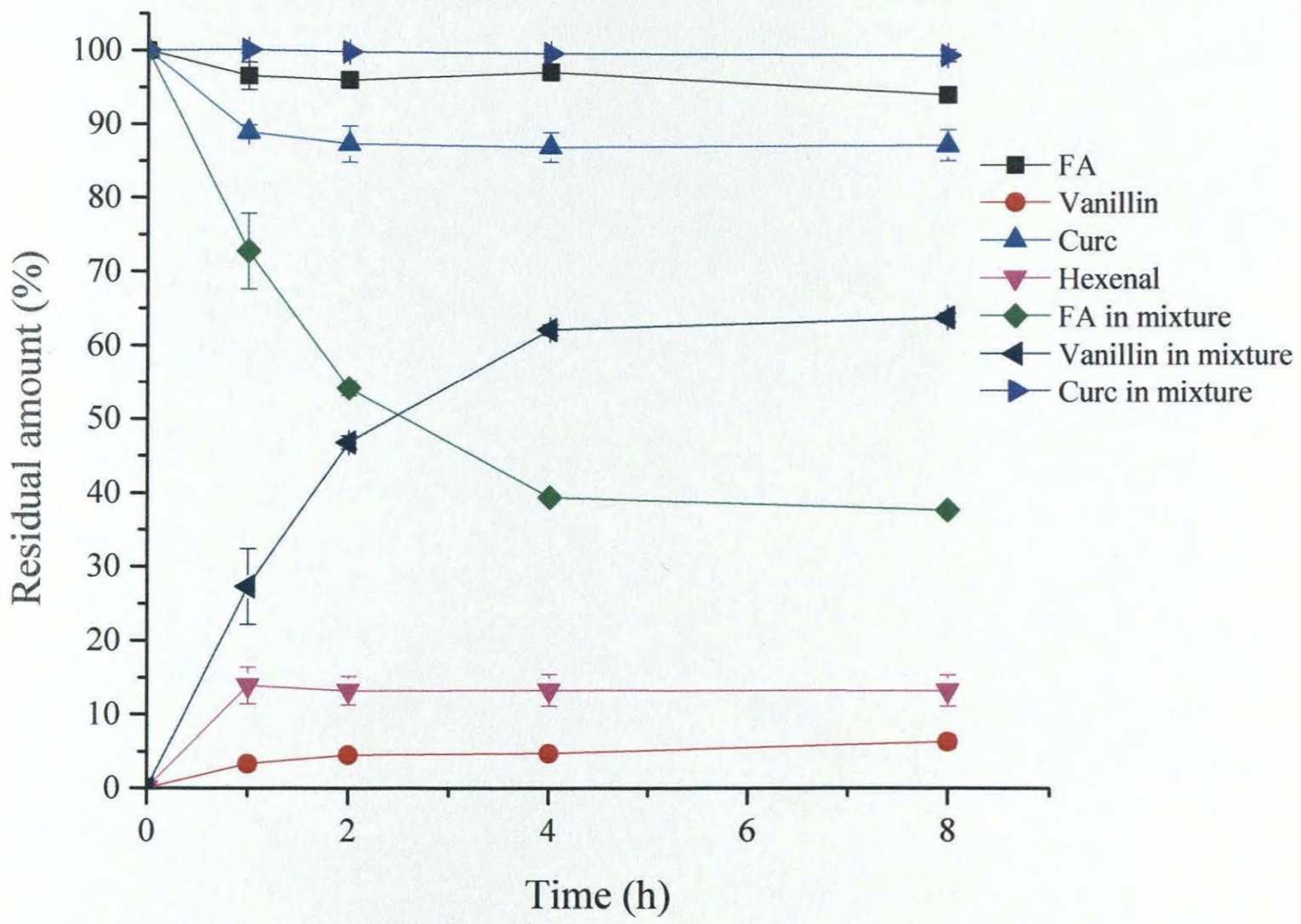

Figure 46. Residual amounts of ferulic acid (FA), curcumin (Curc) and their degradadtion products, upon exposure to diffuse light with time

Figure 46 shows the residual amounts of ferulic acid, curcumin and degradation products of those species upon exposure to diffuse light with time. The structures of the degradation products of curcumin are depicted in figure 47. The percentage of pure ferulic acid remaining in solution after 8 h was 93.8 ± 0.9 %, which indicated that 6.2 ± 0.9 % of ferulic acid had been converted to its degradation product–vanillin. The susceptibility of pure curcumin to diffuse light was two-fold compared to pure ferulic acid. In fact, the percentage of pure curcumin remaining in solution after 8 h was 86.9 ± 2.1 %, which indicated that 13.1 ± 2.1 % of curcumin had been converted to its degradation product – trans-6-(4'-hydroxy-3'-methoxypenyl)-4-dioxo-5-hexanal. Unlike in the case of pure ferulic acid, the residual amount of ferulic acid decreased gradually to reach nearly a minimum over a period of 4 h beyond which it was almost constant, in the mixture of ferulic acid and curcumin. Accordingly, the amount of the degradation product of ferulic acid – vanillin – increased gradually over a period of 4 h beyond which it was almost constant. Interestingly, unlike in the case of pure curcumin, curcumin in the mixture did not show degradation over the period of observation. In fact the residual percentage of curcumin after 8 h was 99.0 ± 0.8%.

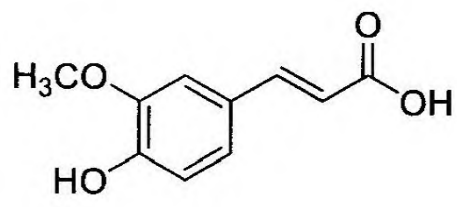

A

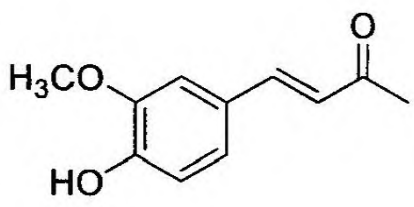

B

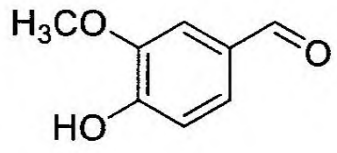

C

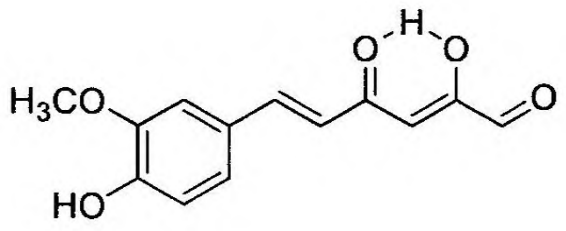

D

Figure 47. Structures of degradation products of curcumin

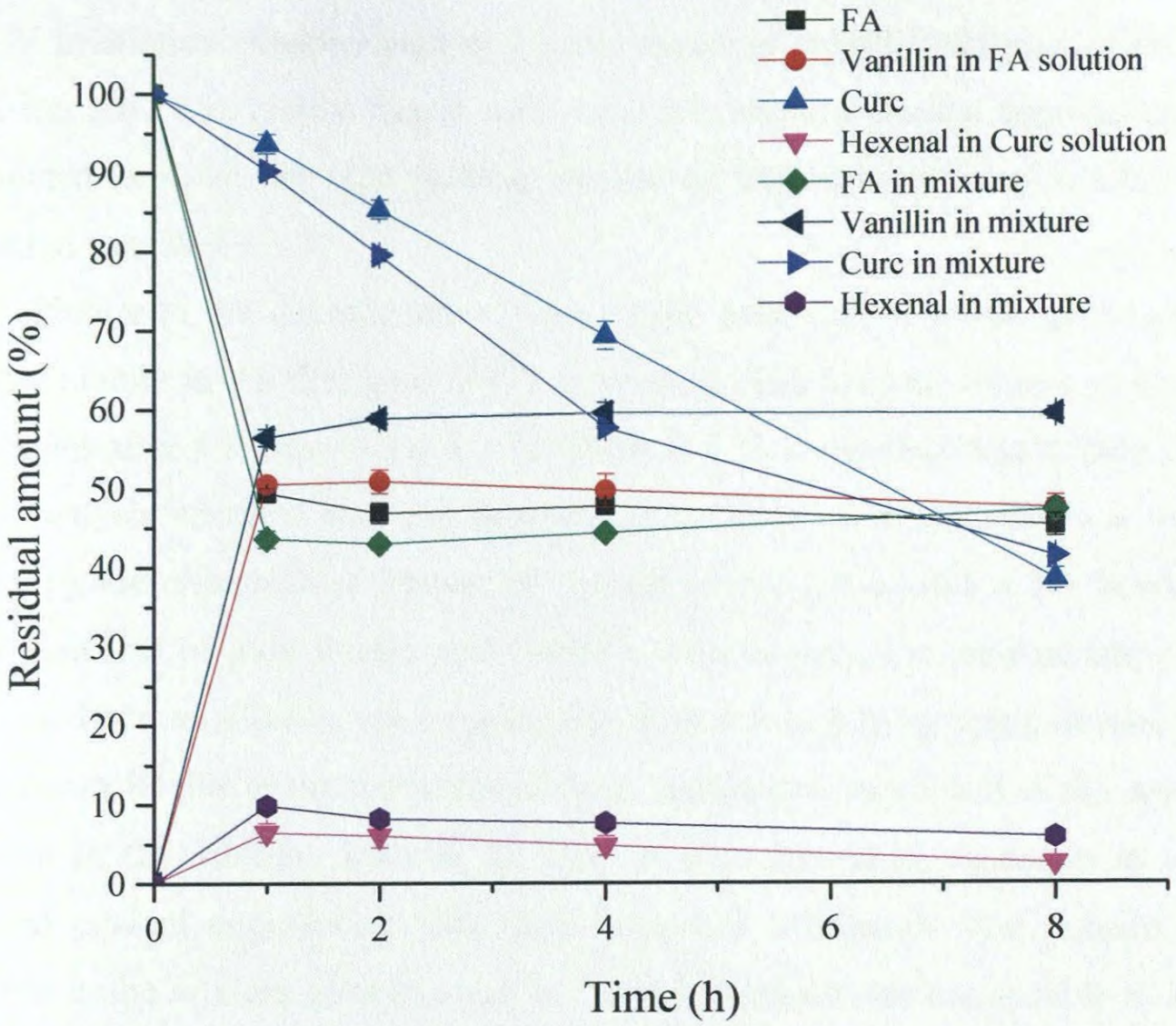

Figure 48. Residual amounts of ferulic acid (FA), curcumin (Curc) and their degradation products, upon exposure to UV light with time

Figure 48 shows the residual amounts of ferulic acid, curcumin and degradation products of those species upon exposure to UV A and UV B radiation concurrently, with time.

The main degradation product of ferulic acid was vanillin, according to the HPLC analysis. The degradation of ferulic acid occurred mainly in the first hour of UV irradiation and the percentage of pure ferulic acid remaining in solution after 1 h was 49.5 ± 0.6 %. This indicated that 50.5 ± 0.6 % of ferulic acid had been converted to its degradation product–vanillin. After the first hour, the amount of ferulic acid and vanillin remained relatively constant; although approximately 4 % of ferulic acid and 3 % of vanillin showed degradation from 1 h to 8 h.

Curcumin showed a number of degradation products upon UV irradiation as revealed by HPLC analysis (see Annexure). Like in the case of exposure to diffuse light, trans-6-(4'-hydroxy-3'-methoxyphenyl)-4-dioxo-5-hexenal was one degradation product. In addition to this hexenal, ferulic acid and vanillin were also present. Moreover, another

compound showed a peak in HPLC chromatogram at 8.7 min as detected at 321 nm after 2 h of UV irradiation. Another peak at 9.0 min appeared in HPLC chromatogram as detected at 321 nm after 8 h. Unlike ferulic acid, curcumin showed gradual degradation with time, as depicted in figure 48. The residual amount of curcumin in solution after 8 h of UV irradiation was 38.3 ± 1.3.

Similar to the degradation of pure ferulic acid, that of ferulic acid in the mixture occurred mainly in the first hour of UV irradiation. The residual amount of ferulic acid in the mixture after 1 h was 43.5 ± 1.1 % which is 6 % lower than that of pure ferulic acid. HPLC analysis revealed that the degradation product of ferulic acid was vanillin (see Annexure), and the residual amount of vanillin after 1 h was 56.5 ± 1.1 % which is 6 % higher than that of pure ferulic acid solution. Interestingly, the residual amounts of both ferulic acid and vanillin increased gradually from 1 h to 8 h, by approximately 3 %. This increase may be due to the formation of these compounds as a result of the degradation of curcumin in the mixture. Like in the case of pure curcumin, curcumin in the mixture exhibited gradual degradation with time, upon UV irradiation. The residual amount of curcumin in the mixture after 8 h was 41.2 ± 0.3 % which was comparable to that of pure curcumin solution after 8 h. One degradation product was the hexenal. Two other degradation products of curcumin were also detected through HPLC analysis, like in the case of irradiation of pure curcumin solution. One peak appeared at 8.7 min which was detected at 321 nm after 2 h and the other peak appeared at 9.0 min which also was detected at 321 nm after 8 h of UV irradiation. Interestingly, the degradation products of both ferulic acid and curcumin, including vanillin and the hexanal, contain a phenolic group, and thus, those species function as antioxidants.

5.3.10 Antioxidant properties

DPPH is a stable free radical of deep purple colour, which presents a strong absorption band in the range of 515–520 nm of the visible spectrum. DPPH accepts an electron or a hydrogen atom in the presence of an antioxidant compound. The colour of the free radical thus reduced is yellow. It is therefore possible to measure the extent of reduction, spectrophotometrically. The antioxidant activity is expressed as the concentration of antioxidant able to reduce the initial DPPH· concentration to 50% (IC_{50}) (Carmona-Jimenez *et al.*, 2014). In this study, methanol solutions of ferulic acid, curcumin, a mixture of ferulic acid and curcumin, and the three products of cocrystallization were exposed to sun light using a sun simulator for 4 h, and their change

in the antioxidant potency was evaluated using the DPPH assay. The results of this study are given in table 20.

Table 20. Antioxidant activities (i.e. IC_{50}) of methanol solutions of ferulic acid, curcumin, a mixture of the two and products of cocrystallization, according to the DPPH assay

Compound / Formulation	**IC_{50} (μM)**	
	Initial	**After 4 h**
Ferulic acid (A)	23.6 ± 0.4	18.7 ± 0.6
Curcumin (B)	17.0 ± 0.9	14.7 ± 0.4
Mixture of ferulic acid and curcumin	16.8 ± 0.5	13.7 ± 0.2
Product of neat grinding (C)	16.2 ± 0.4	12.0 ± 0.4
Product of liquid-assisted grinding (D)	16.2 ± 0.9	13.1 ± 0.3
Product of cocrystallization by solvent evaporation (E)	16.8 ± 0.6	13.4 ± 0.2

According to the initial antioxidant activities, curcumin (B) is a more potent antioxidant than ferulic acid (A). Indeed, this fact has been reported by several authors (Cuvelier, Richard and Berset, 1992). As expected, a mixture of A and B, prepared by mixing methanol solutions of those individual species, and methanol solutions of the three products of cocrystallization showed similar antioxidant activities. This result is consistent with the fact that all of these solutions contained equimolar amounts of the same solutes. This result also indicates that ferulic acid and curcumin in the products of cocrystallization dissociate completely in the methanol medium, and that those species interact in the solution only to the degree that a mixture prepared by simple mixing of A and B would allow. Dissociation of A and B completely in the medium is very important because dissociation of the API from the coformer is an essential requirement for the constitution of pharmaceutically acceptable cocrystals (Brittain, 2013).

Interestingly, ferulic acid and curcumin exhibit synergy when present in equimolar concentrations in methanol, whether prepared by simple mixing or by dissolution of products of cocrystallization. In fact, although the expected antioxidant activity of

solutions containing both A and B was 20.3 μM, the actual antioxidant activities of those solutions were between 16 μM and 17 μM. These values correspond to a synergism of 17.2 – 20.2 %.

The antioxidant potential of ferulic acid increases upon exposure to sun light for 4 h, as indicated by the decreased IC_{50} value. This increase in antioxidant activity may be due to the formation of analogs of ferulic acid, that may function as antioxidants, upon exposure to sun light. As indicated by photostability studies, vanillin possessing antioxidant activity may be formed (Tai *et al.*, 2011). Moreover, formation of vanillic acid from vanillin may occur, contributing to further increase the antioxidant potential. Also, synergistic interactions of ferulic acid and the degradation products of ferulic acid may increase the antioxidant activity of the methanol solution of ferulic.

Like in the case of ferulic acid, the radical scavenging activity of curcumin increases markedly after four hours of irradiation of solar radiation. This increase, also, may be due to the degradation of curcumin, which results in the formation of products possessing antioxidant activity. It has been reported that vanillin, ferulic acid, feruloyl methane and trans-6-(4'-hydroxy-3'-methoxyphenyl)-2,4-dioxo-5-hexenal are the major degradation products of curcumin; and all of these species are known antioxidants. In fact, Wang and coauthors demonstrated that feruloyl methane shows an antioxidant activity comparable to its analogs (Wang *et al.*, 2015). In addition to the major degradation products, numerous other products such as vanillic acid may form. The observed increase in antioxidant activity may be due to either additive or synergistic effects of residual curcumin and those antioxidants.

In accordance with the increase in antioxidant activity observed with ferulic acid and curcumin, all the methanol solutions containing both ferulic acid and curcumin exhibited an increase in the antioxidant activity upon irradiation with solar radiation for 4 h. As explained previously, this increase may be due to the formation of degradation products of both ferulic acid and curcumin, possessing antioxidant activity. As stated previously, additive or synergistic effects of those antioxidant species may enhance the antioxidant potential.

Interestingly, like in the case of initial antioxidant activities, ferulic acid and curcumin exhibit synergy when present in equimolar concentrations in methanol, whether prepared by simple mixing or by dissolution of products of cocrystallization even after 4 h of irradiation of solar radiation. In fact, although the expected antioxidant activity of solutions containing both A and B was 16.7 μM, the actual antioxidant activities of those

solutions were between 12 μM and 14 μM. These values correspond to a synergism of 18 - 28 %.

Evaluation of antioxidant properties of curcumin (B), ferulic acid (A) and equimolar mixtures of those species (i.e. (mixture of A and B), (C), (D), and (E)) revealed that curcumin and ferulic acid show synergism. Thus, using those chemical species together in a pharmaceutical or a cosmeceutical formulation is extremely advantageous. Moreover, the antioxidant activity of eutectic compositions of those APIs increases upon exposure to sun light. Thus, the products of cocrystallization are particularly suitable for topical formulations.

5.4 Conclusion

This study reveals that the cocrystallization methods – neat grinding and liquid-assisted grinding – can be utilized to prepare eutectic mixtures of curcumin and ferulic acid (molar ratio – 1:1), successfully. Furthermore, cocrystallization by solvent evaporation can be utilized to prepare a more crystalline solid form, probably a solid solution of curcumin and ferulic acid. Interestingly, the products of cocrystallization melted at the same temperature, which explains their similar dissolution profiles. Thus, the three methods of cocrystallization used in this study are equally suitable to prepare binary solid composites of curcumin and ferulic acid in the molar ratio 1:1.

The two bioactive compounds used in this study – curcumin and ferulic acid – are thermally stable at storage (25 °C), physiological (37 °C) and emulsion processing (70 °C) temperatures if protected from light, when used either individually or as a mixture (1:1 mol/mol). Upon exposure to diffuse light, ferulic acid exerts a protective effect on curcumin conferring it some extra stability on irradiation. However, curcumin shows degradation upon exposure to UV A and UV B light concurrently. Interestingly, the degradation products of both curcumin and ferulic acid, also, function as antioxidants. The antioxidant assays revealed that curcumin and ferulic acid exhibit a synergistic effect when mixed in the molar ratio 1:1. Also, antioxidant assays confirmed that the degradation products of ferulic acid and curcumin, whether present separately or together as a mixture or as any of the products of cocrystallization, exhibit antioxidant activity and may function synergistically. Therefore, the eutectic composition of curcumin and ferulic acid is especially suitable for topical formulations in both cosmaceuticals and pharmaceuticals.

In sum, the eutectic composition of curcumin and ferulic acid augments solubility, photostability and antioxidant potential of curcumin.

5.5 References

Ahmad, I, Zahin, M., Aqil, F., Hasan, S., Khan, M.S.A. and Owais, M. (2008). Bioactive compounds from *Punica granatum*, *Curcuma longa* and *Zingiber officinale* and their therapeutic potential. *Drugs of the Future* **33(4)**, 329-346.

Anand, P., Kunnumakkara, A.B., Newman, R.A. and Aggarwal, B.B. (2007). Bioavailability of curcumin: problems and promises. *Molecular Pharmaceutics* **4(6)**, 807-18.

Bates, T.R. (1969). Dissolution characteristics of reserpine-polyvinylpyrrolidone co-precipitates. *Journal of Pharmacy and Pharmacology* **21(10)**, 710-712.

Brittain, H.G. (2013). Pharmaceutical cocrystals: The coming wave of new drug substances. *Journal of pharmaceutical sciences* **102(2)**, 311-317.

Carmona-Jiménez, Y., García-Moreno, M.V., Igartuburu, J.M. and Barroso, C.G. (2014). Simplification of the DPPH assay for estimating the antioxidant activity of wine and wine by-products. *Food Chemistry* **165**, 198-204.

Chiou, W.L. and Riegelman, S. (1971). Pharmaceutical applications of solid dispersion systems. *Journal of Pharmaceutcal Sciences,* **60(9)**, 1281-1302.

Chow, S.F., Shi, L., Ng, W.W., Leung, K.H.Y., Nagapudi, K., Sun, C.C. and Chow, A.H.L. (2014). Kinetic entrapment of a hidden curcumin cocrystal with phloroglucinol. *Crystal Growth & Design* **14(10)**, 5079-5089.

Cuvelier, M-E., Richard, H. and Berset, C. (1992). Comparison of the Antioxidative Activity of Some Acid-phenols: Structure-Activity Relationship. *Bioscience, Biotechnology, and Biochemistry* **56(2)**, 324-325.

Das, S.S., Singh, N.P., Agrawal, T., Gupta, P., Tiwari, S.N. and Singh, N.B. (2009). Studies of the solidification behavior and molecular interaction in benzoic acid:o-chloro benzoic acid eutectic system. *Molecular Crystals and Liquid Crystals* **501**, 107-124.

Goldberg, A.H., Gibaldi, M., Kanig, J.L. and Mayersohn, M. (1966). Increasing dissolution rates and gastrointestinal absorption of drugs via solid solutions and eutectic mixtures IV: Chloramphenicol—urea system. *Journal of Pharmaceutical Sciences* **55(6)**, 581-583.

Good, D.J. and Rodríguez-Hornedo, N. (2009). Solubility advantage of pharmaceutical cocrystals. *Crystal Growth & Design* **9(5)**, 2252–2264.

Górniak, A., Wojakowska, A., Karolewicz, B. and Pluta, J. (2011). Phase diagram and dissolution studies of the fenofibrate-acetylsalicylic acid system. *Journal of Thermal Analysis and Calorimetry* **104**, 1195-1200.

Goud, N.R., Suresh, K., Sanphui, P. and Nangia, A. (2012). Fast dissolving eutectic compositions of curcumin. *International Journal of Pharmaceutics* **439**, 63-72.

Hickey, M.B., Peterson, M.L., Scoppettuolo, L.A., Morrisette, S.L., Vetter, A., Guzmán, H., Remenar, J.F., Zhang, Z., Tawa, M.D., Haley, S., Zaworotko, M.J. and Almarsson, Ö. (2007). Performance comparison of a cocrystal of carbamazepine with marketed product. *European Journal of Pharmaceutics and Biopharmaceutics* **67**, 112–119.

Jung, S., Lee, J. and Kim, I.W. (2013). Structures and physical properties of the cocrystals of adefovir dipivoxil with dicarboxylic acids. *Journal of Crystal Growth* **373**, 59-63.

Kudo, S. and Takiyama, H. (2014). Production method of carbamazepine/saccharin cocrystal particles by using two solution mixing based on the ternary phase diagram. *Journal of Crystal Growth* **392**, 87-91.

Lara-Ochoa, F. and Espinosa-Pérez, G. (2007). Cocrystals Definitions. *Supramolecular Chemistry* **19(8)**, 553-557.

Ober, C.A., Montgomery, S.E. and Gupta, R.B. (2013). Formation of itraconazole/L-malic acid cocrystals by gas antisolvent cocrystallization. *Powder Technology* **236**, 122-131.

Ogiwara, T., Satoh, K., Kadoma, Y., Murakami,Y., Unten, S., Atsumi, T., Sakagami, H. and Fujisawa, S. (2002). Radical scavenging activity and cytotoxicity of ferulic acid. *Anticancer Research* **22(5)**, 2711–2717.

Padrela, L., Rodrigues, M.A., Tiago, J., Velaga, S.P., Matos, H.A. and de Azevedo, E.G. (2014). Tuning physicochemical properties of theophylline by cocrystallization using the supercritical fluid enhanced atomization technique. *The Journal of Supercritical Fluids* **86**, 129-136.

Padrela, L., Rodrigues, M.A., Velaga, S.P., Matos, H.A. and de Azevedo, E.G. (2009). Formation of indomethacin-saccharin cocrystals using supercritical fluid technology. *European Journal of Pharmaceutical Sciences* **38**, 9-17

Qiao, N., Li, M., Schlindwein, W., Malek, N., Davies, A. and Trappitt, G. (2011). Pharmaceutical cocrystals: An overview. *International Journal of Pharmaceutics* **419**, 1-11.

Sanphui, P., Goud, N.R., Khandavilli, U.B.R. and Nangia, A. (2011). Fast dissolving curcumin cocrystals. *Crystal Growth & Design* **11(9)**, 4135-4145.

Setyaningsih, W., Saputro, I.E., Palma, M. and Barroso, C.G. (2015). Optimisation and validation of the microwave-assisted extraction of phenolic compounds from rice grains. *Food Chemistry* **169**, 141–149.

Sinha, S., Baboota, S., Ali, M., Kumar, A. and Ali, J. (2009). Solid dispersion: An alternative technique for bioavailability enhancement of poorly soluble drugs. *Journal of dispersion science and technology* **30(10)**, 1458-1473.

Srinivasan, M., Sudheer, A.R. and Menon, V.P. (2007). Ferulic acid: Therapeutic potential through its antioxidant property. *Journal of Clinical Biochemistry and Nutrition* **40**, 92-100.

Swapna, B., Maddileti, D. and Nangia, A. (2014). Cocrystals of the tuberculosis drug isoniazid: Polymorphism, isostructurality, and stability. *Crystal Growth & Design* **14(11)**, 5991-6005.

Tai, A., Sawano, T., Yazama, F. and Ito, H. (2011). Evaluation of antioxidant activity of vanillin by using multiple antioxidant assays. *Biochimica et Biophysica Acta* **1810**, 170-177.

Tønnesen, H.H., Másson, M. and Loftsson, T. (2002). Studies of curcumin and curcuminoids. XXVII. Cyclodextrin complexation: solubility, chemical and photochemical stability. *International Journal of Pharmaceutics* **244**, 127-135.

Trask, A.V., Sam Motherwell, W.D. and Jones, W. (2006). Physical stability enhancement of theophylline via cocrystallization. *International Journal of Pharmaceutics* **320**, 114-123.

Trombino, S., Serini, S., Di Nicuolo, F., Celleno, L., Andò, S., Picci, N., Calviello, G. and Palozza, P. (2004). Antioxidant effect of ferulic acid in isolated membranes and intact cells: Synergistic interactions with α-tocopherol, β-carotene, and ascorbic acid. *Journal of Agricultural Food Chemistry* **52(8)**, 2411-2420.

Wang, W., Guo, J., Zhang, J., Peng, J., Liu, T. and Xin, Z. (2015). Isolation, identification and antioxidant activity of bound phenolic compounds present in rice bran. *Food Chemistry* **171**, 40-49.

Wang, Y-J., Pan, M-H., Cheng, A-L., Lin, L-I., Ho, Y-S., Hsieh, C-Y. and Lin, J-K. (1997). Stability of curcumin in buffer solutions and characterization of its degradation products. *Journal of Pharmaceutical and Biomedical Analysis* **15**, 1867-1876.

ANNEXURE

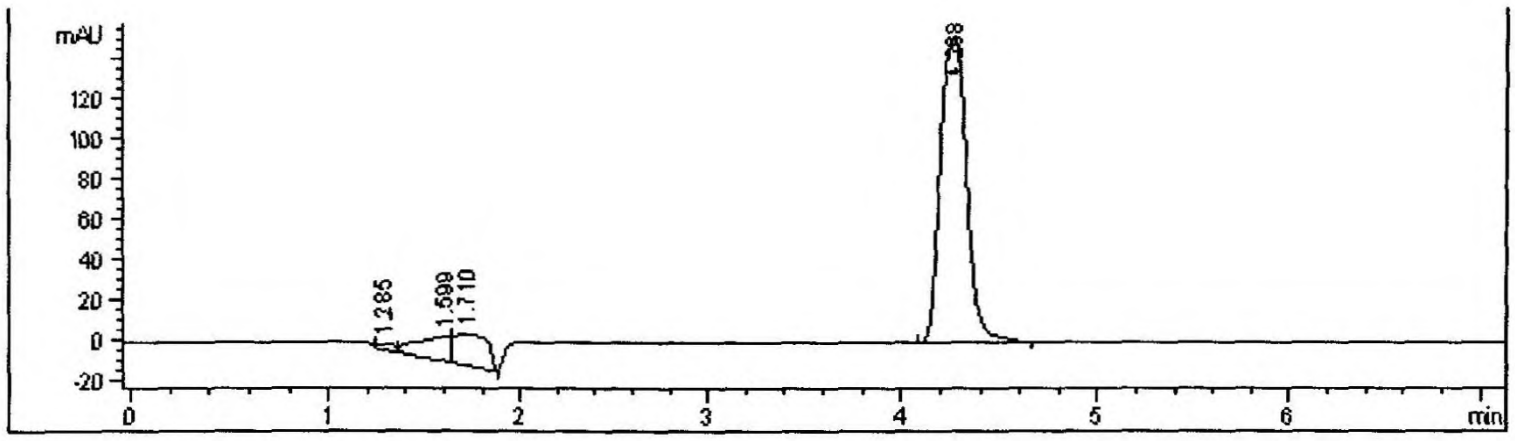

Figure A1. HPLC chromatogram of ferulic acid (321 nm)

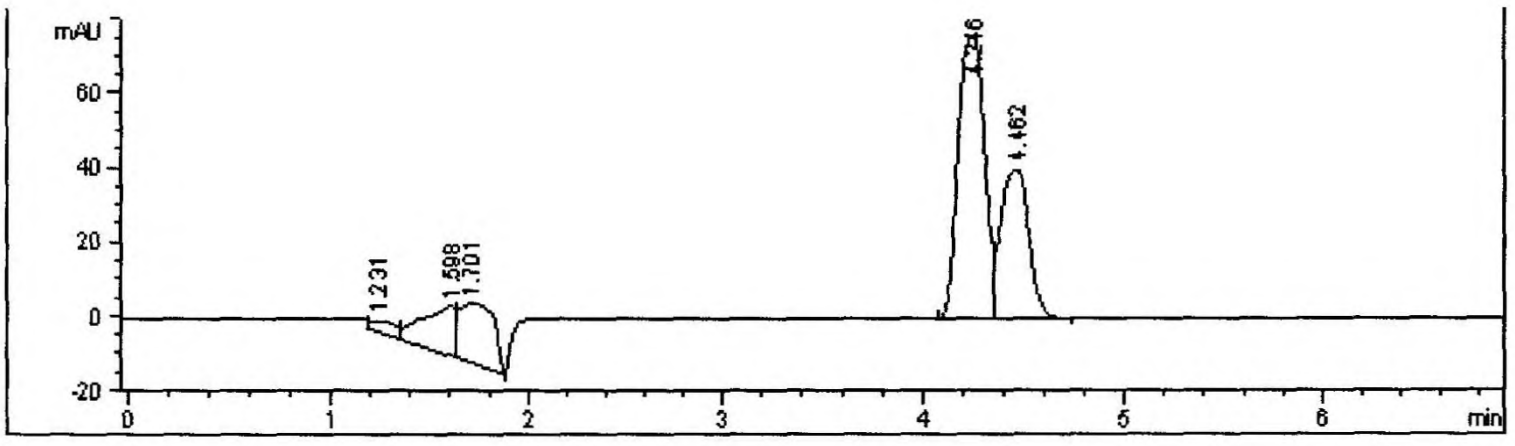

Figure A2. HPLC chromatogram of ferulic acid after 1 h of UV irradiation (321 nm)

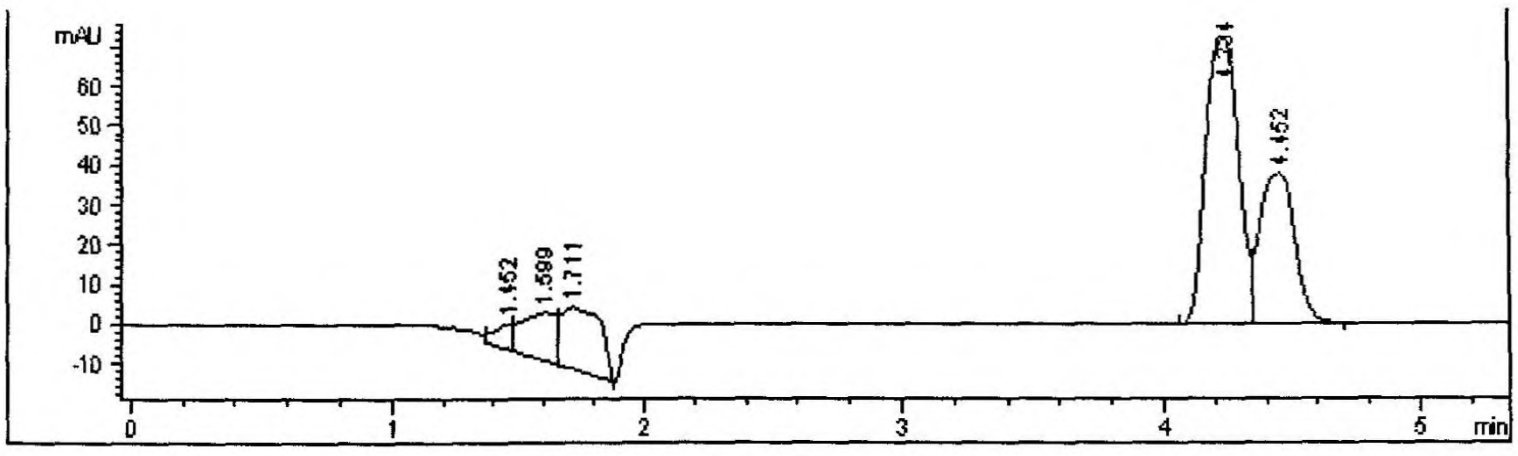

Figure A3. HPLC chromatogram of feruic acid after 8 h of UV irradiation (321 nm)

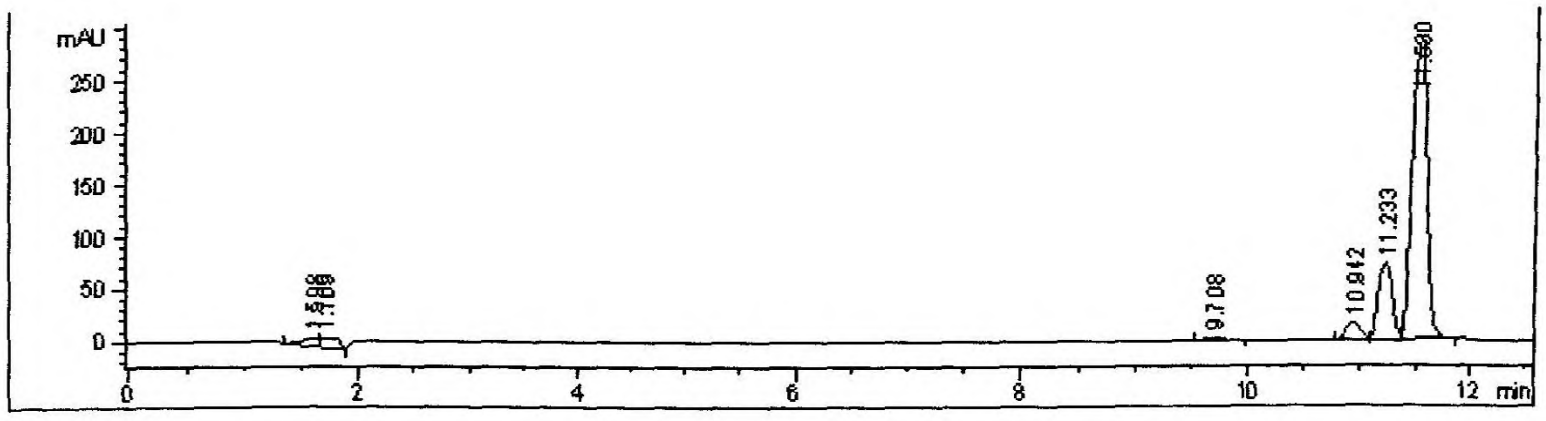

Figure A4. HPLC chromatogram of curcumin (425 nm)

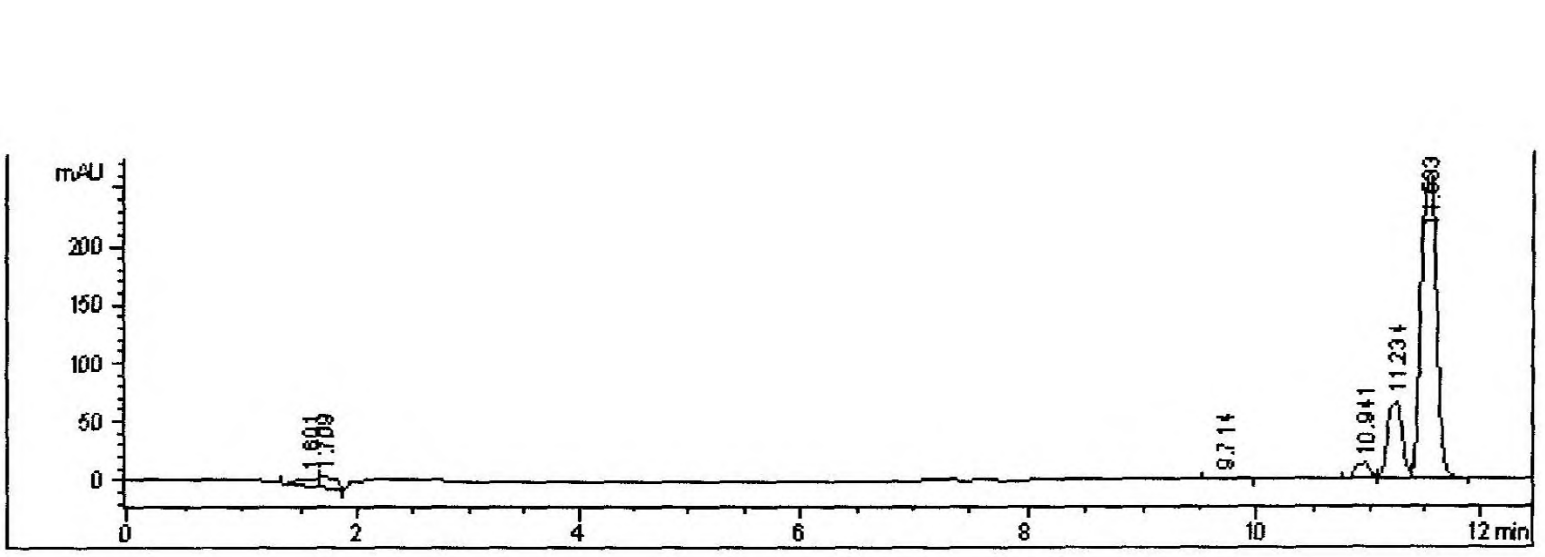

Figure A5. HPLC chromatogram of curcumin after 1 h of UV irradiation (425 nm)

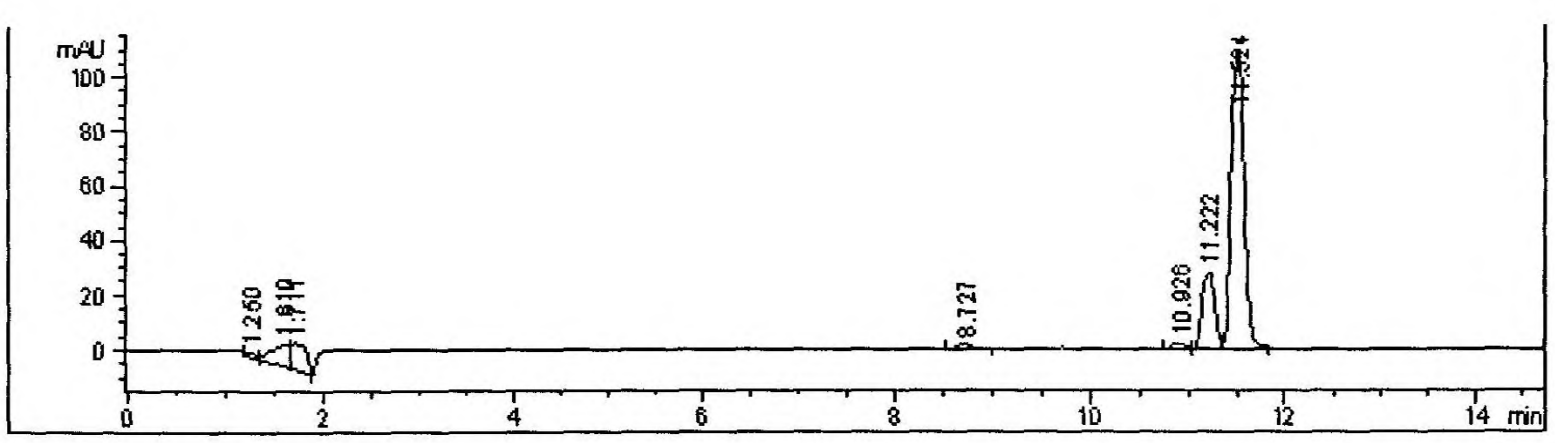

Figure A6. HPLC chromatogram of curcumin after 8 h of UV irradiation (425 nm)

Figure A7. HPLC chromatogram of curcumin (254 nm)

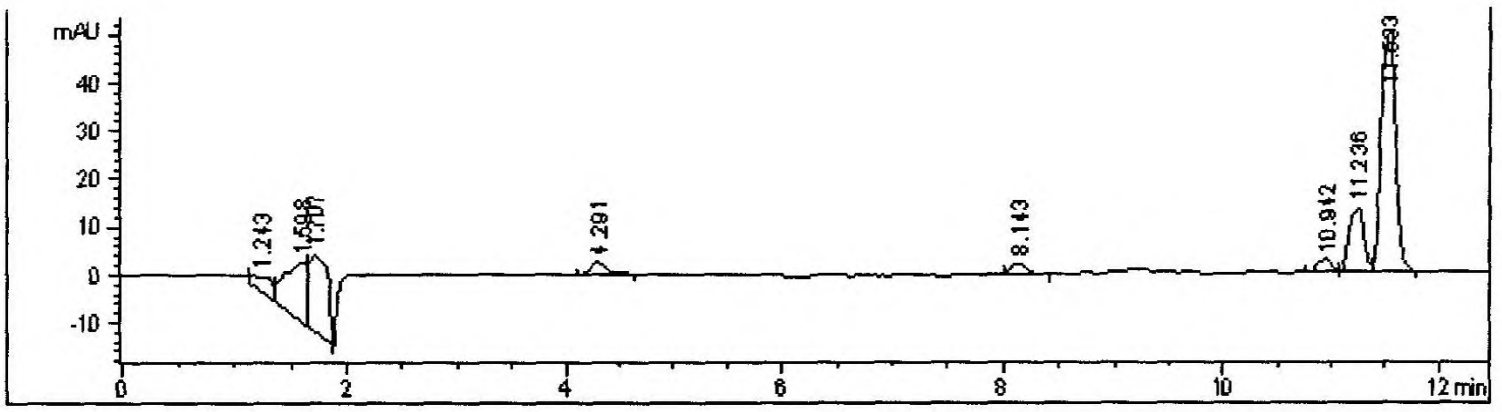

Figure A8. HPLC chromatogram of curcumin solution after 1 h of UV irradiation (254 nm)

Figure A9. HPLC chromatogram of curcumin solution after 8 h of UV irradiation (254 nm)

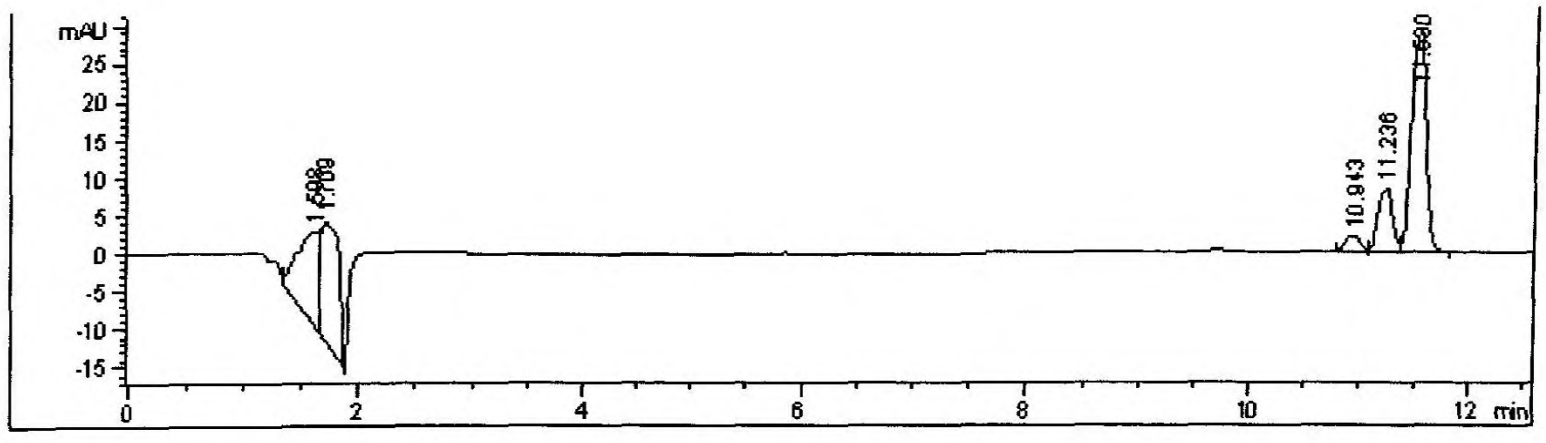

Figure A10. HPLC chromatogram of crucumin (321 nm)

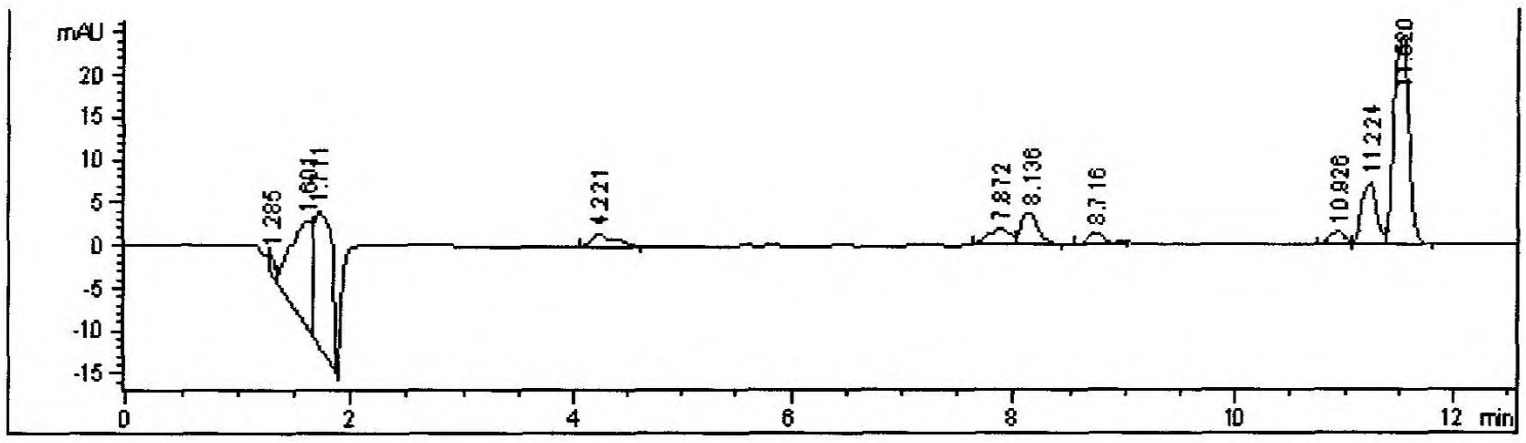

Figure A11. HPLC chromatogram of curcumin solution after 2 h of UV irradaition (321 nm)

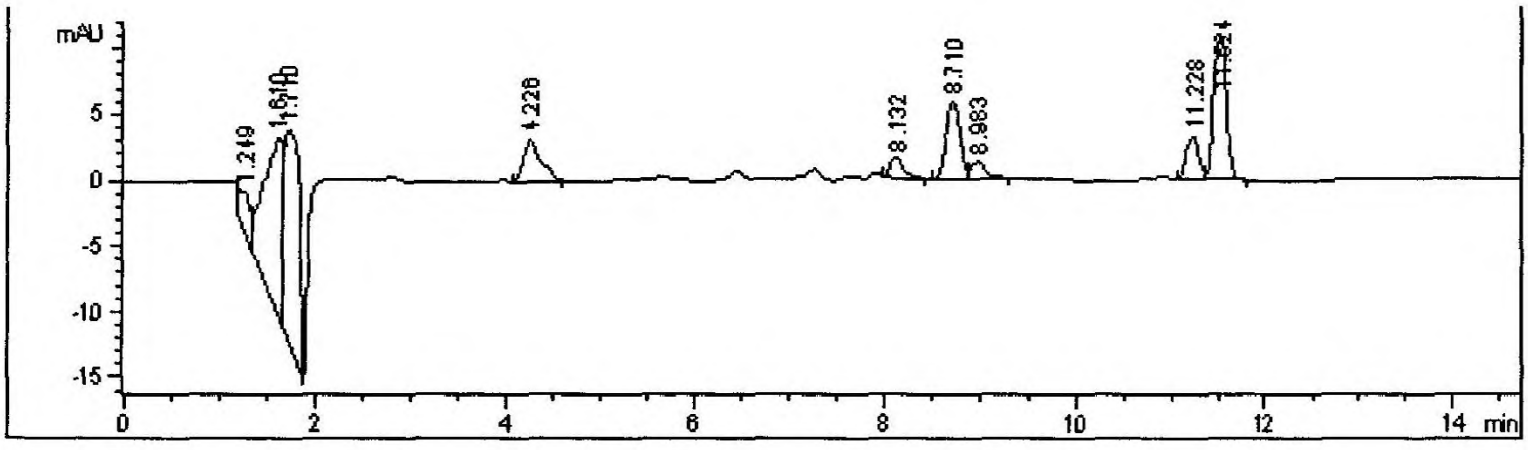

Figure A12. HPLC chromatogram of curcumin solution after 8 h of UV irradiation (321 nm)

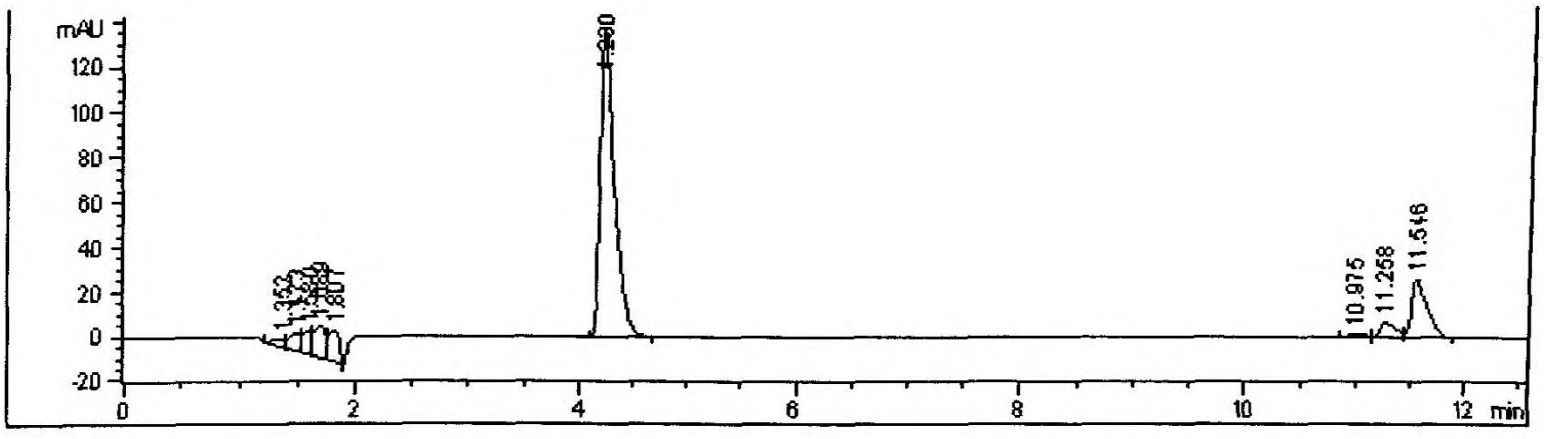

Figure A13. HPLC chromatogram of a solution of ferulic acid and curcumin (321 nm)

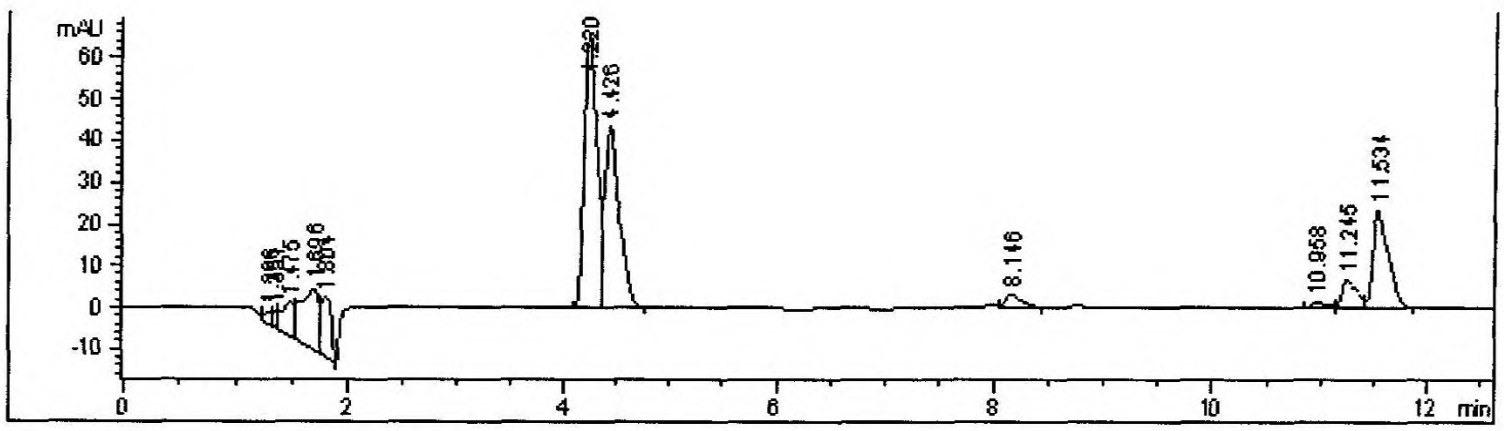

Figure A14. HPLC chromatogram of a solution of ferulic acid and curcumin after 1 h of UV irradiation (321 nm)

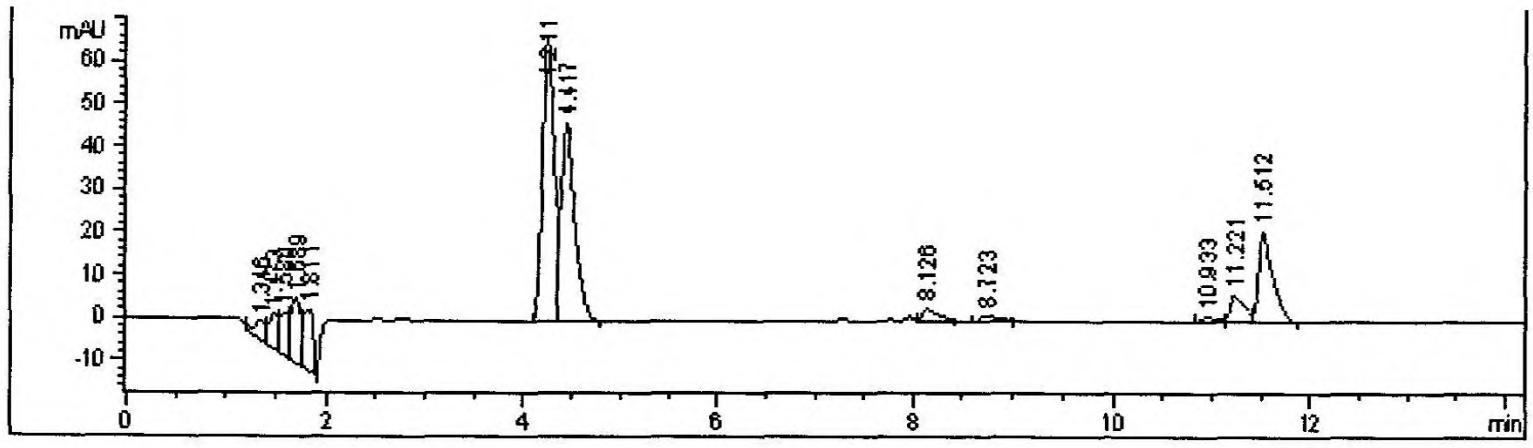

Figure A15. HPLC chromatogram of a solution of ferulic acid and curcumin after 2 h of UV irradiation (321 nm)

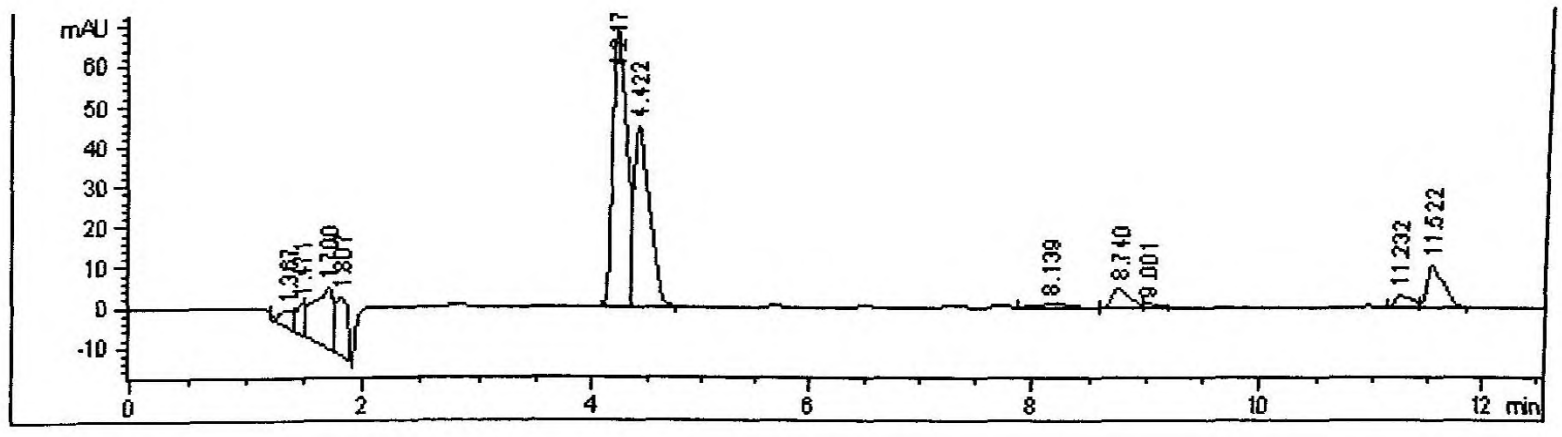

Figure A16. HPLC chromatogram of a solution of ferulic acid and curcumin after 8 h of UV irradiation (321 nm)

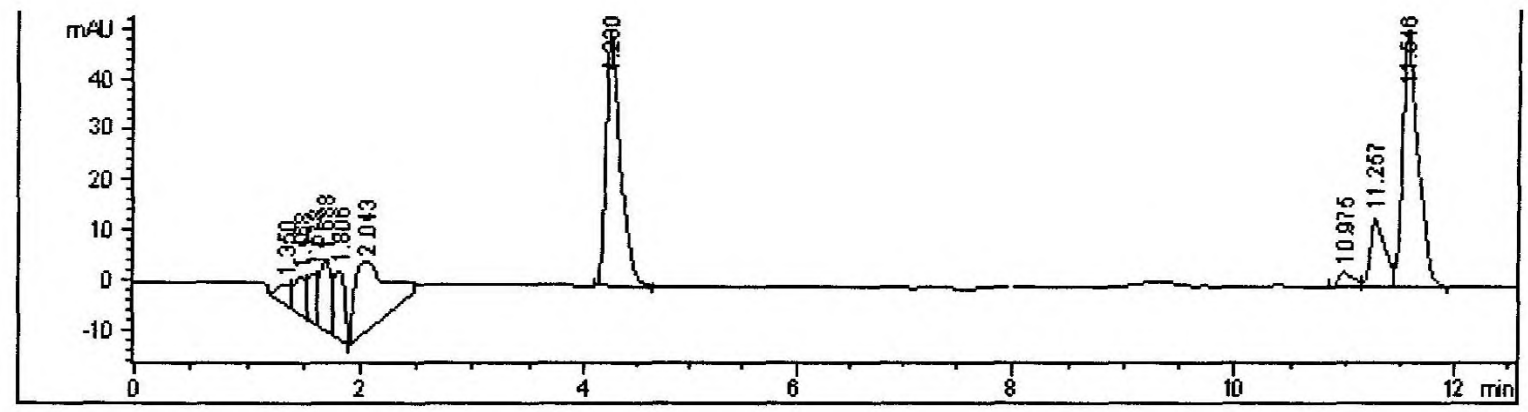

Figure A17. HPLC chromatogram of a solution of ferulic acid and curcumin (254 nm)

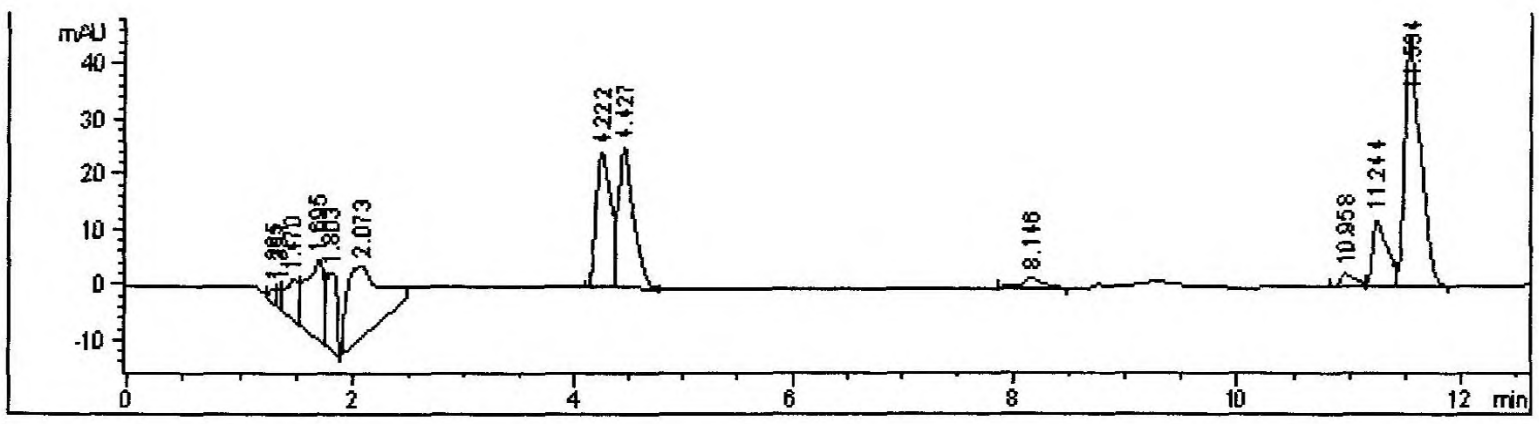

Figure A18. HPLC chromatogram of a solution of ferulic acid and curcumin after 1 h of UV irradiation (254 nm)

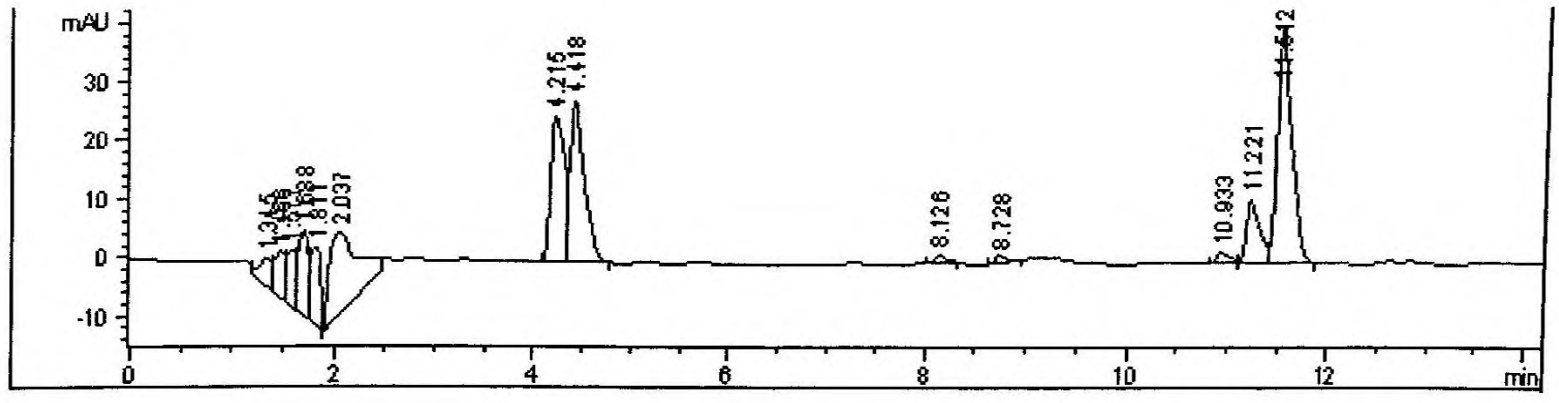

Figure A19. HPLC chromatogram of a solution of ferulic acid and curcumin after 2 h of UV irradiation (254 nm)

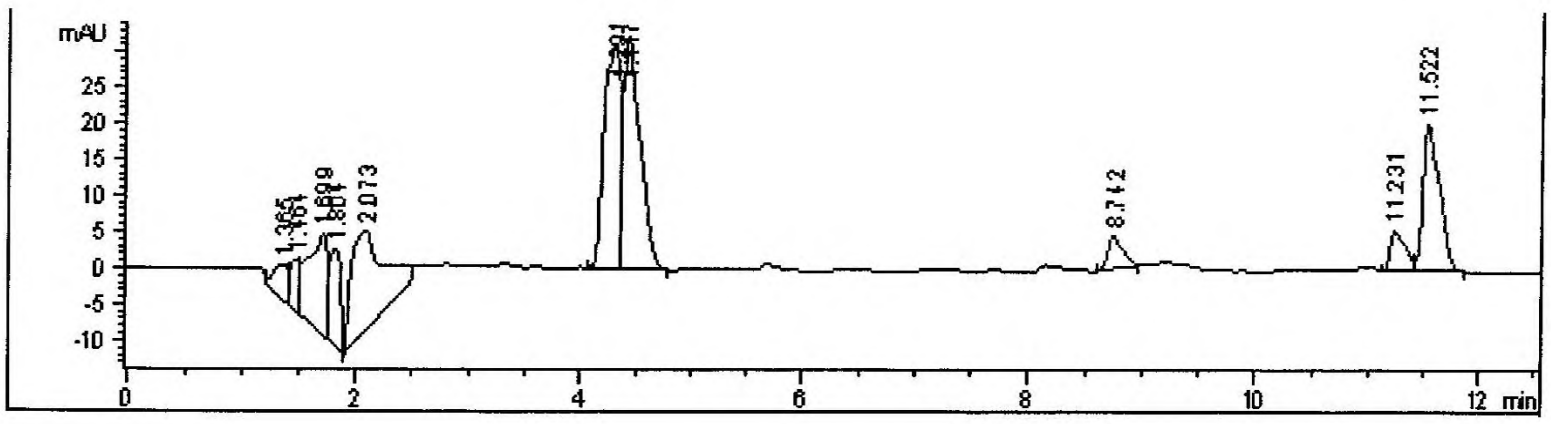

Figure A20. HPLC chromatogram of a solution of ferulic acid and curcumin after 8 h of UV irradiation (254 nm)

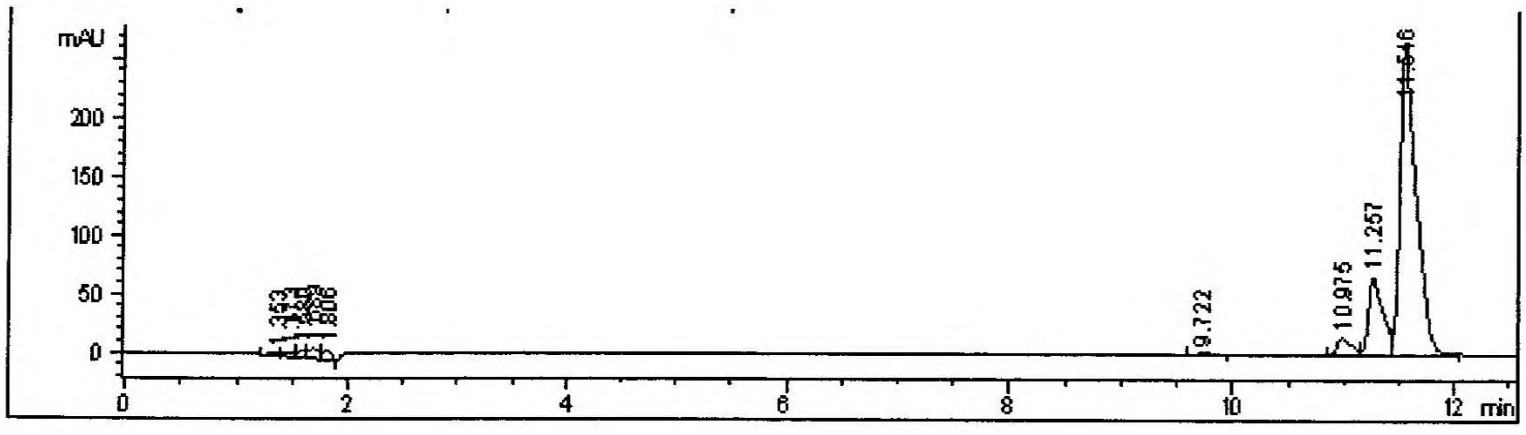

Figure A21. HPLCchromatogram of a soluation of ferulic acid and curcumin (425 nm)

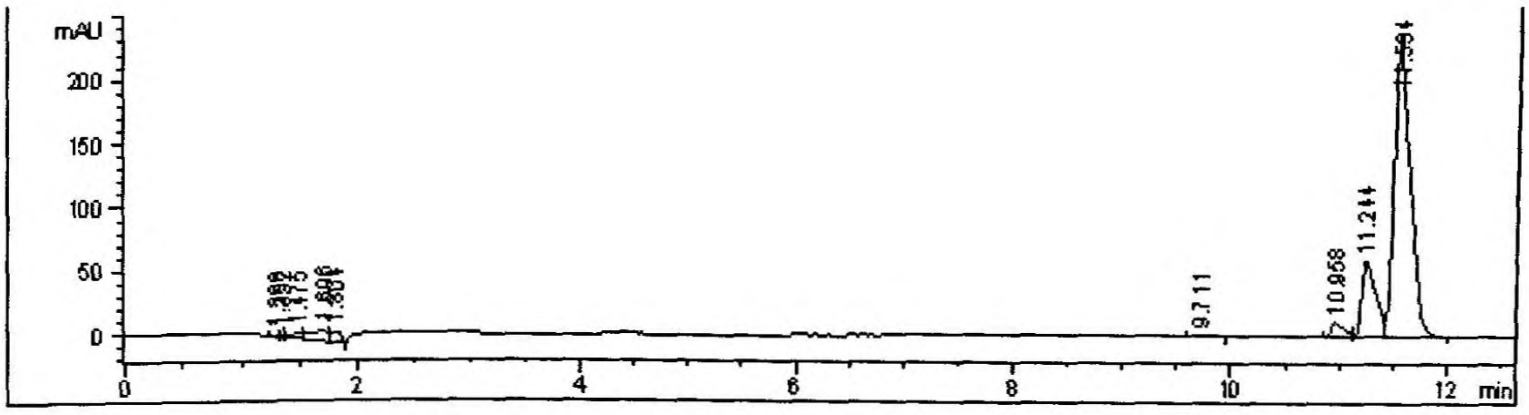

Figure A22. HPLC chromatogram of a solution of ferulic acid and curcumin after 1 h of UV irradiation (425 nm)

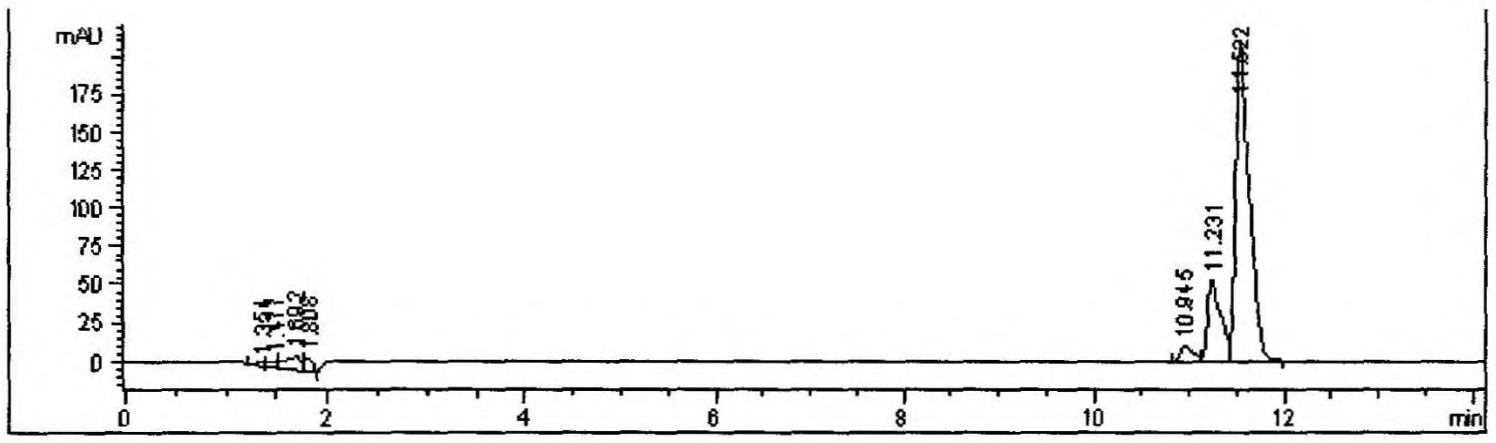

Figure A23. HPLC chromatogram of a solution of ferulic acid and curcumin after 2 h of UV irradiation (425 nm)

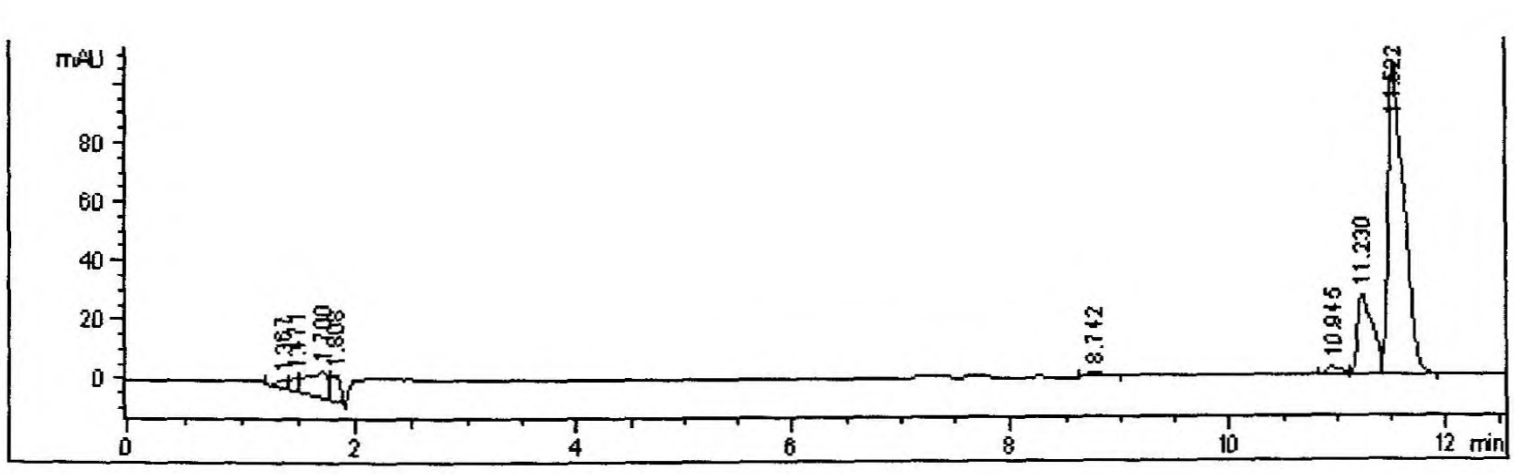

Figure A24. HPLC chromatogram of a solution of ferulic acid and curcumin after 8 h of UV irradiation (425 nm)

National Digitization Project

National Science Foundation

Institute : National Science Foundation

1. Place of Scanning : Sanje (Private) Ltd, Hokandara
2. Date Scanned : 2017/03/31
3. Name of Digitizing Company : Sanje (Private) Ltd, No 435/16, Kottawa Rd, Hokandara North. Arangala, Hokandara
4. Scanning Officer

Name : Angelo Melvin

Signature : A.M.

Certification of Scanning

I hereby certify that the scanning of this document was carried out under my supervision, according to the norms and standards of digital scanning accurately, also keeping with the originality of the original document to be accepted in a court of law.

Certifying Officer

Designation : Information Officer

Name : Renuka Sugathadasa

Signature : R.P. Sugathadasa

Date : .....

"This document/publication was digitized under National Digitization Project of the National Science Foundation, Sri Lanka"